

SUBSTITUENT EFFECTS IN THE MASS SPECTRA

OF

SUBSTITUTED BENZILS

A thesis presented for the degree of
Doctor of Philosophy in Chemistry
in the University of Canterbury,
Christchurch, New Zealand.

by

B.N. McMaster

1972

QD
281
.S67
.M167
1972ABSTRACT

The mass spectra of a series of *m*- and *p*-substituted benzils have been determined at several ionizing voltages below 20 eV, and at 70 eV. The fractional intensities of the molecule-ion (F_M), substituted benzoyl ion (F_X) and unsubstituted benzoyl ion (F_H) were obtained as a function of energy from measured ionization efficiency (IE) curves. Ionization potentials (IP), and appearance potentials for the substituted (AP_X) and unsubstituted (AP_H) benzoyl ions were determined from the IE curves by a semi-logarithmic method. Various correlations of ion intensity and energy parameters with substituent constants (σ^+ , σ) are examined; by the best standards of solution chemistry these are generally poor. Fair correlations are obtained between $\log (F_X/F_H)$ or $AP_X - AP_H$ and σ^+ (σ), and these are interpreted in terms of the expected effect of substituents on the stabilities of the product ions in the decompositions. A good correlation is observed between $\log (F_X/F_H)$ and $AP_X - AP_H$; it suggests that substituents mainly affect F_X/F_H by changing the activation energies for the competing decompositions of the benzil molecule-ions. The competitive shift has a marked effect on these appearance potentials, and in this system $AP - IP$ is therefore not a good measure of the activation energy for the primary decompositions.

CONTENTS

	<u>Page</u>
CHAPTER 1 <u>INTRODUCTION</u>	1
1.1 Mass Spectrometry	1
1.2 This Work	2
CHAPTER 2 <u>GENERAL PRINCIPLES OF MASS SPECTROMETRY</u>	3
2.1 Instrumental Factors	3
2.1.1 Ion Flight Path	3
2.1.2 Flight Times and Types of Ion Observed	4
2.1.3 Metastable Ions	4
2.2 Theoretical Aspects	6
2.2.1 Ionization Processes	6
2.2.2 Decay Processes	7
2.2.3 Quasi-Equilibrium Theory	8
(i) Basic Assumptions	8
(ii) Unimolecular Rate Constants	9
(iii) Kinetic and Competitive Shift Effects	11
(iv) Breakdown Graphs	13
(v) Ion Intensities	16
2.2.4 Comparison with Conventional Chemical Reactions	17
2.3 Substituent Effects	18
2.3.1 Substituent Effects on Decomposition Path- ways	19
2.3.2 Substituent Effects on Internal Energy and Rate Constant Functions	20
(i) Internal Energy Distribution Functions, p(E)	20
(ii) Rate Constant Functions, k(E)	23

	<u>Page</u>
CHAPTER 3 <u>EXPERIMENTAL</u>	27
3.1 Preparation and Purification of Compounds	27
3.1.1 Reagents and Solvents	27
3.1.2 Deoxybenzoins	27
(i) Preparation of Benzylmagnesium Chloride	28
(ii) Preparative Methods	29
3.1.3 Benzils	34
3.2 Mass Spectrometer	35
3.2.1 Instrumental Modifications	35
3.2.2 Semi-Automatic Digital Recording System	36
(i) Ionizing Voltage Control Unit	36
(ii) CAT Input Signal	37
(iii) CAT Read-out System	37
3.2.3 Sample Introduction	38
(i) Inlet Systems	38
(ii) Sample Preparation	39
(iii) General Procedure	41
3.2.4 Source Focussing	42
3.3 Data Collection	44
3.3.1 70 eV Mass Spectra	44
3.3.2 Low Voltage Mass Spectra	44
3.3.3 Ionization Efficiency Curves	45
3.3.4 Calibration of Multiplier Gain	46
CHAPTER 4 <u>ANALYSIS OF IONIZATION EFFICIENCY DATA</u>	48
4.1 Least Squares Procedures	49
4.1.1 Smoothing and Differentiation (SMOOTH)	50
4.1.2 Fitting a Straight Line (LINEAR)	50
4.1.3 Fitting a General Function (LINFIT)	52

	<u>Page</u>
4.2 Preliminary Treatment of Ionization Efficiency	
Data	53
4.2.1 Decoding and Editing (TAPED)	53
4.2.2 Smoothing and Reduction of Data (RAWFIT)	54
4.3 Appearance Potentials	55
4.3.1 Semi-Logarithmic Method	55
4.3.2 Normalization of Semi-Log Curves (SLOG)	59
4.3.3 Calculation of Appearance Potentials (SLAP)	59
4.3.4 Discussion of Errors	62
4.4 Fractional Ion Intensities (FIX)	63
4.5 A Typical Analysis	66
4.5.1 Program RAWFIT	66
4.5.2 Program SLOG	67
4.5.3 Program SLAP	67
4.5.4 Program FIX	67
CHAPTER 5 <u>RESULTS</u>	69
5.1 Mass Spectra (70 and 20 eV)	69
5.2 Mass Spectra (Low Voltage)	70
5.3 Fractional Ion Intensities	71
5.4 Logarithmic Ion Intensity Ratios	72
5.5 Appearance Potentials	73
5.6 Correlation of Results	74
CHAPTER 6 <u>DISCUSSION</u>	75
6.1 General Description of Mass Spectra	75
6.2 Interpretation of Energy and Intensity Data	85
6.2.1 Correlation of Ionization and Appearance Potentials with Substituent Constants	86

	<u>Page</u>
6.2.2 Correlations of Energy Parameters with Substituent Constants	88
6.2.3 Variation of Fractional Ion Intensities with Energy	95
6.2.4 Correlations of Logarithmic Ion Intensity Ratios with Substituent Constants	98
(i) $\text{Log } (F/F_M)$	99
(ii) $\text{Log } (F/1-F_M)$	100
(iii) $\text{Log } (F_X/F_H)$	103
6.2.5 Correlations of Logarithmic Ion Intensity Ratios with Energy Parameters	105
6.3 Conclusion	109
REFERENCES	112
APPENDIX A <u>COMPUTER PROGRAMS</u>	120
APPENDIX B <u>ELECTRONICS</u>	121
ACKNOWLEDGEMENTS	122

TABLES

<u>No.</u>	<u>Title</u>	<u>Following Page</u>
1	Multiplier Gain (G_M)	47
2	Systematic Errors in Appearance Potential Determinations	62
3	Relative Ion Intensities (70 and 20 eV Mass Spectra)	69
4	Measured Fractional Ion Intensities	70
5	Fractional Ion Intensities	71
6	Logarithmic Intensity Ratios	72
7	Logarithmic Intensity Ratios (70 eV)	72
8	Ionization and Appearance Potentials	73
9	Energy Parameters in Substituted Benzils	73
10	Correlations of Energy Parameters with Substituent Constants	74
11	Correlations of $\text{Log } (F/F_M)$ with Substituent Constants	74
12	Correlations of $\text{Log } (F/1-F_M)$ with Substituent Constants	74
13	Correlations of $\text{Log } (F_X/F_H)$ with Substituent Constants	74
14	Correlations of $\text{Log } (F/F_M)$ with (AP-IP)	74
15	Correlation of $\text{Log } (F/1-F_M)$ with (AP-IP)	74
16	Correlations of $\text{Log } (F_X/F_H)$ with $(AP_X - AP_H)$	74
17	Correlations of Logarithmic Intensity Ratios at 70 eV with Substituent Constants and Energy Parameters	74

FIGURES

<u>No.</u>	<u>Title</u>	<u>Following Page</u>
1	Fragmentation Pattern of Benzils	2
2	Ion Flight Path	3
3	Ion Source	3
4	Rate Constant Function, $k(E)$	10
5	Kinetic and Competitive Shift Effects	10
6	Breakdown Graph ($M^+ \rightarrow A^+ \rightarrow B^+$)	13
7	Internal Energy Distribution and Rate Constant Functions	20
8	Semi-Automatic Digital Recording System	36
9	Standard Error of Ionization Efficiency	66
10a	Program SLOG Output: Normalized Semi-Log Curve	67
10b	Program SLOG Output: Unnormalized Semi-Log Curve	67
11	Program SLAP Output	67
12	Systematic Errors in Appearance Potential Determinations	67
13	Normalized Semi-Log Ionization Efficiency Curves for <i>m</i> -Methylbenzil	67
14	Fractional Ion Intensity Curves for <i>m</i> -Methylbenzil	68
15	Effect of Incorrect Zero Threshold on Fractional Ion Intensity Curves	68
16	Relative Ion Intensities (70 and 20 eV Mass Spectra)	69
17	Fractional Ion Intensities	71
18	IP versus σ^+	86
19	AP_H versus σ^+	87
20	AP_X versus σ^+	87
21	AP_H-IP versus σ^+	89
22	AP_X-IP versus σ^+	89

23	AP_H -IP and AP_X -IP versus σ^+ for Bibenzyls	89
24	AP_X - AP_H versus σ^+	90
25	Log (F_H/F_M) versus σ^+ (E = 6.0 eV)	99
26	Log (F_X/F_M) versus σ^+ (E = 6.0 eV)	99
27	Log ($F_H/1-F_M$) versus σ^+ (E = 6.0 eV)	101
28	Log ($F_X/1-F_M$) versus σ^+ ((a) E = 6.0 eV, (b) V = 70.0 eV)	101
29	Log (F_X/F_H) versus σ^+ ((a) E = 6.0 eV, (b) V = 70.0 eV)	103
30	Log (F_H/F_M) versus (AP_H -IP) (E = 6.0 eV)	105
31	Log (F_X/F_M) versus (AP_X -IP) (E = 6.0 eV)	105
32	Log ($F_H/1-F_M$) versus (AP_H -IP) (E = 6.0 eV)	106
33	Log ($F_X/1-F_M$) versus (AP_X -IP) (E = 6.0 eV)	106
34	Log (F_X/F_H) versus (AP_X - AP_H) ((a) E = 6.0 eV, (b) V = 70.0 eV)	107
35	Motor Drive Unit (Ionizing Voltage Control)	121
36	CAT - Tape Punch Interface	121

C H A P T E R 1INTRODUCTION1.1 MASS SPECTROMETRY

Mass spectrometry is widely used as an aid to the determination of molecular structure. Because of its importance, considerable research effort has been directed towards discovering how structural changes affect the mass spectra of molecules. Implicit in this research has been the hope that the factors which control mass spectral decompositions will prove to be similar to those involved in ordinary chemical reactions, thus allowing the extensive knowledge of structural effects in ordinary reactions to be applied to the interpretation of mass spectra.

Striking similarities have been observed between mass spectral reactions and some other, more conventional, chemical processes - particularly pyrolysis and photolysis¹. The similarities suggest² that information obtained from mass spectrometry may help to elucidate the mechanisms of some of these processes, especially the role of carbonium ions (or ion-radicals). Since mass spectral data can be obtained routinely and rapidly on microgram quantities of sample, there are very compelling reasons for exploring the factors influencing mass spectra.

The study of substituent effects has long been an important method of investigating relationships between the structure (both geometric and electronic) of a molecule and its reactions. The pioneering work of Hammett³ stimulated a tremendous amount of research into the effects of substituents

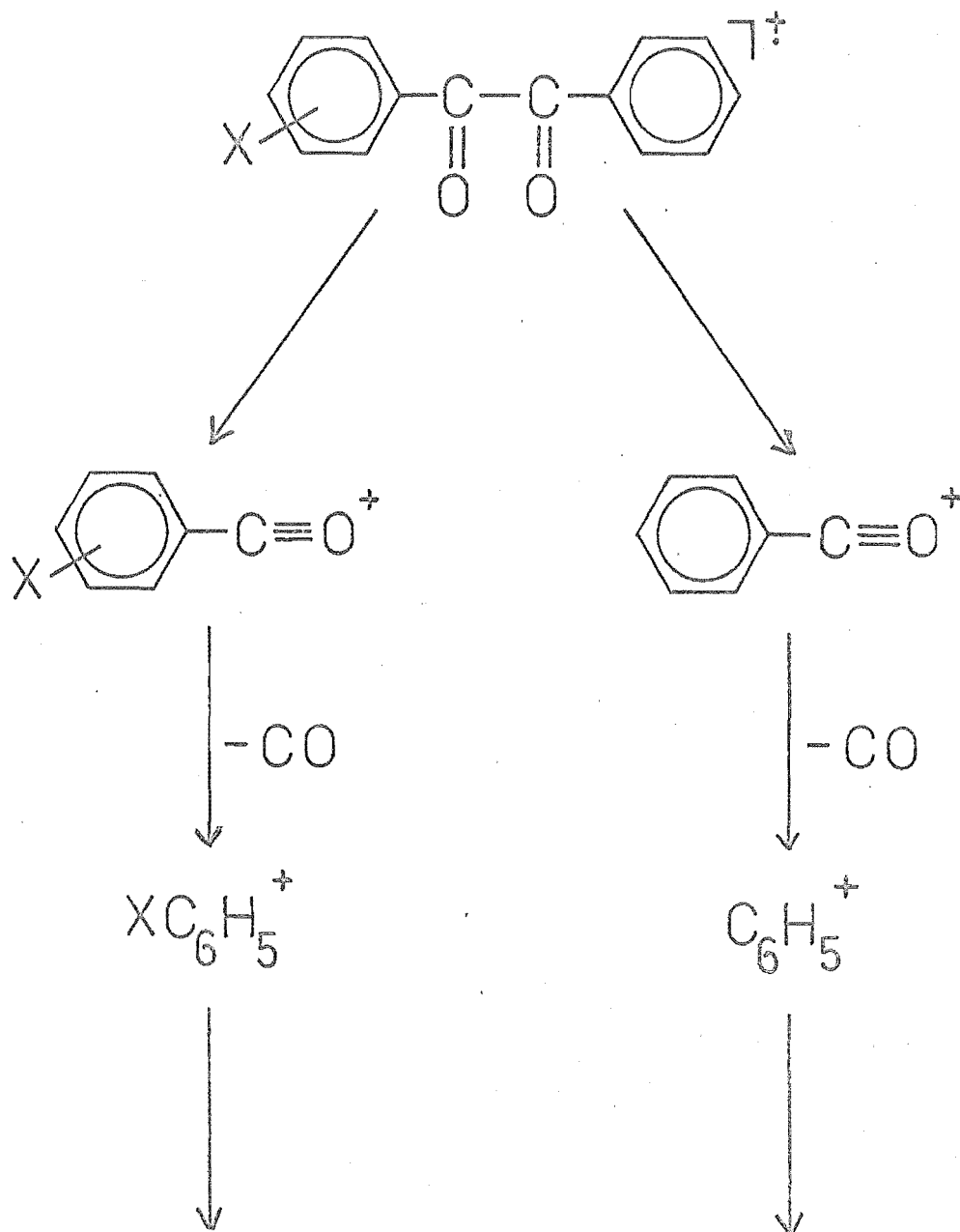
on the reactivity of aromatic systems in both solution⁴ and gas-phase⁵ reactions. More recently such investigations have been extended to mass spectral reactions, and a number of correlations between substituent parameters and ion intensities, as well as appearance potentials, have been reported⁶⁻⁸.

1.2 THIS WORK

This thesis describes the effects of substituents on the ion intensities and appearance potentials in the mass spectra of benzils. These were chosen for study because the substituted and unsubstituted primary fragment ions are formed by the competitive scission of the same bond in the molecule-ion. In addition, these ions are expected to have the well-defined, comparatively stable benzoyl ion structure. There are generally no competing primary decompositions of the molecule-ion, or any secondary decompositions of the primary fragment ions - at least over a sufficient range of energy above their appearance potentials. The central bond breaks readily to give the substituted and unsubstituted benzoyl ions which only decompose by loss of CO about 4 eV above their appearance potentials (Fig. 1). Only for a few substituents (e.g. *m*-NO₂, *m*-CF₃) were other ions formed to any significant extent.

This simple, well-defined behaviour makes the benzils an ideal system for the study of substituent effects in mass spectra, and many of the problems encountered in the interpretation of earlier work⁹ were not evident in this study.

Fig. 1. Fragmentation Pattern of Benzils.



CHAPTER 2GENERAL PRINCIPLES OF MASS SPECTROMETRY2.1 INSTRUMENTAL FACTORS

The general principles¹⁰ of the double-focussing mass spectrometer (A.E.I. MS902) used in this work must be understood before the relationship between a mass spectrum and the molecular rate processes occurring after ionization can be fully appreciated. This section describes some of the instrumental factors which have an important bearing on this relationship; fuller accounts have been given recently in the literature^{11,12,18}.

2.1.1 Ion Flight Path

A double-focussing mass spectrometer consists of an ion source, an electrostatic energy analyser, a magnetic mass analyser, and an ion detector, which are all separated by short field-free regions in the flight path (Fig. 2). Ions formed by electron impact in the source may be withdrawn by a small repeller voltage to enter a short accelerating region where they are accelerated from thermal energies to kinetic energies up to 8 kV (Fig. 3). Because the high accelerating voltage penetrates the ion source slightly, the efficiency of ion extraction is not impaired greatly if the repeller plate is shorted to the ion block. The average time between initial ion formation and acceleration is called the ion source residence time, which for sources of this Nier-type design is about 1-2 μsec ^{13,14}.

After acceleration the ions travel through the first field-free region (15.4 cm) before entering the cylindrical 90°

Fig. 2. Ion Flight Path

Flight Region	Ion Flight Distance (cm)	Type of Ion Formed
Ion Source	_____	Fragment Ions
	0.5	Background
Ion Accelerating Plates	_____	
First Drift Region	15.4	Defocussed Metastable Ions

Electrostatic Analyser	60.8	Background

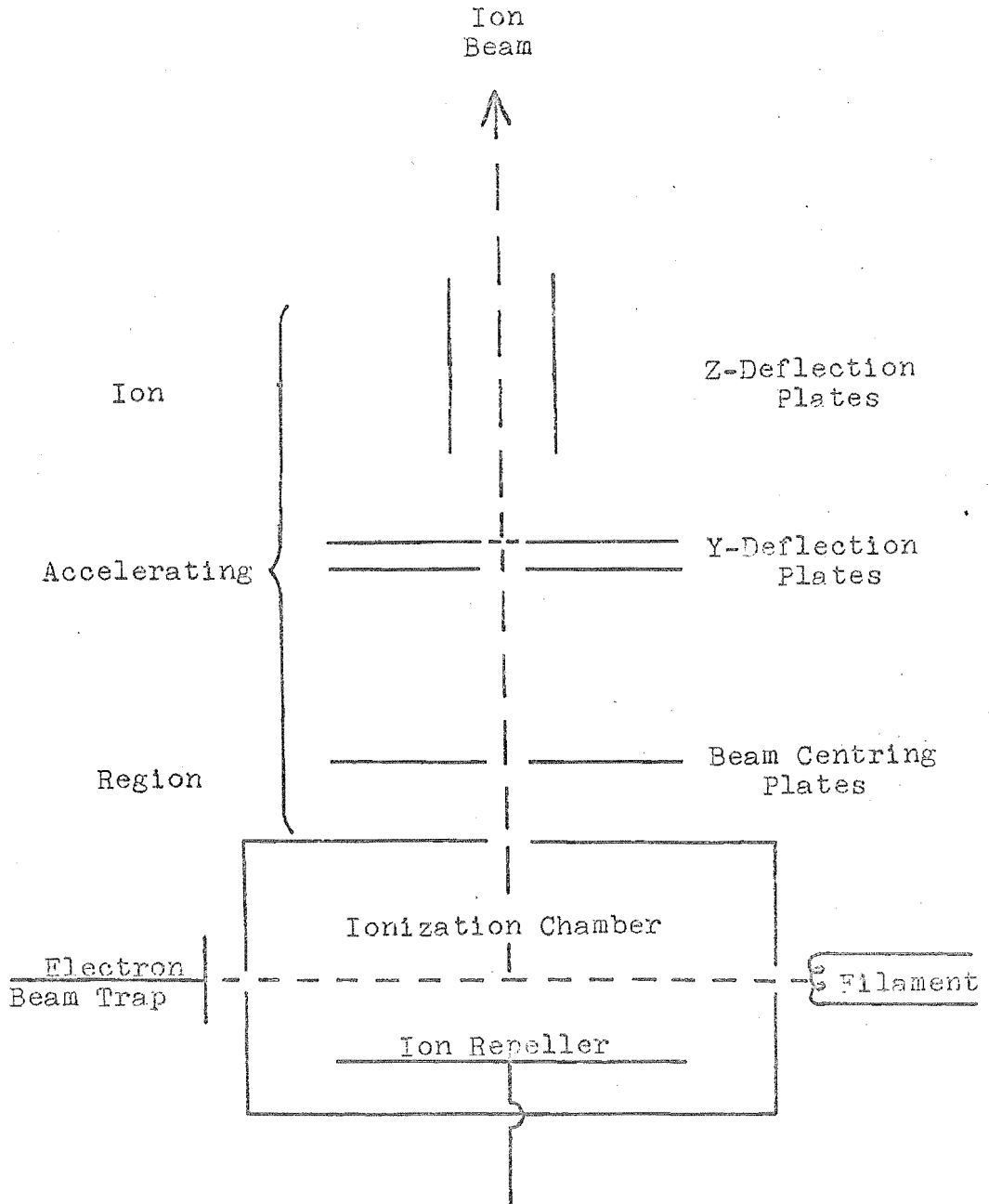
Second Drift Region	54.6	Normal Metastable Ions

Mass Analyser	47.9	Background

Third Drift Region	21.9	Molecule-ions

Ion Detector	_____	

Fig. 3. Ion Source



electrostatic energy analyser (60.8 cm), which transmits only those ions with kinetic energies differing from the desired value by less than $\pm 0.66\%$. The energy-focussed ion beam then passes down the second field-free region (54.6 cm) and enters the 90° magnetic mass analyser (47.9 cm) which separates the ions according to their mass-to-charge (m/e) ratios. The mass-separated ions then strike the collector dynode of the electron multiplier ion detector, or alternatively the Faraday-cup collector, after travelling through a third field-free region (21.9 cm).

2.1.2 Flight Times and Types of Ion Observed

The flight velocity of the accelerated ions is given by

$$v = 1.389 (Ve/m)^{\frac{1}{2}} \text{ cm}/\mu\text{sec} \quad (1)$$

where V is the ion accelerating potential (volt) and m/e is the ion mass/charge ratio (a.m.u.). Since the total flight path from source to collector is 201.1 cm, the total time between formation and detection of the ions may be 15-30 μsec (for the usual range of m/e values of organic ions at 8 kV accelerating voltage). During this time the ions may decompose, and it is possible to experimentally differentiate between ions formed in the source which do not decompose during their flight time (i.e. the normal molecule-ions and fragment ions observed in a mass spectrum), and those which are formed in either of the first two field-free regions of the flight path (i.e. the so-called "metastable" ions^{15,16}).

2.1.3 Metastable Ions

Metastable ions are distinguished from the normal ions only by the dissociative lifetimes of their precursors, which span the narrow range of ion flight times required to reach

the field-free regions (e.g. 5-10 μ sec and 15-20 μ sec respectively).

Two types of metastable ions may be observed in a double-focussing instrument. These correspond to ions formed in the different field-free regions, and are distinguished by the methods used to detect them. Firstly the "normal" metastable ions are those ions formed in the second field-free region which do not decompose before leaving the magnetic analyser. They are observed as weak diffuse peaks in the mass spectrum; their position on the mass scale (m^*) is related to the masses of the precursor (m_1) and daughter (m_2) ions of the "metastable transition" by

$$m^* = m_2^2 / m_1 \quad (2)$$

The metastable ion is actually the daughter ion of the metastable transition, i.e. an ion which is accelerated and energy-analysed as $m/e = m_1$, but is mass-analysed as $m/e = m_2$.

The second type of metastable ion - commonly called "defocussed" metastables - are ions, formed in the first field-free region, which again do not decompose before leaving the magnetic analyser. These can be detected by either of the "defocussing" methods^{17,18} which unambiguously determine all the precursors from which a daughter ion is formed by such metastable transitions.

Ions which are formed in any other regions of the flight path (e.g. during acceleration, energy focussing, or mass analysis) are generally lost from the ion beam although they may contribute to the background¹². Those which decompose after leaving the magnetic analyser, but before striking the collector, are detected simply as the original mass-analysed ion.

2.2 THEORETICAL ASPECTS

Several excellent reviews of the ionization and dissociation processes occurring in a mass spectrometer are available^{11,19-27}, so only a brief description of the main points relevant to this study will be given here.

2.2.1 Ionization Processes

Ionization by electron impact is an example of an inelastic collision and may occur by two general processes - direct ionization and auto-ionization. Auto-ionization refers to multiple-electron excitation of the molecule to an excited metastable state, which then ionizes by spontaneous loss of an electron to form the molecule-ion, usually in an excited state. Direct ionization can be considered^{22,28} as a limiting case of this process, where the lifetime of the excited metastable state of the molecule is of the same order as that for the collision process (i.e. 10^{-16} sec).

Although auto-ionization contributes significantly to the total ionization observed for small molecules (e.g. 90% for H_2 ²⁹), it is expected to be much less important for large molecules. The density of internal energy levels is so high, and the breakdown of selection rules for ionization²² so much more likely in large molecules, that their excited electronic states are unlikely to be metastable with respect to ionization. Direct ionization is a "vertical" transition leading to the formation of molecule-ions which may be in rotationally, vibrationally, and electronically excited states. The nature of these initially formed ionic states will be governed by the transition probabilities from the populated states of the molecule to the accessible states of the ion, and will be determined to a good approximation by the

appropriate Franck-Condon factors as in optical spectroscopy²¹. The two ionization processes obey different threshold laws; because these laws are of crucial importance in analysing ionization efficiency curves³⁰, it is necessary to decide which type of ionization is occurring.

2.2.2 Decay Processes

The decay of the initially prepared states of the molecule-ions may occur by two general processes involving either radiative or radiationless transitions - 'decay' here refers to spontaneous transitions which are irreversible on the time scale of the experiment, as discussed by Berry²⁹. Radiative transitions generally have lifetimes of 10^{-9} - 10^{-7} sec (for "allowed" transitions) up to 10^{-6} - 10^{-3} sec (for "forbidden" transitions). These are generally longer than the lifetimes of the slowest radiationless transitions in polyatomic molecules and so may be ignored.

Radiationless transitions³¹ may be conveniently separated into two categories; those which lead to some type of reaction (e.g. dissociation, isomerization), and those which result in electronic relaxation (e.g. internal conversion, intersystem crossing). Electronic relaxation processes for polyatomic molecules are likely to have lifetimes not much longer than the period of a vibration (10^{-13} - 10^{-14} sec), whereas decomposition reactions of molecule-ions can have much longer lifetimes. Excess energy, which is transferred to excited electronic states of the molecule-ion by the initial ionization process, will therefore be rapidly converted by electronic relaxation processes to excited vibrational and rotational energy in the ground electronic state, or some set

of "isolated" electronic states from which relaxation is comparatively slow.

The internal energy of the molecule-ion is thus assumed to become randomly distributed throughout the vibrational and rotational degrees of freedom of the ground or isolated states in a time which is short compared with the lifetimes of the decomposition processes leading to the formation of the mass spectrum. The assumption that these decompositions could be considered as rate processes similar to those occurring in ordinary chemical reactions led to the formulation of the quasi-equilibrium theory of mass spectra³², which is currently accepted as a sound description of mass spectral reactions^{23,33}.

2.2.3 Quasi-Equilibrium Theory

(i) Basic Assumptions

The first principal assumption of the quasi-equilibrium theory is that the molecule-ions may decompose by various paths through different activated complexes, possibly from different electronic states, and the fragment ions so formed may themselves decompose in the same way if they possess sufficient internal energy. Thus the mass spectrum is considered to be formed by a series of competing consecutive unimolecular decomposition reactions.

The second principle assumption is that the microcanonical ensemble³⁴ describes the distribution of the activated ions which dissociate. This implies that the state of an ion is described completely by its internal energy alone and that any other constants of motion are randomly distributed amongst all their possible values. The assumption is valid if rapid equilibration of the internal energy occurs by electronic

relaxation processes. A corollary of this assumption is that an ion will decompose only when sufficient internal energy has become localised in the degree(s) of freedom associated with the reaction coordinate, so that the rate of a decomposition will depend on the internal energy of the ion.

(ii) Unimolecular Rate Constants

The dependence of the rate constant for unimolecular ion decomposition on internal energy may be derived from any of the unimolecular rate theories (e.g. those due to Slater³⁵, Kassel³⁶, or Marcus^{37,38}), although the quasi-equilibrium assumption leads naturally to the use of Eyring's absolute rate theory³⁹. The general form of the rate constant expression obtained from these statistical mechanical formulations of unimolecular decomposition is given by

$$k(E) = \int_0^{E-E_0} N^\ddagger(E, E_0, \epsilon) d\epsilon / hN(E), \quad E \geq E_0 \quad (3)$$

$$= 0, \quad E < E_0$$

where $N(E)$ is the density-of-states of the decomposing ion containing internal energy E , $N^\ddagger(E, E_0, \epsilon)$ is the density-of-states of the activated complex for the decomposition having a threshold energy E_0 and translational energy ϵ in the reaction coordinate, and h is Planck's constant²³. Since this rate constant expression is an average over all possible rates of passage through the activated complex configuration, it strictly represents a mean lifetime rather than a specific rate.

These derivations ignore quantum tunnelling and interference effects, which recent theoretical studies⁴⁰ suggest may cause the decay of isolated systems to be non-exponential

in certain situations. However, the development of the quantum mechanical formulation of unimolecular decomposition processes is still in its early stages, and the details are too complex to be applied to any but the simplest model systems^{40-42,45}.

Computation of the rate constant function $k(E)$ has been described in detail in a recent review⁴³, and only the general features of these functions relevant to mass spectral ion decompositions will be discussed. The dependence of $k(E)$ on the internal energy is shown schematically in Fig. 4. Below the threshold energy (E_0) the rate constant is zero, but it rises rapidly with increasing energy just above the threshold. At the threshold energy the rate constant has a finite minimum value, $k_{\min}(E_0)$, since the numerator in equation (3) has a minimum value of unity corresponding to a singly degenerate ground state of the activated complex⁴⁴. (More detailed considerations of effects due to the external rotational degrees of freedom suggest⁴⁵ that the minimum rate constant is probably much lower than would be expected from a consideration of only the active internal degrees of freedom.) The existence of a minimum value for the rate constant has important consequences for metastable ions, since these will not be observed if the minimum is greater than about 10^6 sec^{-1} .

All unimolecular decompositions also exhibit a maximum rate constant at high energies which is limited by the time required for the atoms to move through the activated complex configuration - about the period of a vibration for simple bond cleavage reactions ($10^{-13} - 10^{-14} \text{ sec}$). The maximum value is determined by the difference in the density-of-states of the activated complex and the corresponding reactant state,

Fig. 4. Rate Constant Function, $k(E)$.

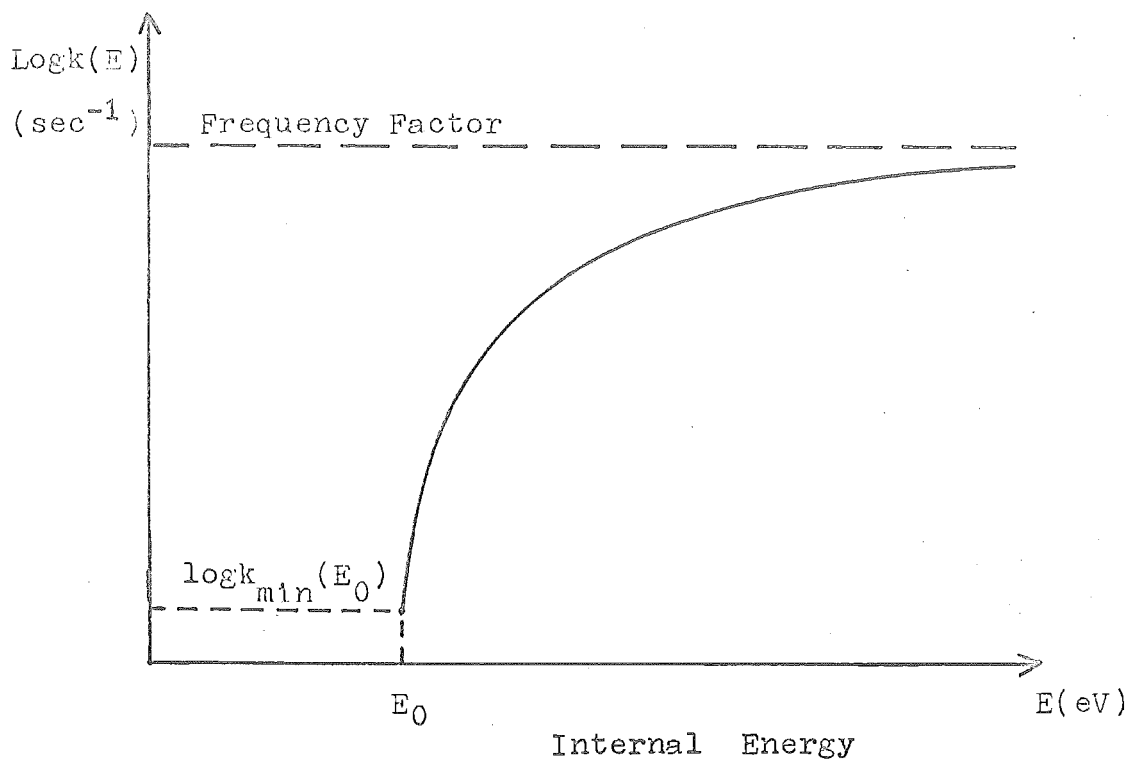
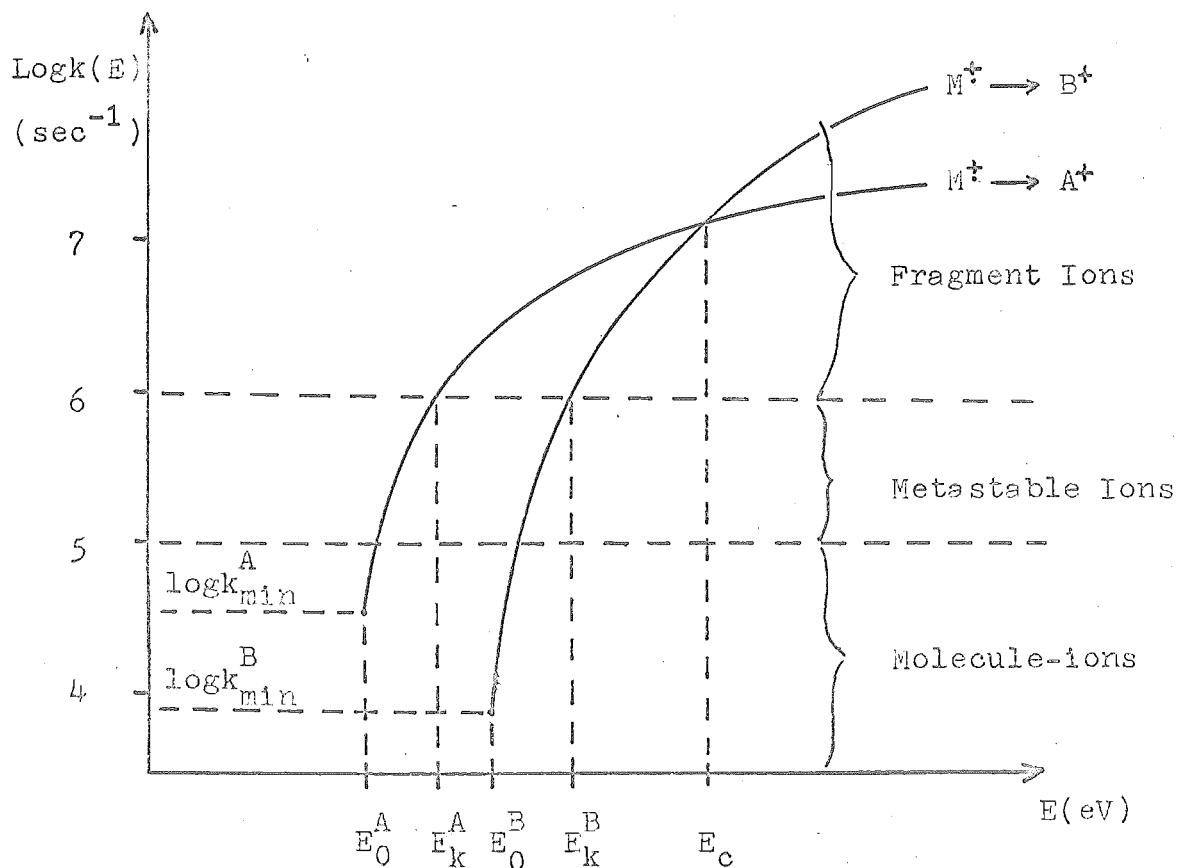


Fig. 5. Kinetic and Competitive Shift Effects.



and is commonly termed the "frequency factor". The general shape of the $k(E)$ function between these limits is primarily determined by the magnitude of the activation energy and the number of active degrees of freedom involved in the reaction. The rise in $k(E)$ with increasing energy is slower for larger activation energies and higher numbers of active degrees of freedom.

(iii) Kinetic and Competitive Shift Effects

The relationship between $k(E)$ and the ion source residence time has a very important bearing on the observed appearance potentials of fragment ions. As Fig. 5 shows, a small excess of internal energy above the activation energy for the decomposition (e.g. E_0^A for $M^\ddagger \rightarrow A^+$) is required to cause $k^A(E)$ to be greater than 10^6 sec^{-1} , the approximate value necessary for decomposition to occur before the ion is ejected from the source. This excess energy, $(E_k^A - E_0^A)$, is termed the "kinetic shift"⁴⁶ and causes the measured appearance potential (AP_m) for the fragment ion (A^+) to be higher than the thermochemical value (AP_t) by approximately $(E_k^A - E_0^A)$; thus

$$AP_t(A^+) = IP(M^\ddagger) + E_0^A \quad (4)$$

$$\text{c.f. } AP_m(A^+) \approx IP(M^\ddagger) + E_k^A. \quad (5)$$

Of course if the minimum rate constant for the decomposition (k_{\min}^A) is greater than 10^6 sec^{-1} , then the kinetic shift will be zero. In this case no metastable ions can be observed for the decomposition, but the reverse argument does not necessarily apply since the metastable ions may simply be too weak to be detected.

When an ion decomposes by competing pathways, a further complication is introduced for all but the lowest energy decomposition. This additional factor is called the "competitive shift"^{8,47} and causes the measured appearance potential(s) for the higher energy decomposition(s) (e.g. $AP_m(B^+)$ for $M^+ \rightarrow B^+$, Fig. 5) to be even higher than expected from the kinetic shift effect; thus

$$AP_m(B^+) > IP(M^+) + E_k^B. \quad (6)$$

This effect arises because the rate constant for the lowest energy decomposition (e.g. $k^A(E)$) is usually substantially greater than the rate constant for the competing decomposition (e.g. $k^B(E)$) at the energy $E = E_k^B$ where B^+ should appear. Hence the proportion of B^+ formed relative to A^+ is so small as to be undetectable until the magnitudes of the competing rate constants become comparable at higher energies. For the situation depicted in Fig. 5, where the higher energy decomposition has a higher frequency factor (causing the $k(E)$ curves to cross), B^+ will appear at an energy somewhere between E_k^B and E_c , where $k^B(E)$ is considerably greater than 10^6 sec^{-1} . In the alternative situation where the $k(E)$ curves do not cross, the size of the competitive shift could be very large indeed. The competitive shift effect will always operate, whether or not the kinetic shift effect is involved, since it depends solely on the relative magnitudes of the rate constants for the competing decompositions.

The major factor influencing the kinetic shift is the activation energy which has a large effect on the minimum rate constant for a decomposition; $k_{\min}(E_0)$ being lower for higher activation energies. The activation energy also affects the

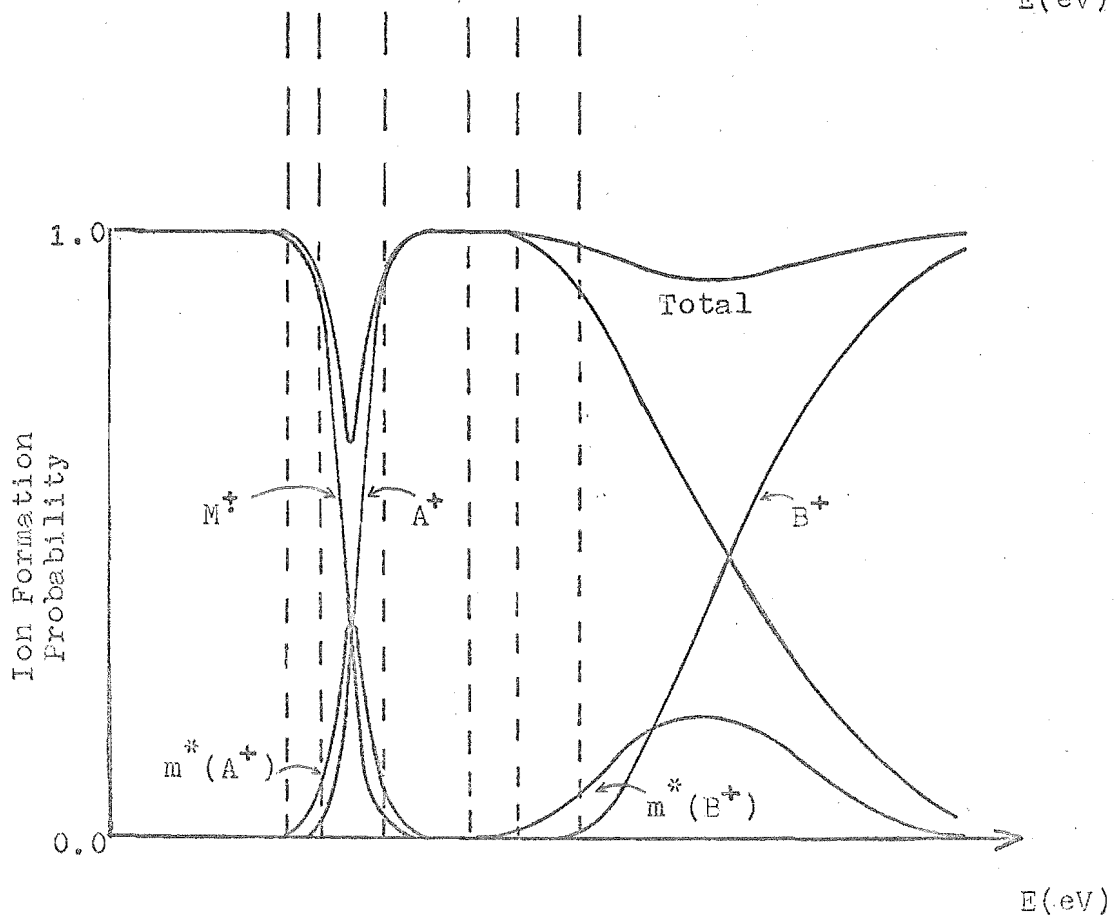
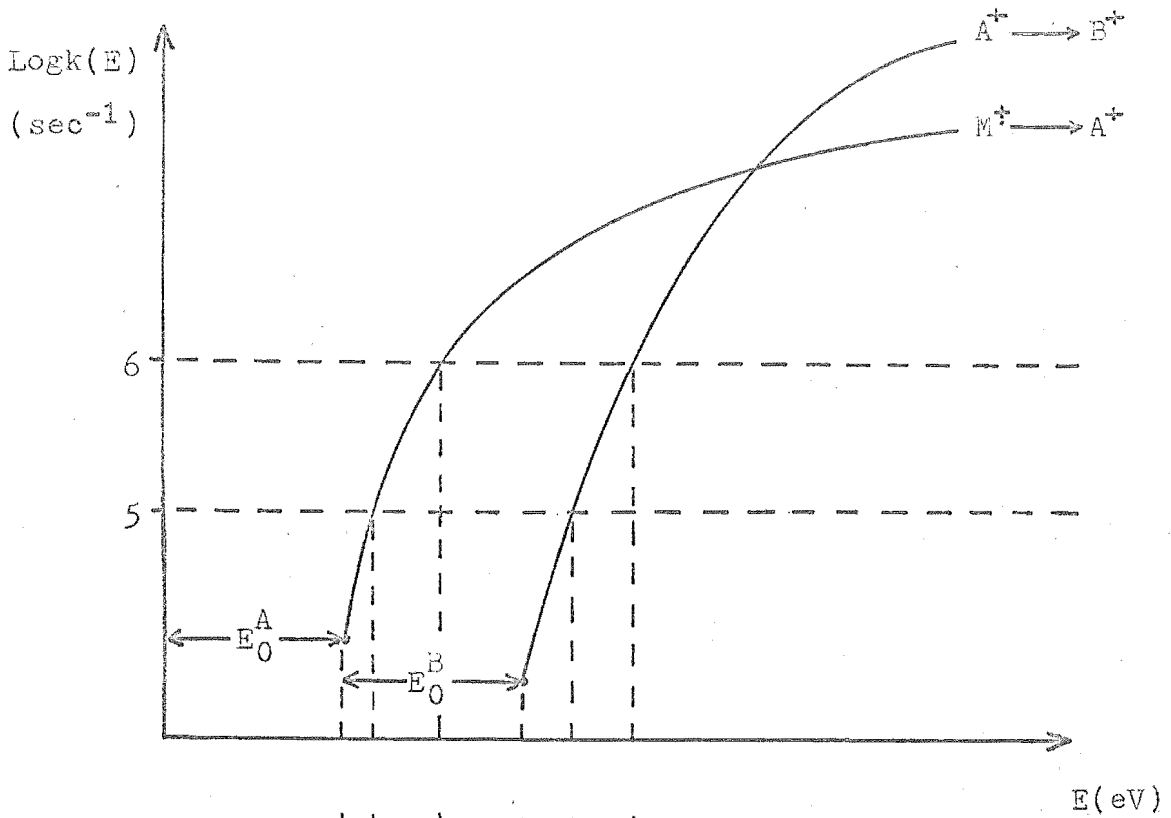
slope of the $k(E)$ curve in such a way as to enhance the first effect. The frequency factor and the number of active degrees of freedom also influence the size of the kinetic shift through their respective effects on the shape of the $k(E)$ curve. The kinetic shift will therefore increase with higher activation energies, lower frequency factors, and more active degrees of freedom for the decomposition. Similar considerations apply to the competitive shift, although here it is the relative magnitudes of these factors which are important.

(iv) Breakdown Graphs

When the fragmentation scheme for a molecule-ion and the corresponding rate constant functions are known, a "breakdown graph" can be calculated from an analysis of the first-order kinetic equations, if allowance is made for the source residence and ion flight times⁴⁸. The breakdown graphs give the relative probabilities of the formation of the various ions observed in a mass spectrum as a function of the internal energy of the molecule-ion; they are one of the most useful applications of the quasi-equilibrium theory.

An example of the breakdown graph obtained for the consecutive decompositions $M^{\dagger} \rightarrow A^{\dagger} \rightarrow B^{\dagger}$ is shown in Fig. 6. The $k(E)$ curves, which are also shown, were calculated from models using parameters corresponding to decompositions of aromatic molecules, so that the general features of the breakdown graph would be appropriate to this work. A notable feature is the wide range of internal energies of the molecule-ion over which metastable ions are observed for the secondary decomposition ($A^{\dagger} \rightarrow B^{\dagger}$), compared with the range for the primary decomposition ($M^{\dagger} \rightarrow A^{\dagger}$). This is a direct consequence of the "fluctuation effect"^{66,67} on the partitioning

Fig. 6. Breakdown Graph ($M^+ \rightarrow A^+ \rightarrow B^+$).



of the excess internal energy of the precursor ion between the decomposition products, which causes A^+ , for example, to have a range of internal energies for a particular value of E . For the same reason the initial rise in the breakdown curve for a secondary fragment ion at the threshold is much slower than that observed for a primary fragment ion. This is why much longer tails are observed on the ionization efficiency curves of secondary fragment ions, making it more difficult to measure their appearance potentials accurately. Another interesting feature of Fig. 6 is the substantial loss of ions occurring at internal energies corresponding to metastable ion formation, as indicated by the total ion formation probability curve, which is simply the sum of the individual breakdown curves. These so-called "missing metastable" ions⁴⁹ are those which form in non-field-free regions of the flight path and are consequently lost from the ion beam.

The relationship between breakdown graphs and ionization efficiency curves is entirely dependent on the threshold laws for ionization. There is some evidence⁵⁰ that the probability of direct ionization varies as the first power of the excess energy of the electron, at least near the threshold. The general theoretical result⁵¹ is that the probability of ionization is given by

$$I(E) = \int_0^E \delta(E-E_c) dE^n \quad (7)$$

where $\delta(E-E_c)$ is a delta function centred on the threshold energy E_c . Thus for $n > 1$,

$$I(E) = (E-E_c)^{n-1}/(n-1)!, \quad E > E_c \quad (8)$$

where n is the number of electrons leaving the collision complex (i.e. $n = 1$ for auto-ionization, and $n = 2$ for direct ionization). Following Morrison's analysis⁵², the second derivative of the ionization efficiency curve is proportional to the sum of the transition probabilities for the formation of the ion convoluted with the reversed electron energy distribution, assuming that only direct ionization is important. When the effect of the spread in electron energies is removed by deconvolution⁵³, the relative amplitudes of the second derivative ionization efficiency (SDIE) curves give the relative probabilities of formation of the ions as a function of the energy transferred by the ionization process. If these deconvoluted SDIE curves are normalised (relative to their sum), they are equivalent to breakdown graphs except for the definition of the energy axis. Since breakdown graphs are calculated as a function of the internal energy of the molecule-ion, they are equivalent to normalised SDIE curves measured at 0°K ; for other temperatures the internal thermal energy of the molecule which will be transferred to the molecule-ion on ionization must be taken into account⁵⁴.

This problem has been discussed by Vestal⁵⁵ who showed that to a fair approximation the thermal energy distribution in the molecule-ion is similar to that in the molecule, but is shifted to higher energies by an amount comparable to the average thermal energy. Using this approximation a modified breakdown graph may be calculated as a function of the transferred energy by convoluting the theoretical breakdown graph with the thermal energy distribution of the molecule.

(v) Ion Intensities

Relative ion intensities are readily obtained by simply measuring the relative peak heights in a mass spectrum. They depend on a number of factors, including ionization cross-sections and threshold laws, and the rates of formation and decomposition of the ions - all molecular properties - as well as ion flight times and ion source conditions (including temperature), which are instrument dependent. Mass spectra therefore differ from other types of spectra which generally measure well-defined physical properties of molecules. Because of this much current research effort is directed towards finding improved methods of analysing mass spectral data, especially to provide more reliable information about the structures and properties of the ions which are formed.

According to the quasi-equilibrium theory, the relative ion intensities in a mass spectrum (at any particular ionizing voltage) may be calculated from the breakdown graph by integrating the individual breakdown curves for each ion over the internal energy distribution function of the molecule-ion. This gives the relative ion intensities with the effect of the electron energy spread removed (i.e. a deconvoluted mass spectrum);

$$I_j(V) = \int_0^V R_j(E) P(E,V) dE \quad (9)$$

where $I_j(V)$ is the deconvoluted relative intensity, $R_j(E)$ is the breakdown curve for the j^{th} ion, and $P(E,V)$ is the internal energy distribution function of the molecule-ion for the particular ionizing voltage V . The function

$$P(E,V) = \sigma(E) (V-E), \quad E < V \quad (10)$$

is often called the "excess energy transfer function", and it depends on both the transition probability function for ionization, $\sigma(E)$, and the ionization threshold law, so that it will change with both molecular structure and the ionizing voltage (for direct ionization). $P(E,V)$ can be obtained experimentally from the total SDIE curve assuming that the same threshold law holds over a sufficient range of energy^{65,70}.

2.2.4 Comparison with Conventional Chemical Reactions

The essential difference between reactions in a mass spectrometer and conventional chemical reactions should be stressed. In the latter, the reacting species are being continuously energized and de-energized by molecular collisions, so that the temperature can be used to describe the distribution of the reactants and activated complexes among their accessible states. This situation does not apply to the rate processes occurring in a mass spectrometer where there are few molecular collisions, and the molecule-ions are energized solely by the initial ionization process. Hence the overall rate constant expressions are quite different, even though the spontaneous dissociation processes occurring in each case are described by the same theory (e.g. RRKM theory^{56,57} in unimolecular gas-phase kinetics). These differences must be borne in mind when considering apparent similarities between mass spectral and conventional chemical reactions.

Although a complete understanding of the factors determining the mass spectrum of a molecule is difficult to attain, there are several reasons for attempting to do this. In many respects the situation in a mass spectrometer, with isolated reactant species, is much simpler than that pertaining

to reactions under conventional conditions, where higher-order rate laws, molecular interactions (including solvent effects), and diffusion effects must also be considered. Since the theories concerning unimolecular decay processes are more highly developed, a more direct comparison between theory and experiment is possible for mass spectra than for many other types of chemical reaction. The complicating factor in mass spectral reactions is the comparatively wide range of energies involved, leading to a corresponding increase in the number of decay processes which can occur.

2.3 SUBSTITUENT EFFECTS

Following McLafferty's original investigation of substituent effects in the mass spectra of aromatic molecules⁵⁸, research in this field has been very active - particularly over the last five years - and several good reviews are now available^{6,11,24,26,59}. However, it is only recently that a fuller appreciation of the various factors which may influence ion intensities has become apparent in the literature. There has been an increasing awareness and application, at least qualitatively^{24,27}, of the quasi-equilibrium theory to the interpretation of mass spectra, and some recent papers have considerably clarified the effect of substituents on ion intensities^{7,8,60}.

Early investigations⁶¹ of the often quite marked variations in ion intensities obtained from aromatic compounds with different substituents, suggested that correlations based on the Hammett equation, used extensively for the rates and equilibria of solution reactions, might also apply to mass spectra. In fact fair correlations between logarithmic

intensity ratios and Hammett sigma constants (σ) were observed for some aromatic compounds⁶. Although such correlations were used as evidence for the structures of ions, and even transition states, in some important types of mass spectral reactions (by analogy with conventional substituent effects), recent work has severely criticised this approach on both empirical⁶² and theoretical⁶³ grounds.

The remainder of this section reviews the factors contributing to substituent effects in mass spectra, and is intended as a background to discussion of the effects observed in this study.

2.3.1 Substituent Effects on Decomposition Pathways

The most obvious effect which changing a substituent in a molecule can have on its mass spectrum is the introduction of new, or different, pathways for ion decompositions. In the most extreme case competitive loss of part, or all, of the substituent may occur more readily than the decomposition(s) whose substituent effect is being studied. A more common situation arises when competing decompositions of the ions are also affected by the substituent, often to varying degrees depending on the nature of the substituent. These irregular substituent effects can only be avoided by choosing substrates which are not prone to undergo alternative competing decompositions. Many of the problems encountered in measuring regular substituent effects in mass spectra arise because such compounds are hard to find.

2.3.2 Substituent Effects on Internal Energy and Rate Constant Functions

When only regular effects of substituents on a particular decomposition pathway are operating, the relative ion intensities obtained will reflect the internal energy distribution functions $p(E)$ and the rate constant functions $k(E)$ for all the decomposing ions, and the effects of substituents on these functions will determine the observed substituent effects on ion intensities. For example the intensity of a primary fragment ion (A^+) will depend on:

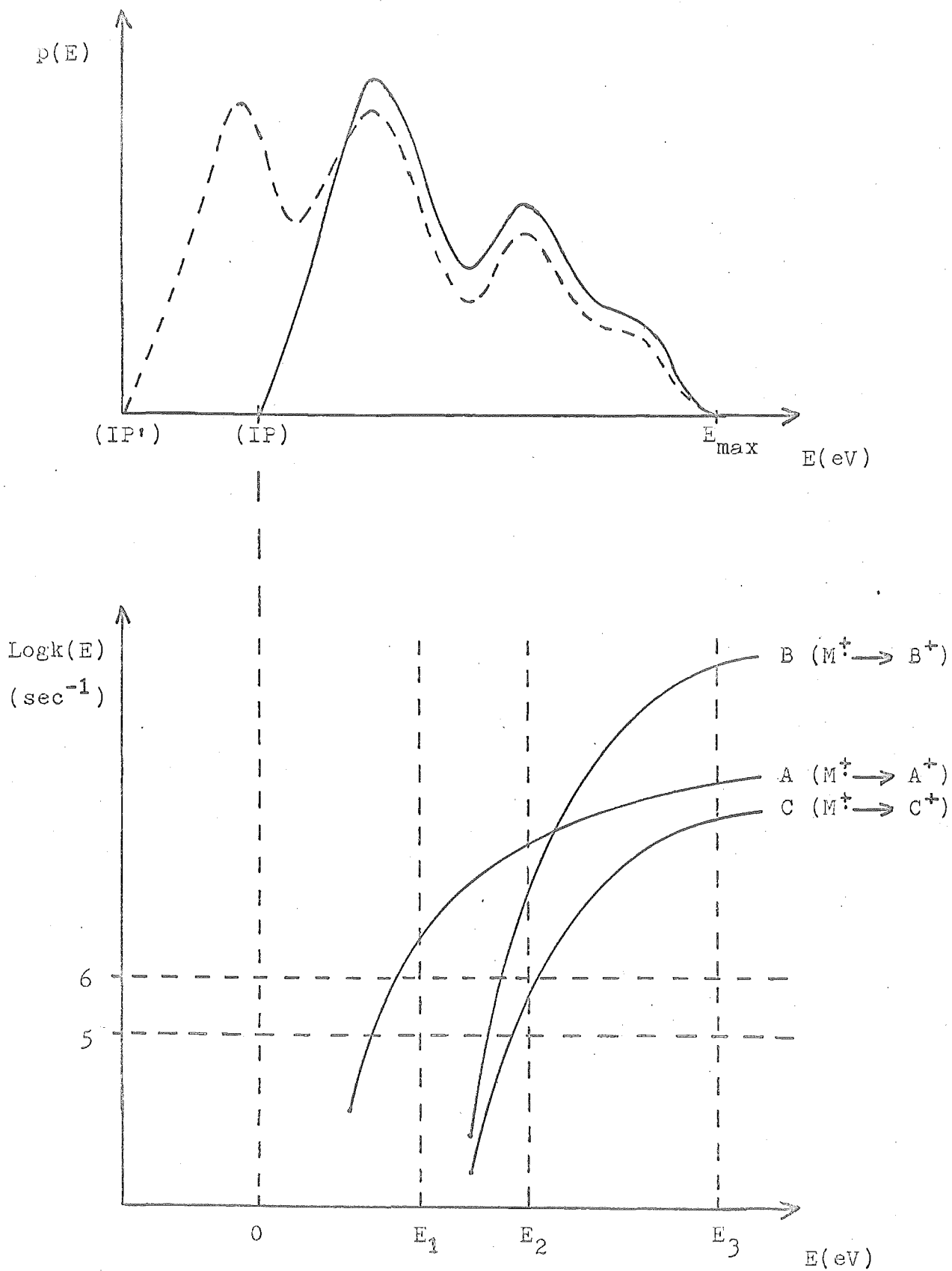
- 1) $p(E)$ function of the molecule-ion (M^+),
- 2) $k(E)$ function for the formation of A^+ ,
- 3) $k(E)$ functions for all the competing decompositions of M^+ ,
- 4) $p(E)$ function of A^+ ,
- 5) $k(E)$ functions for all the decompositions of A^+ .

The manner in which ion intensities depend on the relationship between the internal energy distribution function of a decomposing ion and its corresponding rate constant functions is shown in Fig. 7, where a reasonable $p(E)$ function and logarithmic $k(E)$ curves are plotted against the internal energy E . For the molecule-ion the $p(E)$ function is given by the excess energy transfer function $P(E,V)$ whose lower limit is determined by the ionization potential, and the upper limit (E_{\max}) by the ionizing voltage.

(i) Internal Energy Distribution Functions, $p(E)$

Since ion intensities are determined by the breakdown curves for each ion integrated over the excess energy transfer function, any substituent effect which alters the relationship between $P(E,V)$ and the breakdown curves will modify the corresponding ion intensities.

Fig. 7. Internal Energy Distribution and Rate Constant Functions.



This can happen when the ionization potential is lowered relative to the $k(E)$ curves (as illustrated by the dotted function in Fig. 7), causing a large increase in the relative intensity of M^+ , since a higher proportion of molecule-ions now have insufficient energy to decompose. The relative intensities of the fragment ions (e.g. A^+ , B^+ , C^+ in Fig. 7) are also changed in this situation because the values of $P(E,V)$ over which the breakdown curves for these ions have to be integrated, are now different to those of the original $p(E)$ function.

Substituents may also change the shape of the $p(E)$ function of the molecule-ion through their influence on ionization transition probabilities. Although experimental data concerning this is difficult to obtain, some possible effects are indicated by studies of the photoelectron spectra of substituted benzenes⁶⁴. (The transition probabilities observed in photoelectron spectra are not the same as those obtained in electron impact⁶⁵, because different threshold laws are involved and negligible auto-ionization occurs in photoelectron spectra.) The energy bands observed in these spectra may be broadened or split by the electronic interaction of some substituents with certain π - and σ -molecular orbitals of the aromatic ring; furthermore the degree of splitting seems to depend on the extent of the conjugative interaction between the substituent and the ring. Substituents with lone-pairs can also cause the appearance of new characteristic bands which seem to be due to ionization of these non-bonding electrons.

Since the $p(E)$ functions of primary fragment ions are used in calculating the breakdown curves of the secondary

fragment ions formed from them, the possible effects of substituents on the $p(E)$ functions of fragment ions must also be considered. A fragment ion acquires its internal energy from the partitioning of the excess internal energy $(E-E_0)$ of the precursor ion between the products of the decomposition. Under the quasi-equilibrium hypothesis this partitioning⁶⁶, or "energy fluctuation effect"⁶⁷, is governed by the respective density-of-states functions of the decomposition products. For example, if M^{\dagger} dissociates to give a charged fragment A^+ and a neutral radical $B\cdot$, then the probability that an energy between ϵ and $\epsilon+d\epsilon$ remains as internal energy of A^+ , for a total internal energy E in M^{\dagger} , is given by

$$p(E, \epsilon) d\epsilon = \frac{N_A(\epsilon) \cdot N_B(E-E_0^A - \epsilon) d\epsilon}{\int_0^{E-E_0^A} N_A(\epsilon) \cdot N_B(E-E_0^A - \epsilon) d\epsilon} \quad (11)$$

where N_A and N_B are the density-of-states functions for A^+ and $B\cdot$ respectively, and E_0^A is the activation energy for the formation of A^+ . For each value of E there is thus a distribution of internal energies in a fragment ion ranging from zero to $E-E_0$, and substituents may subtly alter these $p(E)$ functions through their influence on the relevant density-of-states functions.

A further factor which contributes to the form of the excess energy transfer function, and thus influences relative ion intensities, is the ionizing voltage. Referring again to Fig. 7, if E_{\max} were to take the values E_1 , E_2 and E_3 corresponding to different ionizing voltages, then the relative intensities of the ions M^{\dagger} , A^+ , B^+ and C^+ would change markedly, owing to the different $P(E, V)$ functions over

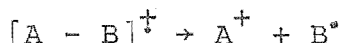
which their respective breakdown curves would have to be integrated. For $E_{\max} = E_1$ only M^+ and A^+ would be formed, whereas for $E_{\max} = E_2$ a small amount of B^+ (c.f. A^+) would also be observed, but probably no C^+ since its rate constant would be too slow to compete effectively at energies up to E_2 . For $E_{\max} = E_3$ the amount of B^+ relative to A^+ would be greater because of its much higher rate constant over a considerable portion of the corresponding $P(E,V)$ function, and C^+ would also be observed but with a much smaller intensity than A^+ . Of course the relative M^+ intensity also decreases with increasing E_{\max} since an increasing proportion of molecules have sufficient energy to decompose. It is therefore important to follow the variation in ion intensities with ionizing voltage, so that this effect can at least be recognized and possibly allowed for, although the advent of new decompositions at higher energies often makes such allowance impracticable.

(ii) Rate Constant Functions, $k(E)$

Substituents alter the rate constant functions mainly through their effect on the activation energy and frequency factor for a decomposition. They may also exert a secondary influence on $k(E)$ curves by changing the number of active internal degrees of freedom, but for large polyatomic ions this effect is usually minor. A substituent which increases only the activation energy E_0 , would cause curve A to change to curve C for example (Fig. 7), where the minimum rate constant and the curvature of the $k(E)$ function are both decreased. Conversely if a substituent increases only the frequency factor, then curve C would change to curve B, this

time causing only a small increase in the rate constant near the threshold but a large increase at higher energies. Thus a change in activation energy will modify breakdown curves strongly near their threshold energies, whereas a change in frequency factor will have a significant effect only at high energies; this combination of effects can lead to large variations in relative ion intensities with changing ionizing voltage.

The activation energy for the simple cleavage reaction of a molecule-ion



is equal to the bond dissociation energy of the ion as given by either of the following thermochemical relationships^{25,68}

$$E_0(A^+) = \Delta H_f(A^+) + \Delta H_f(B^{\bullet}) - \Delta H_f([AB]^{\ddagger}) \quad (12)$$

$$E_0(A^+) = IP(A^{\bullet}) + D(A-B) - IP(AB) \quad (13)$$

where ΔH_f is the enthalpy of formation and D is the bond dissociation energy. (These relationships assume that the activation energy for the reverse reaction is negligible, which is reasonable since most ion-radical or ion-molecule recombination reactions have very low threshold energies.) Substituents can therefore be considered to alter activation energies by changing the ionization potentials of the molecule-ion and the charged fragment, or by changing the bond dissociation energy of the neutral molecule. The manner in which particular substituents are likely to affect these quantities, especially the bond strength term, might be predictable from the extensive knowledge of substituent effects

available for ordinary reactions. However, unusual effects may operate for the ionization potential terms, since the electronic states involved in the fragmentation process might be different from those in the ionization processes - a situation not usually met in chemical reactions of systems at thermal equilibrium. A further obvious difference concerns the multiplicities of the electronic states involved, which are often doublet (or quartet) states for many of the ions observed in mass spectra compared with the singlet (or triplet) states usually involved in ordinary chemical reactions. Little is known about the differences these factors might make to the extensively studied pattern of substituent effects observed in solution⁴ and gas-phase⁵ reactions.

Since frequency factors depend on the structural differences (e.g. in vibrational and rotational states) between the reactant ion and the activated complex, large changes in frequency factors are expected only for different types of decomposition; e.g. simple dissociations compared with rearrangements. Direct cleavage reactions generally occur via a "loose" activated complex⁶⁹ in which some vibrational degrees of freedom (e.g. torsional or bending modes) become "loosened" to rotational degrees of freedom in passing to the activated complex. Since rotations have a much higher density-of-states than vibrations, the frequency factor is larger than would otherwise be expected. Conversely rearrangement reactions generally have "tight" activated complexes with lower frequency factors. In such reactions some rotational degrees of freedom are usually constrained to become weak vibrations in the activated complex because of the incipient bond formation which occurs between the atoms or groups

participating in the rearrangement. Substituents will therefore have a marked effect on frequency factors only if they cause the number of free rotors to change in passing from the reactant ion to the activated complex⁸. This will occur, for example, when a substituent acting as a free rotor in the decomposing ion becomes constrained to undergo torsional vibrations in the activated complex, because of increased conjugation between the substituent and the aromatic ring. Furthermore a substituent may affect other free rotors similarly, since conjugative effects can be transmitted across the aromatic system.

C H A P T E R 3EXPERIMENTAL3.1 PREPARATION AND PURIFICATION OF COMPOUNDS

Melting points are uncorrected. Infrared spectra were recorded on a Shimadzu IR27G spectrophotometer; n.m.r. spectra on a Varian A60 spectrometer (CCl₄ solvent and TMS internal standard); high resolution mass spectra on an A.E.I. MS902 spectrometer (70 eV, resolving power 10,000). Analytical g.l.c. analyses were performed on a Varian Aerograph 1200 Hi Fi III using a SE-30 column.

3.1.1 Reagents and Solvents

Thionyl chloride (Riedel de Haen) was distilled from quinoline and the fraction boiling at 76-84° was redistilled from raw linseed oil⁷²; it had b.p. 75.5-76° (lit.⁷¹ 78.8°/746 mm).

Benzyl chloride (B.D.H. Lab Reagent) was dried over calcium chloride and distilled, b.p. 73-74°/11 mm (lit.⁷¹ 179°).

Diethyl ether was distilled from conc. sulphuric acid and stored over sodium wire⁷³.

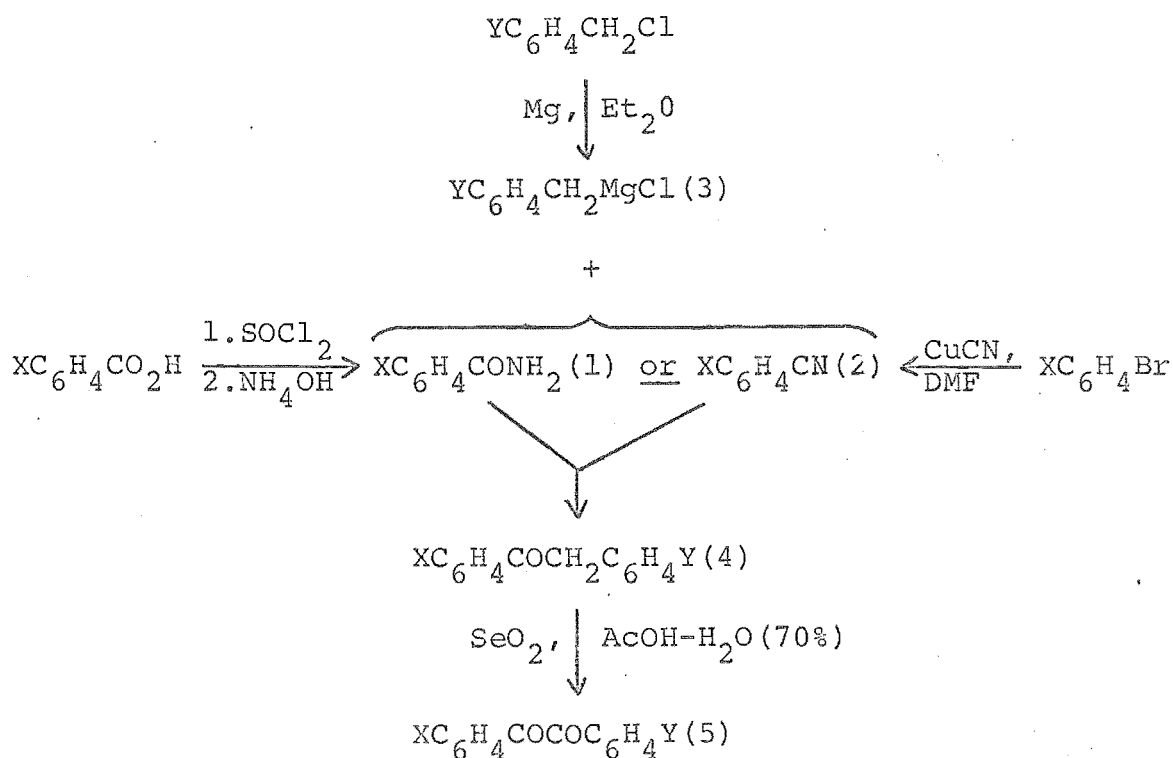
Benzene was distilled off phosphorus pentoxide and stored over sodium wire.

3.1.2 Deoxybenzoins (Scheme 1)

The mono-substituted deoxybenzoins (4) were usually prepared by reacting the substituted benzamide (1), or preferably the benzonitrile (2), with an ether solution of benzylmagnesium chloride (3) according to the method of Jenkins⁷⁴, to give the benzoyl-substituted deoxybenzoin (ring position of the substituent (X) is denoted by *meta* or *para*).

Alternatively the substituted benzylmagnesium chloride was reacted with benzonitrile to give the benzyl-substituted deoxybenzoin (ring position of the substituent (Y) is denoted by *meta*' or *para*'). Good yields were obtained only when the Grignard reagent was prepared carefully to avoid formation of the bibenzyl coupling product; the deoxybenzoin were not purified before being oxidized to the benzils (5). For some substituents alternative procedures were necessary, and these involved the modification of substituents on the deoxybenzoin or benzil substrates.

Scheme 1



(i) Preparation of Benzylmagnesium Chloride

Magnesium turnings (B.D.H., "for Grignard") (4.86g, 0.20 mol) were placed in a 3-necked round bottom flask (250 ml) fitted with a strong mechanical stirrer, dropping funnel, and a double-surface condenser, which was connected via a T-joint adapter to allow solvents to be removed, or reagents to be

added, while the system was under reflux. A dry nitrogen atmosphere was maintained at all times. After flame-drying the glass-ware and magnesium turnings under a stream of nitrogen, sodium dried ether (50 ml) was placed in the flask and cooled to 0°. A solution of benzyl chloride (23 ml, 0.20 mol) in ether (50 ml) was added dropwise while stirring continuously, and the reaction usually started within a few minutes. The temperature was kept at 0° during the addition of the benzyl chloride and then allowed to rise to room temperature. G.l.c. analysis of a hydrolysed sample of the dark-green benzyl-magnesium chloride solution showed that this procedure gave only a few percent of bibenzyl.

(ii) Preparative Methods

(a) *m*-Methyldeoxybenzoin:

m-Toluic acid (B.D.H.; 19.0g, 0.130 mol) was treated with thionyl chloride (12.5 ml) overnight to give the acid chloride, which was added to a mixture of ammonia (0.880; 50 ml) and ice (50 g). Crystallization from ether gave *m*-toluamide as white needles (13.1 g, 70%), m.p. 94-96° (lit.⁷¹ 97°).

m-Toluamide (6.76 g, 50 mmol) was slowly added to a refluxing ether solution of benzylmagnesium chloride (0.20 mol) with stirring. The mixture was refluxed for two days, hydrolysed with dil. sulphuric acid, and the organic layer was separated. After washing with water, aqueous sodium carbonate and water, the ether solution was dried (MgSO₄) and the solvent and toluene removed to give *m*-methyldeoxybenzoin as an orange solid (9.7 g, 90% crude), n.m.r. δ 7.69 (m, 2H); 7.14 (m, 2H); 7.13 (s, 5H); 4.05 (s, 2H); 2.17 (s, 3H).

(b) *m*-Methoxydeoxybenzoin:

m-Methoxybenzoic acid (Light; 88.5 g, 0.582 mol) was treated with thionyl chloride (50 ml) in dry benzene (100 ml) under reflux, and then amidated to give *m*-methoxybenzamide, which was crystallized from water as plates (58.8 g, 67%), m.p. 132-134° (lit.⁷⁶ 133-133.5°).

m-Methoxybenzamide (8.10 g, 55 mmol) was refluxed with an ether solution of benzylmagnesium chloride (0.2 mol) for two days. The usual workup gave *m*-methoxydeoxybenzoin as an orange solid (12.3 g, 98% crude), n.m.r. δ 7.43 (m, 3H); 7.16 (s, 5H); 7.1-6.9 (m, 1H); 4.08 (s, 2H); 3.66 (s, 3H).

(c) *m*-Chlorodeoxybenzoin:

m-Chlorotoluene (Chemische Fabrik, purum) was converted⁷⁷ to *m*-chlorobenzoic acid (52% yield), m.p. 155-156° (lit.⁷¹ 155°).

m-Chlorobenzoic acid was amidated as usual to give *m*-chlorobenzamide, which was crystallized from water (69% yield), m.p. 133-135° (lit.⁷¹ 134.5°).

m-Chlorobenzamide (4.85 g, 31 mmol) and benzene (100 ml) were added to an ether solution of benzylmagnesium chloride (0.13 mol), and most of the ether was distilled off. After refluxing the mixture for 3½ days the usual workup gave *m*-chlorodeoxybenzoin⁷⁴ as a dark orange solid (7.10 g, 94% crude), n.m.r. δ 7.9-7.7 (m, 2H); 7.35 (t, 2H); 7.17 (s, 5H); 4.18 (s, 2H).

(d) *p*-Fluorodeoxybenzoin:

p-Fluorobenzoic acid (Light; 10.0g, 71 mmol) was refluxed with thionyl chloride (20 ml) and amidated to give *p*-fluorobenzamide (6.21 g, 63%), which was recrystallized from water, m.p. 152-155° (lit.⁸³ 154.5°); identical (i.r.) with an authentic sample⁷⁶.

p-Fluorobenzamide (4.70 g, 34 mmol) and benzene (100 ml) were added to an ether solution of benzylmagnesium chloride (0.17 mol), most of the ether was distilled off, and the mixture was refluxed for three days. *p*-Fluorodeoxybenzoin was obtained as a yellow solid (5.76 g, 80% crude) after the usual workup.

(e) *p*-Bromodeoxybenzoin:

p-Bromobenzonitrile (Aldrich; 21.7 g, 0.12 mol) was refluxed with an ether solution of benzylmagnesium chloride (0.26 mol) for two days, giving *p*-bromodeoxybenzoin as a white solid (27.0 g, 82%), m.p. 114-115° (lit.⁸⁵ 114-115°), n.m.r. δ 7.87 (d, 2H); 7.55 (d, 2H); 7.27 (s, 5H); 4.21 (s, 2H).

(f) *p*-Phenyldeoxybenzoin:

p-Bromobiphenyl (Light; 10.0 g, 43 mmol) was refluxed with cuprous cyanide (5.05 g, 49 mmol) in *N*-dimethylformamide (20 ml) with stirring for one day. Workup according to Friedman and Shechter's method⁷⁹ gave *p*-cyanobiphenyl⁸² as discoloured plates (8.6 g, 100% crude) which were treated with decolourising charcoal.

p-Cyanobiphenyl (7.5 g, 40 mmol) was refluxed with an ether solution of benzylmagnesium chloride (86 mmol) for 1½ days giving *p*-phenyldeoxybenzoin as a white solid (8.0 g, 73%) which was recrystallized from methanol as colourless plates, m.p. 146-148° (lit.⁸⁴ 140°).

(g) *m*-Trifluoromethyldeoxybenzoin:

m-Trifluoromethylbromobenzene (Koch-Light; 22.5 g, 0.10 mol) was refluxed with cuprous cyanide (10.3 g, 0.11 mol) in *N*-dimethylformamide (20 ml) for 8 hr. Vacuum distillation of the brown liquid obtained after workup⁷⁹ gave *m*-trifluoromethylbenzotrile as a clear liquid (8.87 g, 52%), b.p. 84°/34 mm (lit.⁸⁰ 94-95°/40 mm).

m-Trifluoromethylbenzotrile (8.85 g, 52 mmol) was refluxed with an ether solution of benzylmagnesium chloride (0.16 mol) for one day, giving *m*-trifluoromethyldeoxybenzoin as an orange oil (13.4 g, 98% crude), n.m.r. δ 8.2-8.0 (m, 2H); 7.7-7.4 (m, 2H); 7.16 (s, 5H); 4.13 (s, 2H).

(h) *m*-Bromodeoxybenzoin:

The complex obtained by adding benzotrile (80 ml, 0.78 mol) to anhydrous aluminium trichloride (233 g, 1.55 mol) with vigorous stirring, was brominated (20 ml, 0.78 mol) at 80° for 12 hr⁷⁸. The dark oil obtained on hydrolysis in conc. hydrochloric acid (100 ml) and ice (1 Kg), was extracted with ether and the extracts were washed and dried (MgSO₄). After distilling off the ether and unreacted benzotrile (0.36 mol), the residue was dissolved in hexane and treated with decolourising charcoal, giving colourless prisms of *m*-bromobenzotrile at 0° (20.0 g, 0.12 mol, 27%), m.p. 37-39° (lit.⁷⁸ 37-38°).

m-Bromobenzotrile (7.28 g, 40 mmol) was refluxed with an ether solution of benzylmagnesium chloride (85 mmol) for 12 hr, to give *m*-bromodeoxybenzoin as a yellow solid (11.0 g, 40 mmol, 100% crude), n.m.r. δ 8.00 (t, 1H); 7.74 (doublet of triplets, 1H); 7.47 (doublet of triplets, 1H); 7.13 (d, 1H); 7.12 (s, 5H); 4.01 (s, 2H).

(i) *m*-Cyanodeoxybenzoin:

m-Bromodeoxybenzoin (50.0 g, 0.18 mol) was refluxed with cuprous cyanide (19.5 g, 0.21 mol) in *N*-dimethylformamide (50 ml) for 6 hr. The brown solid obtained on workup⁷⁹ was purified by eluting it through an alumina column with petroleum ether (50-70)-benzene mixtures, giving *m*-cyanodeoxybenzoin (23.3 g, 58%) as white prisms from alcohol, m.p. 86.5-87.5°, ν_{\max} 2230, 1690 cm^{-1} ; n.m.r. δ 8.20 (d, 1H); 8.09 (t, 1H); 7.7-7.5 (m, 2H); 7.22 (s, 5H); 4.18 (s, 2H).

(j) *m*-Formyldeoxybenzoin:

m-Cyanodeoxybenzoin (3.00 g, 13.5 mmol) was reacted with anhydrous stannous chloride⁸¹ (75 mmol) in a solution of hydrogen chloride in ether⁸² (75 ml), and the resulting aldimine stannichloride complex was decomposed in boiling water to give *m*-formyldeoxybenzoin as a white solid (2.50 g, 82%), ν_{\max} 1710, 1670, 1600 cm^{-1} ; n.m.r. δ 10.07 (s, 1H); 8.50 (t, 1H); 8.26 (doublet of triplets, 1H); 8.06 (doublet of triplets, 1H); 7.68 (d, 1H); 7.29 (s, 5H); 4.33 (s, 2H).

(k) *m'*-Fluorodeoxybenzoin:

m-Fluorobenzyl bromide (Aldrich; 10 ml, 87 mmol) was converted to *m*-fluorobenzylmagnesium bromide by the usual procedure, and refluxed with benzonitrile (4.1 ml, 40 mmol) for 2½ days, to give *m'*-fluorodeoxybenzoin as a red-brown oil (10 g), n.m.r. δ 8.00-7.83 (m, 2H); 7.43 (d, 2H); 7.34 (d, 1H); 7.00 (m, 3H); 6.85 (m, 1H); 4.13 (s, 2H).

(l) *m'*-Nitrodeoxybenzoin:

m'-Nitrodeoxybenzoin was obtained from a sample prepared by Fischer⁸⁹ which had m.p. 82°.

3.1.3 Benzils

The mono-substituted benzils were prepared by oxidation of the deoxybenzoins with 1.1 equivalents of selenium dioxide (B.D.H.) according to the method of Corey and Schaefer⁸⁵. No impurities were detected in their mass spectra.

(a) Benzil (Hopkin and Williams) was recrystallized from alcohol to give yellow needles, m.p. 95-96° (lit.⁷¹ 95°).

(Found: m/e 210.0682; $C_{14}H_{10}O_2$ requires mol. wt. 210.0681.)

(b) *m*-Fluorobenzil was chromatographed on a silica gel column with petroleum ether (50-70)-benzene mixtures, and gave pale yellow needles from alcohol, m.p. 101.5-102.5° (lit.⁸⁷ 100.5-101°). (Found: m/e 228.0589; $C_{14}H_9O_2F$ requires mol. wt. 228.0587.)

(c) *p*-Fluorobenzil was chromatographed on a silica gel column with petroleum ether (50-70)-benzene mixtures, and gave yellow prisms from methanol, m.p. 62-62.5° (lit.⁸⁷ 63.5-64.5°).

(Found: m/e 228.0584; $C_{14}H_9O_2F$ requires mol. wt. 228.0587.)

(d) *m*-Chlorobenzil was purified by column chromatography and gave yellow prisms from alcohol, m.p. 89-90° (lit.⁸⁶ 86°).

(Found: m/e 244.0293; $C_{14}H_9O_2Cl$ requires mol. wt. 244.0291.)

× (e) *m*-Bromobenzil gave yellow prisms from alcohol, m.p. 82-83°. (Found: m/e 287.9782; $C_{14}H_9O_2Br$ requires mol. wt. 287.9786.)

(f) *p*-Bromobenzil gave pale yellow needles from alcohol, m.p. 86.5-87° (lit.⁸⁵ 86-87°). (Found: m/e 287.9780; $C_{14}H_9O_2Br$ requires mol. wt. 287.9786.)

× (g) *m*-Methylbenzil gave pale yellow prisms from alcohol, m.p. 93.5-94.5°. (Found: m/e 224.0834; $C_{15}H_{12}O_2$ requires mol. wt. 224.0837.)

- (h) *m*-Methoxybenzil gave pale yellow prisms from alcohol, m.p. 90-91^o. (Found: *m/e* 240.0783; C₁₅H₁₂O₃ requires mol. wt. 240.0786.)
- (i) *p*-Phenylbenzil was chromatographed on a silica gel column with petroleum ether (50-70)-benzene mixtures, giving a yellow oil which crystallized from cold petroleum ether (50-70) as a pale yellow powder, m.p. 96-97^o (lit.⁸⁸ 104-105^o). (Found: *m/e* 286.0995; C₂₀H₁₄O₂ requires mol. wt. 286.0994.)
- (j) *m*-Formylbenzil was purified by column chromatography and gave pale yellow prisms from alcohol, m.p. 84.5-85^o. (Found: *m/e* 238.0630; C₁₅H₁₀O₃ requires mol. wt. 238.0630.)
- (k) *m*-Cyanobenzil gave orange-yellow prisms from alcohol, m.p. 86.5-87.5^o. (Found: *m/e* 235.0629; C₁₅H₉NO₂ requires mol. wt. 235.0633.)
- (l) *m*-Trifluoromethylbenzil gave yellow plates from alcohol, m.p. 67-68^o. (Found: *m/e* 278.0560; C₁₅H₉O₂F₃ requires mol. wt. 278.0555.)
- (m) *m*-Nitrobenzil gave pale yellow prisms from alcohol, m.p. 120-121^o (lit.⁹⁰ 120^o). (Found: *m/e* 255.0525; C₁₄H₉NO₄ requires mol. wt. 255.0532.)

3.2 MASS SPECTROMETER

3.2.1 Instrumental Modifications

The instrument used was an A.E.I. MS902 double-focussing high resolution mass spectrometer, which was equipped with some standard modifications designed to improve and extend its capabilities. The most important of these for this work, was a modified ion beam focussing system for the source⁹¹. Prior to the introduction of this modification, it was very difficult to obtain optimum focussing of the ion beam - a prerequisite

to obtaining good ionization efficiency data. The original focussing controls were interdependent and their range of adjustment was sometimes insufficient. The new system showed a much reduced degree of interdependence between the focussing controls, and a maximum in the ion current could always be obtained if the source was clean.

Other modifications included a head amplifier gain kit, which provided a ten times increase in amplification of the ion detector signal, and a digital read-out for the collector meter. This was obtained by connecting a digital voltmeter (International Electronics; Type DSV4), reading to four significant figures, across the scaling resistor of the collector meter. A semi-automatic digital recording system for measuring ionization efficiency data was also constructed, and is described in the next section.

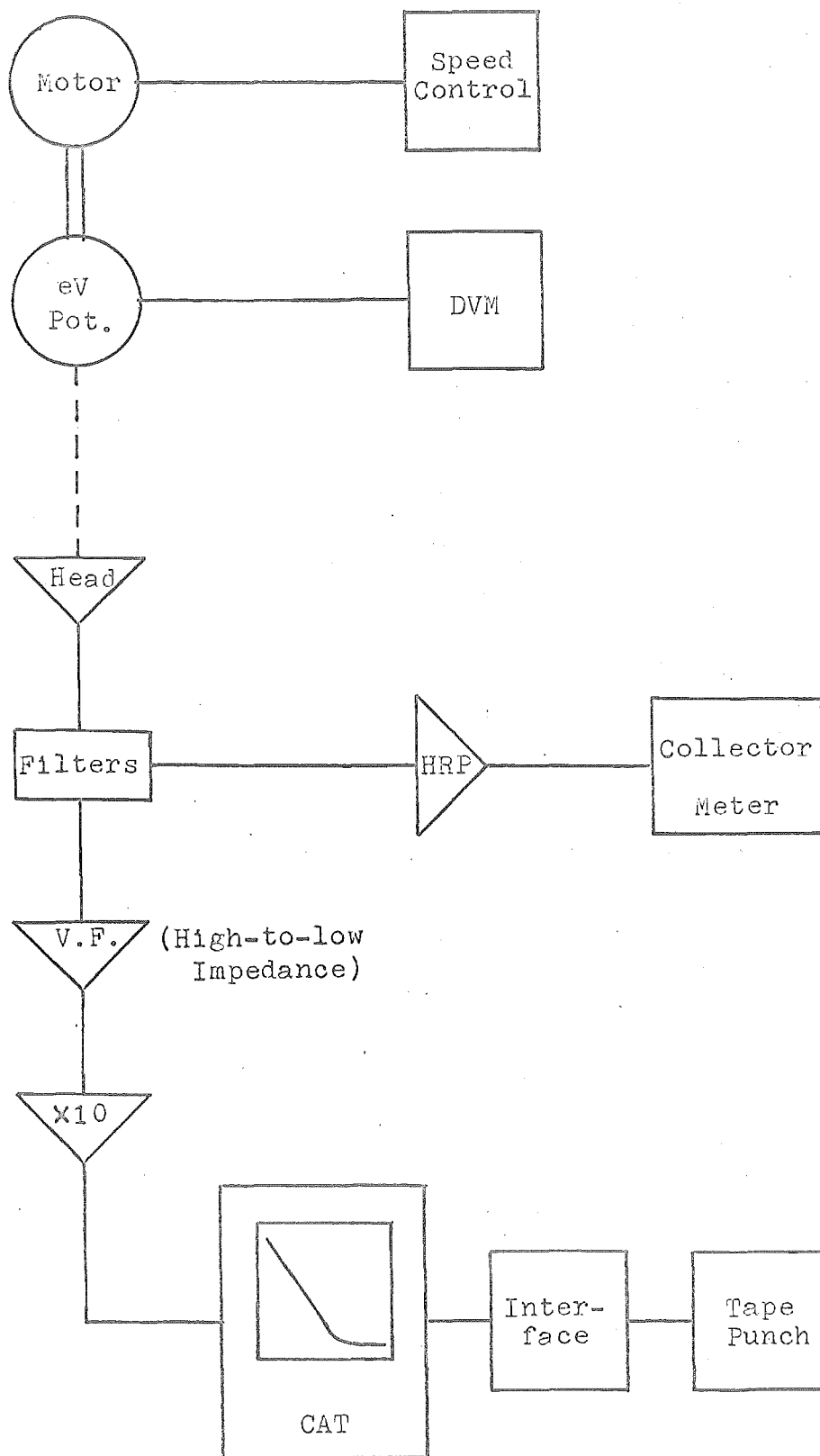
3.2.2 Semi-Automatic Digital Recording System

This data collection system was designed to obtain ionization efficiency data, and was based on a 1024 channel time-averaging-computer (Varian C1024, CAT) which was used to digitise and store the ion signal at constant time intervals while the ionizing voltage was scanned mechanically (Fig. 8).

(i) Ionizing Voltage Control Unit

The potentiometer controlling the electron beam voltage was replaced by a very free-running 10-turn helipot (Beckman; Series A, 10K, $\pm 0.5\%$ linearity) giving a 9 volt change in the ionizing voltage per revolution. An electromagnetic clutch (Oliver Pell; MC7) connected the helipot spindle to the drive unit of a synchronous motor (Phillips; AU 5100/91), which was powered by a continuously variable frequency supply (Appendix B). The motor shaft speed was 250 rev/min (at a frequency of

Fig. 8. Semi-Automatic Digital Recording System.



50 Hz), and this was reduced to $3\frac{1}{3}$ rev/min by a 75:1 reduction gear unit (Phillips; AU 5300/80 DP). The voltage scan rate was decreased to a convenient value of 6 volt/min ($2/3$ rev/min) by reducing the supply frequency, so that a 5 volt scan was obtained using the 50 sec scan setting on the CAT. The electron beam voltage was displayed on a digital voltmeter (Weston; Model 1290) which replaced the original meter, and read to 0.01 volt over the range 0-25 volt. (A switching device was incorporated to enable it to read to 0.1 volt over the range 0-100 volt.)

(ii) CAT Input Signal

In order to match the input impedance of the CAT, the ion signal output from the bandwidth filter was fed through a high-to-low impedance voltage follower; to reduce the multiplier gain required to obtain a sufficient ion signal, an amplifier ($\times 10$) was inserted between the voltage follower and the CAT input. In this way the signal was amplified after removing most of the noise with the bandwidth filter, rather than by increasing the multiplier gain which gave unacceptable noise levels at high multiplier settings.

(iii) CAT Read-out System

Once stored in the CAT, the ionization efficiency data was punched on 7-track paper tape using a Creed Model 25 punch unit. The binary values of each channel address and its contents were transmitted to the punch through a specially designed interface unit (Appendix B). The two numbers (for each channel) were punched in a compact binary format, enabling a complete scan (1024 channels) to be stored on about 45 feet of tape. Although the maximum speed of the punch was 28 characters/sec, it was run at about $1/3$ this rate to

avoid the punching errors which occurred at higher speeds; a complete scan (5120 characters) therefore took about 6 minutes to punch. At the end of each tape record (i.e. a scan) an "end-of-record" character (middle 5 tracks punched) was punched manually.

3.2.3 Sample Introduction

(i) Inlet systems

This instrument possessed three standard systems for introducing samples into the ion source: a cold inlet system for gases, an all-glass heated inlet system (AGHIS) for liquids, and a heated direct insertion system (HDIS) for solids. Extra introduction ports were provided in the source housing for alternative inlet systems, and one of these was used for a modified gas inlet system to introduce a reference gas (xenon) into the source at a constant, readily controlled pressure.

This inlet system consisted of a backing pump connected to an oil diffusion pump, which evacuated a small vacuum line containing two inlet ports and an exit line to the ion source. The flow of gas through the exit line was controlled by a variable needle-valve (Granville-Phillips; Series 203), and could be adjusted to any desired value. The operation of this system was quite simple. A small reservoir (250 ml), filled to a few mtorr pressure with xenon, was connected to an inlet port and the line was evacuated until no residual gases were detected on opening the needle-valve to the source. The vacuum line was then isolated from the diffusion pump and the stop-cock to the gas reservoir was opened (with the needle-valve closed). The xenon was then admitted to the source by opening the needle-valve until the desired flow-

rate was attained. A constant source pressure of about 5×10^{-6} torr could be maintained over a long period using this technique. However, it was noticed that the source ionization gauge reading (pressure) slowly increased to about $1\frac{1}{2}$ times its initial reading over a period of $\frac{1}{2}$ -1 hour; the ion current did not change during this time. The reason for this effect is not known, but the xenon pressure was always allowed to equilibrate for at least one hour before its reading was taken.

The AGHIS was only used to introduce the reference compound (N-heptacosatrifluorobutylamine) to the source for high-resolution mass measurements. Attempts were made to use it for some of the benzils, but sufficient source pressures could not be obtained, even at temperatures (250-300°) which were apparently high enough to cause pyrolysis of the samples. At these temperatures much higher $[\text{C}_6\text{H}_5\text{CO}^+]/[\text{M}^+]$ intensity ratios were observed than when using the direct insertion system. A constant source pressure could not be maintained with the unheated direct insertion probe, but when the HDIS became available a technique was devised to overcome this critical problem with the introduction of the solid samples.

(ii) Sample Preparation

The ionization efficiency curves of all the major ions in the mass spectra of the benzils, usually five or more ions at low ionizing voltages (not counting isotopic species), had to be measured for the purposes of this study. The most efficient way to do this was to obtain all the curves for a compound in one experiment, keeping the ion source conditions constant throughout, so that only one reference curve (xenon)

was required for each experiment. Contact potentials between the electron-gun filament and the ion chamber block can change markedly with different source pressures⁹², and it was important that these changes be kept to a minimum so that the calibration of the ionizing voltage scale with the reference curve was correct. Since it took 8-10 minutes to record and punch a single ionization efficiency curve, the source pressure had to be kept constant for up to 1½ hours. This requirement posed a major problem when introducing solid samples with the HDIS.

The usual method with the HDIS was to pack the sample in a melting point tube cut to the requisite length, and push it into the cup on the probe tip, which was packed with silica wool (previously heated at 400° overnight), so that it protruded about ¼". This method enabled the sample pressure in the source to be kept constant for only a few minutes, since it proved very difficult to control the rate of vaporization of the sample by varying the temperature of the probe tip. However, a simple modification of this procedure enabled a constant sample pressure to be maintained for up to two hours.

About ¼" of sample was packed into a melting point tube cut to the correct length, and just melted over a hot lamp. A ½" plug of silica wool was pushed into the molten sample so that the wool was impregnated with the sample. Care was taken that none of the sample rose above the top of the wool plug. The sample was allowed to cool, and a further plug (½") of silica wool was pushed in. The tube was then placed in the cup of the HDIS probe as usual, and inserted into the source. When the probe temperature was gradually raised the

sample vaporized smoothly off the silica wool on melting, and its pressure could be controlled by adjusting the temperature of the probe. Over the period of an experiment, minor adjustments to the probe temperature were required to maintain the constant source pressure. These adjustments were made while the previous scan was being punched, allowing enough time for the pressure to reach equilibrium at the desired value for each scan.

(iii) General Procedure

A clean ion source was essential to obtain satisfactory ionization efficiency data. Sometimes an apparently clean source gave unsatisfactory results, and this was usually traced to small ion burns around the electron-gun assembly; replacement of the filament with a clean one generally rectified this problem. Whenever an ion source (or part) was replaced, it was baked overnight in the instrument (100-150°). If the source was baked between each experiment for a few hours, and overnight about every two days, it often proved satisfactory for a week or more if not used for any other work. The general procedure followed in introducing a sample for ionization efficiency experiments is described below.

The source housing and ion chamber block were allowed to equilibrate at temperatures of 80 (± 10)° and 120 (± 10)° respectively, depending on the melting point of the sample (generally in the range 80-100°). These temperatures were high enough to prevent any condensation of the sample on the source, but not so high that they caused the sample to melt when it was inserted in the HDIS probe and so prevent control of its pressure with the probe heater. The AGHIS and direct

insertion lock were kept at similar temperatures to avoid condensation on their inlet ports. The xenon was admitted through the variable leak and allowed to equilibrate at about 5×10^{-6} torr pressure. The sample was then introduced and the probe temperature adjusted to give a total source pressure of about 1×10^{-5} torr. The temperature required to do this was often considerably higher than the melting point of the sample owing to the efficient insulation provided by the silica wool surrounding the sample tube. It was generally found that the probe temperature had to be gradually increased during an experiment to maintain a constant source pressure, since the sample slowly sublimed through the silica wool, moving further away from the probe heater.

3.2.4 Source Focussing

Good source focussing is essential to obtain reproducible ionization efficiency data. Precautions were taken to minimise the variable effects on ion chamber potentials due to cross-fields and space-charge^{92,93}. All ionization efficiency and ion intensity data were measured with the ion repeller plate shorted to the ion chamber block, and at a trap current of 10 μ a - the lowest setting available. Although the low electron beam current produces a considerable sacrifice in sensitivity, and hence the attainable signal-to-noise ratio of the ion current, it is necessary to accept this in view of the variable space-charge effects observed at higher currents⁹³. Since the most sensitive maximum in the ion current is obtained near an ion repeller setting of zero potential difference between it and the ion chamber block, practically no loss in sensitivity is suffered by shorting them. Variations in the penetration of the ion accelerating

potential into the ion chamber were minimised by measuring all data at a constant voltage (8 kV).

The source focussing controls were optimized using the most intense peak present in the mass spectrum. Except for high resolution measurements, the source exit slit was set just under the maximum width, and the collector slit was set to give a flat-topped peak. The ion beam was set in the middle of the monitor valley using the " ΔV " control to trim the ion accelerating voltage, and the beam focussing controls were adjusted. The "beam centring", "Z-deflection", "Y-deflection", and "source focus" controls were optimised in that order; the ΔV control was then readjusted to make the top of the peak flat (adjustment of the Y-deflection control can cause this to become skewed). This cycle of adjustments was repeated until the maximum ion current was obtained, then the "analyser focus" and magnet horizontal settings were checked. These are particularly important for high resolution work. The focussing was performed at the ionizing voltage at which the measurements were to be made (e.g. 15eV for ionization efficiency data), since the focussing changed considerably at different voltages - especially above 20 eV.

The focussing was tested for ionization efficiency work by recording the curve for xenon (m/e 132), and displaying it on the CAT oscilloscope. If the ionization efficiency curve appeared to be linear above the threshold, the source focussing was considered acceptable. If not it was refocussed and if no improvement was obtained, the source was removed for inspection and cleaning.

3.3 DATA COLLECTION

3.3.1 70 eV Mass Spectra

The standard 70 eV mass spectra were recorded at low resolving power ($M/\Delta M \approx 1,000$, 10% valley) and 100 μ a trap current; the background spectrum was checked to be negligible. The multiplier gain was set so that the base peak gave less than half the full-scale deflection on the galvanometer trace ($\times 1$) of the chart recorder, to ensure that the recorded ion intensities did not suffer from saturation of the multiplier response. Saturation occurred for the largest peaks if the gain was much higher than this, and it was indicated by excessive values for the ^{13}C isotope peak. The ion intensities were digitized and averaged from two or three chart recordings by manual measurement of the peak heights. Spectra were also recorded at high multiplier gains to enable weak normal metastable ion peaks to be detected. Mass measurements were performed at high resolution ($M/\Delta M \approx 15,000$, 10% valley) by the "peak-matching" procedure, using N-heptacosatrifluorobutylamine as the mass standard; all measured masses were within 5 ppm of the required values.

3.3.2 Low Voltage Mass Spectra

Low resolution mass spectra were also recorded at nominal ionizing voltages of 20, 18, 16, 14, 12 and 10 eV. The purpose of these measurements was to obtain accurate relative ion intensity data, which could be used to apply corrections to the relative ion intensities calculated from ionization efficiency curves. This was necessary because of the small variations in source pressure which occurred when different curves were being measured. The following method

of measuring ion intensities gave accurate data, and was also fast enough to ensure that variations in the source pressure at each ionizing voltage were negligible. The time required to perform the measurements at each voltage was 5-10 minutes, depending on the number of peaks to be measured.

At each ionizing voltage the source focussing was checked, and the major ions present (i.e. intensities greater than $\sum_{i=0} = 0.1\%$) were tuned onto the collector in turn. The multiplier was adjusted to give a suitable reading on the digital voltmeter connected in parallel with the collector meter, and the peak was then just detuned so that the collector meter zero could be set correctly. On retuning the peak the ion signal was read from the digital voltmeter, and a correction was made for the multiplier gain. Although isotopic peaks were not measured, the ^{13}C peak was checked to ensure that the gain used was low enough to avoid saturation of the multiplier response.

3.3.3 Ionization Efficiency Curves

Ionization efficiency curves were obtained for the major ions present in the mass spectra at low ionizing voltages, and for the reference ion (Xe^+ , m/e 132), in the following manner. The ion was tuned onto the collector and the ionizing voltage was decreased below the threshold voltage of the ion, so that the collector zero could be adjusted to give a digitized value ca. 100 for the sub-threshold region of the ionization efficiency curve. The ionizing voltage was set to the desired starting value (e.g. 5 eV above the threshold), and the multiplier gain was adjusted to give the maximum ion signal accepted by the CAT on its most sensitive input range (approx. 2.8 volt on a CAT "attenuator" setting 1); this

gives a digitized value *ca.* 1200. The CAT "scan time" was set to 50 sec, and the frequency control for the ionizing voltage drive unit was adjusted to ramp down the required voltage (e.g. 6 eV), so that the last 100 or so data channels recorded the flat sub-threshold region of the curve. The CAT scan was triggered automatically when the clutch was switched on; when the scan had finished (as indicated on the oscilloscope display) the clutch was switched off manually, leaving the final value of the ionizing voltage displayed on the digital voltmeter. (This recording system could be improved by making the "end-of-scan" pulse generated in the CAT trigger a relay to switch off the clutch automatically).

Experience showed that the optimum signal-to-noise (S/N) ratio was obtained with a bandwidth filter setting of 50 Hz. A lower setting caused the curves to have low-frequency noise which could not be removed with the analytical smoothing methods used in the data analysis. In principle the S/N ratio could be improved by accumulating many scans in the CAT memory, but the ratio increases only as the square root of the number of scans. The present method of scanning was too slow to allow any significant improvement to be made in this way; there was usually only just sufficient time to record and punch all the ionization efficiency curves before the sample eventually ran out.

3.3.4 Calibration of Multiplier Gain

The multiplier gain had to be calibrated so that relative ion intensities could be obtained from the measured intensities, which invariably employed different multiplier gains for different ions. This was carried out using the $C_6H_5CO^+$ ion (m/e 105) in the mass spectrum of benzil. The source pressure and ionizing voltage were adjusted so that

no saturation of the multiplier response occurred at the highest gains used. The ion signals at both the HRP (multiplier) and LRP (Faraday cup) collectors were measured from the digital voltmeter at various multiplier settings, care being taken to ensure that the collector zero was correctly adjusted before each reading. The multiplier gain was then calculated (as a function of the multiplier setting) as the ratio

$$G_M = I_{\text{HRP}}/I_{\text{LRP}} \quad (14)$$

and is given in Table 1. These values were used to convert the measured ion intensities to the same relative scale, assuming that discrimination effects in the multiplier response for the various ions were negligible⁹⁴.

CHAPTER 4ANALYSIS OF IONIZATION EFFICIENCY DATA

One of the principal aims of this work was to develop numerical data analysis procedures which would extract the maximum amount of useful information from the experimental ionization efficiency (IE) curves. In view of the direct relationship between theoretically calculated breakdown curves and normalized, deconvoluted second-derivative ionization efficiency (SDIE) curves (see Chapter 2.2.3 (iv)), attempts were first made to compute SDIE curves from the experimental data. However, the accuracy of the data measured using the present system was too low for such computations to be satisfactory; this was due to the low signal-to-noise (S/N) ratio obtained when measuring the very weak ion signal near the threshold voltage. It was recently shown⁹⁵ that data of sufficient precision to derive reliable SDIE curves could be obtained using a much more sophisticated computer-operated system, which performed time-averaging of the experimental IE curves over several thousand scans.

Because of the insurmountable problems encountered with the "derivative" method^{52,92} of analysing the experimental IE curves, a less sophisticated approach was used to extract ionization and appearance potentials from the measured IE curves. The conventional methods for doing this have been extensively discussed^{93,96}, and generally depend on various interpretations of the shape of an IE curve near its threshold. These include the "vanishing current" methods of Smyth⁹⁷ and Warren⁹⁸, and the "logarithmic methods" due to Honig and

Wannier⁹⁹, Lossing et al.¹⁰⁰, and Dibeler and Reese¹⁰¹. A modification of the logarithmic methods was used in this work because these are the ones generally favoured in studies of this type.

Fractional ion intensities were also calculated from the IE curves because then the energy scale could be corrected to its true value, rather than using intensities measured at a number of nominal ionizing voltages. Furthermore this method allowed the fractional ion intensities to be calculated at any desired energy intervals (up to several volts above the threshold voltage), so that the variation of the relative intensities with ionizing voltage could be analyzed in more detail than would otherwise be possible.

This chapter describes the numerical procedures which were used to analyse the experimental data, with reference to the computer programs which were developed specifically for this work. After a general discussion of the various programs, a brief description of the different stages of a typical analysis is given in section 4.5 to illustrate the use of the programs with examples of the outputs obtained from them. A complete listing of the computer programs is given in Appendix A.

4.1 LEAST SQUARES PROCEDURES

The method of least squares¹⁰² was used extensively to overcome the problems associated with the processing of data containing considerable random noise. Three different least squares programs were used in the data analysis; two had simple applications requiring only a single cycle of refinement, and the third was a general least squares program adapted from

ORGLS¹⁰³. They were all written as subroutines for use with the other data analysis programs, and are briefly described below.

4.1.1 Smoothing and Differentiation (SMOOTH)

Data obtained at uniformly spaced values of the independent variable can be fitted to a polynomial function of any desired order by a simple convolution procedure¹⁰⁴, described by

$$\hat{y}_j = \frac{\sum_{i=-m}^m c_i y_{j+i}}{N}, \quad j = m+1, \dots, n-m \quad (15)$$

where y_j ($j = 1, \dots, n$) is an observed point, \hat{y}_j is the corresponding value estimated by a least squares fit over $2m+1$ points, c_i is the set of convoluting integers, and N is the associated normalizing constant. The set $\{c_i\}$ may be chosen such that the \hat{y}_j values give the least squares estimate of the k^{th} order derivative of the polynomial fitted to the observed values $(y_{j-m}, \dots, y_{j+m})$, where k may range up to the order of the polynomial. It is merely necessary to judge what degree polynomial gives the best fit to the observed data over segments of $2m+1$ points, m being chosen as desired. A second order polynomial was considered to be sufficient for the IE curves obtained in this work, and the subroutine SMOOTH performs quadratic smoothing or differentiation using this method.

4.1.2 Fitting a Straight Line (LINEAR)

The data points $(y_i, x_i; i = 1, \dots, n)$ were fitted to the straight line

$$\hat{y}_i = \hat{a} + \hat{b}x_i \quad (16)$$

using least squares estimates for the linear parameters (\hat{a} , \hat{b}) which minimise the sum of the weighted squares of the residuals

$$E = \sum_i w_i (y_i - \hat{y}_i)^2 \quad (17)$$

where w_i is the weight of the i^{th} point. The parameter estimates were obtained from the equations

$$\hat{a} = \frac{(\sum_i w_i x_i^2 \cdot \sum_i w_i y_i - \sum_i w_i x_i \cdot \sum_i w_i y_i)}{(\sum_i w_i \cdot \sum_i w_i x_i^2 - (\sum_i w_i x_i)^2)} \quad (18a)$$

$$\hat{b} = \frac{(\sum_i w_i \cdot \sum_i w_i x_i y_i - \sum_i w_i x_i \cdot \sum_i w_i y_i)}{(\sum_i w_i \cdot \sum_i w_i x_i^2 - (\sum_i w_i x_i)^2)} \quad (18b)$$

and the standard deviations (\hat{s}_a , \hat{s}_b) of these estimates, together with the correlation coefficient (r), from the expressions

$$\hat{s}_a^2 = s^2 / (\sum_i w_i x_i^2 - (\sum_i w_i x_i)^2 / \sum_i w_i) \quad (19a)$$

$$\hat{s}_b^2 = s^2 \cdot \sum_i w_i / (\sum_i w_i \cdot \sum_i w_i x_i^2 - (\sum_i w_i x_i)^2) \quad (19b)$$

$$r = \frac{\sum_i w_i \cdot \sum_i w_i x_i y_i - \sum_i w_i x_i \cdot \sum_i w_i y_i}{(\sum_i w_i \cdot \sum_i w_i x_i^2 - (\sum_i w_i x_i)^2)^{1/2} (\sum_i w_i \cdot \sum_i w_i y_i^2 - (\sum_i w_i y_i)^2)^{1/2}} \quad (19c)$$

where

$$s^2 = \frac{\sum_i w_i \cdot \sum_i w_i y_i^2 - (\sum_i w_i y_i)^2 - \frac{(\sum_i w_i \cdot \sum_i w_i x_i y_i - \sum_i w_i x_i \cdot \sum_i w_i y_i)^2}{(\sum_i w_i \cdot \sum_i w_i x_i^2 - (\sum_i w_i x_i)^2)}}{(n-2) \cdot \sum_i w_i} \quad (19d)$$

Although this subroutine has provision for weighting the data, unit weights were generally employed since LINEAR was only used

when simple straight line fits were required without iterative refinement to discard points lying well off the line (e.g. see 4.3.2).

4.1.3 Fitting a General Function (LINFIT)

The general least squares method^{102c} uses a Taylor expansion about a point in parameter space to refine initial estimates of the parameters of an arbitrary function to give the best fit to a set of observations. More than one cycle of refinement is required to converge on the final solution, unless the function fitted to the data is linear in the variable parameters. Although the applications in this work involved such linear functions, the refinement was continued over a few cycles so that observations could be rejected if their weighted residuals were too high; new estimates of the parameters were then computed with these points excluded from the least squares analysis.

Subroutine LINFIT was set up in the same way as ORGLS to allow a number of options using the subroutines PRELIM, CALC, and TEST, which were called at different stages by LINFIT. PRELIM was called before the least squares analysis started and set up the data arrays, computed the standard deviations used to weight the data, and provided initial estimates for the parameters and other associated variables. For each cycle of refinement, the contribution of each observation to the matrix and vector of the normal equations was calculated after calling CALC, which computed the value of the function from the current values of the parameters and the independent variables associated with each observation, and also obtained the derivatives of the function with respect to the variable

parameters. The matrix was then tested for singularities and inverted by MATINV which used the Choleski matrix-inversion procedure¹⁰⁵. At the end of each refinement cycle, after computing the revised estimates of the parameters and their standard deviations, TEST was called and could be used to check the parameters (modifying them if necessary), or the convergence of the refinement by testing the agreement factor. Unless the refinement was terminated by TEST (or because of a singular matrix), it was continued for the specified number of cycles and a final calculation of the parameter estimates was performed. These estimates were then printed out, together with their standard deviations, the correlation matrix, and the agreement factor.

4.2 PRELIMINARY TREATMENT OF IONIZATION EFFICIENCY DATA

4.2.1 Decoding and Editing (TAPED)

The paper tape data was decoded using a special Assembler subroutine (BNMCM), written in the department by R.J. Dellaca, which translated the characters read from the paper tape, and stored the decoded values of the digitized ion signal in the elements of a data array according to their channel number. Because of occasional mispunchings on the tapes and recurring problems with reading the tapes into the computer, it was convenient to have the decoded data punched on cards in an easily readable integer format (20 points per card, 52 cards per tape record), so that spurious data could be corrected by simply repunching a card. A listing of the raw data was edited manually for this purpose; although time-consuming, this process had to be done only once, and it avoided having to include data-checking routines in the computer programs.

4.2.2 Smoothing and Reduction of Data (RAWFIT)

Analytically smooth ionization efficiency curves were required for the calculation of the fractional ion intensities (see 4.4), and originally for the attempted calculations of the SDIE curves. Since the low signal-to-noise ratio of the experimental IE data allowed only the broad features of these curves to be discerned, the smoothing was done by fitting a sequence of linear segments to the experimental IE curves using the general least squares subroutine (LINFIT). Each linear segment spanned 0.2 eV (i.e. about 34 data points for the usual 6 eV scan), giving thirty segments in all, and the ordinate values at the end-points of each segment were the parameters adjusted by least squares. This simple technique possessed a number of advantages over other smoothing methods for the data obtained in this work. Most importantly it successfully removed all the noise from the experimental data (except for very low frequency noise), and the smoothed IE curves which could be reconstructed from the linear segments with subroutine DATCOM (using quadratic smoothing to even out the changes in slope between successive segments) reproduced the broad features of the original curves very closely. Further advantages were that the data files were reduced from over 1000 points per scan to only 35 parameters or less (including the voltage scan parameters), and that the ionization efficiency could be calculated at any desired intervals of the ionizing voltage by simple linear interpolation procedures.

The estimated standard deviations (σ_y) of the end-points (y) of each linear segment provide a measure of the variation in the error of the ion signal with its magnitude. Plots of $\log \sigma_y$ against $\log y$ (Fig. 9) showed that the relation between

σ_y and y was well described by

$$\sigma_y = cy^\alpha, \quad \alpha = 0.50 (\pm 0.01). \quad (20)$$

This has important consequences in deciding on the correct weighting scheme to use when estimating parameters from the experimental data (e.g. appearance potentials, see 4.3). The relation

$$\sigma_y = cy^{\frac{1}{2}} \quad (21)$$

was used in all cases where weighting schemes were employed in estimating parameters by least squares.

4.3 APPEARANCE POTENTIALS

4.3.1 Semi-logarithmic Method

The semi-logarithmic method^{100,101} for determining ionization and appearance potentials is generally performed by measuring the intensities (I_V) of the sample and reference ions relative to their respective intensities at 50 (I_{50}) or 70 eV (I_{70}), over the range of ionizing voltages (V) where these relative intensities (e.g. I_V/I_{50}) lie between 0.1 and 1%. Plots of the logarithm of these normalized ion intensity curves (e.g. $\log(I_V/I_{50})$) against the ionizing voltage are generally linear and parallel (with suitable choice of the reference ion) over this range, and the appearance potential is obtained from the voltage difference between the parallel sections of the two curves. This method is easy to perform experimentally since intensity-voltage measurements need be taken only at several selected values lying in the range $I_V/I_{50} \approx 0.1 - 1\%$. However, this arbitrary normalization procedure is simply equivalent to the subtraction of a

constant value (e.g. $\log I_{50}$) from the unnormalized logarithmic IE curve ($\log I_V$). It therefore merely shifts the $\log I_V$ curve down the ordinate scale, and assumes that this will make the linear portions of these curves coincide (on the normalized ordinate scale). This assumption supposes that the IE curves have the same shape from the threshold right up to an ionizing voltage of 50 (70) eV; it is not justified, especially for different types of ions (e.g. fragment ions compared with molecule-ions), but is necessary when complete ionization efficiency curves are not available.

In this work, IE curves were available up to about 5 eV above the threshold energy and a normalization procedure which avoided the disadvantage of the standard method was developed. This procedure scales the logarithmic IE curves to the same size over the short energy range from just below the threshold to about 5 eV above the threshold; it thus shows up differences in the shapes of the $\log I_V$ curves near the threshold but does not make assumptions about the behaviour of the IE curves at higher energies. These differences in the $\log I_V$ curves arise from the expected changes in the functional dependence of the ionization efficiency on the ionizing voltage for different types of ions, and they must be recognized if estimates are to be obtained for the systematic errors they cause in using the semi-log method.

The normalization procedure adopted was carried out as follows. The multiplier gain was set to give the same ion signal for each IE curve at an ionizing voltage about 5 eV above the threshold. This starting energy for the decreasing voltage scan was such that the last 100 channels of the CAT

recorded the flat sub-threshold region of the IE curve (see section 3.3.3). Since the $\log I_V$ curve increases with energy only slowly at this point (Fig. 10b), the precise starting voltage used is not critical for this normalization procedure, but it should be about the same energy above the threshold for each curve. Before recording the IE curve the ion signal in the flat sub-threshold region was adjusted to give a measurable value (I_0), which then has to be adjusted to the same value (I_Z) for all the IE curves. I_Z was set to 1.0 so that the logarithm of the normalized IE curve (I_V^N) was zero for the sub-threshold region (if I_Z was set to zero, $\log I_V^N$ would be minus infinity in this region). The normalized IE curves were thus obtained from the expression

$$I_V^N = I_V - I_0 + 1.0 \quad (22)$$

and examples of the semi-log plots ($\log I_V^N$) are shown in Fig. 13. The advantages of this normalization procedure are that the normalized semi-log plots are referenced correctly to their zero ordinate value, and are also scaled to the same size. This procedure hence gives a more correct correspondence between the ordinates of the different $\log I_V$ curves than does the standard method, which does not reference the semi-log curves to the same zero value (unless the IE curves have exactly the same shapes from the threshold to 50 (70) eV).

The problem is now to decide the value of the normalized logarithmic intensity scale at which the voltage differences between the semi-log curves should be measured to derive the appearance potentials. For ions of the same type (e.g. molecule-ions), the ionization efficiency should show the same functional dependence on the ionizing voltage; the corresponding

normalized semi-log curves will therefore have the same shapes. In particular the normalized ionization efficiency near the threshold may be described by an exponential of the form

$$I_V^N = C \exp(\beta V) \quad (23a)$$

where C is a constant representing the zero correction factor, and the exponent β gives the degree of dependence on the ionizing voltage V ; β is therefore expected to vary with the type of ion. Hence a linear region whose slope depends on the value of β will be observed near the threshold of the normalized semi-log curve

$$\log_e I_V^N = \log_e C + \beta V, \quad (23b)$$

and this behaviour was found for all the IE curves measured in this work (e.g. Fig. 13). The linear regions generally spanned ordinate values centred around $\log I_V^N = 1.0$, and their slopes were the same for the reference ion and the molecule-ion, and slightly less for the primary fragment ions. The slopes observed for the secondary fragment ions were always much less than that for the reference ion - behaviour expected from a consideration of typical breakdown curves for these ions (see section 2.2.3(iv)).

The appearance potentials reported in this work were determined from the voltage difference between the normalized semi-log curves measured at an ordinate value of $\log I_V^N = 1.0$ (on the arbitrary scale applying to this data), because this corresponded to the middle of the linear regions of the curves. The ion intensity at this point ($I_V^N = 10$) is approximately 1% of the intensity 5 eV above the threshold

($I_V^N \approx 1000$), so these appearance potentials can be described as 1% values measured with reference to the ion intensity 5 eV above the threshold. The systematic errors introduced by this arbitrary choice of ordinate value are discussed in section 4.3.4.

4.3.2 Normalization of Semi-log Curves (SLOG)

Because the experimental IE data was so noisy, it was necessary to use a trial-and-error method to determine the best value of the normalizing constant (I_0) to subtract from the IE curve to adjust its zero intensity value. The raw IE curve was first smoothed (SMOOTH) and a straight line was fitted to the first 50 points (LINEAR) to obtain an approximate normalizing constant. This value was then corrected by an input parameter and the normalized semi-log curve was calculated and plotted on the line-printer (SPLOT). Visual inspection of this plot (Fig. 10) showed whether the normalization was satisfactory, i.e. giving the sub-threshold region a value close to zero.

Straight line segments were also fitted to overlapping portions of this semi-log curve (e.g. 40-point segments starting at every 20th point), and the values of the intercepts and gradients of these line segments were printed out. Together with the general appearance of the plot, these parameters were used to decide where the end-points of the linear region of the semi-log curve were situated; these end-points were required for the next program (SLAP).

4.3.3 Calculation of Appearance Potentials (SLAP)

The straight line

$$y = p_1 + p_2x \quad (25)$$

was fitted to the selected linear portion of the semi-log curve using LINFIT; y is the logarithm of the normalized, quadratically smoothed IE curve (obtained from SLOG) at a nominal ionizing voltage x . The data points were weighted according to the estimated standard deviations of y , calculated to within a scaling factor c from the expression

$$\sigma_y = \frac{c(y')^{-\frac{1}{2}}}{2.303} \quad (26)$$

where y' is the normalized ionization efficiency (i.e. $y' \equiv I_V^N$, $y = \log y'$). The agreement factor calculated by LINFIT is the weighted average of the deviations between the observed and calculated points, and may be regarded as the average ratio of the observed deviations to the corresponding estimated standard deviations obtained from equation (26). The scaling factor (c) in this equation was adjusted to make the agreement factor close to unity so that the estimated standard deviations closely represented the actual observed deviations, assuming that these deviations were due to random experimental error. Points which deviated from the line by more than $3\sigma_y$ were then given zero weight (the usual criterion for eliminating occasional spurious data points), and the refinement of the parameters (p_1, p_2) was continued until the agreement factor did not change in successive cycles. The nominal ionizing voltage (x) at $y = 1.0$ and its estimated standard deviation (σ_x) were calculated from the least squares estimates of the parameters (p_1, p_2) and their standard deviations (S_1, S_2) using the expressions^{102a},

$$x = (1.0 - p_1)/p_2 \quad (27a)$$

$$\sigma_x = x \left[\left(\frac{S_1}{1.0-p_1} \right)^2 + \left(\frac{S_2}{p_2} \right)^2 \right]^{1/2} \quad (27b)$$

Fig. 11 shows an example of the output from program SLAP.

The corrected appearance potential (v) was obtained by adding to the derived value (x) the difference between the ionization potential of xenon (12.130 eV) and the measured value (x_r) of the xenon reference curve, so that

$$v = x - x_r + 12.130 \text{ eV} \quad (28a)$$

$$\sigma_v = (\sigma_x^2 + \sigma_r^2)^{1/2}. \quad (28b)$$

Weighted means (\bar{v}) of the appearance potentials (v_i , $i = 1, \dots, n$) measured for each ion, and estimated standard deviations of the means ($\sigma_{\bar{v}}$), were calculated from the following expressions^{102b},

$$\bar{v} = \frac{\sum_i w_i v_i}{\sum_i w_i} \quad (29a)$$

$$\sigma_{\bar{v}} = \left(\frac{1}{(\sum_i w_i)^2} \right)^{1/2} \quad (29b)$$

$$\sigma_{\bar{v}} = \left(\frac{\sum_i (v_i - \bar{v})^2}{n(n-1)} \right)^{1/2} \quad (29c)$$

where the weights (w_i) of the individual determinations were given by

$$w_i = \frac{1}{\sigma_{v_i}^2}, \quad i = 1, \dots, n. \quad (29d)$$

The larger of the alternative estimates of $\sigma_{\bar{v}}$ (29b, 29c) has been quoted in the results, and the individual measurements (v_i) were usually within $2\sigma_{\bar{v}}$ of the mean value (Table 8).

4.3.4 Discussion of Errors

The estimates of the standard deviations of the appearance potentials determined in the previous section (4.3.3) reflect only the errors due to the random noise on the experimental IE curves. Further systematic errors are introduced because of differences in the slopes of the linear regions of the normalized semi-log curves for different types of ions (Fig. 13). These differences in the slopes for the reference ion, compared with the fragment ions, cause the measured appearance potentials (v) to depend on the value of the ordinate (y) chosen to determine x and x_r (see equations (27) and (28)). For example, Fig. 12 shows the typical case where the slope for the reference ion is greater than that for the fragment ion. If the appearance potential (v') is determined at a value of the ordinate (y') lower than 1.0 (used in this work), then the measured voltage difference ($x' - x_r'$) between the linear regions of the semi-log curves is smaller, causing v' to be less than v by the same amount. Upper limits to the systematic errors in the appearance potentials due to this effect can be obtained by determining \bar{v}' for $y = 0$ and comparing these values with those obtained at $y = 1$. These calculations were performed for a few of the compounds and the results are presented in Table 2. The differences (Δv) observed for the ionization potentials are of the same order as the estimated standard deviations, and are therefore of little consequence. Significant differences (about 0.1 - 0.2 eV) are observed for the primary fragment ions, and large differences (about 0.5 - 1.0 eV) for the secondary fragment ions. Since the appearance potentials of the secondary fragment ions were not

Table 2

Systematic Errors in Appearance Potential Determinations^a

Compound	<i>m/e</i>	\bar{v} ($\sigma_{\bar{v}}$) ^b	\bar{v}' ($\sigma_{\bar{v}'}$) ^c	Δv ^d
(a) Benzil	210	9.20 (.03)	9.22 (.04)	0.02
	105	9.87 (.03)	9.81 (.06)	-0.06
	77	13.8 (.1)	13.4 (.1)	-0.4
(b) <i>m</i> -Fluorobenzil	228	9.23 (.02)	9.25 (.03)	0.02
	123	10.42 (.05)	10.15 (.05)	-0.27
	105	9.76 (.05)	9.56 (.05)	-0.20
	95	13.7 (.2)	13.2 (.2)	-0.5
	77	13.8 (.2)	13.4 (.2)	-0.4
(c) <i>m</i> -Methylbenzil	224	9.05 (.03)	9.01 (.02)	-0.04
	119	9.57 (.03)	9.45 (.03)	-0.12
	105	9.93 (.03)	9.76 (.03)	-0.16
	91	13.60 (.04)	13.18 (.03)	-0.4 ₂
	77	14.01 (.05)	13.2 (.1)	-0.8
(d) <i>m</i> -Formylbenzil	238	9.14 (.05)	9.13 (.05)	-0.01
	133	10.34 (.05)	10.12 (.05)	-0.22
	105	9.88 (.04)	9.70 (.03)	-0.18
	77	13.67 (.05)	13.12 (.04)	-0.55

^a All values in electron volts (eV).

^b Mean and e.s.d. determined at $\log(\text{normalized IE}) = 1$.

^c Mean and e.s.d. determined at $\log(\text{normalized IE}) = 0$.

^d $\Delta v = \bar{v}' - \bar{v}$ (approx. upper limit for the systematic error).

used in the correlations of the results they are not considered further, except to note that the tabulated values may be subject to large systematic errors - as is usually the case for such measurements.

The systematic errors in the appearance potentials of the primary fragment ions must be considered because they are significant, and because they form the basis of the conclusions reached in this work. Where correlations involve the differences between the appearance potentials for the substituted (AP_X) and unsubstituted (AP_H) ions, the systematic errors (Δv) are about the same and hence will cancel (to within the estimated standard deviations of the measurements). Where the correlations involve the appearance potentials themselves, the systematic errors will have practically no effect on the slope and the degree of the correlation because the Δv values for these ions have the same sign and are of similar magnitude. The same remarks will apply to correlations involving the differences between the appearance potentials and the ionization potentials.

4.4 FRACTIONAL ION INTENSITIES (FIX)

The fractional ion intensities of the major ions in the low voltage mass spectra were calculated as a function of energy from the smoothed ionization efficiency curves, obtained from the program RAWFIT (see section 4.2). A number of correction factors had to be applied to these calculated IE curves (DATCOM) to obtain the fractional ion intensities. The voltage scan parameters were adjusted to make the measured appearance potential obtained from the normalized IE curve (see section 4.3) coincide with the mean value determined for the particular ion. The curves were corrected for the

multiplier gain (Table 1), and also for the contributions of the other isotopic peaks of the ion. A final correction was applied by comparing the calculated fractional ion intensities with the values measured directly at several ionizing voltages. Before this could be done, the corrected IE curves for the molecule-ion and the primary fragment ions had to be extrapolated to higher energies so that the fractional intensities of these ions could be calculated up to 9-10 eV above the ionization potential. A simple linear extrapolation gave satisfactory agreement with the measured fractional intensities.

The measured fractional intensities (Table 4) were plotted as a function of the nominal ionizing voltage so that they could be compared with plots of the calculated curves obtained as a function of the corrected ionizing voltage (electron energy) using the subroutines FLOG and PLOT. Since these two energy scales may differ by a constant (but unknown) amount, the plots were shifted relative to each other along the energy axis until the threshold energies were in best agreement. Correction factors for the fractional intensity curves of each ion were then obtained by comparing the relative heights of the curves over the whole energy range. An example of the agreement generally obtained is shown in Fig. 14.

An important factor in calculating these fractional ion intensity curves was the determination of the correct threshold energies of the IE curves. These values were difficult to determine from the corrected IE curves because of the asymptotic approach to the zero level of the ion signal. However, the trial-and-error method employed was facilitated by using the fractional ion intensity scale, especially for

the important primary fragment ions, because their threshold energies usually occurred where the total ion intensity was still low, so that small errors in their calculated intensities (caused by using an incorrect value for the zero intensity) were greatly magnified in their fractional intensities. This effect caused large fluctuations to occur near the thresholds of the fractional intensity curves for these ions (e.g. Fig. 15), but had no effect at higher energies. The correct threshold energy was therefore taken as the value which gave the fractional intensity curve showing a smooth increase with energy near the threshold. This factor was much less important for the secondary fragment ions since their fractional intensities were so low that a small error in the zero intensity level had no observable effect.

The calculated fractional ion intensity curves were used to obtain the various ion intensity ratios employed in the analysis of this data. The curves had two advantages for this purpose - they referred to the true ionizing voltage (rather than the nominal voltage, as for the directly measured intensities), and the intensity ratios could be computed at any desired energy intervals, thus permitting a detailed analysis of the variation in these ratios with energy.

To make the energy scales comparable for the different compounds, the scales were converted from the (true) ionizing voltage (V) to an "excess energy" scale (E) defined by

$$E = V - IP \quad (30)$$

where IP is the ionization potential. This scale gives the mean excess energy of the electron beam above the ionization

potential and should not be confused with the internal energy of the molecule-ion. No allowance has been made for the energy distribution of the electron beam (which has a half-width of about 0.6 eV), and therefore the ionizing energy at $E = 0$ does not represent the energy where the molecule-ion has zero internal energy; negative values of E reflect the width of the electron energy distribution.

4.5 A TYPICAL ANALYSIS

This section illustrates the procedure followed in analysing the ionization efficiency data obtained from a typical experiment with *m*-methylbenzil (M-MBZl). The outputs from the various computer programs are shown graphically where possible.

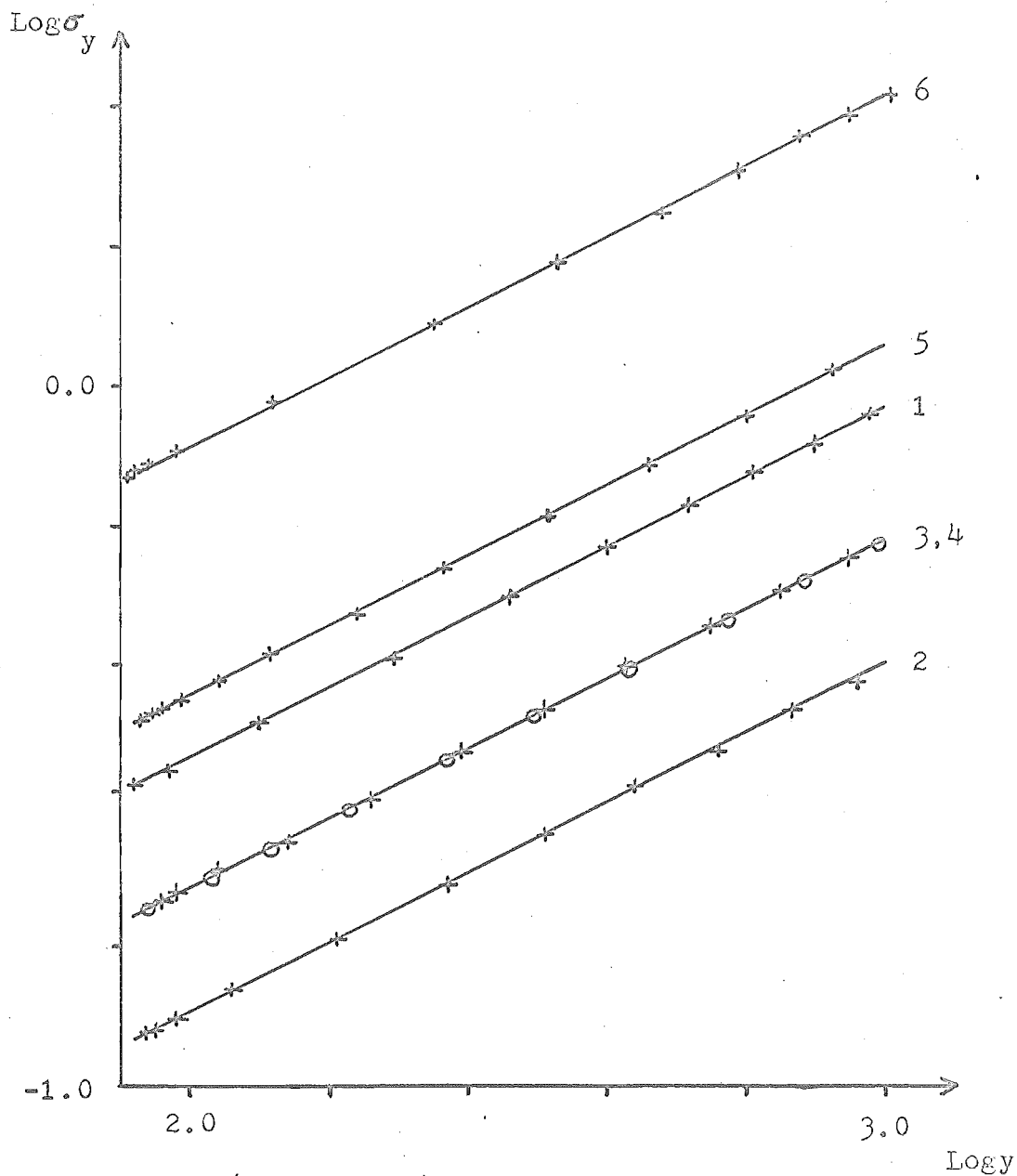
4.5.1 Program RAWFIT

The least squares estimates of the end-points (y) of the linear segments fitted to an experimental IE curve are punched on cards, together with the voltage scan parameters. These parameters are used as input data to compute smooth replicas of the noisy experimental IE curves when such smoothed curves are required, for example in the calculation of fractional ion intensities or for plotting purposes.

The relation between the root mean square value of the noise and the magnitude of the ion signal is illustrated in Fig. 9. This is a plot of $\log \sigma_y$ against $\log y$ (obtained from RAWFIT, section 4.2.2) for the reference ion and the major ions in the mass spectrum of *m*-methylbenzil, and it shows that σ_y varies as the square root of y . The values of α (equation 20) are given by the slopes of the lines.

Fig. 9. Standard Error of Ionization Efficiency.

(IE Curves for m-Methylbenzil)



	<u>m/e</u>	<u>Slope</u> (α)
1.	224	0.50
2.	119	0.50
3.	105	0.50
4.	91	0.50
5.	77	0.50
6.	132	0.51 (ref.)

4.5.2 Program SLOG

A specimen output from this program is shown for the molecule-ion (m/e 224) of *m*-methylbenzil in Fig. 10a. The unnormalized semi-log curve ($\log I_V$, without the zero threshold correction) is shown (Fig. 10b) for comparison with the normalized curve ($\log I_V^N$). The intercept (CONST) and slope (SLOPE) values for the overlapping linear segments (INTERVAL) fitted to the semi-log curve are also tabulated.

4.5.3 Program SLAP

The input parameters for this program are given under the heading (Fig. 11) EXPERIMENTAL DATA, and include the scaling factor c (EST ERROR CONST) for the estimated standard deviations σ_y of the semi-log values y (see equation 26), and the appropriate zero threshold correction and the interval for fitting the straight line obtained from program SLOG (c.f. Fig. 10). The output parameters include the agreement factor referred to in section 4.3.3 (SQRTF), and the uncorrected voltages (x) at which $y = 0$ and 1 (EPT and VPT respectively, c.f. Fig. 12).

Fig. 13 illustrates the differences in the slopes of the linear regions of the normalized semi-log plots for the different types of ions formed by *m*-methylbenzil. The semi-log curves were computed from the smoothed IE curves obtained from RAWFIT using the same normalization procedure as SLOG.

4.5.4 Program FIX

The calculated fractional ion intensities obtained from this program are tabulated as a function of the corrected ionizing voltage for comparison with the measured values in Table 4. Fig. 14 shows a plot of these fractional intensity

FIG. 10(a) Program SLOG Output: Normalized Semi-Log IE Curve

(7-12-71)M-MEZL (3) M/E=224, 13.00- 7.0CEV/10 MA.P= 8.5F-1/B/W= 50C/S.

EXPERIMENTAL DATA -

INITIAL SCAN VOLTAGE = 7.00
FINAL SCAN VOLTAGE = 12.00

LENGTH OF INTERVAL FOR QUADRATIC SMOOTHING OF C-ORDER DERIVATIVE = 41. POINTS

ZERO THRESHOLD CORRECTION -

ADJUSTED ZERO VALUE = 1.00
CALCULATED CORRECTION = 77.08

SEMI-LOG PLOT PARAMETERS -

LOG10(I.E.) AT VPT = 1.00
MINIMUM SLOPE VALUE = 0.10
PLCT SCALE FACTOR = 30.00

CALCULATED APPEARANCE POTENTIAL VALUES -

INTERVAL	CONST(ESD)	SLOPE(ESD)	CORR	EPT	VPT
300-320	-0.174737	0.140150E+01	0.232229	0.6629	7.52
320-340	-0.180933	0.140201E+01	0.146635	0.6727	7.447
340-360	-0.186429	0.140242E+01	0.172912	0.6800	7.394
360-380	-0.192100	0.140283E+01	0.241000	0.6850	7.344
380-400	-0.197941	0.140324E+01	0.247799	0.6889	7.300
400-420	-0.203945	0.140365E+01	0.345779	0.6920	7.260
420-440	-0.210104	0.140406E+01	0.424115	0.6943	7.225
440-460	-0.216419	0.140447E+01	0.483781	0.6959	7.195
460-480	-0.222890	0.140488E+01	0.524115	0.6968	7.168
480-500	-0.229517	0.140529E+01	0.546379	0.6972	7.143
500-520	-0.236300	0.140570E+01	0.560443	0.6973	7.119
520-540	-0.243240	0.140611E+01	0.566299	0.6973	7.096
540-560	-0.250337	0.140652E+01	0.573979	0.6972	7.074
560-580	-0.257591	0.140693E+01	0.583495	0.6970	7.053
580-600	-0.265002	0.140734E+01	0.594849	0.6967	7.033
600-620	-0.272570	0.140775E+01	0.608042	0.6963	7.014
620-640	-0.280295	0.140816E+01	0.623075	0.6958	6.996
640-660	-0.288177	0.140857E+01	0.639958	0.6953	6.979
660-680	-0.296216	0.140898E+01	0.658691	0.6948	6.963
680-700	-0.304412	0.140939E+01	0.679274	0.6943	6.948
700-720	-0.312765	0.140980E+01	0.701707	0.6938	6.933
720-740	-0.321275	0.141021E+01	0.726000	0.6933	6.919
740-760	-0.330042	0.141062E+01	0.752163	0.6928	6.905
760-780	-0.339066	0.141103E+01	0.779206	0.6923	6.891
780-800	-0.348347	0.141144E+01	0.807129	0.6918	6.877
800-820	-0.357885	0.141185E+01	0.835942	0.6913	6.863
820-840	-0.367680	0.141226E+01	0.865655	0.6908	6.850
840-860	-0.377731	0.141267E+01	0.896278	0.6903	6.837
860-880	-0.388038	0.141308E+01	0.927811	0.6898	6.824
880-900	-0.398601	0.141349E+01	0.960254	0.6893	6.811
900-920	-0.409420	0.141390E+01	0.993607	0.6888	6.798
920-940	-0.420495	0.141431E+01	1.027870	0.6883	6.785
940-960	-0.431826	0.141472E+01	1.063043	0.6878	6.772
960-980	-0.443413	0.141513E+01	1.099126	0.6873	6.760
980-1000	-0.455256	0.141554E+01	1.136119	0.6868	6.748

INDEX

LOG(I.E.)

VALUE

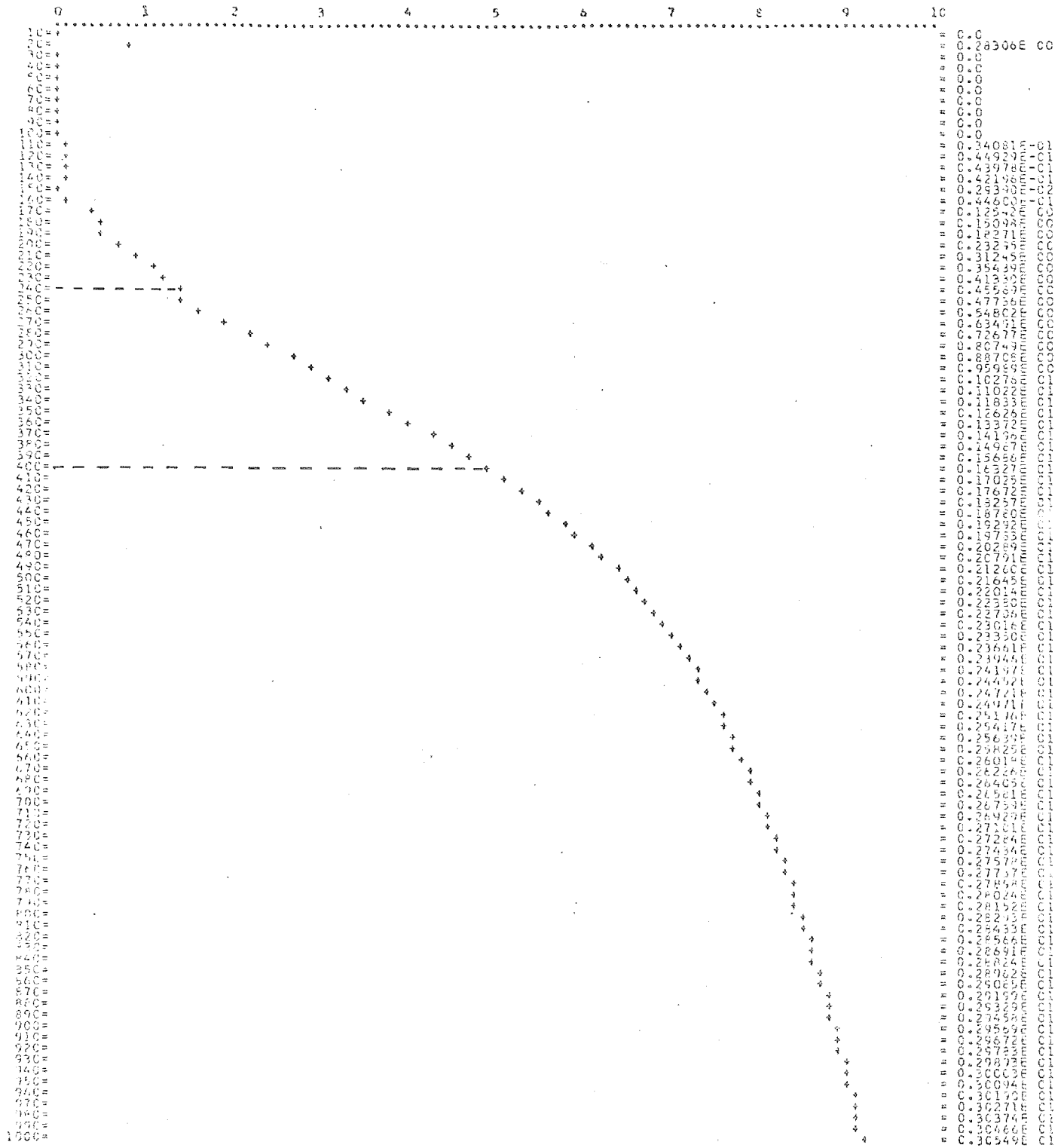


FIG. 10(b) Program SLOG Output: Unnormalized Semi-Log IE Curve

(7-12-71)H-MBZ1 (5) M/E=224, 13.00- 7.00EV/10 MA,P= 8.5E-6,I/N= 50C/S.

EXPERIMENTAL DATA -

INITIAL SCAN VOLTAGE = 7.00
 FINAL SCAN VOLTAGE =13.00

LENGTH OF INTERVAL FOR QUADRATIC SMOOTHING OF C-ORDER DERIVATIVE = 41. POINTS

ZERO THRESHOLD CORRECTION -

ADJUSTED ZERO VALUE = 78.08
 CALCULATED CORRECTION = 0.00

SEMI-LOG PLOT PARAMETERS -

LOGIC(I.E.) AT VPT = 1.00
 MINIMUM SLOPE VALUE = 0.10
 PLOT SCALE FACTOR = 30.00

CALCULATED APPEARANCE POTENTIAL VALUES -

INTERVAL	CONST(ESD)	SLOPE(ESD)	CDRR	EPT	VPT
280- 300	0.90495E 00(0.8840E-02)	0.11649E 00(0.1010E-02)	0.99886	-7.74	0.81
300- 320	0.75227E 00(0.6798E-01)	0.13576E 00(0.2995E-02)	0.99355	-1.61	2.81
320- 340	0.48232E 00(0.2309E-01)	0.23533E 00(0.2653E-02)	0.99776	0.26	4.70
340- 360	0.75363E 00(0.6018E-01)	0.20204E 00(0.4431E-02)	0.99560	2.49	5.80
360- 380	0.11358E 00(0.4986E-01)	0.26736E 00(0.7431E-02)	0.9999	3.62	6.37
380- 400	0.17573E 00(0.2134E-01)	0.21421E 00(0.3603E-02)	0.9987	4.32	6.73
400- 420	0.20104E 00(0.9128E-01)	0.22713E 00(0.3643E-02)	0.9999	4.70	6.93
420- 440	0.15017E 00(0.8716E-02)	0.43862E 00(0.3304E-02)	0.9999	4.60	6.88
440- 460	0.20498E 00(0.2342E-01)	0.47325E 00(0.2419E-02)	0.9995	4.96	7.08
460- 480	0.26344E 00(0.4417E-01)	0.42222E 00(0.2464E-02)	0.9995	5.15	7.18
480- 500	0.19213E 00(0.2233E-01)	0.43010E 00(0.3207E-02)	0.9995	4.47	6.79
500- 520	0.16743E 00(0.1671E-01)	0.40536E 00(0.1863E-02)	0.9996	4.13	6.60
520- 540	0.15363E 00(0.1497E-01)	0.37971E 00(0.1463E-02)	0.9997	4.01	6.53
540- 560	0.14101E 00(0.1597E-01)	0.37937E 00(0.2277E-02)	0.9999	3.72	6.35
560- 580	0.10198E 00(0.1182E-01)	0.34154E 00(0.1119E-02)	0.9998	2.98	5.91
580- 600	0.10370E 00(0.1365E-01)	0.34324E 00(0.1203E-02)	0.9998	3.02	5.93
600- 620	0.73353E 00(0.1973E-01)	0.21545E 00(0.3580E-02)	0.9998	2.33	5.51
620- 640	0.46707E 00(0.1069E-01)	0.24780E 00(0.1835E-02)	0.9992	1.61	5.07
640- 660	0.37748E 00(0.1049E-01)	0.24311E 00(0.1410E-02)	0.9998	1.34	4.93
660- 680	0.19187E 00(0.1059E-01)	0.25397E 00(0.1410E-02)	0.9995	0.71	4.50
680- 700	0.19918E 00(0.1120E-01)	0.24415E 00(0.5594E-03)	0.9999	0.31	4.25
700- 720	0.10067E 00(0.1189E-01)	0.23597E 00(0.1059E-02)	0.9997	0.11	4.10
720- 740	0.10070E 00(0.1109E-01)	0.23036E 00(0.1507E-02)	0.9992	-0.32	3.52
740- 760	0.11170E 00(0.1276E-01)	0.22813E 00(0.1143E-02)	0.9994	-0.93	3.45
760- 780	0.67700E 00(0.1191E-01)	0.20511E 00(0.1120E-02)	0.9995	-1.54	2.54
780- 800	0.46761E 00(0.8873E-01)	0.20890E 00(0.5024E-02)	0.9999	-2.09	2.70
800- 820	0.26070E 00(0.2340E-02)	0.20331E 00(0.6132E-02)	0.9998	-2.46	2.46
820- 840	0.40503E 00(0.1156E-01)	0.20464E 00(0.6747E-02)	0.9998	-2.17	2.52
840- 860	0.61245E 00(0.1189E-01)	0.19883E 00(0.6765E-02)	0.9995	-3.49	1.78
860- 880	0.57227E 00(0.1075E-01)	0.19648E 00(0.6929E-02)	0.9996	-2.93	3.15
880- 900	0.88139E 00(0.1181E-01)	0.17883E 00(0.7611E-02)	0.9994	-2.96	0.80
900- 920	0.78094E 00(0.1240E-01)	0.17929E 00(0.4731E-02)	0.9999	-5.10	0.71
920- 940	0.19111E 00(0.1263E-01)	0.16075E 00(0.1027E-02)	0.9992	-6.35	-1.03
940- 960	0.12140E 00(0.1263E-01)	0.14608E 00(0.2731E-02)	0.9995	-5.55	-1.60
960-1000	0.11647E 00(0.9598E-02)	0.14927E 00(0.7531E-02)	0.9995	-7.30	-1.10

INDEX

LOG(I.E.)

VALUE

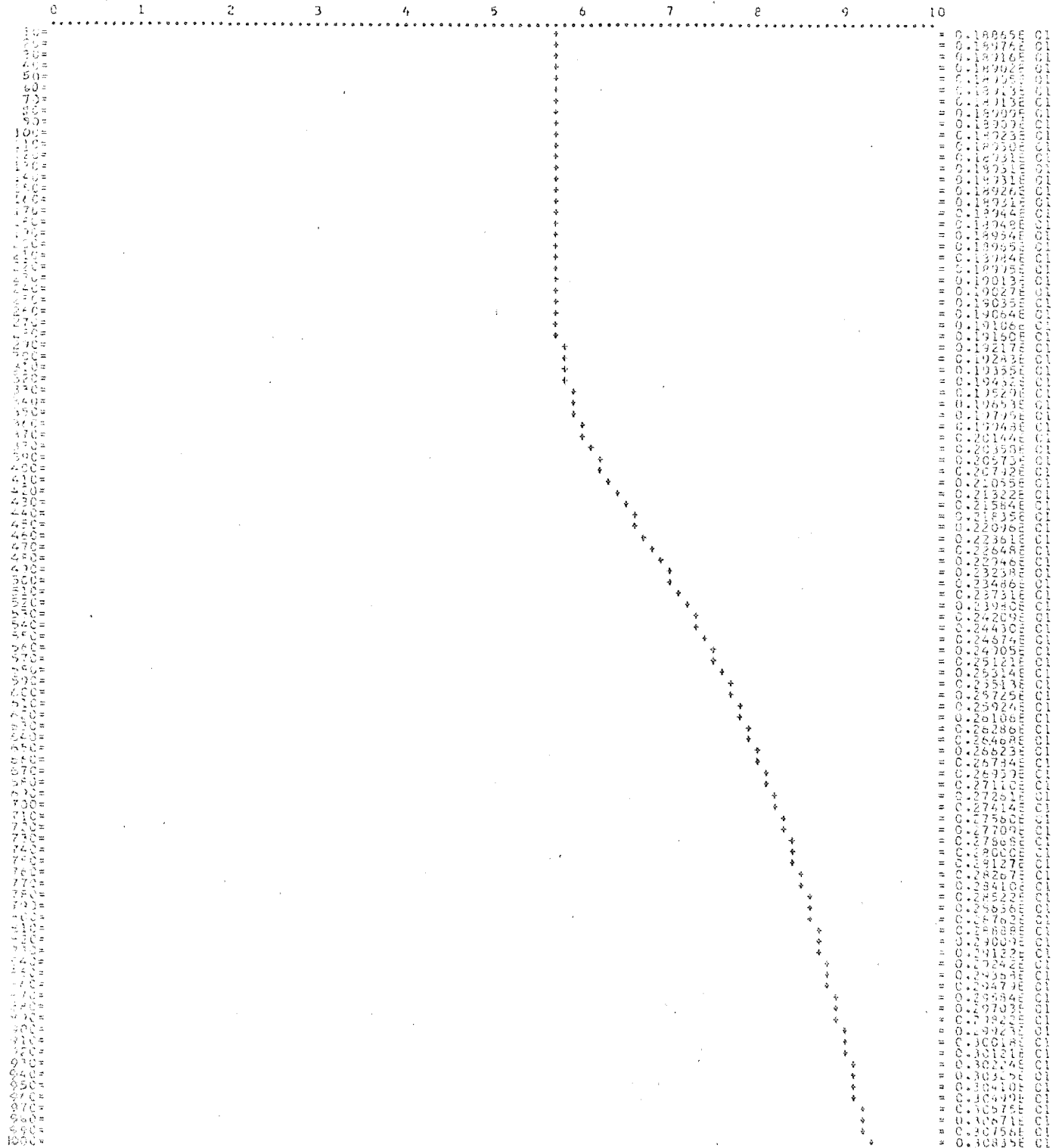


FIG. 11 Program SLAP Output

RECORD NUMBER 1 (7-12-71)M-MBZ (3) M/E=224, 12.00- 7.00EV/10 MA, P= 2.5E-4.8/W= 50G/S.

EXPERIMENTAL DATA -
 INITIAL SCAN VOLTAGE = 7.00
 FINAL SCAN VOLTAGE = 13.00
 EST ERROR CONSTANT = 0.06
 MAX ERROR ALLOWED = 3.00

LENGTH OF INTERVAL FOR QUADRATIC SMOOTHING OF 0-ORDER DERIVATIVE = 41. POINTS

ADJUSTED ZERO VALUE = 1.00
 CALCULATED CORRECTION = 77.08
 LOG(CIT(.5)) AT VPT = 1.00

INTERVAL FOR L-S FIT -
 INITIAL DATA POINT = 240
 FINAL DATA POINT = 400

LEAST-SQUARES FIT OF STRAIGHT LINE TO SEMI-LOG I.E. CURVE -

DERIVATIVES PROGRAMMED BY USER
 WEIGHTS TO BE SUPPLIED BY USER
 PARAMETERS TO BE ESTIMATED FROM RAW DATA
 CORRECTED PARAMETERS NOT TO BE SAVED FOR LATER USE
 NUMBER OF CYCLES IN THIS JOB IS 4
 NUMBER OF PARAMETERS READ IS 2
 NUMBER OF PARAMETERS TO BE VARIED IS 2
 NUMBER OF OBSERVATIONS READ IS 161

INPUT DATA

I	P(I)	KI(I)	DI(I)
1	-0.100000E 02	1	0.0
2	0.100000E 01	1	0.0

CALCULATED Y BASED ON PARAMETERS BEFORE CYCLE 1
 AGREEMENT FACTORS BASED ON PARAMETERS BEFORE CYCLE 1
 NUMBER OF D.O.F. IS 159.
 SUM(W*(O-C)**2) IS 0.173E 08
 SORTF(SUM(W*(O-C)**2)/(D.O.F.)) IS 329.5393
 PARAMETERS AFTER LEAST SQUARES CYCLE 1

	OLD	CHANGE	NEW	ERROR
1	-0.100000E 02	-0.562012E 00	-0.105620E 02	0.224050E-01
2	0.100000E 01	0.306895E 00	0.130689E 01	0.246953E-02

ESTIMATED AGREEMENT FACTORS BASED ON PARAMETERS AFTER CYCLE 1
 NUMBER OF D.O.F. IS 159.
 SUM(W*(O-C)**2) IS 0.176E 08
 SORTF(SUM(W*(O-C)**2)/(D.O.F.)) IS 1.0521
 CALCULATED Y BASED ON PARAMETERS BEFORE CYCLE 2

REJECTED DATA POINTS - ICXIG I YO(I) YC CY WCY

AGREEMENT FACTORS BASED ON PARAMETERS BEFORE CYCLE 2
 NUMBER OF D.O.F. IS 159.
 SUM(W*(O-C)**2) IS 0.192E 08
 SORTF(SUM(W*(O-C)**2)/(D.O.F.)) IS 1.1003
 PARAMETERS AFTER LEAST SQUARES CYCLE 2

	OLD	CHANGE	NEW	ERROR
1	-0.100000E 02	-0.309645E-01	-0.103096E 02	0.239847E-01

NUMBER OF D.O.F. IS 159.

SUM(W*(O-C)**2) IS 0.140E 03

SQRTF(SUM(W*(O-C)**2)/(D.O.F.)) IS 1.0944

CALCULATED Y BASED ON PARAMETERS BEFORE CYCLE 3

REJECTED DATA POINTS	I	ICRIG	I	YC(I)	YC	DY	WCY
	399		160	0.162567E 01	0.163771E 01	-0.120411E-01	-0.300309E 01
	400		161	0.163269E 01	0.164540E 01	-0.127039E-01	-0.319411E 01

AGREEMENT FACTORS BASED ON PARAMETERS BEFORE CYCLE 3

NUMBER OF D.O.F. IS 157.

SUM(W*(O-C)**2) IS 0.171E 03

SQRTF(SUM(W*(O-C)**2)/(D.O.F.)) IS 1.0442

PARAMETERS AFTER LEAST SQUARES CYCLE 3

	OLD	CHANGE	NEW	ERROR
1	-0.105227E 02	-0.225917E-01	-0.106152E 02	0.226749E-01
2	0.131026E 01	0.254065E-02	0.131280E 01	0.250203E-02

ESTIMATED AGREEMENT FACTORS BASED ON PARAMETERS AFTER CYCLE 3

NUMBER OF D.O.F. IS 157.

SUM(W*(O-C)**2) IS 0.169E 03

SQRTF(SUM(W*(O-C)**2)/(D.O.F.)) IS 1.0385

CALCULATED Y BASED ON PARAMETERS BEFORE CYCLE 4

REJECTED DATA POINTS	I	ICRIG	I	YC(I)	YC	DY	WCY
	399		160	0.162567E 01	0.162887E 01	-0.122046E-01	-0.329326E 01
	400		161	0.163269E 01	0.164657E 01	-0.126817E-01	-0.349024E 01

AGREEMENT FACTORS BASED ON PARAMETERS BEFORE CYCLE 4

NUMBER OF D.O.F. IS 157.

SUM(W*(O-C)**2) IS 0.169E 03

SQRTF(SUM(W*(O-C)**2)/(D.O.F.)) IS 1.0385

PARAMETERS AFTER LEAST SQUARES CYCLE 4

	OLD	CHANGE	NEW	ERROR
1	-0.106152E 02	-0.259140E-03	-0.106155E 02	0.226740E-01
2	0.131280E 01	0.287493E-04	0.131283E 01	0.250194E-02

ESTIMATED AGREEMENT FACTORS BASED ON PARAMETERS AFTER CYCLE 4

NUMBER OF D.O.F. IS 157.

SUM(W*(O-C)**2) IS 0.169E 03

SQRTF(SUM(W*(O-C)**2)/(D.O.F.)) IS 1.0385

CALCULATED Y BASED ON PARAMETERS BEFORE CYCLE 5

REJECTED DATA POINTS	I	ICRIG	I	YC(I)	YC	DY	WCY
	399		160	0.162567E 01	0.163589E 01	-0.122122E-01	-0.329517E 01
	400		161	0.163269E 01	0.164658E 01	-0.126903E-01	-0.349240E 01

AGREEMENT FACTORS BASED ON PARAMETERS BEFORE CYCLE 5

NUMBER OF D.O.F. IS 157.

SUM(W*(O-C)**2) IS 0.169E 03

SQRTF(SUM(W*(O-C)**2)/(D.O.F.)) IS 1.0385

CORRELATION MATRIX

1	1.000-1.000
2	1.000

CALCULATED APPEARANCE POTENTIAL = EPT (E.S.D.) VPT (E.S.D.)
 8.0860 (0.0231) 8.8477 (0.0241)

Fig. 12. Systematic Errors in Appearance Potential Determinations:

'VPT' : $y = 1.0$

'EPT' : $y' = 0.0$

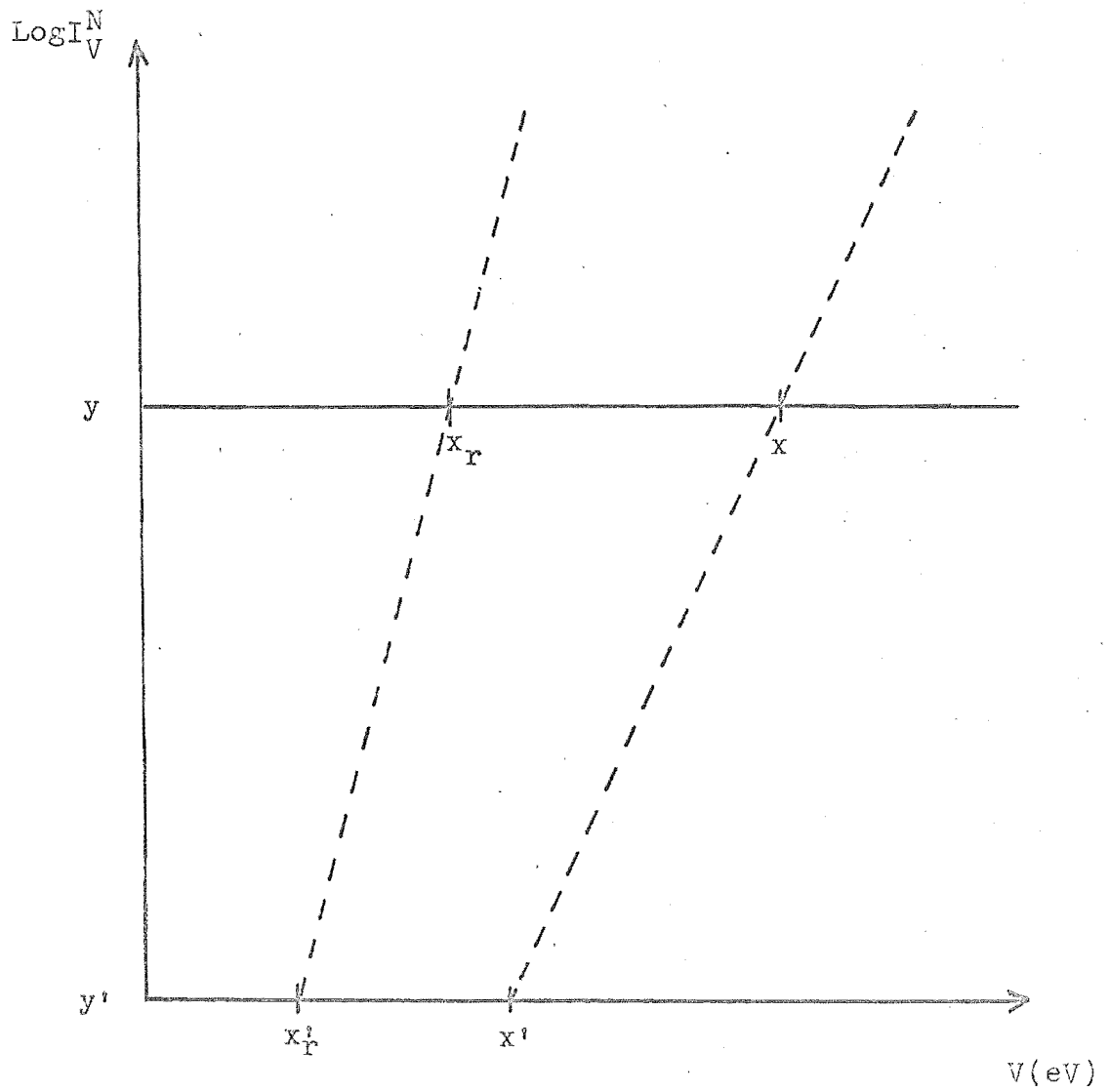
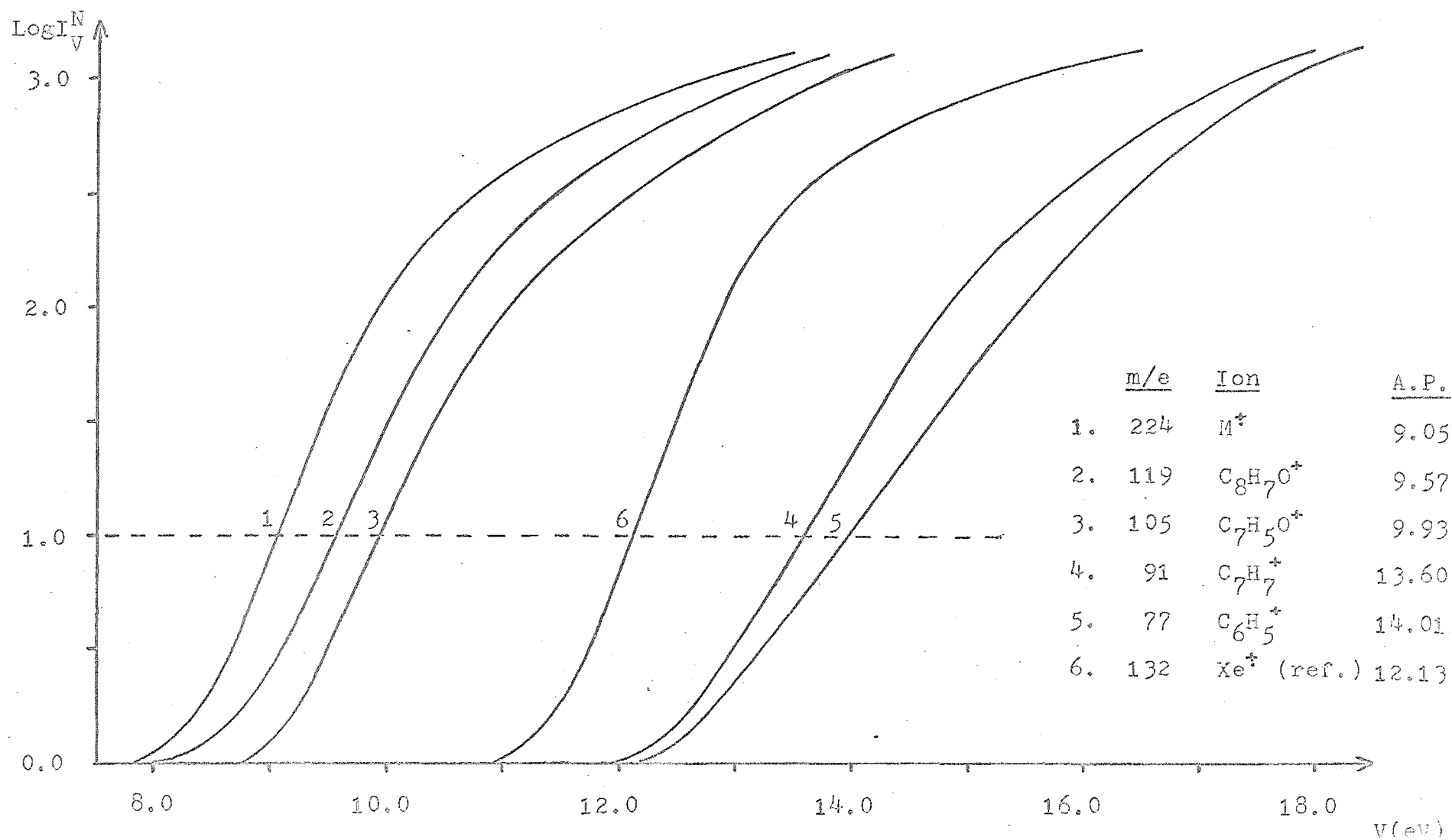


Fig. 13. Normalized Semi-Log Ionization Efficiency Curves for m-Methylbenzil.



curves for the major ions in the mass spectrum of *m*-methylbenzil (some of the curves are multiplied by a scale factor). The measured fractional intensities are marked by the crosses to illustrate the agreement obtained between the calculated and measured values.

Fig. 15 illustrates the effect of using an incorrect value for the threshold of the ion intensity, particularly for the primary fragment ion having the lowest appearance potential (i.e. m/e 119(2) for *m*-methylbenzil).

Fig. 14

M-METHYLBENZIL

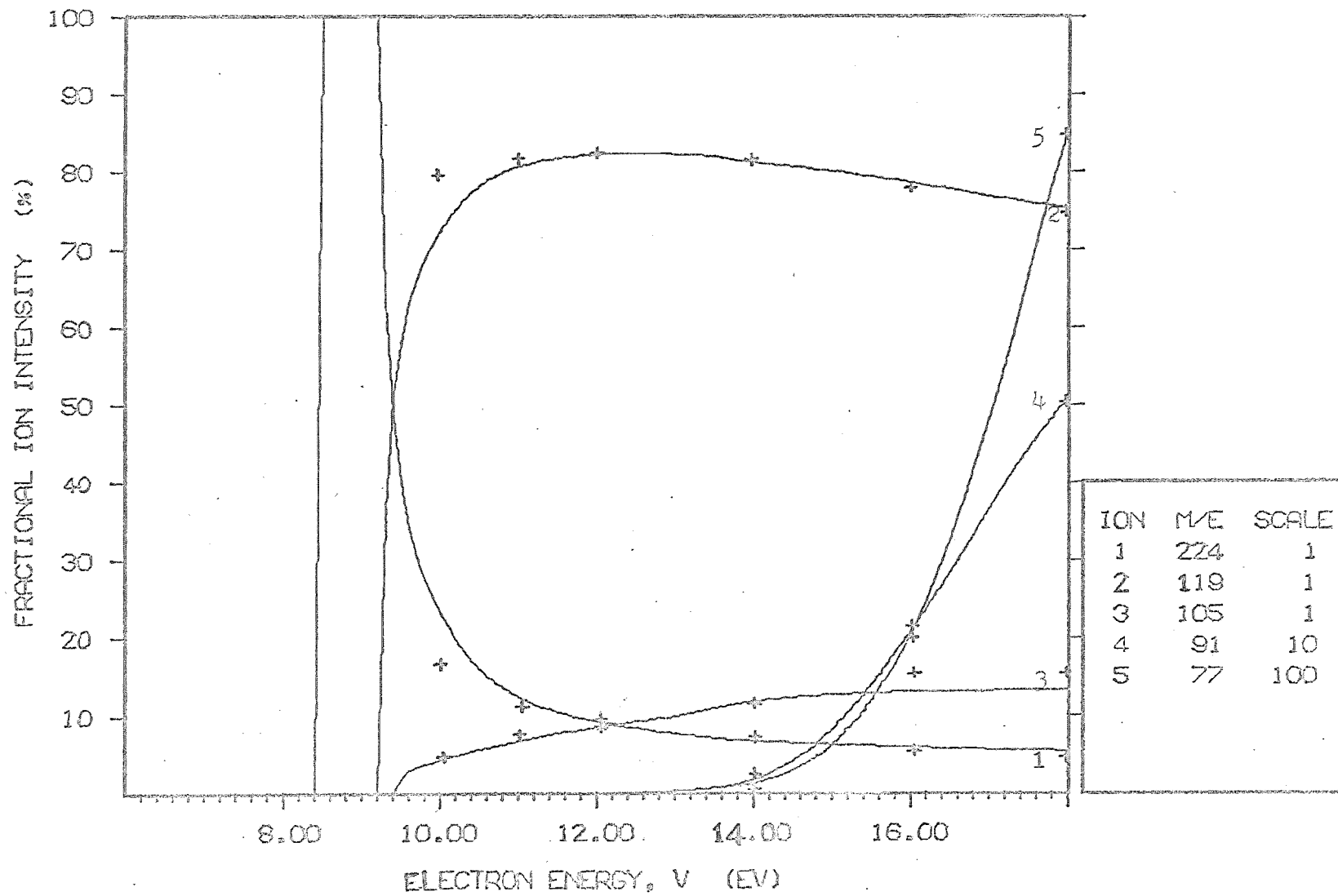
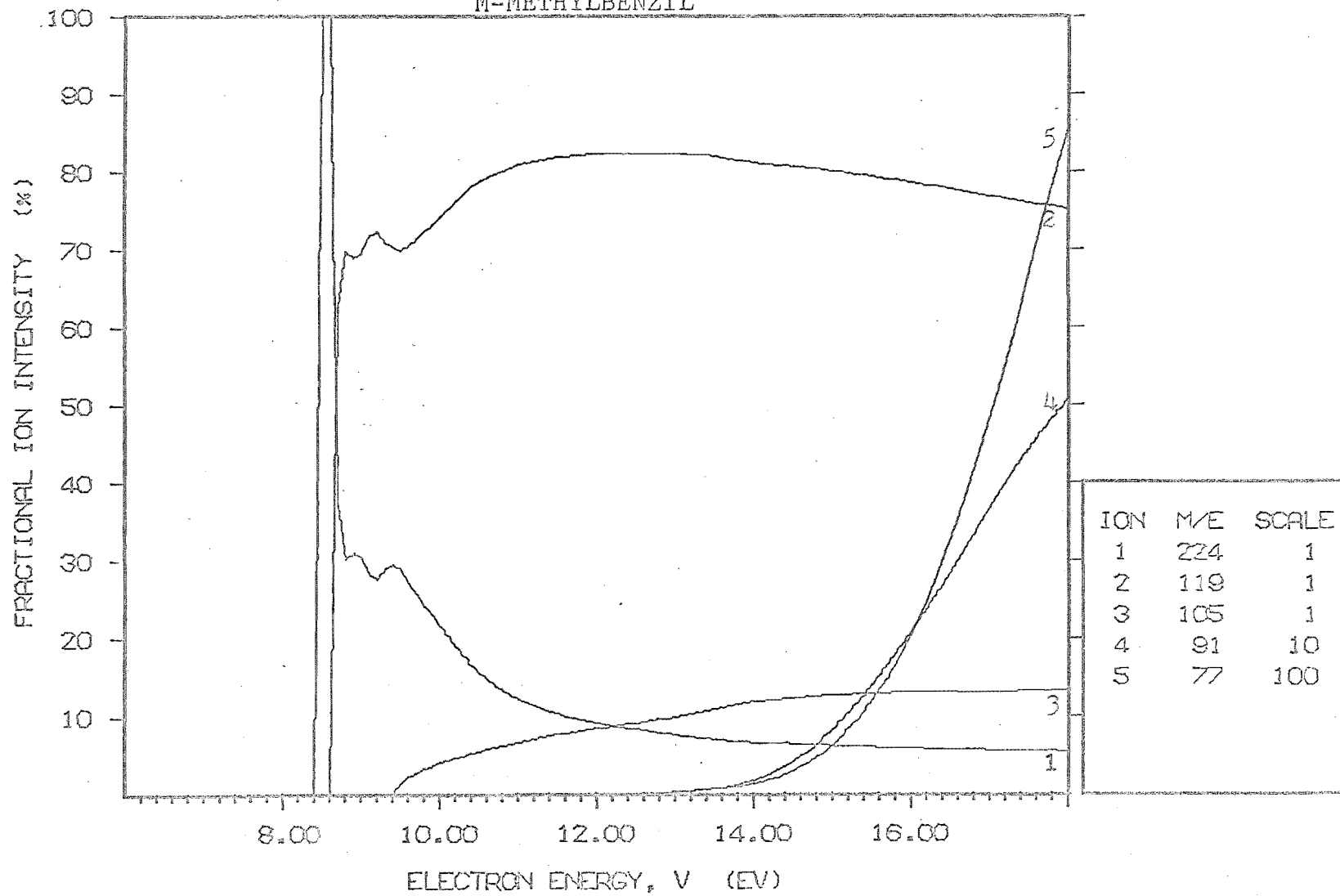


Fig. 15 Effect of Incorrect Zero Threshold Intensity
M-METHYLBENZIL



C H A P T E R 5

RESULTS

5.1 MASS SPECTRA (70 and 20 eV)

The mass spectra of the benzils, measured at nominal ionizing voltages of 70 and 20 eV as described in section 3.3.1, are shown in Fig. 16 (a-m). These plots show the mean values of the ion intensities measured relative to the base peak (100%) from at least three separate chart recordings. They have not been corrected for isotopic contributions. The relative ion intensities (I_{rel}) tabulated in Table 3(a-m) were obtained from the same data, but the intensities for each ion have been corrected for isotopic contributions (the tabulated m/e value refers to the isotope of lowest mass). The estimated standard deviations ($\sigma_{\bar{Y}}$) of the mean relative intensities (\bar{Y}) were calculated from the expression^{102b}

$$\sigma_{\bar{Y}} = \left(\frac{\sum_{i=1}^n (Y_i - \bar{Y})^2}{n(n-1)} \right)^{1/2} \quad (31)$$

Where the composition of an ion was in doubt it was determined by mass measurement.

Table 3

Relative Ion Intensities (70 and 20 eV Mass Spectra)

m/e	Ion	70 eV		20 eV	
		I _{rel}	(e.s.d.)	I _{rel}	(e.s.d.)
210	C ₁₄ H ₁₀ O ₂ ⁺	5.6	(0.4)	4.9	(0.9)
105	C ₇ H ₅ O ⁺	100		100	
77	C ₆ H ₅ ⁺	37.7	(0.5)	10.9	(0.8)
76	C ₆ H ₄ ⁺	1.2	(0.1)		
75	C ₆ H ₃ ⁺	0.7	(0.2)		
74	C ₆ H ₂ ⁺	0.8	(0.2)		
51	C ₄ H ₃ ⁺	13.9	(0.5)	0.3	(0.1)
50	C ₄ H ₂ ⁺	3.6	(0.3)		

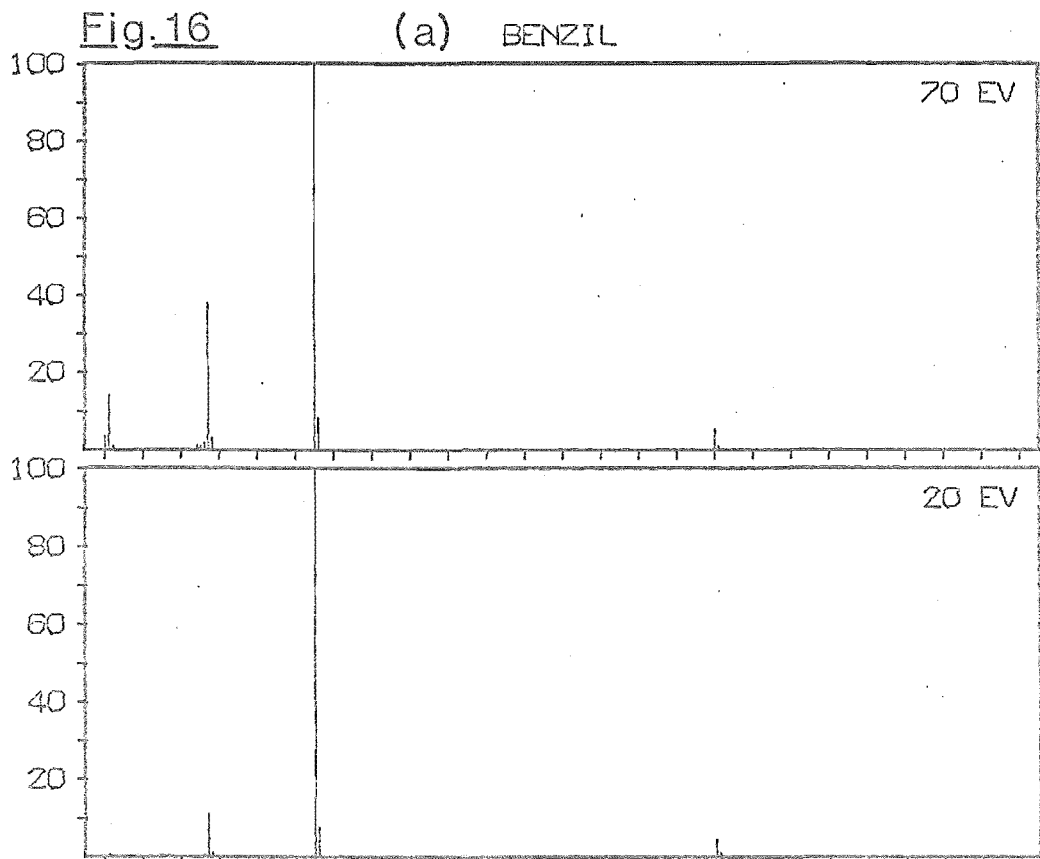


Table 3

Relative Ion Intensities (70 and 20 eV Mass Spectra)

(b) *m*-Fluorobenzil

<i>m/e</i>	Ion	70 eV		20 eV	
		<i>I</i> _{rel}	(e.s.d.)	<i>I</i> _{rel}	(e.s.d.)
228	C ₁₄ H ₉ O ₂ F ⁺	2.3	(0.4)	2.5	(0.4)
123	C ₇ H ₄ OF ⁺	15.0	(0.4)	12.0	(0.4)
105	C ₇ H ₅ O ⁺	100		100	
95	C ₆ H ₄ F ⁺	16.0	(0.4)	3.9	(0.6)
94	C ₆ H ₃ F ⁺	0.7	(0.1)		
77	C ₆ H ₅ ⁺	37.6	(0.9)	15.0	(1.1)
76	C ₆ H ₄ ⁺	1.3	(0.2)		
75	C ₆ H ₃ ⁺	6.8	(0.5)		
74	C ₆ H ₂ ⁺	1.5	(0.2)		
69	C ₄ H ₂ F ⁺	1.2	(0.1)		
51	C ₄ H ₃ ⁺	12.5	(0.4)		
50	C ₄ H ₂ ⁺	4.0	(0.2)		

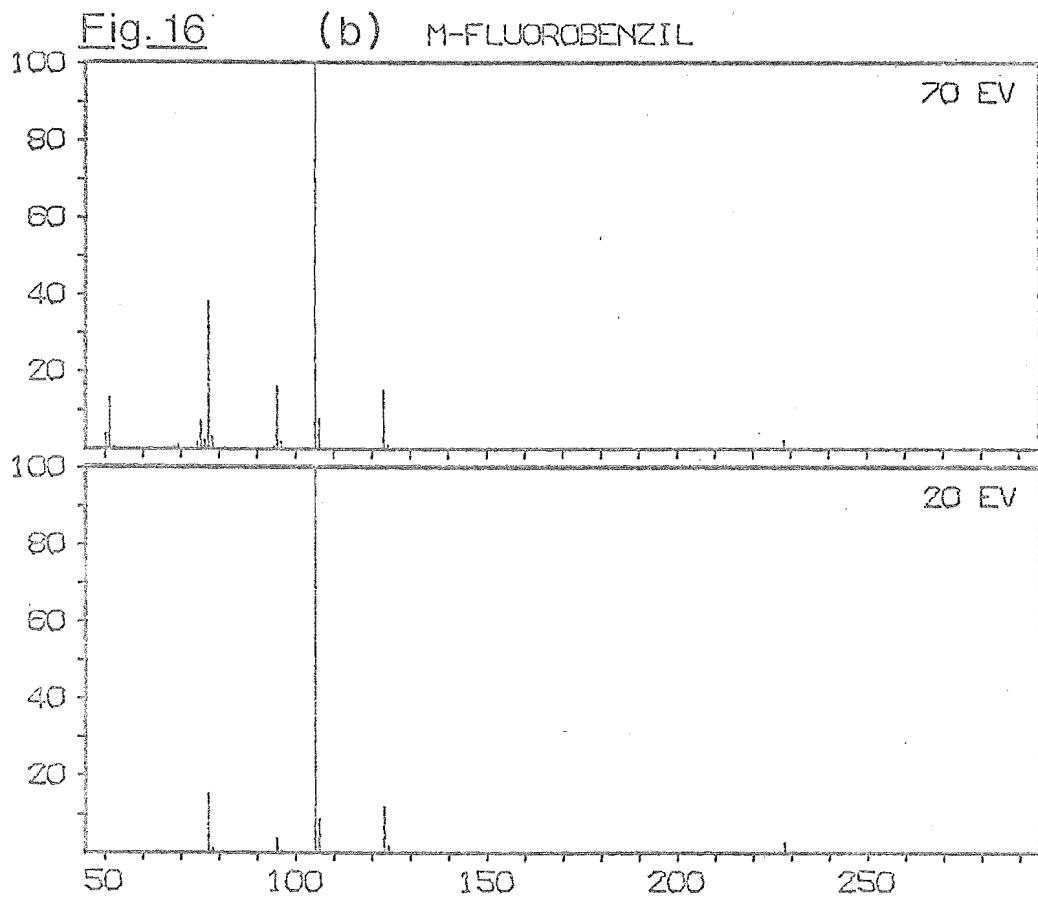


Table 3

Relative Ion Intensities (70 and 20 eV Mass Spectra)

(c) *p*-Fluorobenzil

<i>m/e</i>	Ion	70 eV		20 eV	
		<i>I</i> _{rel}	(e.s.d.)	<i>I</i> _{rel}	(e.s.d.)
228	$C_{14}H_9O_2F^+$	2.6	(0.0)	2.5	(0.0)
215		0.5	(0.0)	0.9	(0.0)
123	$C_7H_4OF^+$	44.1	(0.1)	36.6	(0.2)
105	$C_7H_5O^+$	100		100	
95	$C_6H_4F^+$	17.6	(0.0)	4.0	(0.0)
94	$C_6H_3F^+$	0.7	(0.0)		
77	$C_6H_5^+$	28.2	(0.1)	10.6	(0.1)
76	$C_6H_4^+$	0.8	(0.0)		
75	$C_6H_3^+$	5.3	(0.0)		
74	$C_6H_2^+$	1.1	(0.0)		
69	$C_4H_2F^+$	1.0	(0.0)		
51	$C_4H_3^+$	8.2	(0.1)		
50	$C_4H_2^+$	2.8	(0.0)		

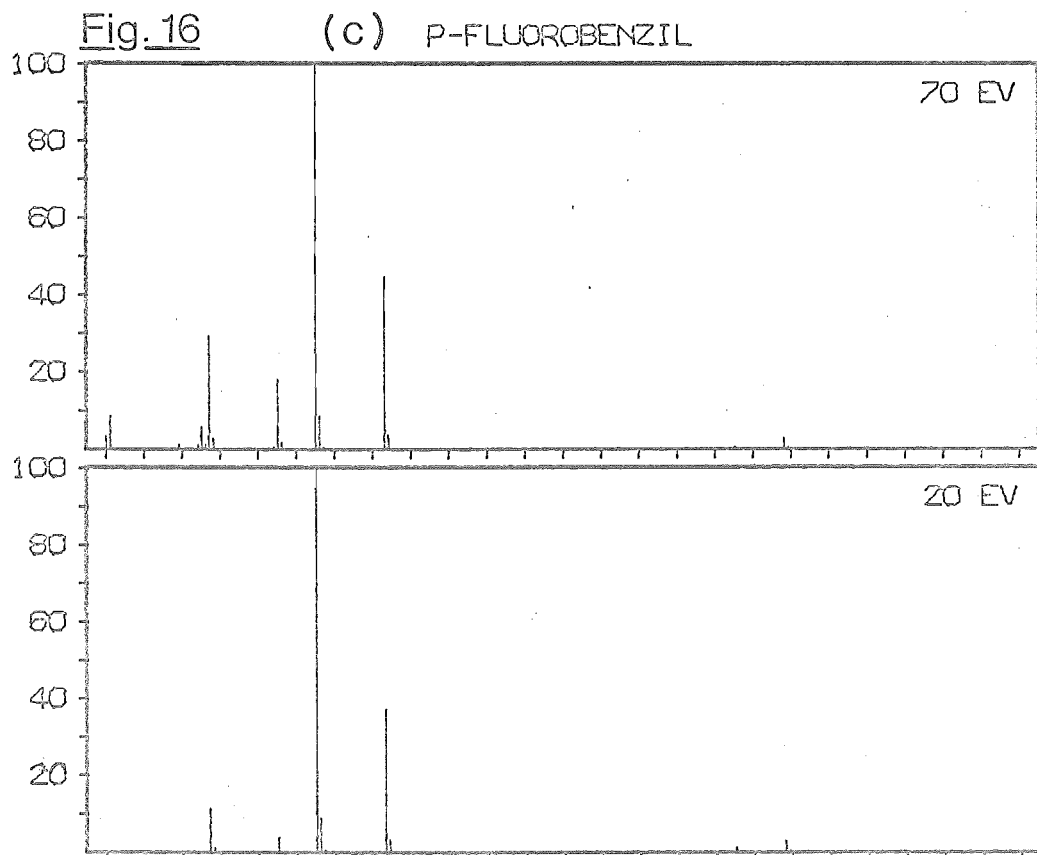


Table 3

Relative Ion Intensities (70 and 20 eV Mass Spectra)

(d) *m*-Chlorobenzil

<i>m/e</i>	Ion	70 eV		20 eV	
		<i>I</i> _{rel}	(e.s.d.)	<i>I</i> _{rel}	(e.s.d.)
244	C ₁₄ H ₉ O ₂ Cl ⁺	2.4	(0.2)	2.3	(0.3)
139	C ₇ H ₄ OCl ⁺	15.7	(0.8)	10.6	(0.5)
111	C ₆ H ₄ Cl ⁺	11.1	(0.6)	2.8	(0.5)
105	C ₇ H ₅ O ⁺	100		100	
77	C ₆ H ₅ ⁺	29.7	(0.6)	5.9	(0.0)
76	C ₆ H ₄ ⁺	1.7	(0.2)		
75	C ₆ H ₃ ⁺	5.9	(0.4)		
74	C ₆ H ₂ ⁺	1.5	(0.2)		
51	C ₄ H ₃ ⁺	9.2	(0.5)		
50	C ₄ H ₂ ⁺	4.2	(0.3)		

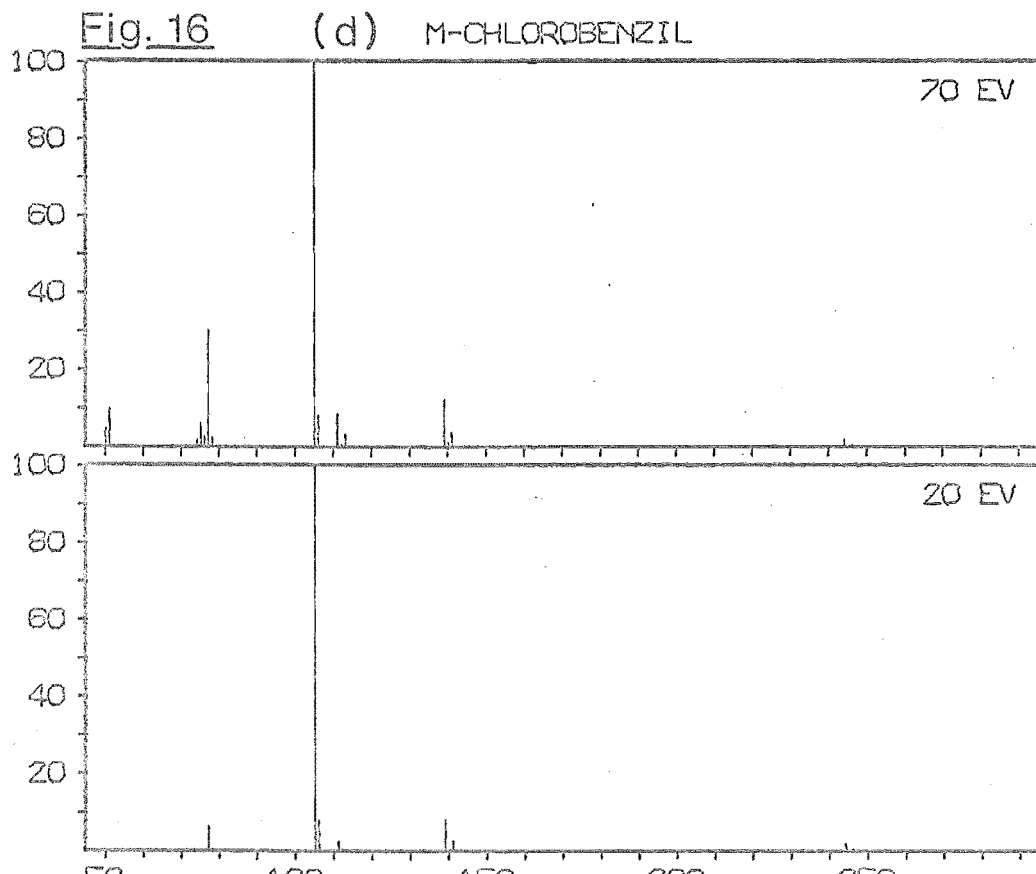


Table 3

Relative Ion Intensities (70 and 20 eV Mass Spectra)

(e) *m*-Bromobenzil

<i>m/e</i>	Ion	70 eV		20 eV	
		<i>I</i> _{rel}	(e.s.d.)	<i>I</i> _{rel}	(e.s.d.)
288	C ₁₄ H ₉ O ₂ Br ⁺	1.7	(0.0)	1.9	(0.0)
183	C ₇ H ₄ OBr ⁺	12.0	(0.1)	9.7	(0.0)
155	C ₆ H ₄ Br ⁺	8.1	(0.0)	3.3	(0.0)
105	C ₇ H ₅ O ⁺	100		100	
77	C ₆ H ₅ ⁺	21.2	(0.2)	7.2	(0.2)
76	C ₆ H ₄ ⁺	4.2	(0.0)		
75	C ₆ H ₃ ⁺	3.6	(0.0)		
74	C ₆ H ₂ ⁺	1.0	(0.0)		
51	C ₄ H ₃ ⁺	5.2	(0.1)		
50	C ₄ H ₂ ⁺	3.5	(0.0)		

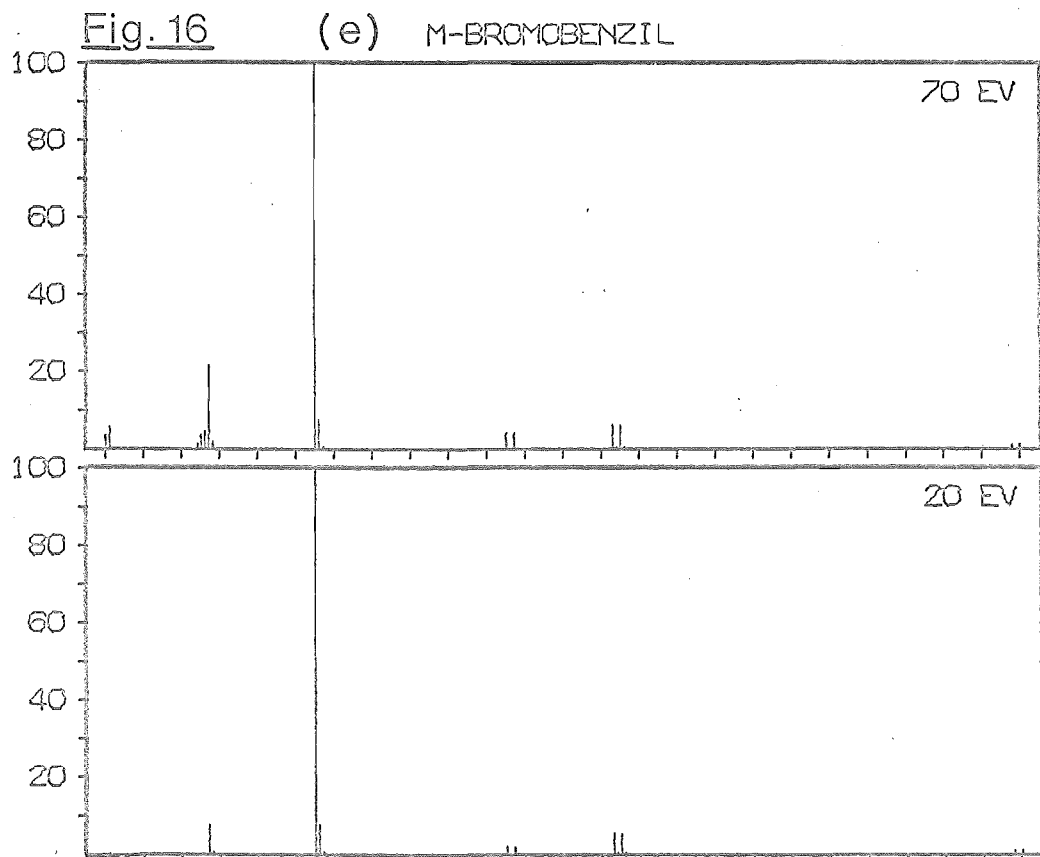


Table 3

Relative Ion Intensities (70 and 20 eV Mass Spectra)

(f) *p*-Bromobenzil

m/e	Ion	70 eV		20 eV	
		I _{rel}	(e.s.d.)	I _{rel}	(e.s.d.)
288	C ₁₄ H ₉ O ₂ Br ⁺	4.7	(0.4)	5.2	(0.4)
183	C ₇ H ₄ OBr ⁺	38.4	(0.5)	34.4	(0.3)
155	C ₆ H ₄ Br ⁺	14.8	(0.4)	3.6	(0.1)
105	C ₇ H ₅ O ⁺	100		100	
77	C ₆ H ₅ ⁺	29.3	(0.7)	5.3	(0.5)
76	C ₆ H ₄ ⁺	8.5	(0.3)		
75	C ₆ H ₃ ⁺	7.3	(0.3)		
74	C ₆ H ₂ ⁺	2.6	(0.2)		
51	C ₄ H ₃ ⁺	8.3	(0.1)		
50	C ₄ H ₂ ⁺	2.8	(0.0)		

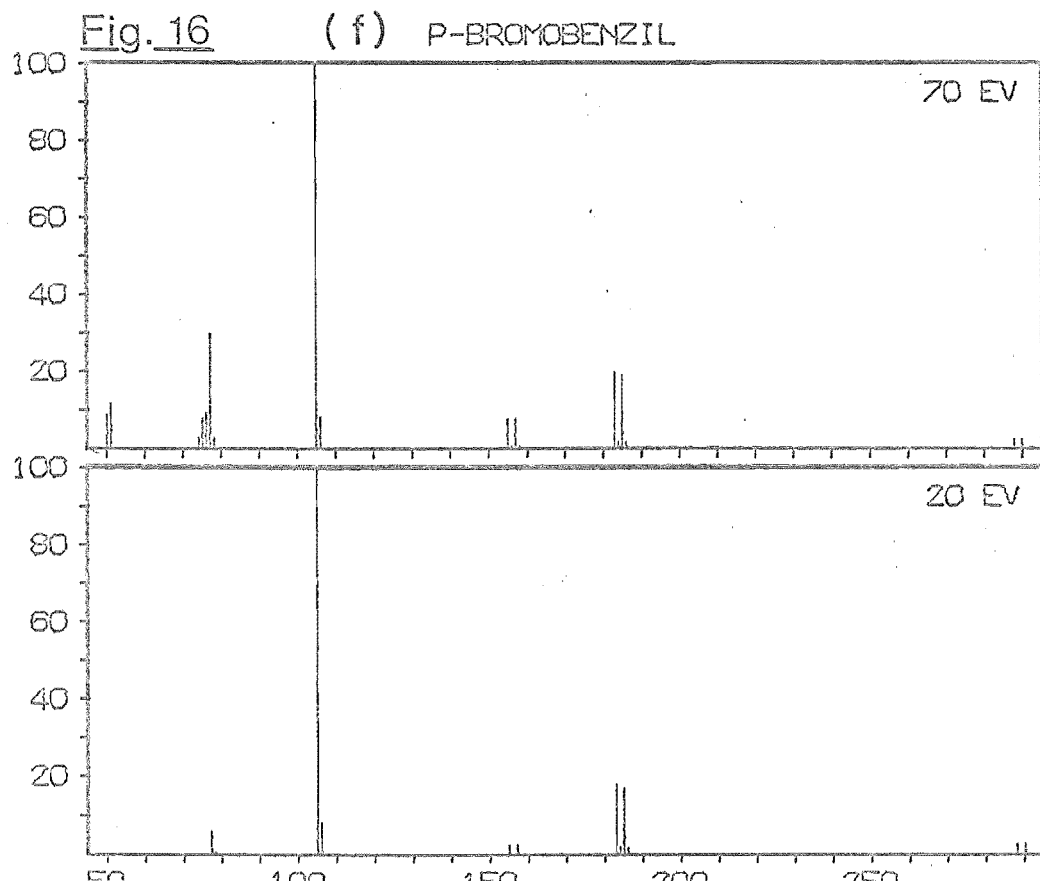


Table 3

Relative Ion Intensities (70 and 20 eV Mass Spectra)

(g) <i>m</i> -Methylbenzil		70 eV		20 eV	
<i>m/e</i>	Ion	<i>I</i> _{rel}	(e.s.d.)	<i>I</i> _{rel}	(e.s.d.)
224	C ₁₅ H ₁₂ O ₂ ⁺	6.1	(0.8)	6.6	(0.9)
119	C ₈ H ₇ O ⁺	100		100	
105	C ₇ H ₅ O ⁺	37.7	(0.9)	30.0	(1.3)
91	C ₇ H ₇ ⁺	30.2	(0.9)	12.7	(0.6)
90	C ₇ H ₆ ⁺	1.1	(0.3)		
89	C ₇ H ₅ ⁺	1.8	(0.3)		
77	C ₆ H ₅ ⁺	19.7	(0.9)	3.5	(0.8)
76	C ₆ H ₄ ⁺	0.9	(0.2)		
65	C ₅ H ₅ ⁺	9.4	(0.8)	0.7	(0.6)
63	C ₅ H ₃ ⁺	1.9	(0.4)		
51	C ₄ H ₃ ⁺	7.7	(0.8)		
50	C ₄ H ₂ ⁺	2.2	(0.4)		
41	C ₃ H ₅ ⁺	1.2	(0.2)		
39	C ₃ H ₃ ⁺	3.8	(0.4)		

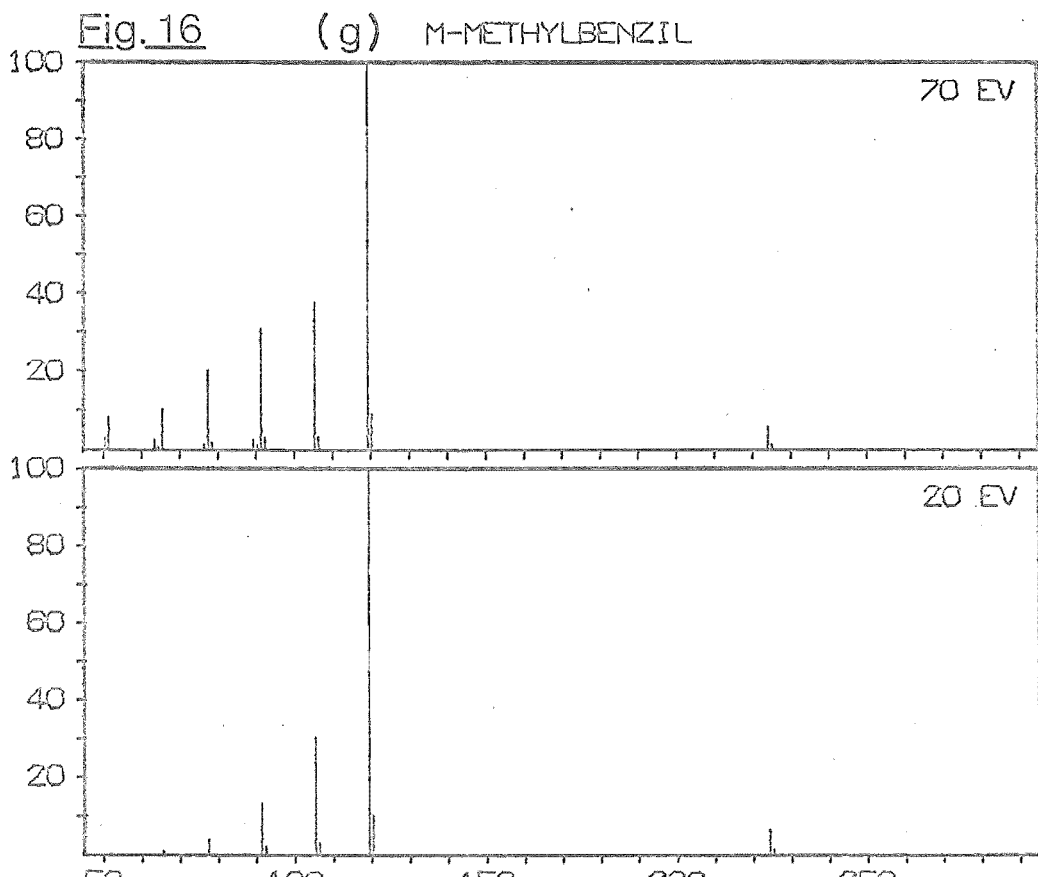


Table 3

Relative Ion Intensities (70 and 20 eV Mass Spectra)

(h) *m*-Methoxybenzil

<i>m/e</i>	Ion	70 eV		20 eV	
		<i>I</i> _{rel}	(e.s.d.)	<i>I</i> _{rel}	(e.s.d.)
240	C ₁₅ H ₁₂ O ₃ ⁺	11.0	(0.1)	13.0	(0.0)
135	C ₈ H ₇ O ₂ ⁺	100		100	
107	C ₇ H ₇ O ⁺	17.5	(0.2)	9.8	(0.1)
105	C ₇ H ₅ O ⁺	41.8	(0.4)	32.6	(0.0)
92	C ₆ H ₄ O ⁺	7.1	(0.2)	0.8	(0.0)
77	C ₆ H ₅ ⁺	28.8	(0.4)	5.8	(0.0)
76	C ₆ H ₄ ⁺	1.4	(0.0)		
64	C ₅ H ₄ ⁺	3.4	(0.1)		
63	C ₅ H ₃ ⁺	2.1	(0.1)		
51	C ₄ H ₃ ⁺	5.3	(0.1)		
50	C ₄ H ₂ ⁺	1.9	(0.0)		

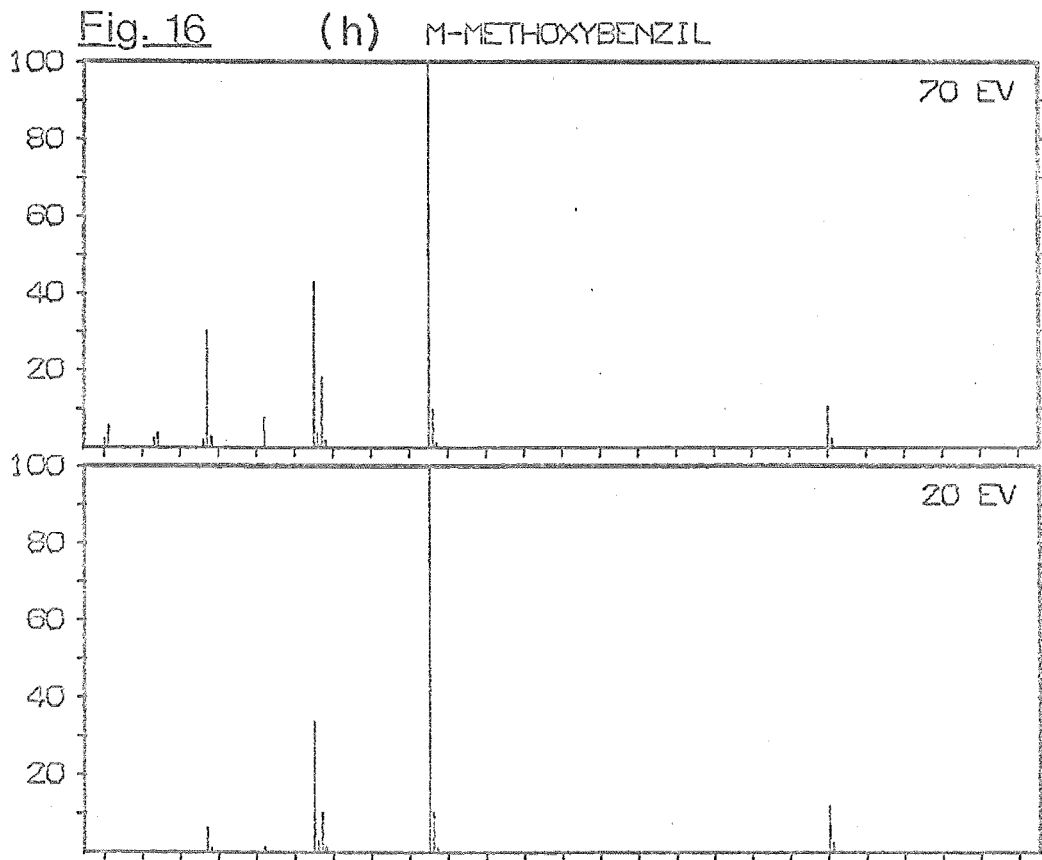


Table 3

Relative Ion Intensities (70 and 20 eV Mass Spectra)

(i) <i>p</i> -Phenylbenzil		70 eV		20 eV	
<i>m/e</i>	Ion	<i>I</i> _{rel}	(e.s.d.)	<i>I</i> _{rel}	(e.s.d.)
286	C ₂₀ H ₁₄ O ₂ [†]	1.2	(0.2)	1.6	(0.4)
181	C ₁₃ H ₉ O ⁺	100		100	
153	C ₁₂ H ₉ ⁺	15.6	(1.4)	7.0	(0.2)
152	C ₁₂ H ₈ [†]	37.4	(1.9)	2.2	(0.3)
151	C ₁₂ H ₇ ⁺	9.4	(1.1)	0.7	(0.2)
150	C ₁₂ H ₆ [†]	2.4	(0.6)		
127	C ₁₀ H ₇ ⁺	4.6	(0.8)		
126	C ₁₀ H ₆ [†]	2.9	(0.6)		
105	C ₇ H ₅ O ⁺	18.6	(1.3)	7.8	(0.4)
102	C ₈ H ₆ [†]	1.9	(0.5)		
101	C ₈ H ₅ ⁺	1.1	(0.4)		
77	C ₆ H ₅ ⁺	26.4	(1.9)	0.6	(0.2)
76	C ₆ H ₄ [†]	3.0	(0.7)		
75	C ₆ H ₃ ⁺	2.6	(0.6)		
74	C ₆ H ₂ [†]	1.7	(0.5)		
63	C ₅ H ₃ ⁺	2.0	(0.6)		
51	C ₄ H ₃ ⁺	13.6	(1.5)		
50	C ₄ H ₂ [†]	3.9	(0.9)		

Fig. 16

(i) P-PHENYLBENZIL

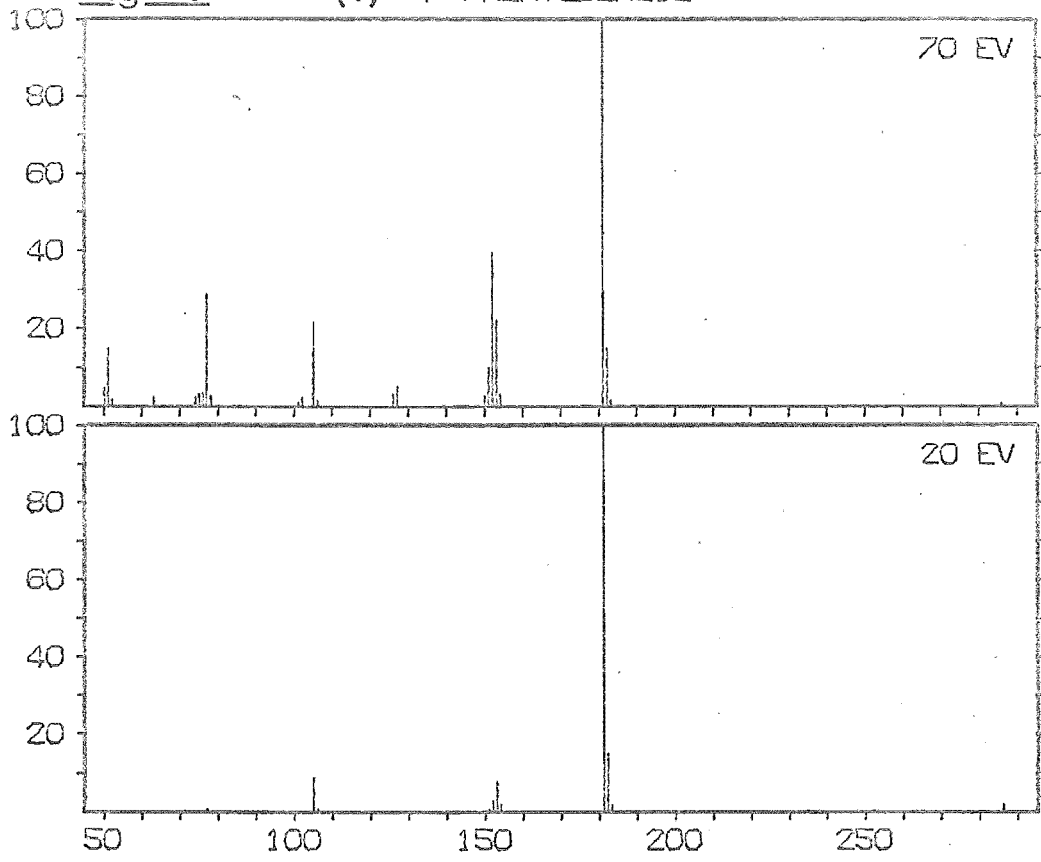


Table 3

Relative Ion Intensities (70 and 20 eV Mass Spectra)

(j) *m*-Formylbenzil

<i>m/e</i>	Ion	70 eV		20 eV	
		<i>I</i> _{rel}	(e.s.d.)	<i>I</i> _{rel}	(e.s.d.)
238	C ₁₅ H ₁₀ O ₃ ⁺	2.1	(0.1)	1.6	(0.2)
133	C ₈ H ₅ O ₂ ⁺	11.9	(0.3)	8.1	(0.4)
105	C ₇ H ₅ O ⁺	100		100	
77	C ₆ H ₅ ⁺	28.3	(0.0)	6.6	(0.2)
76	C ₆ H ₄ ⁺	2.0	(0.1)		
75	C ₆ H ₃ ⁺	0.9	(0.1)		
51	C ₄ H ₃ ⁺	9.3	(0.2)		
50	C ₄ H ₂ ⁺	2.6	(0.2)		

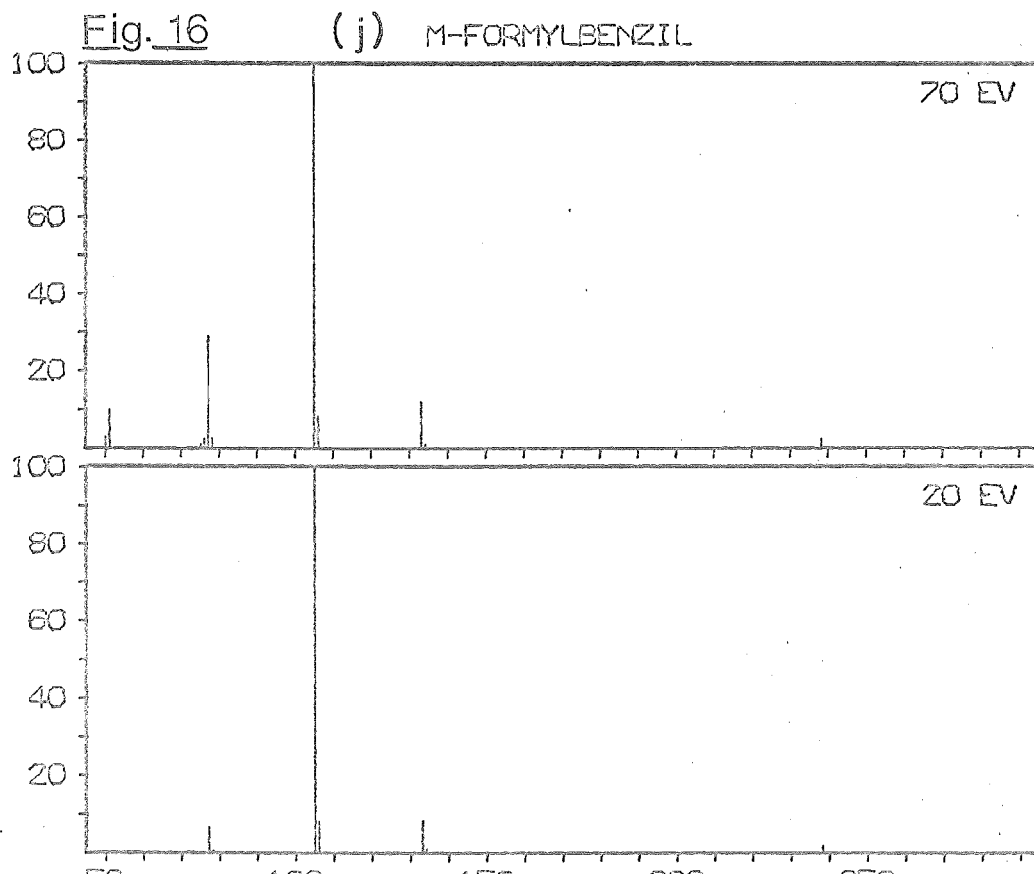


Table 3

Relative Ion Intensities (70 and 20 eV Mass Spectra)

(k) *m*-Cyanobenzil

<i>m/e</i>	Ion	70 eV		20 eV	
		<i>I</i> _{rel}	(e.s.d.)	<i>I</i> _{rel}	(e.s.d.)
235	C ₁₄ H ₉ ON ⁺	0.6	(0.1)	0.6	(0.3)
130	C ₈ H ₄ ON ⁺	4.8	(0.2)	2.9	(0.4)
105	C ₇ H ₅ O ⁺	100		100	
102	C ₇ H ₄ N ⁺	8.2	(0.0)	1.2	(0.3)
77	C ₆ H ₅ ⁺	37.3	(0.3)	15.7	(0.3)
76	C ₆ H ₄ ⁺	2.9	(0.2)		
75	C ₆ H ₃ ⁺	3.5	(0.3)		
74	C ₆ H ₂ ⁺	1.2	(0.2)		
51	C ₄ H ₃ ⁺	13.1	(0.4)		
50	C ₄ H ₂ ⁺	4.1	(0.2)		

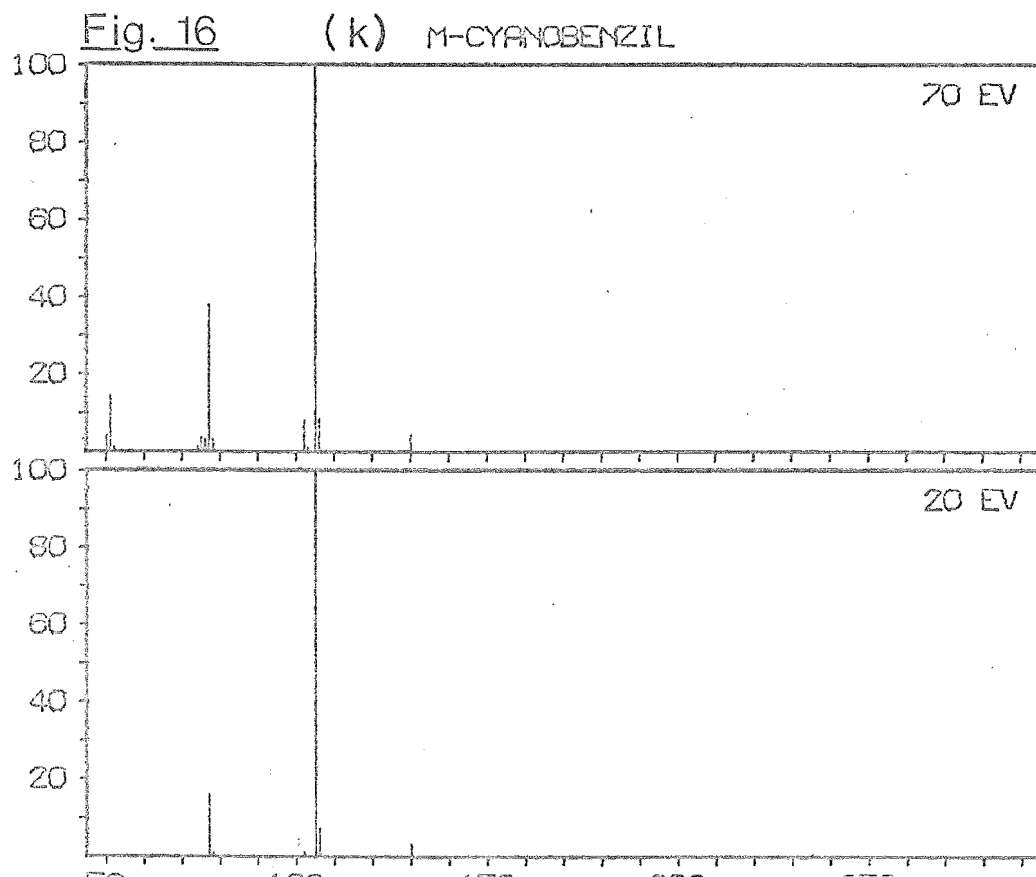


Table 3

Relative Ion Intensities (70 and 20 eV Mass Spectra)

(1) *m*-Trifluoromethylbenzil

<i>m/e</i>	Ion	70 eV		20 eV	
		<i>I</i> _{rel}	(e.s.d.)	<i>I</i> _{rel}	(e.s.d.)
278	$C_{15}H_9O_2F_3^+$	2.5	(0.8)	1.6	(0.2)
259	$C_{15}H_9O_2F_2^+$	2.4	(0.5)		
173	$C_8H_4OF_3^+$	9.9	(1.0)	1.9	(1.0)
145	$C_7H_4F_3^+$	9.7	(0.5)		
105	$C_7H_5O^+$	100		100	
95	$C_3H_2F_3^+$	1.8	(0.3)		
77	$C_6H_5^+$	25.9	(0.9)	4.1	(0.1)
76	$C_6H_4^+$	1.1	(0.1)		
75	$C_3HF_2^+$	1.6	(0.3)		
51	$C_4H_3^+$	6.2	(0.6)		
50	$C_4H_2^+$	2.0	(0.4)		

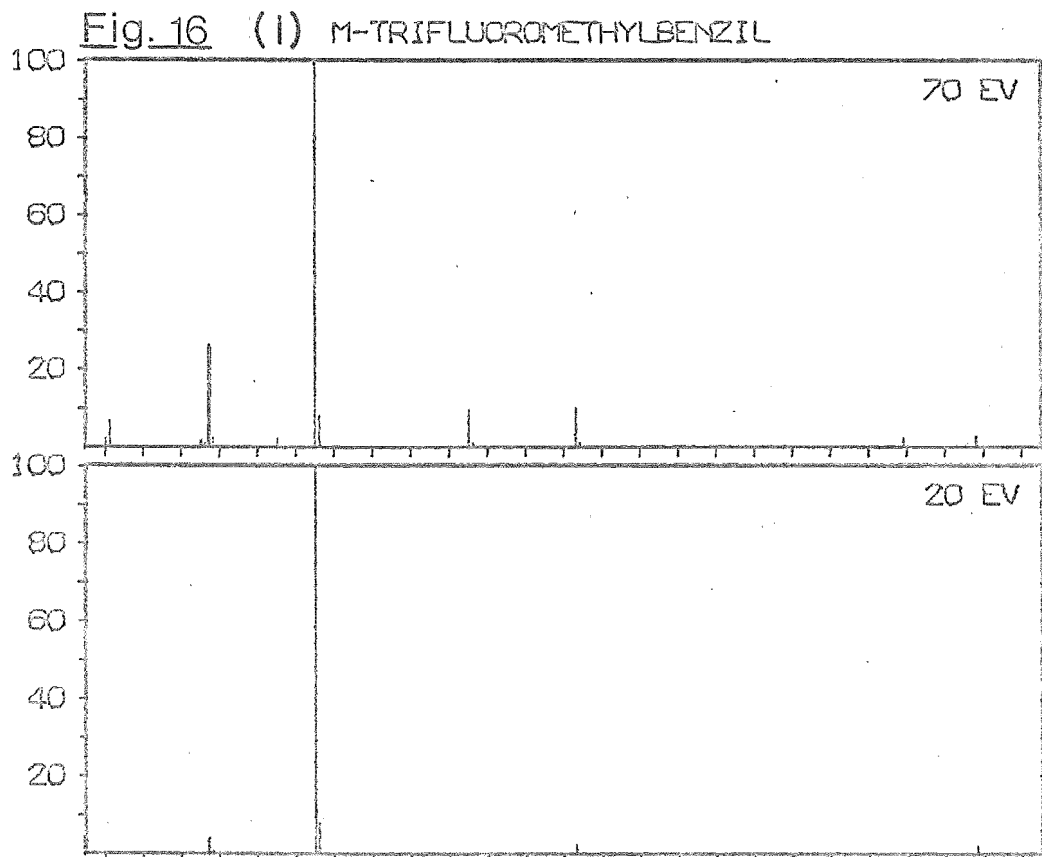
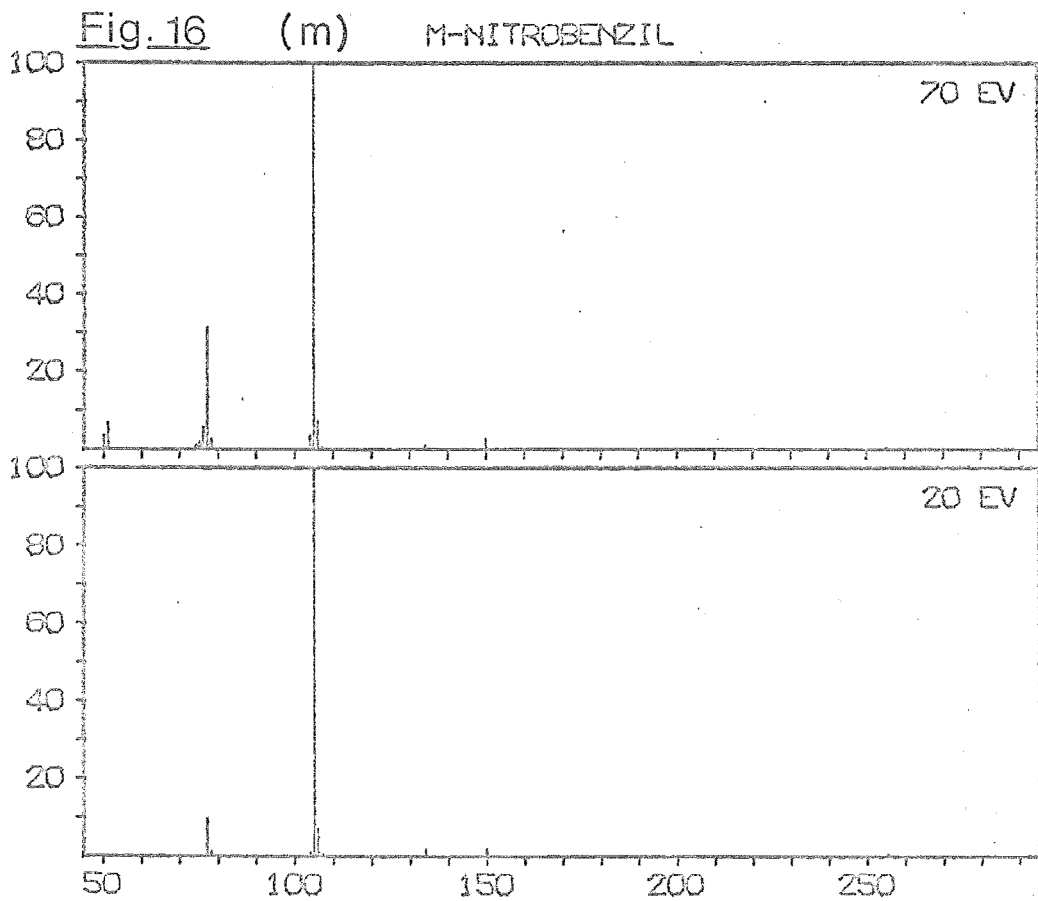


Table 3

Relative Ion Intensities (70 and 20 eV Mass Spectra)

(m) *m*-Nitrobenzil

<i>m/e</i>	Ion	70 eV		20 eV	
		<i>I</i> _{rel}	(e.s.d.)	<i>I</i> _{rel}	(e.s.d.)
255	C ₁₄ H ₉ O ₄ N ⁺	0.5	(0.0)	0.3	(0.0)
150	C ₇ H ₄ O ₃ N ⁺	2.7	(0.0)	1.8	(0.0)
134	C ₇ H ₄ O ₂ N ⁺	1.1	(0.0)	1.3	(0.0)
105	C ₇ H ₅ O ⁺	100		100	
104	C ₇ H ₄ O ⁺	3.4	(0.0)	1.1	(0.0)
77	C ₆ H ₅ ⁺	30.7	(0.8)	9.2	(0.4)
76	C ₆ H ₄ ⁺	5.4	(0.1)		
75	C ₆ H ₃ ⁺	1.5	(0.0)		
74	C ₆ H ₂ ⁺	0.8	(0.0)		
51	C ₄ H ₃ ⁺	5.8	(0.2)		
50	C ₄ H ₂ ⁺	3.6	(0.0)		



5.2 MASS SPECTRA (LOW VOLTAGE)

Table 4(a-m) gives the measured fractional ion intensities in the mass spectra (section 3.3.2). These values are the means of at least four separate measurements, and have been corrected for the contributions of other isotopes. The estimated standard deviations (given in brackets) were again determined from equation 31. For comparison, the fractional ion intensities calculated from the IE curves as described in section 4.4 are also tabulated; the nominal and corrected ionizing voltage scales of these two sets of data may differ by up to 0.4 eV.

Table 4

(a) Benzil

NOMINAL IONIZING VOLTAGE (EV)	MEASURED		FRACTIONAL	ION		INTENSITIES	
	210	105	M/E	77			
10.0	0.234 (.033)	0.766 (.033)	0.0	(.0)	0.0	(.0)	0.0 (.0)
12.0	0.103 (.015)	0.894 (.015)	0.0	(.0)	0.0	(.0)	0.0 (.0)
14.0	0.056 (.009)	0.931 (.008)	0.003	(.001)	0.0	(.0)	0.0 (.0)
16.0	0.057 (.007)	0.920 (.005)	0.023	(.003)	0.0	(.0)	0.0 (.0)
18.0	0.048 (.005)	0.889 (.002)	0.063	(.004)	0.0	(.0)	0.0 (.0)
20.0	0.040 (.005)	0.848 (.001)	0.112	(.005)	0.0	(.0)	0.0 (.0)

EXCESS ENERGY (EV)	ELECTRON ENERGY (EV)	FRACTIONAL		ION	INTENSITIES		TOTAL INTENSITY (ARB UNITS)
		210	105	M/E	77		
0.80	10.00	0.2380	0.7120	0.0	0.0	0.0	0.1562E 02
2.80	12.00	0.0909	0.9091	0.0	0.0	0.0	0.3544E 03
4.80	14.00	0.0643	0.9337	0.0020	0.0	0.0	0.1144E 04
6.80	16.00	0.0546	0.9187	0.0267	0.0	0.0	0.2094E 04
8.80	18.00	0.0495	0.8867	0.0638	0.0	0.0	0.3134E 04
10.80	20.00	0.0469	0.8702	0.0828	0.0	0.0	0.4177E 04

Table 4 (b) m-Fluorobenzil

NOMINAL IONIZING VOLTAGE (eV)	MEASURED FRACTIONAL ION INTENSITIES					
	228	123	M/E 105	95	77	
10.0	0.091 (.002)	0.0 (.0)	0.909 (.002)	0.0 (.0)	0.0 (.0)	
12.0	0.020 (.003)	0.017 (.001)	0.961 (.002)	0.0 (.0)	0.0 (.0)	
14.0	0.015 (.002)	0.030 (.002)	0.952 (.001)	0.0 (.0)	0.0 (.0)	
16.0	0.012 (.001)	0.048 (.002)	0.920 (.002)	0.004 (.0)	0.016 (.001)	
18.0	0.011 (.001)	0.063 (.002)	0.872 (.003)	0.012 (.001)	0.043 (.001)	
20.0	0.010 (.001)	0.075 (.001)	0.810 (.001)	0.023 (.001)	0.063 (.001)	

EXCESS ENERGY (eV)	ELECTRON ENERGY (eV)	FRACTIONAL ION INTENSITIES					TOTAL INTENSITY (ARB UNITS)
		228	123	M/E 105	95	77	
0.77	10.00	0.0761	0.0	0.9239	0.0	0.0	0.8321E 01
2.77	12.00	0.0205	0.0172	0.9623	0.0	0.0	0.2267E 03
4.77	14.00	0.0148	0.0350	0.9492	0.0002	0.0008	0.6616E 03
6.77	16.00	0.0131	0.0464	0.9223	0.0038	0.0144	0.1124E 04
8.77	18.00	0.0120	0.0496	0.8830	0.0117	0.0437	0.1636E 04
10.77	20.00	0.0114	0.0510	0.8592	0.0174	0.0610	0.2156E 04

Table 4 (c) p-Fluorobenzil

NOMINAL IONIZING VOLTAGE (EV)	MEASURED FRACTIONAL ION INTENSITIES				
	228	123	M/E 105	95	77
10.0	0.120 (.004)	0.071 (.004)	0.757 (.010)	0.0 (.0)	0.0 (.0)
12.0	0.033 (.001)	0.137 (.008)	0.903 (.017)	0.0 (.0)	0.0 (.0)
14.0	0.026 (.001)	0.176 (.003)	0.789 (.015)	0.0 (.0)	0.0 (.0)
16.0	0.021 (.002)	0.196 (.006)	0.753 (.008)	0.003 (.0)	0.012 (.001)
18.0	0.018 (.001)	0.206 (.001)	0.716 (.004)	0.010 (.001)	0.035 (.002)
20.0	0.017 (.001)	0.220 (.001)	0.666 (.001)	0.024 (.001)	0.061 (.001)

EXCESS ENERGY (EV)	ELECTRON ENERGY (EV)	FRACTIONAL ION INTENSITIES					TOTAL INTENSITY (ARB UNITS)
		228	123	M/E 105	95	77	
0.88	10.00	0.1241	0.0858	0.7901	0.0	0.0	0.1366E 02
2.88	12.00	0.0334	0.1456	0.8210	0.0	0.0	0.3559E 03
4.88	14.00	0.0241	0.1805	0.7945	0.0001	0.0008	0.1079E 04
6.88	16.00	0.0213	0.1962	0.7667	0.0025	0.0133	0.1891E 04
8.88	18.00	0.0197	0.1972	0.7359	0.0110	0.0362	0.2776E 04
10.88	20.00	0.0138	0.1968	0.7168	0.0177	0.0499	0.3677E 04

Table 4 (d) m-Chlorobenzil

NOMINAL IONIZING VOLTAGE (EV)	MEASURED FRACTIONAL ION INTENSITIES							
	244	139	M/E 111		105	77		
10.0	0.148 (.007)	0.0 (.0)	0.0 (.0)	0.852 (.007)	0.0 (.0)			
12.0	0.075 (.003)	0.024 (.001)	0.0 (.0)	0.901 (.003)	0.0 (.0)			
14.0	0.044 (.001)	0.047 (.002)	0.0 (.0)	0.907 (.003)	0.0 (.0)			
16.0	0.035 (.001)	0.065 (.001)	0.006 (.0)	0.886 (.001)	0.099 (.0)			
18.0	0.030 (.001)	0.085 (.002)	0.017 (.001)	0.834 (.003)	0.033 (.001)			
20.0	0.024 (.0)	0.096 (.003)	0.027 (.004)	0.786 (.008)	0.068 (.003)			

EXCESS ENERGY (EV)	ELECTRON ENERGY (EV)	FRACTIONAL ION INTENSITIES					TOTAL INTENSITY (ARB UNITS)
		244	139	M/E 111	105	77	
0.84	10.00	0.1726	0.0	0.0	0.8274	0.0	0.9453E 01
2.84	12.00	0.0582	0.0274	0.0	0.9144	0.0	0.2000E 03
4.84	14.00	0.0414	0.0503	0.0004	0.9072	0.0007	0.5706E 03
6.84	16.00	0.0357	0.0633	0.0076	0.8814	0.0120	0.9873E 03
8.84	18.00	0.0323	0.0663	0.0202	0.8418	0.0394	0.1453E 04
10.84	20.00	0.0304	0.0676	0.0278	0.8181	0.0560	0.1925E 04

Table 4 (e) m-Bromobenzil

NOMINAL IONIZING VOLTAGE (EV)	MEASURED		FRACTIONAL		ION INTENSITIES	
	288	183	M/E	155	105	77
10.0	0.111 (.003)	0.0 (.0)	0.0 (.0)	0.889 (.003)	0.0 (.0)	
12.0	0.054 (.0)	0.030 (.001)	0.0 (.0)	0.915 (.001)	0.0 (.0)	
14.0	0.036 (.0)	0.042 (.001)	0.0 (.0)	0.919 (.001)	0.0 (.0)	
16.0	0.031 (.001)	0.064 (.001)	0.003 (.0)	0.895 (.002)	0.007 (.0)	
18.0	0.026 (.0)	0.077 (.001)	0.011 (.0)	0.861 (.001)	0.025 (.0)	
20.0	0.023 (.0)	0.085 (.001)	0.021 (.0)	0.820 (.002)	0.051 (.0)	

EXCESS ENERGY (EV)	ELECTRON ENERGY (EV)	FRACTIONAL		ION INTENSITIES		TOTAL INTENSITY (ARB UNITS)	
		288	183	M/E	155		105
0.90	10.00	0.1626	0.0015	0.0	0.8359	0.0	0.2993E 02
2.90	12.00	0.0500	0.0239	0.0	0.9261	0.0	0.5326E 03
4.90	14.00	0.0353	0.0473	0.0002	0.9166	0.0005	0.1603E 04
6.90	16.00	0.0310	0.0638	0.0031	0.8948	0.0073	0.2837E 04
8.90	18.00	0.0287	0.0693	0.0092	0.8710	0.0217	0.4147E 04
10.90	20.00	0.0275	0.0719	0.0132	0.8565	0.0308	0.5468E 04

Table 4 (f) p-Bromobenzil

NOMINAL IONIZING VOLTAGE (EV)	MEASURED FRACTIONAL ION INTENSITIES				
	288	183	M/E 155	105	77
10.0	0.122 (.007)	0.118 (.005)	0.0 (.0)	0.760 (.004)	0.0 (.0)
12.0	0.044 (.002)	0.175 (.004)	0.0 (.0)	0.776 (.002)	0.0 (.0)
14.0	0.027 (.001)	0.204 (.006)	0.0 (.0)	0.765 (.004)	0.0 (.0)
16.0	0.022 (.001)	0.232 (.003)	0.006 (.001)	0.728 (.004)	0.011 (.001)
18.0	0.019 (.001)	0.244 (.002)	0.021 (.001)	0.676 (.001)	0.040 (.001)
20.0	0.014 (.001)	0.234 (.003)	0.036 (.001)	0.639 (.007)	0.078 (.003)

EXCESS ENERGY (EV)	ELECTRON ENERGY (EV)	FRACTIONAL ION INTENSITIES					TOTAL INTENSITY (ARB UNITS)
		288	183	M/E 155	105	77	
0.89	10.00	0.0932	0.1206	0.0	0.7862	0.0	0.2046E 02
2.89	12.00	0.0351	0.1889	0.0	0.7761	0.0	0.3667E 03
4.89	14.00	0.0259	0.2248	0.0005	0.7477	0.0011	0.1079E 04
6.89	16.00	0.0226	0.2370	0.0089	0.7161	0.0154	0.1908E 04
8.89	18.00	0.0204	0.2320	0.0253	0.6753	0.0470	0.2852E 04
10.89	20.00	0.0192	0.2279	0.0368	0.6502	0.0658	0.3822E 04

Table 4 (g) m-Methylbenzyl

NOMINAL IONIZING VOLTAGE (EV)	MEASURED FRACTIONAL ION INTENSITIES				
	224	119	M/E 105	91	77
10.0	0.162 (.010)	0.796 (.011)	0.042 (.001)	0.0 (.0)	0.0 (.0)
12.0	0.088 (.003)	0.822 (.003)	0.090 (.002)	0.0 (.0)	0.0 (.0)
14.0	0.069 (.002)	0.816 (.004)	0.113 (.001)	0.0 (.0)	0.0 (.0)
16.0	0.052 (.002)	0.778 (.003)	0.152 (.002)	0.021 (.001)	0.0 (.0)
18.0	0.042 (.004)	0.746 (.002)	0.154 (.003)	0.050 (.001)	0.009 (.001)
20.0	0.035 (.004)	0.706 (.002)	0.168 (.002)	0.074 (.002)	0.018 (.001)

EXCESS ENERGY (EV)	ELECTRON ENERGY (EV)	FRACTIONAL ION INTENSITIES					TOTAL INTENSITY (ARB UNITS)
		224	119	M/E 105	91	77	
0.95	10.00	0.2325	0.7234	0.0441	0.0	0.0	0.2400E 02
2.95	12.00	0.0915	0.8228	0.0857	0.0	0.0	0.3764E 03
4.95	14.00	0.0671	0.8116	0.1193	0.0018	0.0001	0.1041E 04
6.95	16.00	0.0596	0.7853	0.1317	0.0209	0.0021	0.1720E 04
8.95	18.00	0.0548	0.7528	0.1332	0.0507	0.0085	0.2468E 04
10.95	20.00	0.0519	0.7320	0.1334	0.0689	0.0138	0.3230E 04

Table 4 (h) m-Methoxybenzil

NOMINAL IONIZING VOLTAGE (eV)	MEASURED FRACTIONAL ION INTENSITIES					
	240	135	M/E 107	105	77	
10.0	0.453 (.003)	0.510 (.004)	0.0 (.0)	0.037 (.001)	0.0 (.0)	
12.0	0.223 (.001)	0.681 (.001)	0.0 (.0)	0.096 (.001)	0.0 (.0)	
14.0	0.151 (.001)	0.712 (.001)	0.0 (.0)	0.135 (.001)	0.0 (.0)	
16.0	0.126 (.001)	0.676 (.004)	0.018 (.001)	0.177 (.003)	0.0 (.0)	
18.0	0.103 (.001)	0.647 (.002)	0.042 (.001)	0.194 (.002)	0.014 (.001)	
20.0	0.084 (.002)	0.611 (.006)	0.062 (.002)	0.207 (.001)	0.035 (.001)	

EXCESS ENERGY (eV)	ELECTRON ENERGY (eV)	FRACTIONAL ION INTENSITIES					TOTAL INTENSITY (ARB UNITS)
		240	135	M/E 107	105	77	
1.25	10.00	0.5220	0.4563	0.0	0.0217	0.0	0.3482E 01
3.25	12.00	0.2346	0.6748	0.0	0.0906	0.0	0.3155E 02
5.25	14.00	0.1569	0.7068	0.0015	0.1348	0.0	0.8377E 02
7.25	16.00	0.1282	0.6994	0.0164	0.1549	0.0010	0.1414E 03
9.25	18.00	0.1130	0.6771	0.0399	0.1589	0.0112	0.2047E 03
11.25	20.00	0.1028	0.6515	0.0559	0.1577	0.0321	0.2736E 03

Table 4

(i) p-Phenylbenzil

NOMINAL IONIZING VOLTAGE (eV)	MEASURED		FRACTIONAL	ION	INTENSITIES	
	286	181	M/E	153	105	77
10.0	0.266 (.003)	0.734 (.003)	0.0	(.0)	0.0	(.0)
12.0	0.080 (.001)	0.902 (.002)	0.0	(.0)	0.011 (.001)	0.0
14.0	0.052 (.001)	0.916 (.001)	0.006	(.001)	0.023 (.001)	0.0
16.0	0.042 (.003)	0.914 (.001)	0.010	(.001)	0.032 (.003)	0.0
18.0	0.033 (.001)	0.871 (.003)	0.042	(.001)	0.052 (.001)	0.003 (.0)
20.0	0.026 (.001)	0.831 (.003)	0.072	(.001)	0.065 (.001)	0.007 (.0)

EXCESS ENERGY (eV)	ELECTRON ENERGY (eV)	FRACTIONAL		ION	INTENSITIES		TOTAL INTENSITY (ARB UNITS)
		286	181	M/E	153	105	
1.41	10.00	0.1837	0.8138	0.0	0.0025	0.0	0.3866E 02
3.41	12.00	0.0725	0.9159	0.0	0.0116	0.0	0.3073E 03
5.41	14.00	0.0512	0.9237	0.0007	0.0242	0.0003	0.8128E 03
7.41	16.00	0.0447	0.9084	0.0145	0.0513	0.0009	0.1369E 04
9.41	18.00	0.0408	0.8754	0.0438	0.0333	0.0034	0.1983E 04
11.41	20.00	0.0330	0.8430	0.0607	0.0337	0.0038	0.2643E 04

Table 4 (j) m-Formylbenzil

NOMINAL IONIZING VOLTAGE (EV)	MEASURED		FRACTIONAL	ION	INTENSITIES	
	238	133	M/E	105	77	
10.0	0.160 (.001)	0.0 (.0)	0.840 (.001)	0.0 (.0)	0.0 (.0)	
12.0	0.049 (.001)	0.020 (.001)	0.928 (.001)	0.0 (.0)	0.0 (.0)	
14.0	0.029 (.001)	0.033 (.001)	0.935 (.001)	0.003 (.001)	0.0 (.0)	
16.0	0.026 (.001)	0.054 (.001)	0.910 (.001)	0.011 (.001)	0.0 (.0)	
18.0	0.022 (.001)	0.051 (.001)	0.883 (.001)	0.034 (.001)	0.0 (.0)	
20.0	0.019 (.001)	0.070 (.001)	0.842 (.001)	0.070 (.001)	0.0 (.0)	

EXCESS ENERGY (EV)	ELECTRON ENERGY (EV)	FRACTIONAL		ION	INTENSITIES		TOTAL INTENSITY (ARB UNITS)
		238	133	M/E	105	77	
0.86	10.00	0.1904	0.0078	0.8018	0.0	0.0	0.8710E 01
2.86	12.00	0.0437	0.0210	0.9352	0.0	0.0	0.2374E 03
4.86	14.00	0.0296	0.0373	0.9322	0.0009	0.0	0.7515E 03
6.86	16.00	0.0252	0.0499	0.9119	0.0130	0.0	0.1340E 04
8.86	18.00	0.0230	0.0537	0.8860	0.0373	0.0	0.1969E 04
10.86	20.00	0.0218	0.0555	0.8702	0.0525	0.0	0.2604E 04

Table 4 (k) m-Cyanobenzil

NOMINAL IONIZING VOLTAGE (EV)	MEASURED		FRACTIONAL	ION	INTENSITIES	
	235	130	M/E	105	102	77
12.0	0.016 (.001)	0.0 (.0)	0.983 (.002)	0.0 (.0)	0.0 (.0)	0.0 (.0)
14.0	0.011 (.001)	0.005 (.0)	0.981 (.001)	0.0 (.0)	0.0 (.0)	0.0 (.0)
16.0	0.009 (.0)	0.010 (.001)	0.964 (.003)	0.0 (.0)	0.016 (.002)	0.016 (.002)
18.0	0.007 (.0)	0.015 (.001)	0.929 (.004)	0.002 (.0)	0.050 (.004)	0.050 (.004)
20.0	0.006 (.001)	0.018 (.001)	0.878 (.003)	0.006 (.0)	0.093 (.003)	0.093 (.003)

EXCESS ENERGY (EV)	ELECTRON ENERGY (EV)	FRACTIONAL		ION	INTENSITIES		TOTAL INTENSITY (ARB UNITS)
		235	130	M/E	102	77	
0.70	10.00	0.0848	0.0	0.9152	0.0	0.0	0.5915E 01
2.70	12.00	0.0156	0.0013	0.9830	0.0	0.0	0.2415E 03
4.70	14.00	0.0107	0.0041	0.9845	0.0	0.0007	0.7733E 03
6.70	16.00	0.0093	0.0112	0.9647	0.0002	0.0147	0.1345E 04
8.70	18.00	0.0084	0.0145	0.9242	0.0020	0.0509	0.1984E 04
10.70	20.00	0.0078	0.0161	0.8928	0.0057	0.0776	0.2654E 04

Table 4 (I) m-Trifluoromethylbenzil

NOMINAL IONIZING VOLTAGE (eV)	MEASURED FRACTIONAL ION INTENSITIES					
	*****	*****	*****	*****	*****	*****
	278	173	M/E 145	105	77	
12.0	0.017 (.0)	0.004 (.0)	0.0 (.0)	0.976 (.001)	0.0 (.0)	
14.0	0.010 (.001)	0.010 (.001)	0.0 (.0)	0.976 (.001)	0.0 (.0)	
16.0	0.008 (.0)	0.020 (.001)	0.0 (.0)	0.960 (.001)	0.010 (.001)	
18.0	0.007 (.0)	0.033 (.001)	0.002 (.0)	0.919 (.002)	0.037 (.001)	
20.0	0.006 (.0)	0.042 (.001)	0.008 (.0)	0.864 (.003)	0.077 (.002)	

EXCESS ENERGY (eV)	ELECTRON ENERGY (eV)	FRACTIONAL ION INTENSITIES					TOTAL INTENSITY (ARB UNITS)
		*****	*****	*****	*****	*****	
		278	173	M/E 145	105	77	
0.66	10.00	0.0637	0.0	0.0	0.9363	0.0	0.9673E 01
2.66	12.00	0.0156	0.0052	0.0	0.9792	0.0	0.2839E 03
4.66	14.00	0.0102	0.0111	0.0000	0.9779	0.0008	0.9392E 03
6.66	16.00	0.0078	0.0187	0.0004	0.9587	0.0129	0.1733E 04
8.66	18.00	0.0067	0.0214	0.0027	0.9216	0.0417	0.2608E 04
10.66	20.00	0.0060	0.0225	0.0059	0.8943	0.0634	0.3518E 04

Table 4 (m) m-Nitrobenzil

NOMINAL IONIZING VOLTAGE (EV)	MEASURED		FRACTIONAL		ION INTENSITIES	
	255	150	M/E	134	105	77
10.0	0.115 (.004)	0.0 (.0)	0.0 (.0)	0.885 (.004)	0.0 (.0)	
12.0	0.030 (.004)	0.0 (.0)	0.018 (.001)	0.948 (.005)	0.0 (.0)	
14.0	0.021 (.003)	0.0 (.0)	0.020 (.001)	0.953 (.005)	0.003 (.001)	
16.0	0.016 (.002)	0.007 (.001)	0.018 (.001)	0.940 (.001)	0.015 (.003)	
18.0	0.014 (.002)	0.013 (.001)	0.017 (.001)	0.902 (.005)	0.049 (.005)	
20.0	0.012 (.002)	0.017 (.002)	0.014 (.001)	0.847 (.012)	0.105 (.012)	

EXCESS ENERGY (EV)	ELECTRON ENERGY (EV)	FRACTIONAL		ION INTENSITIES		TOTAL INTENSITY (ARB UNITS)	
		255	150	M/E	134		105
0.67	10.00	0.1250	0.0	0.0126	0.8624	0.0	0.8472E 01
2.67	12.00	0.0302	0.0006	0.0192	0.9500	0.0	0.2970E 03
4.67	14.00	0.0198	0.0026	0.0193	0.9565	0.0012	0.1068E 04
6.67	16.00	0.0165	0.0063	0.0182	0.9394	0.0161	0.2033E 04
8.67	18.00	0.0149	0.0088	0.0171	0.9025	0.0519	0.3102E 04
10.67	20.00	0.0139	0.0097	0.0164	0.8776	0.0766	0.4203E 04

5.3 FRACTIONAL ION INTENSITIES

The fractional ion intensities of the major ions in the low voltage mass spectra of the benzils are tabulated in Table 5(a-m) as a function of the excess energy, $V-IP$ (see section 4.4). The corresponding plots of these data are shown in Fig. 17(a-m) to illustrate how they vary with energy.

Table 5

(a) BENZIL

EXCESS ENERGY (EV)	ELECTRON ENERGY (EV)	FRACTIONAL ION INTENSITIES					TOTAL INTENSITY (ARB UNITS)
		210 (1)	(2)	M/E 105 (3)	77 (4)	(5)	
-1.00	8.20	0.0	0.0	0.0	0.0	0.0	0.0
-0.50	8.70	1.0000	0.0	0.0	0.0	0.0	0.2553E-01
0.0	9.20	1.0000	0.0	0.0	0.0	0.0	0.4371E 00
0.50	9.70	0.4004	0.0	0.5996	0.0	0.0	0.5720E 01
1.00	10.20	0.2354	0.0	0.7646	0.0	0.0	0.2702E 02
1.50	10.70	0.1531	0.0	0.8469	0.0	0.0	0.7892E 02
2.00	11.20	0.1169	0.0	0.8831	0.0	0.0	0.1632E 03
2.50	11.70	0.0979	0.0	0.9021	0.0	0.0	0.2743E 03
3.00	12.20	0.0872	0.0	0.9128	0.0	0.0	0.4127E 03
3.50	12.70	0.0798	0.0	0.9199	0.0004	0.0	0.5839E 03
4.00	13.20	0.0729	0.0	0.9264	0.0007	0.0	0.7855E 03
4.50	13.70	0.0668	0.0	0.9318	0.0013	0.0	0.1009E 04
5.00	14.20	0.0629	0.0	0.9344	0.0027	0.0	0.1235E 04
5.50	14.70	0.0600	0.0	0.9341	0.0060	0.0	0.1464E 04
6.00	15.20	0.0577	0.0	0.9305	0.0117	0.0	0.1700E 04
6.50	15.70	0.0557	0.0	0.9241	0.0202	0.0	0.1943E 04
7.00	16.20	0.0539	0.0	0.9147	0.0314	0.0	0.2197E 04
7.50	16.70	0.0524	0.0	0.9049	0.0427	0.0	0.2457E 04
8.00	17.20	0.0511	0.0	0.8968	0.0521	0.0	0.2718E 04
8.50	17.70	0.0501	0.0	0.8901	0.0598	0.0	0.2978E 04
9.00	18.20	0.0492	0.0	0.8846	0.0662	0.0	0.3239E 04
9.50	18.70	0.0484	0.0	0.8798	0.0717	0.0	0.3499E 04
10.00	19.20	0.0478	0.0	0.8757	0.0765	0.0	0.3760E 04

Fig. 17

(a) BENZIL

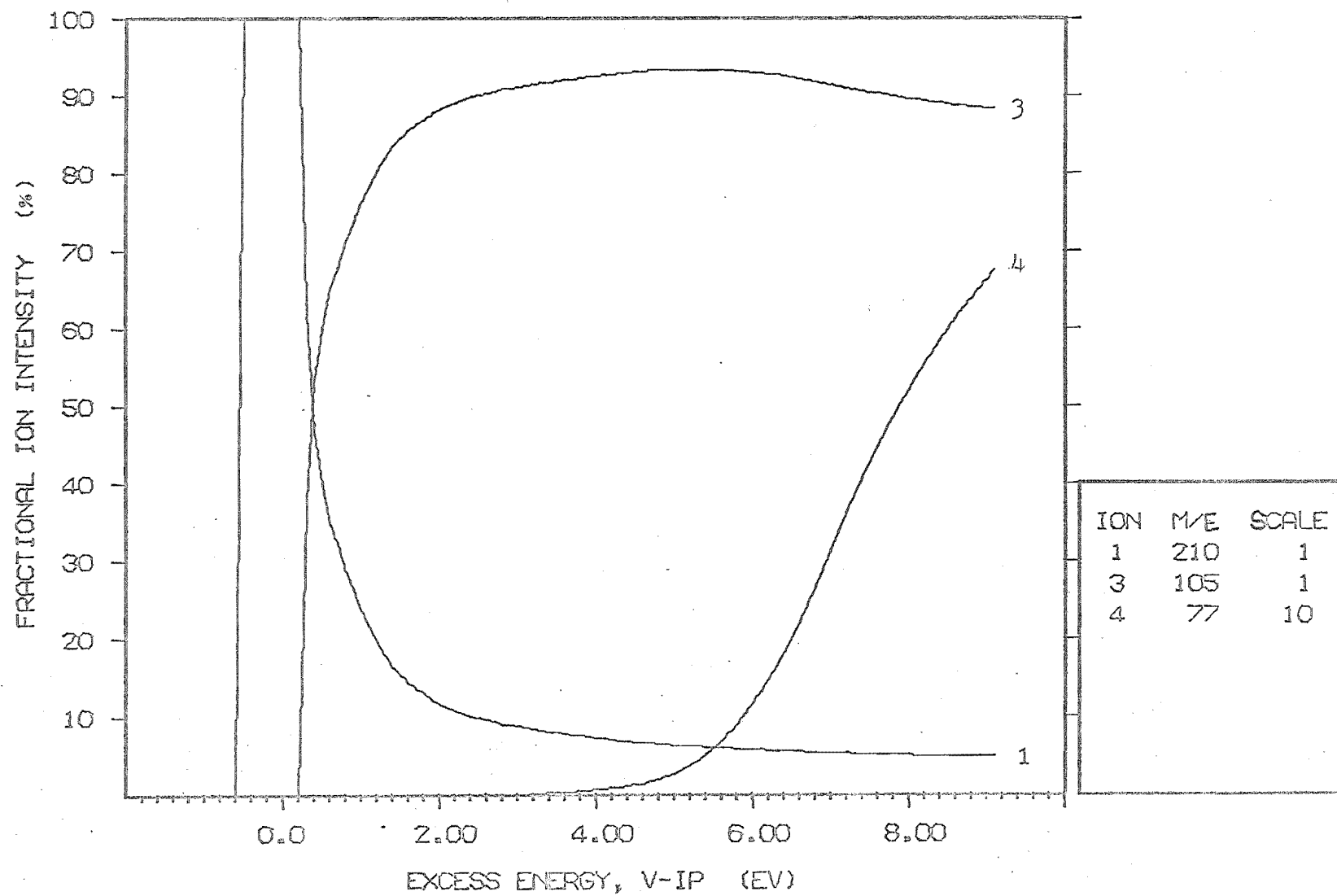


Table 5

(b) M-FLUCROBENZIL

EXCESS ENERGY (EV)	ELECTRON ENERGY (EV)	FRACTIONAL		ION	INTENSITIES		TOTAL INTENSITY (ARB UNITS)
		228 (1)	123 (2)	M/E 105 (3)	95 (4)	77 (5)	
-1.00	8.23	0.0	0.0	0.0	0.0	0.0	0.0
-0.50	8.73	1.0000	0.0	0.0	0.0	0.0	0.2884E-02
0.0	9.23	1.0000	0.0	0.0	0.0	0.0	0.6424E-01
0.50	9.73	0.1153	0.0	0.8847	0.0	0.0	0.2893E 01
1.00	10.23	0.0585	0.0	0.9415	0.0	0.0	0.1614E 02
1.50	10.73	0.0362	0.0081	0.9557	0.0	0.0	0.4939E 02
2.00	11.23	0.0270	0.0122	0.9608	0.0	0.0	0.1039E 03
2.50	11.73	0.0222	0.0155	0.9623	0.0	0.0	0.1780E 03
3.00	12.23	0.0194	0.0188	0.9618	0.0	0.0	0.2714E 03
3.50	12.73	0.0176	0.0228	0.9596	0.0	0.0	0.3761E 03
4.00	13.23	0.0161	0.0271	0.9566	0.0	0.0002	0.4871E 03
4.50	13.73	0.0151	0.0320	0.9523	0.0001	0.0004	0.6015E 03
5.00	14.23	0.0145	0.0371	0.9467	0.0004	0.0013	0.7128E 03
5.50	14.73	0.0140	0.0408	0.9411	0.0009	0.0031	0.8255E 03
6.00	15.23	0.0136	0.0436	0.9347	0.0018	0.0063	0.9403E 03
6.50	15.73	0.0133	0.0455	0.9270	0.0030	0.0111	0.1053E 04
7.00	16.23	0.0130	0.0470	0.9180	0.0046	0.0175	0.1180E 04
7.50	16.73	0.0127	0.0480	0.9073	0.0064	0.0256	0.1306E 04
8.00	17.23	0.0124	0.0487	0.8967	0.0085	0.0327	0.1435E 04
8.50	17.73	0.0122	0.0493	0.8874	0.0107	0.0405	0.1565E 04
9.00	18.23	0.0120	0.0498	0.8795	0.0125	0.0462	0.1696E 04
9.50	18.73	0.0118	0.0502	0.8727	0.0142	0.0512	0.1826E 04
10.00	19.23	0.0116	0.0505	0.8668	0.0156	0.0554	0.1956E 04

Fig. 17

(b) M-FLUOROBENZIL

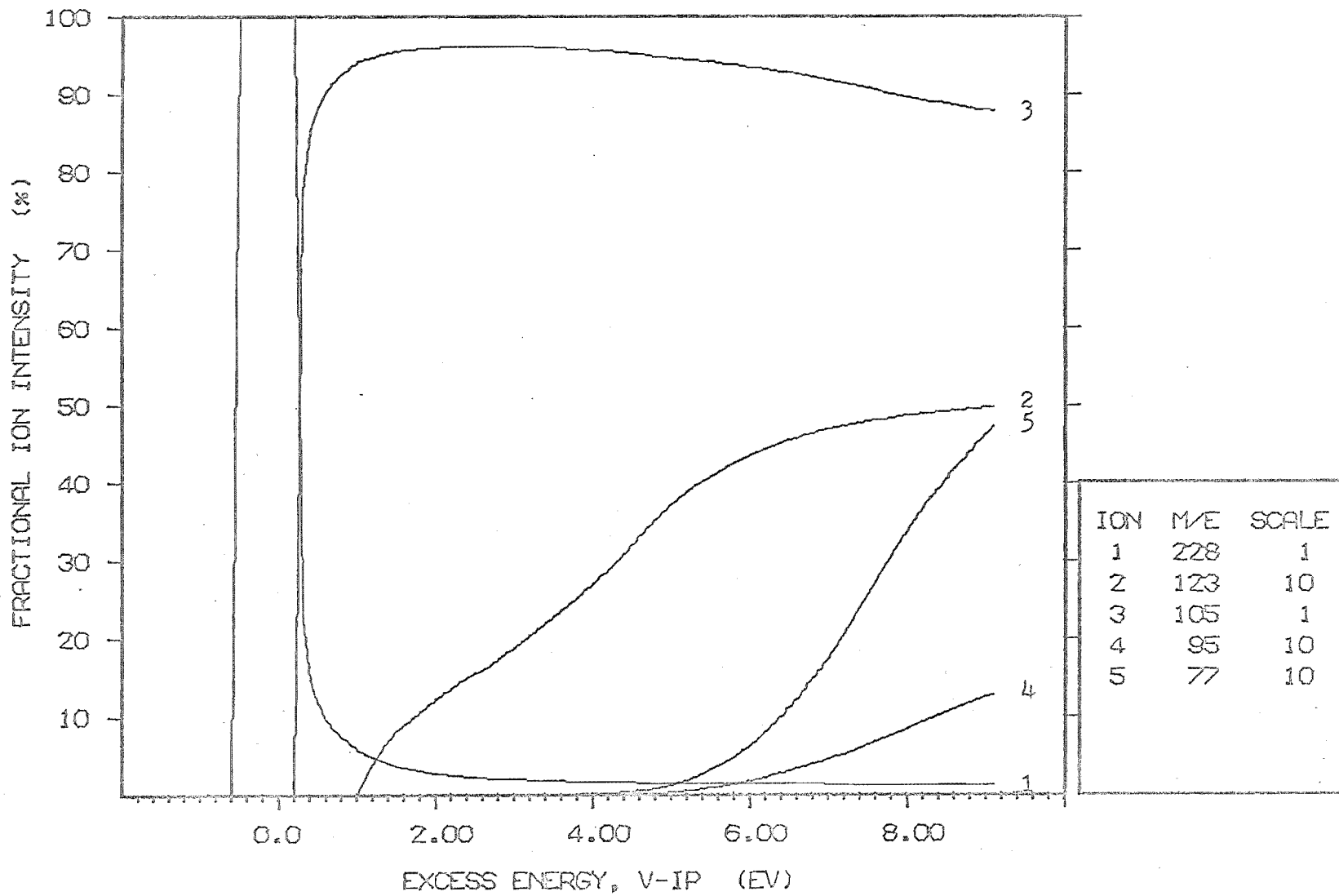


Table 5

(c) P-FLUCROBENZIL

EXCESS ENERGY (EV)	ELECTRON ENERGY (EV)	FRACTIONAL ION INTENSITIES					TOTAL INTENSITY (ARB UNITS)
		228 (1)	123 (2)	M/E 105 (3)	95 (4)	77 (5)	
-1.00	8.12	0.0	0.0	0.0	0.0	0.0	0.0
-0.50	8.62	1.0000	0.0	0.0	0.0	0.0	0.5894E-02
0.0	9.12	1.0000	0.0	0.0	0.0	0.0	0.1265E 00
0.50	9.62	0.2032	0.0589	0.7379	0.0	0.0	0.3453E 01
1.00	10.12	0.1079	0.0925	0.7996	0.0	0.0	0.1963E 02
1.50	10.62	0.0653	0.1101	0.8246	0.0	0.0	0.6379E 02
2.00	11.12	0.0459	0.1269	0.8271	0.0	0.0	0.1433E 03
2.50	11.62	0.0374	0.1387	0.8238	0.0	0.0	0.2527E 03
3.00	12.12	0.0324	0.1476	0.8200	0.0	0.0	0.3917E 03
3.50	12.62	0.0295	0.1567	0.8138	0.0	0.0	0.5517E 03
4.00	13.12	0.0268	0.1647	0.8084	0.0	0.0	0.7346E 03
4.50	13.62	0.0251	0.1739	0.8007	0.0001	0.0003	0.9284E 03
5.00	14.12	0.0239	0.1823	0.7927	0.0001	0.0010	0.1125E 04
5.50	14.62	0.0230	0.1883	0.7858	0.0004	0.0026	0.1324E 04
6.00	15.12	0.0223	0.1923	0.7792	0.0008	0.0053	0.1525E 04
6.50	15.62	0.0217	0.1949	0.7724	0.0016	0.0093	0.1731E 04
7.00	16.12	0.0212	0.1965	0.7648	0.0029	0.0146	0.1942E 04
7.50	16.62	0.0208	0.1972	0.7568	0.0046	0.0207	0.2158E 04
8.00	17.12	0.0203	0.1974	0.7487	0.0067	0.0269	0.2380E 04
8.50	17.62	0.0199	0.1973	0.7410	0.0092	0.0326	0.2604E 04
9.00	18.12	0.0196	0.1971	0.7344	0.0115	0.0373	0.2830E 04
9.50	18.62	0.0193	0.1970	0.7288	0.0135	0.0413	0.3055E 04
10.00	19.12	0.0191	0.1969	0.7239	0.0152	0.0448	0.3280E 04

Fig. 17

(c) P-FLUOROBENZIL

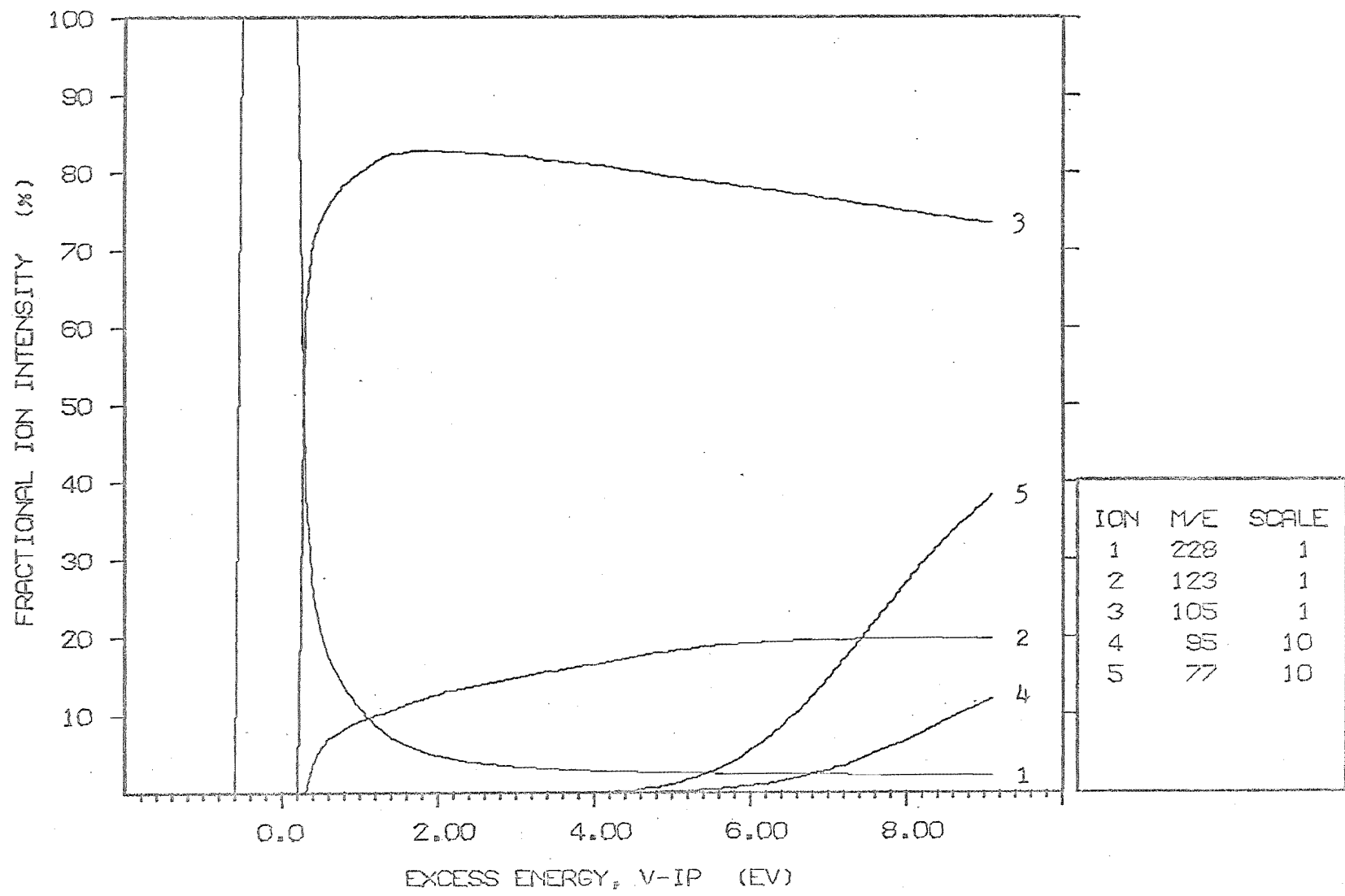


Table 5

(d) M-CHLOROBENZIL

EXCESS ENERGY (EV)	ELECTRON ENERGY (EV)	FRACTIONAL ION INTENSITIES					TOTAL INTENSITY (ARB UNITS)
		244 (1)	139 (2)	M/E 105 (3)	111 (4)	77 (5)	
-1.00	8.16	0.0	0.0	0.0	0.0	0.0	0.0
-0.50	8.66	1.0000	0.0	0.0	0.0	0.0	0.9277E-02
0.0	9.16	1.0000	0.0	0.0	0.0	0.0	0.1382E 00
0.50	9.66	0.2436	0.0	0.7564	0.0	0.0	0.2972E 01
1.00	10.16	0.1473	0.0060	0.8467	0.0	0.0	0.1487E 02
1.50	10.66	0.1000	0.0140	0.8860	0.0	0.0	0.4304E 02
2.00	11.16	0.0765	0.0200	0.9035	0.0	0.0	0.8867E 02
2.50	11.66	0.0635	0.0244	0.9120	0.0	0.0	0.1503E 03
3.00	12.16	0.0562	0.0291	0.9147	0.0	0.0	0.2256E 03
3.50	12.66	0.0509	0.0345	0.9146	0.0	0.0	0.3111E 03
4.00	13.16	0.0463	0.0402	0.9134	0.0	0.0002	0.4047E 03
4.50	13.66	0.0430	0.0459	0.9105	0.0002	0.0004	0.5023E 03
5.00	14.16	0.0407	0.0521	0.9056	0.0006	0.0009	0.6028E 03
5.50	14.66	0.0290	0.0566	0.9006	0.0017	0.0021	0.7041E 03
6.00	15.16	0.0376	0.0598	0.8947	0.0034	0.0044	0.8072E 03
6.50	15.66	0.0365	0.0621	0.8873	0.0057	0.0083	0.9132E 03
7.00	16.16	0.0354	0.0637	0.8784	0.0086	0.0139	0.1023E 04
7.50	16.66	0.0344	0.0648	0.8681	0.0118	0.0209	0.1137E 04
8.00	17.16	0.0335	0.0655	0.8571	0.0152	0.0287	0.1254E 04
8.50	17.66	0.0328	0.0660	0.8474	0.0183	0.0355	0.1372E 04
9.00	18.16	0.0321	0.0664	0.8395	0.0210	0.0411	0.1490E 04
9.50	18.66	0.0316	0.0668	0.8324	0.0232	0.0460	0.1609E 04
10.00	19.16	0.0311	0.0671	0.8265	0.0251	0.0502	0.1727E 04

Fig. 17

(d) M-CHLOROBENZIL

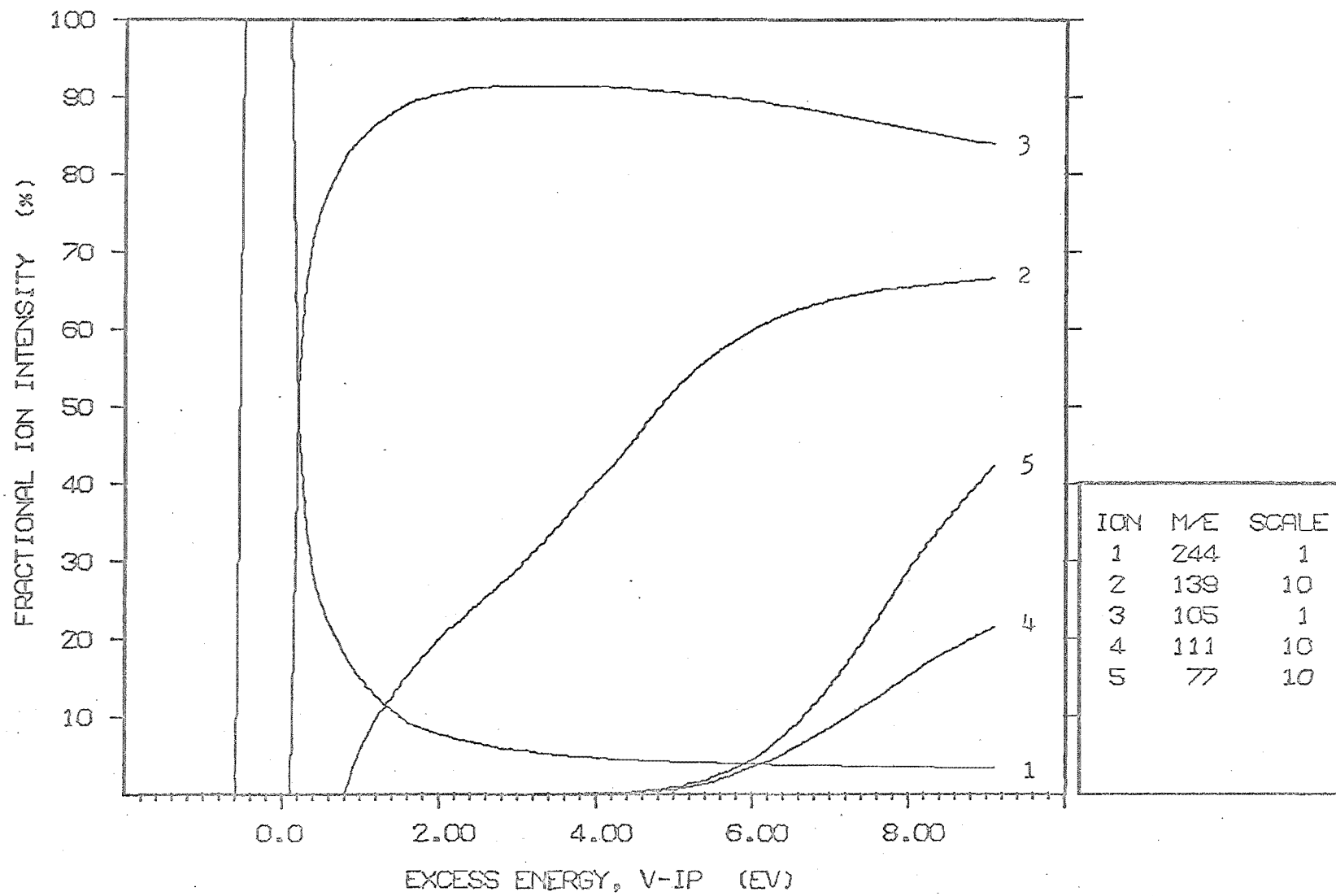


Table 5

(e) m-BROMOBENZILE

EXCESS ENERGY (EV)	ELECTRON ENERGY (EV)	FRACTIONAL		ION	INTENSITIES		TOTAL INTENSITY (ARB UNITS)
		288 (1)	183 (2)	M/E 105 (3)	155 (4)	77 (5)	
-1.00	8.10	0.0	0.0	0.0	0.0	0.0	0.0
-0.50	8.60	1.0000	0.0	0.0	0.0	0.0	0.1370E-01
0.0	9.10	1.0000	0.0	0.0	0.0	0.0	0.3394E 00
0.50	9.60	0.2582	0.0	0.7418	0.0	0.0	0.7817E 01
1.00	10.10	0.1475	0.0027	0.8498	0.0	0.0	0.3903E 02
1.50	10.60	0.0924	0.0070	0.9005	0.0	0.0	0.1160E 03
2.00	11.10	0.0663	0.0127	0.9210	0.0	0.0	0.2432E 03
2.50	11.60	0.0555	0.0189	0.9257	0.0	0.0	0.3928E 03
3.00	12.10	0.0487	0.0251	0.9262	0.0	0.0	0.5722E 03
3.50	12.60	0.0437	0.0308	0.9255	0.0	0.0	0.7980E 03
4.00	13.10	0.0399	0.0363	0.9237	0.0	0.0001	0.1068E 04
4.50	13.60	0.0370	0.0425	0.9202	0.0001	0.0002	0.1363E 04
5.00	14.10	0.0350	0.0485	0.9156	0.0002	0.0007	0.1663E 04
5.50	14.60	0.0336	0.0544	0.9100	0.0006	0.0014	0.1967E 04
6.00	15.10	0.0325	0.0587	0.9048	0.0013	0.0028	0.2275E 04
6.50	15.60	0.0316	0.0619	0.8994	0.0022	0.0050	0.2586E 04
7.00	16.10	0.0308	0.0643	0.8936	0.0034	0.0079	0.2903E 04
7.50	16.60	0.0302	0.0661	0.8874	0.0049	0.0115	0.3225E 04
8.00	17.10	0.0296	0.0674	0.8811	0.0065	0.0154	0.3552E 04
8.50	17.60	0.0291	0.0685	0.8751	0.0081	0.0192	0.3882E 04
9.00	18.10	0.0287	0.0695	0.8701	0.0095	0.0223	0.4213E 04
9.50	18.60	0.0283	0.0703	0.8658	0.0107	0.0250	0.4543E 04
10.00	19.10	0.0280	0.0709	0.8621	0.0117	0.0273	0.4873E 04

Fig. 17

(e) M-BROMOBENZIL

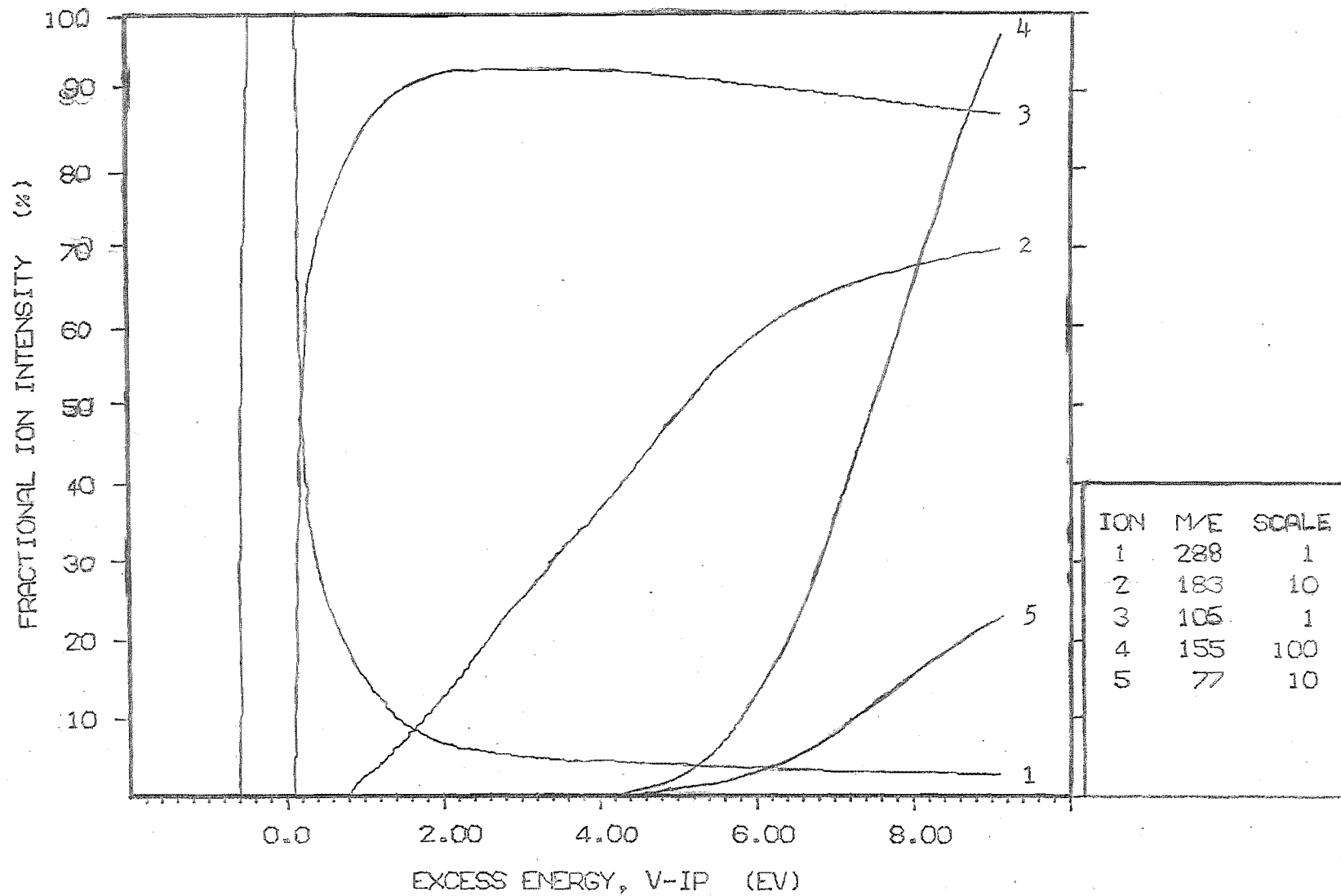


Table 5

(f) p-BROMOBENZIL

EXCESS ENERGY (EV)	ELECTRON ENERGY (EV)	FRACTIONAL ION INTENSITIES					TOTAL INTENSITY (ARB UNITS)
		288 (1)	183 (2)	M/E 105 (3)	155 (4)	77 (5)	
-1.00	8.11	0.0	0.0	0.0	0.0	0.0	0.0
-0.50	8.61	1.0000	0.0	0.0	0.0	0.0	0.1039E-01
0.0	9.11	1.0000	0.0	0.0	0.0	0.0	0.1489E 00
0.50	9.61	0.1386	0.0943	0.7672	0.0	0.0	0.5467E 01
1.00	10.11	0.0839	0.1265	0.7396	0.0	0.0	0.2763E 02
1.50	10.61	0.0593	0.1473	0.7935	0.0	0.0	0.7919E 02
2.00	11.11	0.0459	0.1670	0.7872	0.0	0.0	0.1603E 03
2.50	11.61	0.0387	0.1801	0.7812	0.0	0.0	0.2663E 03
3.00	12.11	0.0343	0.1913	0.7744	0.0	0.0	0.3982E 03
3.50	12.61	0.0316	0.2006	0.7678	0.0	0.0	0.5534E 03
4.00	13.11	0.0290	0.2090	0.7617	0.0	0.0002	0.7321E 03
4.50	13.61	0.0271	0.2180	0.7542	0.0002	0.0006	0.9250E 03
5.00	14.11	0.0257	0.2264	0.7460	0.0006	0.0013	0.1123E 04
5.50	14.61	0.0247	0.2317	0.7390	0.0017	0.0028	0.1323E 04
6.00	15.11	0.0238	0.2350	0.7317	0.0037	0.0058	0.1527E 04
6.50	15.61	0.0231	0.2367	0.7234	0.0064	0.0104	0.1738E 04
7.00	16.11	0.0225	0.2370	0.7140	0.0096	0.0170	0.1957E 04
7.50	16.61	0.0218	0.2362	0.7034	0.0135	0.0250	0.2185E 04
8.00	17.11	0.0213	0.2348	0.6926	0.0176	0.0337	0.2421E 04
8.50	17.61	0.0208	0.2332	0.6823	0.0220	0.0417	0.2663E 04
9.00	18.11	0.0203	0.2317	0.6735	0.0261	0.0483	0.2905E 04
9.50	18.61	0.0200	0.2305	0.6650	0.0295	0.0540	0.3148E 04
10.00	19.11	0.0196	0.2295	0.6576	0.0325	0.0588	0.3390E 04

Fig. 17

(f) P-BROMOBENZIL

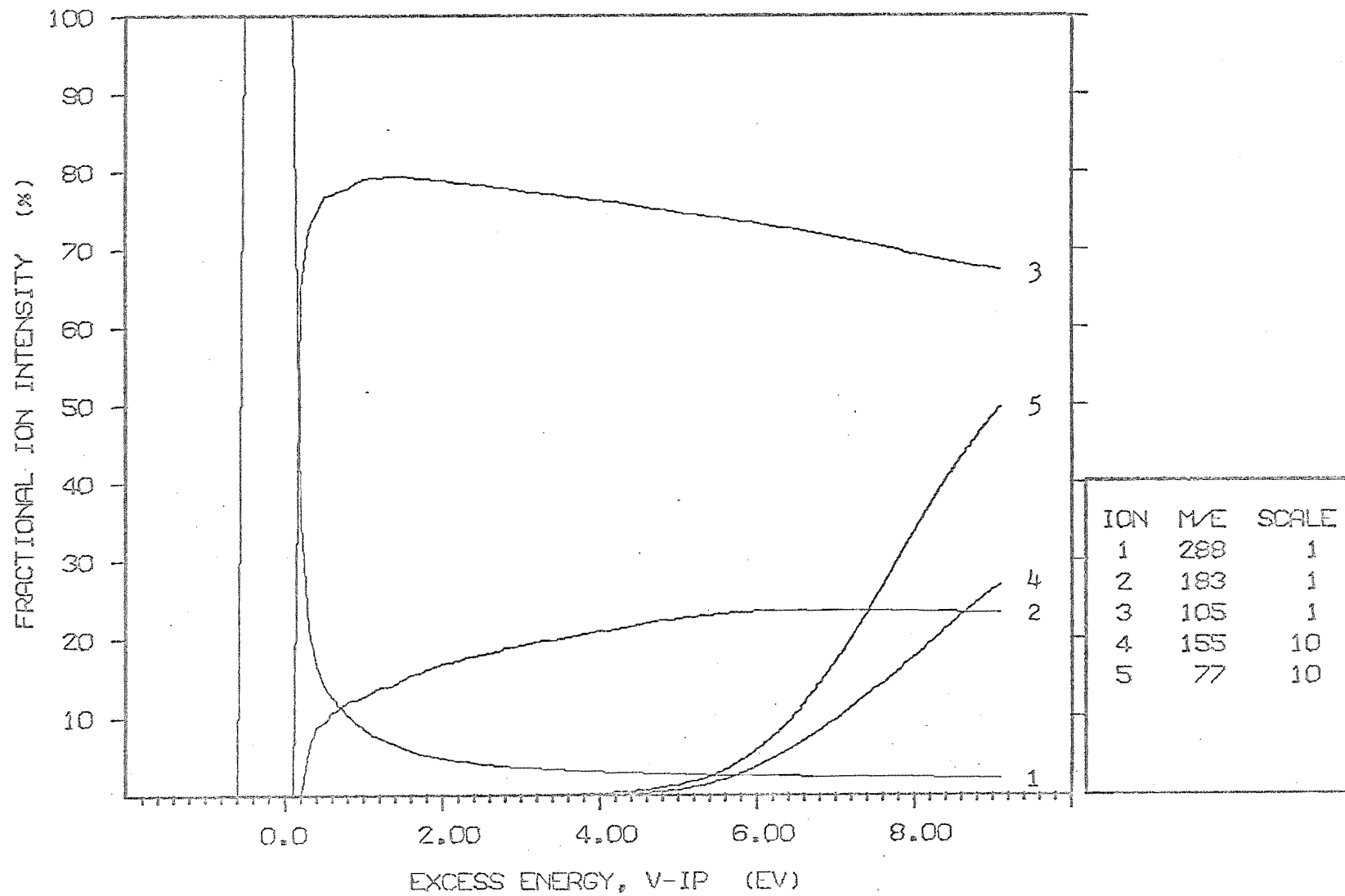


Table 5

(g) M-METHYLBENZIL

EXCESS ENERGY (eV)	ELECTRON ENERGY (eV)	FRACTIONAL		ION	INTENSITIES		TOTAL INTENSITY (ARB UNITS)
		224 (1)	119 (2)	M/E 105 (3)	91 (4)	77 (5)	
-1.00	8.05	0.0	0.0	0.0	0.0	0.0	0.0
-0.50	8.55	1.0000	0.0	0.0	0.0	0.0	0.2031E-01
0.0	9.05	1.0000	0.0	0.0	0.0	0.0	0.3874E 00
0.50	9.55	0.3831	0.5980	0.0189	0.0	0.0	0.5259E 01
1.00	10.05	0.2251	0.7299	0.0450	0.0	0.0	0.2707E 02
1.50	10.55	0.1551	0.7857	0.0592	0.0	0.0	0.7721E 02
2.00	11.05	0.1216	0.8089	0.0694	0.0	0.0	0.1560E 03
2.50	11.55	0.1026	0.8191	0.0783	0.0	0.0	0.2615E 03
3.00	12.05	0.0906	0.8231	0.0863	0.0	0.0	0.3902E 03
3.50	12.55	0.0827	0.8234	0.0939	0.0001	0.0	0.5442E 03
4.00	13.05	0.0756	0.8227	0.1013	0.0003	0.0000	0.7186E 03
4.50	13.55	0.0700	0.8184	0.1107	0.0008	0.0001	0.8928E 03
5.00	14.05	0.0668	0.8110	0.1199	0.0020	0.0002	0.1057E 04
5.50	14.55	0.0645	0.8057	0.1248	0.0046	0.0003	0.1221E 04
6.00	15.05	0.0626	0.7998	0.1281	0.0088	0.0007	0.1389E 04
6.50	15.55	0.0610	0.7928	0.1304	0.0146	0.0013	0.1560E 04
7.00	16.05	0.0595	0.7849	0.1318	0.0217	0.0022	0.1737E 04
7.50	16.55	0.0581	0.7766	0.1327	0.0292	0.0034	0.1919E 04
8.00	17.05	0.0568	0.7677	0.1330	0.0375	0.0050	0.2106E 04
8.50	17.55	0.0557	0.7594	0.1331	0.0450	0.0069	0.2295E 04
9.00	18.05	0.0547	0.7521	0.1332	0.0513	0.0087	0.2487E 04
9.50	18.55	0.0538	0.7459	0.1333	0.0568	0.0103	0.2677E 04
10.00	19.05	0.0531	0.7405	0.1333	0.0615	0.0116	0.2868E 04

Fig. 17

(g) M-METHYLBENZIL

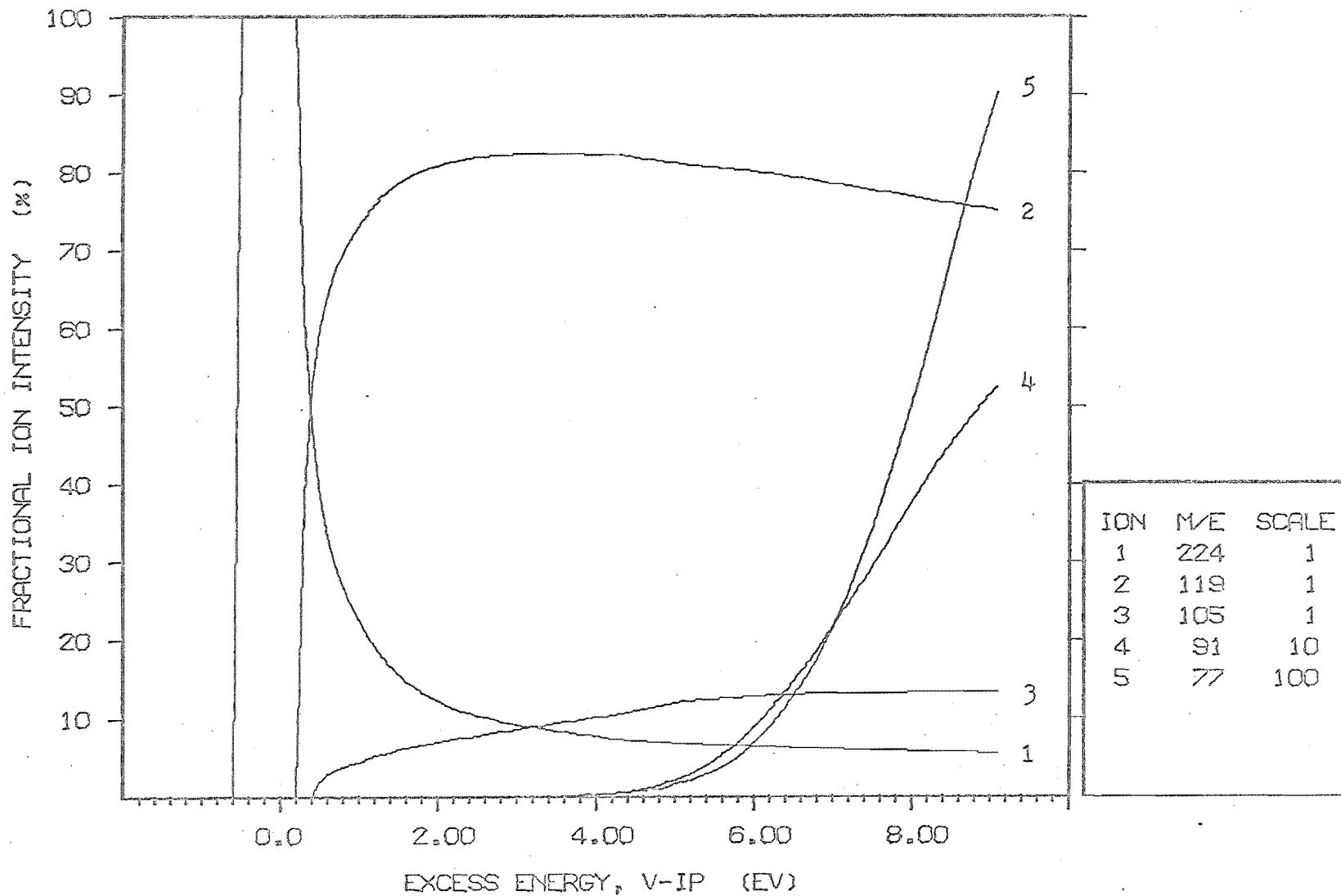


Table 5

(h) M-METHOXYBENZIL

EXCESS ENERGY (eV)	ELECTRON ENERGY (eV)	FRACTIONAL ION INTENSITIES					TOTAL INTENSITY (ARB. UNITS)
		240 (1)	135 (2)	M/E 105 (3)	107 (4)	77 (5)	
-1.00	7.75	0.0	0.0	0.0	0.0	0.0	0.0
-0.50	8.25	1.0000	0.0	0.0	0.0	0.0	0.4637E-02
0.0	8.75	1.0000	0.0	0.0	0.0	0.0	0.7196E-01
0.50	9.25	0.8034	0.1966	0.0	0.0	0.0	0.5260E 00
1.00	9.75	0.6011	0.3989	0.0	0.0	0.0	0.2106E 01
1.50	10.25	0.4529	0.5128	0.0343	0.0	0.0	0.5447E 01
2.00	10.75	0.3512	0.5931	0.0557	0.0	0.0	0.1080E 02
2.50	11.25	0.2879	0.6404	0.0717	0.0	0.0	0.1794E 02
3.00	11.75	0.2487	0.6664	0.0849	0.0	0.0	0.2661E 02
3.50	12.25	0.2215	0.6831	0.0954	0.0	0.0	0.3727E 02
4.00	12.75	0.1985	0.6944	0.1071	0.0	0.0	0.4957E 02
4.50	13.25	0.1787	0.7025	0.1185	0.0003	0.0	0.6310E 02
5.00	13.75	0.1630	0.7064	0.1296	0.0010	0.0	0.7693E 02
5.50	14.25	0.1516	0.7070	0.1389	0.0024	0.0	0.9079E 02
6.00	14.75	0.1431	0.7065	0.1455	0.0049	0.0	0.1049E 03
6.50	15.25	0.1364	0.7047	0.1503	0.0085	0.0001	0.1192E 03
7.00	15.75	0.1308	0.7015	0.1536	0.0135	0.0006	0.1339E 03
7.50	16.25	0.1250	0.6973	0.1559	0.0192	0.0016	0.1490E 03
8.00	16.75	0.1218	0.6925	0.1575	0.0251	0.0032	0.1643E 03
8.50	17.25	0.1180	0.6868	0.1584	0.0312	0.0057	0.1801E 03
9.00	17.75	0.1146	0.6803	0.1588	0.0371	0.0092	0.1964E 03
9.50	18.25	0.1114	0.6736	0.1588	0.0425	0.0137	0.2131E 03
10.00	18.75	0.1086	0.6670	0.1586	0.0471	0.0186	0.2301E 03

Fig. 17

(h) M-METHOXYBENZIL

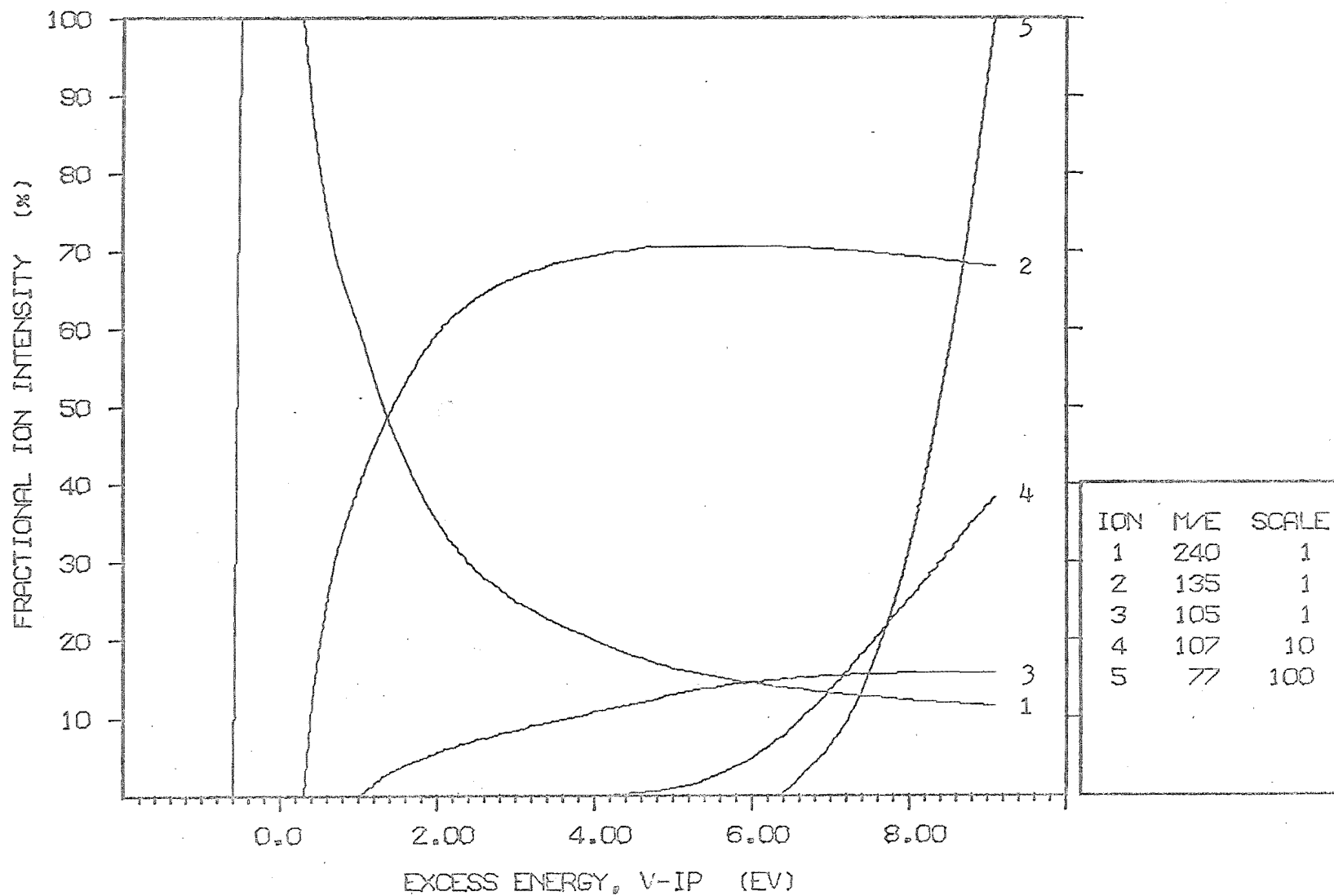


Table 5

(i) P-PHENYLBENZIL

EXCESS ENERGY (EV)	ELECTRON ENERGY (EV)	FRACTIONAL ION INTENSITIES					TOTAL INTENSITY (ARB UNITS)
		286 (1)	181 (2)	M/E 105 (3)	153 (4)	152 (5)	
-1.00	7.59	0.0	0.0	0.0	0.0	0.0	0.0
-0.50	8.09	1.0000	0.0	0.0	0.0	0.0	0.1485E-01
0.0	8.59	1.0000	0.0	0.0	0.0	0.0	0.2079E 00
0.50	9.09	0.4299	0.5701	0.0	0.0	0.0	0.2593E 01
1.00	9.59	0.2511	0.7489	0.0	0.0	0.0	0.1350E 02
1.50	10.09	0.1716	0.8253	0.0030	0.0	0.0	0.3971E 02
2.00	10.59	0.1222	0.8725	0.0053	0.0	0.0	0.8652E 02
2.50	11.09	0.0960	0.8963	0.0077	0.0	0.0	0.1513E 03
3.00	11.59	0.0844	0.9055	0.0101	0.0	0.0	0.2208E 03
3.50	12.09	0.0709	0.9170	0.0121	0.0	0.0	0.2249E 03
4.00	12.59	0.0634	0.9216	0.0148	0.0	0.0	0.4375E 03
4.50	13.09	0.0576	0.9248	0.0174	0.0	0.0	0.5674E 03
5.00	13.59	0.0535	0.9247	0.0213	0.0002	0.0	0.7028E 03
5.50	14.09	0.0507	0.9234	0.0247	0.0008	0.0	0.8371E 03
6.00	14.59	0.0487	0.9215	0.0272	0.0022	0.0	0.9725E 03
6.50	15.09	0.0471	0.9184	0.0291	0.0049	0.0000	0.1110E 04
7.00	15.59	0.0457	0.9136	0.0304	0.0094	0.0001	0.1250E 04
7.50	16.09	0.0445	0.9072	0.0314	0.0157	0.0002	0.1395E 04
8.00	16.59	0.0434	0.8993	0.0321	0.0233	0.0005	0.1544E 04
8.50	17.09	0.0424	0.8905	0.0327	0.0315	0.0011	0.1698E 04
9.00	17.59	0.0414	0.8821	0.0330	0.0387	0.0021	0.1854E 04
9.50	18.09	0.0406	0.8739	0.0333	0.0448	0.0037	0.2012E 04
10.00	18.59	0.0399	0.8657	0.0335	0.0500	0.0061	0.2175E 04

Fig. 17

(i) P-PHENYLBENZIL

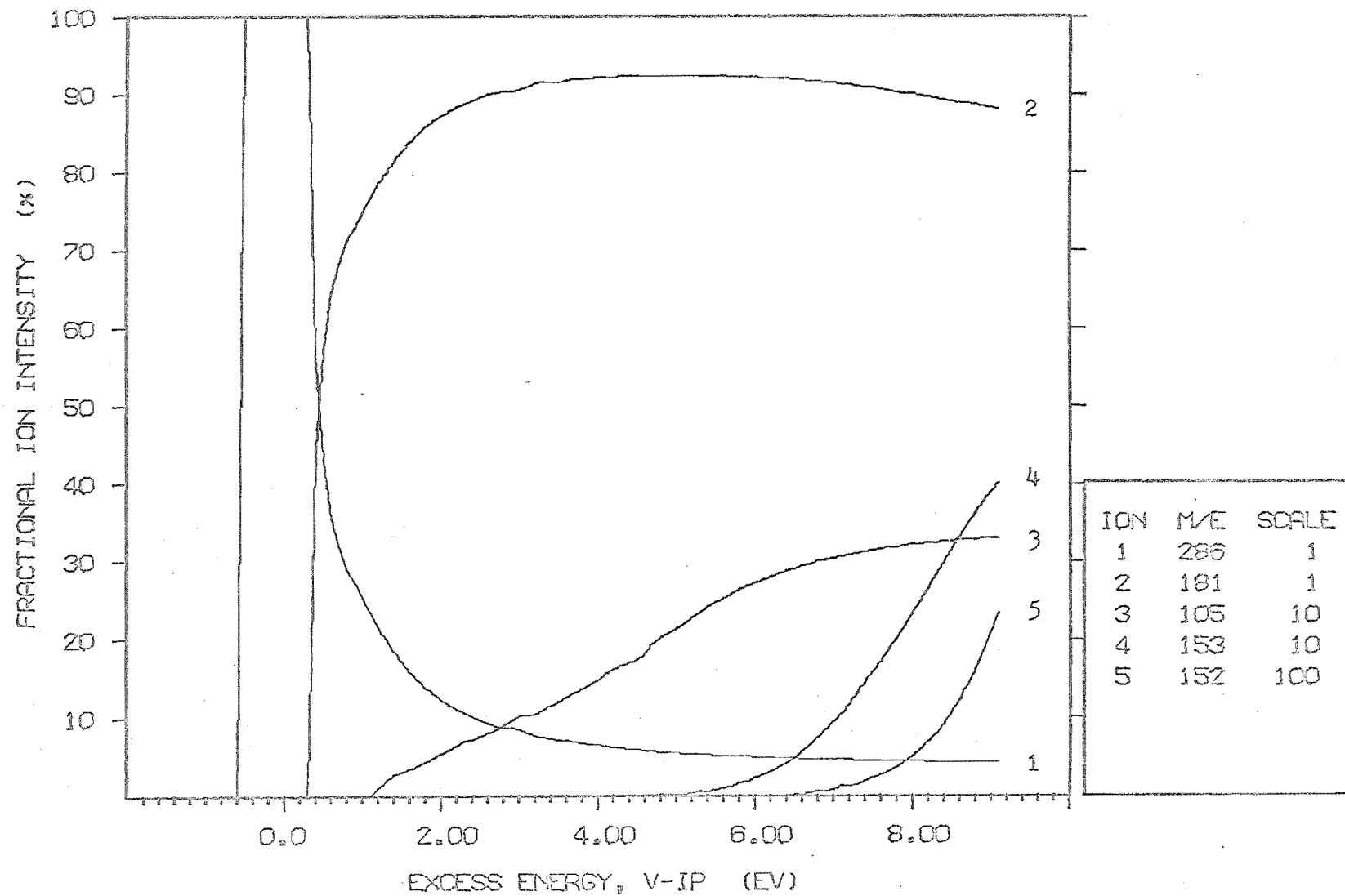


Table 5

(j) M-FORMYLBENZIL

EXCESS ENERGY (EV)	ELECTRON ENERGY (EV)	FRACTIONAL ION INTENSITIES					TOTAL INTENSITY (ARB UNITS)
		238 (1)	133 (2)	M/E 105 (3)	77 (4)	77 (5)	
-1.00	8.14	0.0	0.0	0.0	0.0	0.0	0.0
-0.50	8.64	1.0000	0.0	0.0	0.0	0.0	0.1167E-01
0.0	9.14	1.0000	0.0	0.0	0.0	0.0	0.1564E 00
0.50	9.64	0.4600	0.0	0.5400	0.0	0.0	0.1669E 01
1.00	10.14	0.1622	0.0092	0.8286	0.0	0.0	0.1302E 02
1.50	10.64	0.0879	0.0131	0.8989	0.0	0.0	0.4492E 02
2.00	11.14	0.0611	0.0163	0.9226	0.0	0.0	0.1005E 03
2.50	11.64	0.0491	0.0192	0.9317	0.0	0.0	0.1739E 03
3.00	12.14	0.0422	0.0219	0.9359	0.0	0.0	0.2644E 03
3.50	12.64	0.0379	0.0249	0.9371	0.0	0.0	0.3738E 03
4.00	13.14	0.0342	0.0286	0.9372	0.0	0.0	0.5055E 03
4.50	13.64	0.0311	0.0335	0.9350	0.0003	0.0	0.6484E 03
5.00	14.14	0.0291	0.0388	0.9309	0.0011	0.0	0.7914E 03
5.50	14.64	0.0277	0.0432	0.9264	0.0027	0.0	0.9361E 03
6.00	15.14	0.0266	0.0463	0.9217	0.0054	0.0	0.1082E 04
6.50	15.64	0.0257	0.0486	0.9163	0.0093	0.0	0.1231E 04
7.00	16.14	0.0250	0.0503	0.9102	0.0145	0.0	0.1383E 04
7.50	16.64	0.0244	0.0516	0.9035	0.0205	0.0	0.1537E 04
8.00	17.14	0.0238	0.0525	0.8965	0.0273	0.0	0.1693E 04
8.50	17.64	0.0233	0.0532	0.8900	0.0335	0.0	0.1854E 04
9.00	18.14	0.0229	0.0539	0.8846	0.0387	0.0	0.2013E 04
9.50	18.64	0.0226	0.0544	0.8799	0.0431	0.0	0.2172E 04
10.00	19.14	0.0223	0.0548	0.8759	0.0470	0.0	0.2331E 04

Fig. 17

(j) M-FORMYLBENZIL

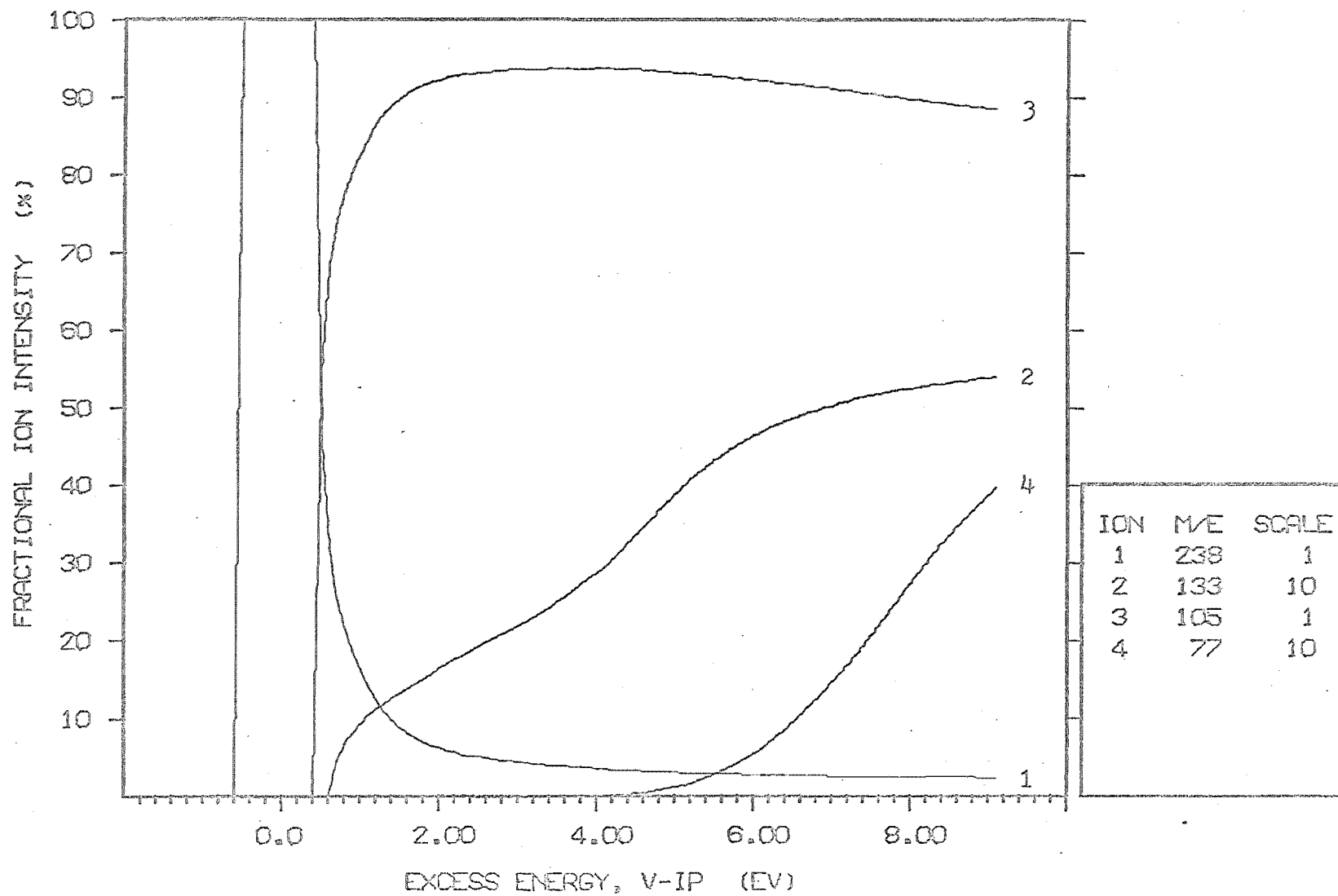


Table 5

(k) m-CYANOBENZIL

EXCESS ENERGY (EV)	ELECTRON ENERGY (EV)	FRACTIONAL ION INTENSITIES					TOTAL INTENSITY (ARB UNITS)
		235 (1)	130 (2)	M/E 105 (3)	102 (4)	77 (5)	
-1.00	8.30	0.0	0.0	0.0	0.0	0.0	0.0
-0.50	8.80	1.0000	0.0	0.0	0.0	0.0	0.4699E-02
0.0	9.30	1.0000	0.0	0.0	0.0	0.0	0.6893E-01
0.50	9.80	0.1176	0.0	0.8824	0.0	0.0	0.2757E 01
1.00	10.30	0.0555	0.0	0.9445	0.0	0.0	0.1526E 02
1.50	10.80	0.0306	0.0002	0.9691	0.0	0.0	0.4243E 02
2.00	11.30	0.0210	0.0008	0.9783	0.0	0.0	0.1116E 03
2.50	11.80	0.0168	0.0012	0.9821	0.0	0.0	0.1990E 03
3.00	12.30	0.0143	0.0016	0.9842	0.0	0.0	0.3110E 03
3.50	12.80	0.0126	0.0019	0.9855	0.0	0.0	0.4434E 03
4.00	13.30	0.0116	0.0026	0.9859	0.0	0.0	0.5819E 03
4.50	13.80	0.0109	0.0036	0.9851	0.0	0.0004	0.7184E 03
5.00	14.30	0.0104	0.0050	0.9831	0.0	0.0014	0.8561E 03
5.50	14.80	0.0100	0.0068	0.9797	0.0000	0.0035	0.9960E 03
6.00	15.30	0.0096	0.0089	0.9743	0.0000	0.0070	0.1139E 04
6.50	15.80	0.0094	0.0106	0.9677	0.0001	0.0122	0.1285E 04
7.00	16.30	0.0091	0.0119	0.9597	0.0003	0.0190	0.1436E 04
7.50	16.80	0.0089	0.0129	0.9505	0.0006	0.0271	0.1591E 04
8.00	17.30	0.0087	0.0137	0.9399	0.0010	0.0367	0.1751E 04
8.50	17.80	0.0084	0.0143	0.9285	0.0017	0.0471	0.1917E 04
9.00	18.30	0.0083	0.0148	0.9184	0.0024	0.0560	0.2084E 04
9.50	18.80	0.0081	0.0153	0.9097	0.0034	0.0635	0.2251E 04
10.00	19.30	0.0080	0.0156	0.9020	0.0044	0.0700	0.2419E 04

Fig. 17

(k) M-CYANOBENZIL

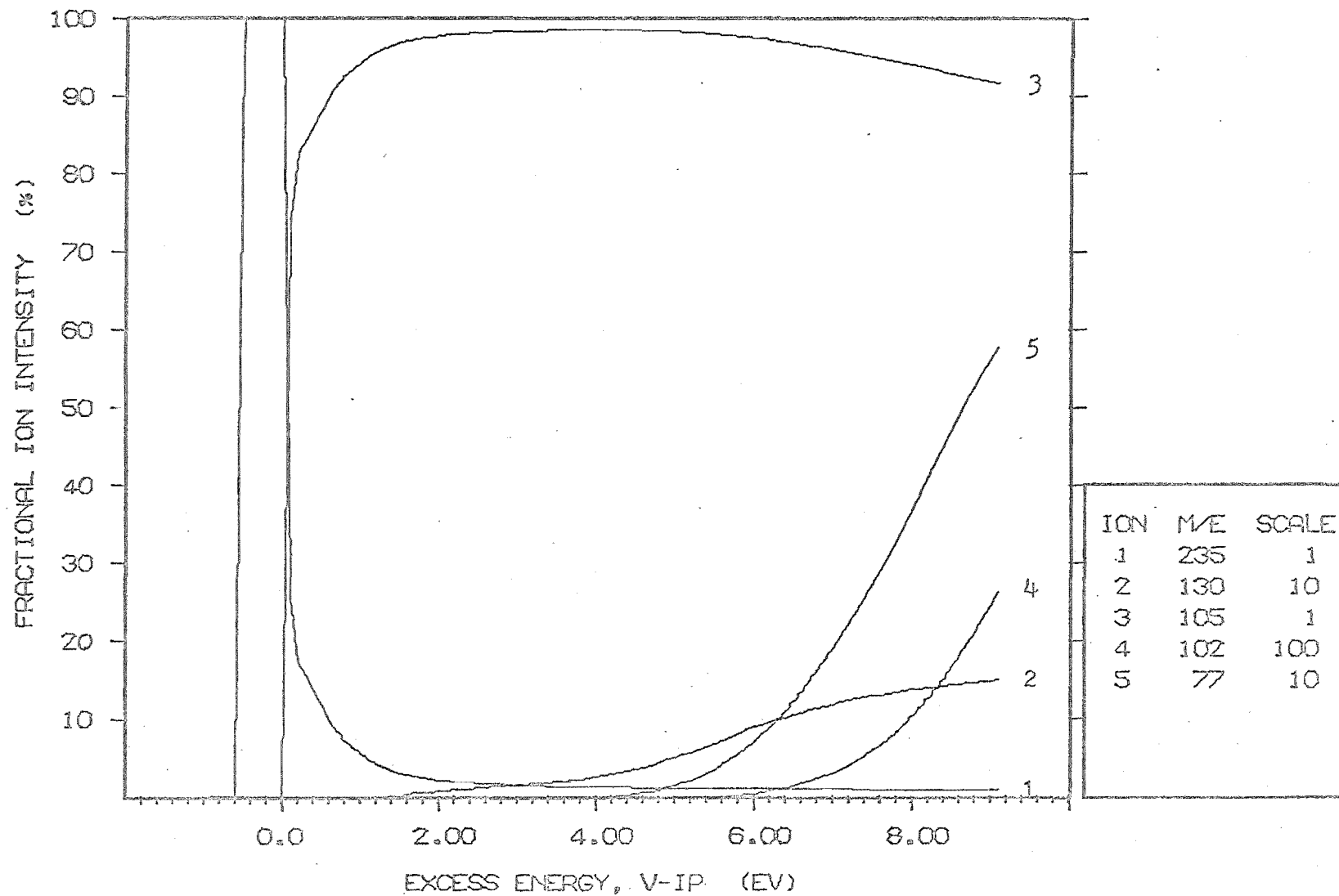


Table 5

(I) M-TRIFLUOROMETHYLBENZIL

EXCESS ENERGY (EV)	ELECTRON ENERGY (EV)	FRACTIONAL ION INTENSITIES					TOTAL INTENSITY (ARB UNITS)
		278 (1)	173 (2)	M/E 105 (3)	145 (4)	77 (5)	
-1.00	8.34	0.0	0.0	0.0	0.0	0.0	0.0
-0.50	8.84	1.0000	0.0	0.0	0.0	0.0	0.5965E-02
0.0	9.34	1.0000	0.0	0.0	0.0	0.0	0.8643E-01
0.50	9.84	0.0735	0.0	0.9265	0.0	0.0	0.5617E 01
1.00	10.34	0.0407	0.0015	0.9578	0.0	0.0	0.2555E 02
1.50	10.84	0.0270	0.0032	0.9698	0.0	0.0	0.7170E 02
2.00	11.34	0.0206	0.0041	0.9752	0.0	0.0	0.1476E 03
2.50	11.84	0.0164	0.0050	0.9786	0.0	0.0	0.2465E 03
3.00	12.34	0.0142	0.0059	0.9798	0.0	0.0	0.3694E 03
3.50	12.84	0.0128	0.0073	0.9800	0.0	0.0	0.5164E 03
4.00	13.34	0.0117	0.0088	0.9795	0.0	0.0000	0.6883E 03
4.50	13.84	0.0106	0.0105	0.9784	0.0000	0.0005	0.8779E 03
5.00	14.34	0.0096	0.0125	0.9763	0.0000	0.0016	0.1070E 04
5.50	14.84	0.0089	0.0148	0.9726	0.0001	0.0035	0.1265E 04
6.00	15.34	0.0083	0.0168	0.9675	0.0002	0.0067	0.1463E 04
6.50	15.84	0.0079	0.0183	0.9611	0.0003	0.0112	0.1666E 04
7.00	16.34	0.0075	0.0194	0.9530	0.0006	0.0172	0.1875E 04
7.50	16.84	0.0072	0.0202	0.9438	0.0010	0.0242	0.2099E 04
8.00	17.34	0.0070	0.0208	0.9343	0.0017	0.0317	0.2310E 04
8.50	17.84	0.0067	0.0213	0.9245	0.0024	0.0394	0.2536E 04
9.00	18.34	0.0065	0.0216	0.9156	0.0034	0.0464	0.2763E 04
9.50	18.84	0.0063	0.0220	0.9081	0.0043	0.0525	0.2991E 04
10.00	19.34	0.0062	0.0222	0.9016	0.0051	0.0576	0.3218E 04

Fig. 17

(I) M-TRIFLUOROMETHYLBENZIL

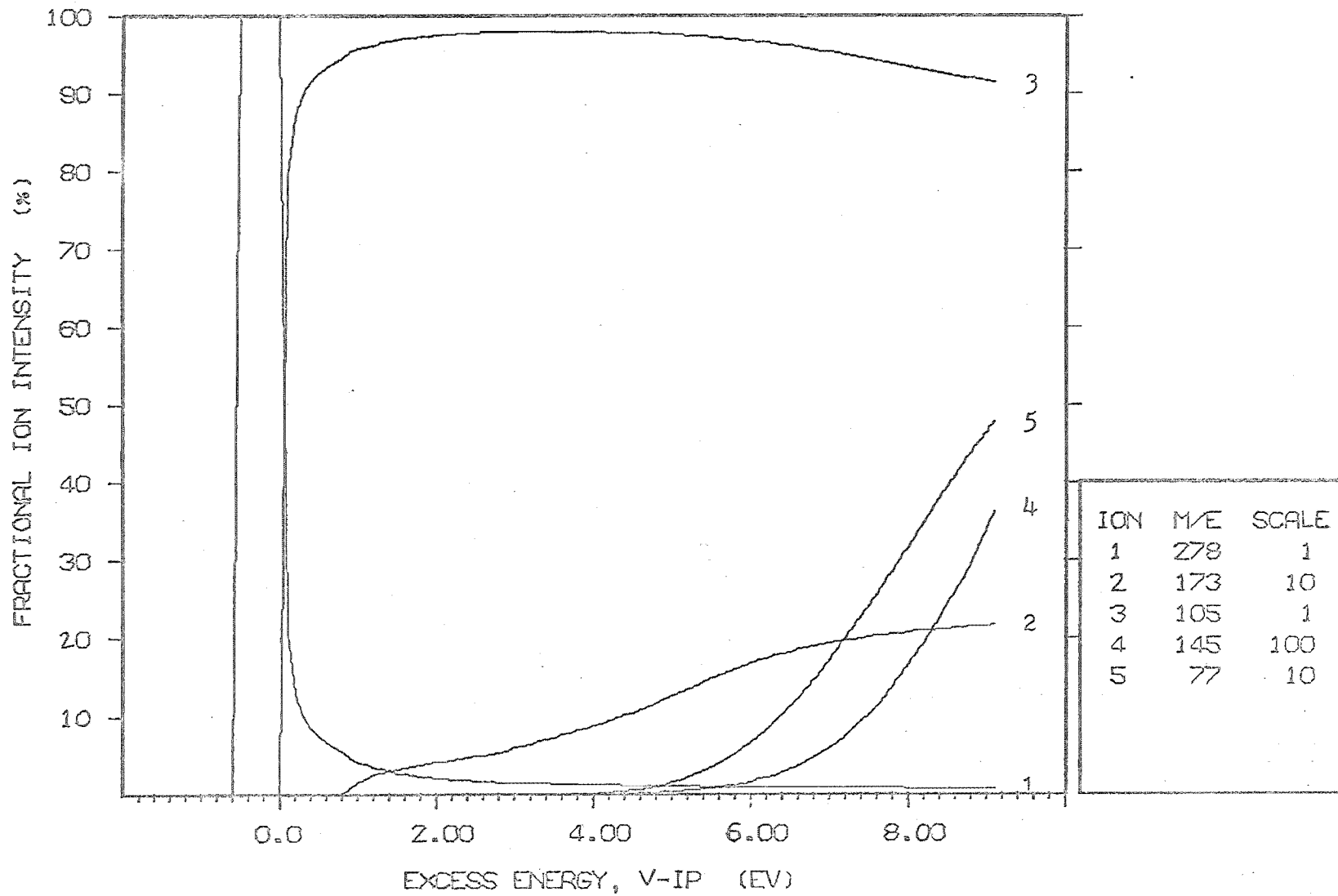


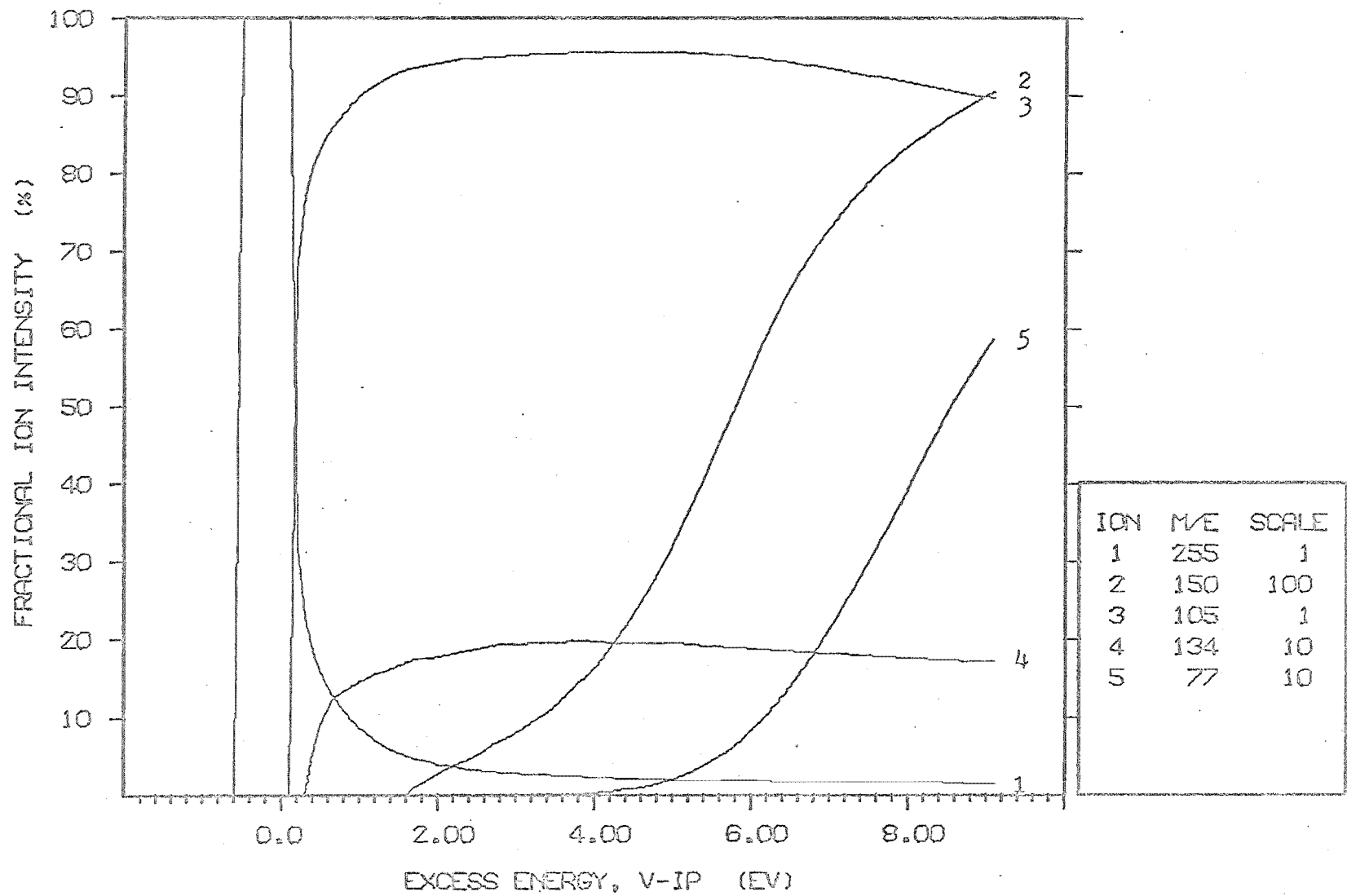
Table 5

(m) M-NITROBENZIL

EXCESS ENERGY (EV)	ELECTRON ENERGY (EV)	FRACTIONAL ION INTENSITIES					TOTAL INTENSITY (ARB UNITS)
		255 (1)	150 (2)	M/E 105 (3)	134 (4)	77 (5)	
-1.00	8.33	0.0	0.0	0.0	0.0	0.0	0.0
-0.50	8.83	1.0000	0.0	0.0	0.0	0.0	0.8857E-02
0.0	9.33	1.0000	0.0	0.0	0.0	0.0	0.1298E 00
0.50	9.83	0.1559	0.0	0.8348	0.0093	0.0	0.4441E 01
1.00	10.33	0.0858	0.0	0.8997	0.0145	0.0	0.2297E 02
1.50	10.83	0.0535	0.0	0.9298	0.0167	0.0	0.6857E 02
2.00	11.33	0.0389	0.0003	0.9429	0.0179	0.0	0.1466E 03
2.50	11.83	0.0318	0.0005	0.9488	0.0188	0.0	0.2530E 03
3.00	12.33	0.0274	0.0008	0.9523	0.0195	0.0	0.3930E 03
3.50	12.83	0.0246	0.0011	0.9545	0.0196	0.0	0.5625E 03
4.00	13.33	0.0223	0.0016	0.9559	0.0196	0.0002	0.7585E 03
4.50	13.83	0.0203	0.0023	0.9567	0.0193	0.0008	0.9982E 03
5.00	14.33	0.0189	0.0032	0.9555	0.0194	0.0020	0.1222E 04
5.50	14.83	0.0180	0.0043	0.9528	0.0190	0.0044	0.1459E 04
6.00	15.33	0.0173	0.0055	0.9483	0.0187	0.0081	0.1700E 04
6.50	15.83	0.0167	0.0065	0.9419	0.0183	0.0138	0.1942E 04
7.00	16.33	0.0162	0.0073	0.9340	0.0180	0.0212	0.2202E 04
7.50	16.83	0.0157	0.0079	0.9250	0.0177	0.0297	0.2464E 04
8.00	17.33	0.0153	0.0083	0.9152	0.0174	0.0393	0.2733E 04
8.50	17.83	0.0150	0.0087	0.9054	0.0172	0.0490	0.3009E 04
9.00	18.33	0.0147	0.0090	0.8972	0.0169	0.0571	0.3285E 04
9.50	18.83	0.0144	0.0092	0.8903	0.0168	0.0640	0.3559E 04
10.00	19.33	0.0142	0.0095	0.8843	0.0166	0.0699	0.3834E 04

Fig. 17

(m) M-NITROBENZIL



5.4 LOGARITHMIC ION INTENSITY RATIOS

The various logarithmic intensity ratios used to correlate the results of this work were calculated from the fractional ion intensities of the molecule-ion (F_M), and the substituted (F_X) and unsubstituted (F_H) benzoyl ions; the logarithmic ratios are tabulated in Table 6 (a-m) as a function of both the excess energy and the electron energy (i.e. corrected ionizing voltage) for the low voltage mass spectra. The corresponding ratios for the 70 eV spectra are given in Table 7 (a-m).

Table 6

(a) BENZIL

EXCESS ENERGY (EV)	ELECTRON ENERGY (EV)	LOGARITHMIC INTENSITY RATIOS				
		FX/FM	FH/FM	FX/I-FM	FH/I-FM	FX/FH

-1.00	8.20	0.0	0.0	0.0	0.0	0.0
-0.50	8.70	0.0	0.0	0.0	0.0	0.0
0.0	9.20	0.0	0.0	0.0	0.0	0.0
0.50	9.70	0.0	0.18	0.0	-0.00	0.0
1.00	10.20	0.0	0.51	0.0	0.00	0.0
1.50	10.70	0.0	0.74	0.0	0.00	0.0
2.00	11.20	0.0	0.88	0.0	-0.00	0.0
2.50	11.70	0.0	0.96	0.0	0.00	0.0
3.00	12.20	0.0	1.02	0.0	0.00	0.0
3.50	12.70	0.0	1.06	0.0	-0.00	0.0
4.00	13.20	0.0	1.10	0.0	-0.00	0.0
4.50	13.70	0.0	1.14	0.0	-0.00	0.0
5.00	14.20	0.0	1.17	0.0	-0.00	0.0
5.50	14.70	0.0	1.19	0.0	-0.00	0.0
6.00	15.20	0.0	1.21	0.0	-0.01	0.0
6.50	15.70	0.0	1.22	0.0	-0.01	0.0
7.00	16.20	0.0	1.23	0.0	-0.01	0.0
7.50	16.70	0.0	1.24	0.0	-0.02	0.0
8.00	17.20	0.0	1.24	0.0	-0.02	0.0
8.50	17.70	0.0	1.25	0.0	-0.03	0.0
9.00	18.20	0.0	1.25	0.0	-0.03	0.0
9.50	18.70	0.0	1.26	0.0	-0.03	0.0
10.00	19.20	0.0	1.26	0.0	-0.04	0.0
-1.20	8.00	0.0	0.0	0.0	0.0	0.0
-0.70	8.50	0.0	0.0	0.0	0.0	0.0
-0.20	9.00	0.0	0.0	0.0	0.0	0.0
0.30	9.50	0.0	-0.22	0.0	0.00	0.0
0.80	10.00	0.0	0.39	0.0	0.0	0.0
1.30	10.50	0.0	0.66	0.0	0.00	0.0
1.80	11.00	0.0	0.83	0.0	-0.00	0.0
2.30	11.50	0.0	0.93	0.0	-0.00	0.0
2.80	12.00	0.0	1.00	0.0	0.00	0.0
3.30	12.50	0.0	1.05	0.0	-0.00	0.0
3.80	13.00	0.0	1.09	0.0	-0.00	0.0
4.30	13.50	0.0	1.13	0.0	-0.00	0.0
4.80	14.00	0.0	1.16	0.0	-0.00	0.0
5.30	14.50	0.0	1.18	0.0	-0.00	0.0
5.80	15.00	0.0	1.20	0.0	-0.00	0.0
6.30	15.50	0.0	1.22	0.0	-0.01	0.0
6.80	16.00	0.0	1.23	0.0	-0.01	0.0
7.30	16.50	0.0	1.23	0.0	-0.02	0.0
7.80	17.00	0.0	1.24	0.0	-0.02	0.0
8.30	17.50	0.0	1.25	0.0	-0.03	0.0
8.80	18.00	0.0	1.25	0.0	-0.03	0.0
9.30	18.50	0.0	1.26	0.0	-0.03	0.0
9.80	19.00	0.0	1.26	0.0	-0.04	0.0
10.30	19.50	0.0	1.26	0.0	-0.04	0.0
10.80	20.00	0.0	1.27	0.0	-0.04	0.0

Table 6

(b) M-FLUOROBENZIL

EXCESS ENERGY (EV)	ELECTRON ENERGY (EV)	LOGARITHMIC INTENSITY RATIOS				
		FX/FM	FH/FM	FX/1-FM	FH/1-FM	FX/FH
-1.00	8.23	0.0	0.0	0.0	0.0	0.0
-0.50	8.73	0.0	0.0	0.0	0.0	0.0
0.0	9.23	0.0	0.0	0.0	0.0	0.0
0.50	9.73	0.0	0.88	0.0	0.00	0.0
1.00	10.23	0.0	1.21	0.0	0.00	0.0
1.50	10.73	-0.65	1.42	-2.07	-0.00	-2.07
2.00	11.23	-0.34	1.55	-1.90	-0.01	-1.90
2.50	11.73	-0.16	1.64	-1.80	-0.01	-1.79
3.00	12.23	-0.01	1.69	-1.72	-0.01	-1.71
3.50	12.73	0.11	1.74	-1.63	-0.01	-1.62
4.00	13.23	0.23	1.77	-1.56	-0.01	-1.55
4.50	13.73	0.33	1.80	-1.49	-0.01	-1.47
5.00	14.23	0.41	1.81	-1.42	-0.02	-1.41
5.50	14.73	0.46	1.83	-1.38	-0.02	-1.36
6.00	15.23	0.50	1.84	-1.35	-0.02	-1.33
6.50	15.73	0.53	1.84	-1.34	-0.03	-1.31
7.00	16.23	0.56	1.85	-1.32	-0.03	-1.29
7.50	16.73	0.58	1.86	-1.31	-0.04	-1.28
8.00	17.23	0.59	1.86	-1.31	-0.04	-1.27
8.50	17.73	0.61	1.86	-1.30	-0.05	-1.26
9.00	18.23	0.62	1.87	-1.30	-0.05	-1.25
9.50	18.73	0.63	1.87	-1.29	-0.05	-1.24
10.00	19.23	0.64	1.87	-1.29	-0.06	-1.23
-1.23	8.00	0.0	0.0	0.0	0.0	0.0
-0.73	8.50	0.0	0.0	0.0	0.0	0.0
-0.23	9.00	0.0	0.0	0.0	0.0	0.0
0.27	9.50	0.0	0.51	0.0	-0.00	0.0
0.77	10.00	0.0	1.08	0.0	-0.00	0.0
1.27	10.50	-0.90	1.33	-2.24	-0.00	-2.23
1.77	11.00	-0.46	1.50	-1.97	-0.00	-1.96
2.27	11.50	-0.23	1.61	-1.84	-0.01	-1.83
2.77	12.00	-0.08	1.67	-1.76	-0.01	-1.75
3.27	12.50	0.06	1.72	-1.67	-0.01	-1.66
3.77	13.00	0.17	1.76	-1.60	-0.01	-1.58
4.27	13.50	0.28	1.79	-1.52	-0.01	-1.51
4.77	14.00	0.37	1.81	-1.45	-0.02	-1.43
5.27	14.50	0.44	1.82	-1.40	-0.02	-1.38
5.77	15.00	0.49	1.83	-1.37	-0.02	-1.34
6.27	15.50	0.52	1.84	-1.34	-0.03	-1.32
6.77	16.00	0.55	1.85	-1.33	-0.03	-1.30
7.27	16.50	0.57	1.85	-1.32	-0.03	-1.28
7.77	17.00	0.59	1.86	-1.31	-0.04	-1.27
8.27	17.50	0.60	1.86	-1.30	-0.04	-1.26
8.77	18.00	0.61	1.87	-1.30	-0.05	-1.25
9.27	18.50	0.63	1.87	-1.30	-0.05	-1.24
9.77	19.00	0.63	1.87	-1.29	-0.06	-1.24
10.27	19.50	0.64	1.87	-1.29	-0.06	-1.23
10.77	20.00	0.65	1.88	-1.29	-0.06	-1.23

Table 6

(c) P-FLUOROBENZIL

EXCESS ENERGY (EV)	ELECTRON ENERGY (EV)	LOGARITHMIC INTENSITY RATIOS *****				
		FX/FM	FH/FM	FX/1-FM	FH/1-FM	FX/FH
-1.00	8.12	0.0	0.0	0.0	0.0	0.0
-0.50	8.62	0.0	0.0	0.0	0.0	0.0
0.0	9.12	0.0	0.0	0.0	0.0	0.0
0.50	9.62	-0.54	0.56	-1.13	-0.03	-1.10
1.00	10.12	-0.07	0.87	-0.98	-0.05	-0.94
1.50	10.62	0.23	1.10	-0.93	-0.05	-0.87
2.00	11.12	0.44	1.26	-0.88	-0.06	-0.81
2.50	11.62	0.57	1.34	-0.84	-0.07	-0.77
3.00	12.12	0.66	1.40	-0.82	-0.07	-0.74
3.50	12.62	0.73	1.44	-0.79	-0.08	-0.72
4.00	13.12	0.79	1.48	-0.77	-0.08	-0.69
4.50	13.62	0.84	1.50	-0.75	-0.09	-0.66
5.00	14.12	0.88	1.52	-0.73	-0.09	-0.64
5.50	14.62	0.91	1.53	-0.72	-0.09	-0.62
6.00	15.12	0.94	1.54	-0.71	-0.10	-0.61
6.50	15.62	0.95	1.55	-0.70	-0.10	-0.60
7.00	16.12	0.97	1.56	-0.70	-0.11	-0.59
7.50	16.62	0.98	1.56	-0.70	-0.11	-0.58
8.00	17.12	0.99	1.57	-0.70	-0.12	-0.58
8.50	17.62	1.00	1.57	-0.70	-0.12	-0.57
9.00	18.12	1.00	1.57	-0.70	-0.13	-0.57
9.50	18.62	1.01	1.58	-0.70	-0.13	-0.57
10.00	19.12	1.01	1.58	-0.70	-0.13	-0.57
-1.12	8.00	0.0	0.0	0.0	0.0	0.0
-0.62	8.50	0.0	0.0	0.0	0.0	0.0
-0.12	9.00	0.0	0.0	0.0	0.0	0.0
0.38	9.50	-0.85	0.45	-1.32	-0.02	-1.30
0.88	10.00	-0.16	0.80	-1.01	-0.04	-0.96
1.38	10.50	0.17	1.06	-0.95	-0.05	-0.89
1.88	11.00	0.40	1.23	-0.89	-0.06	-0.83
2.38	11.50	0.54	1.33	-0.85	-0.07	-0.78
2.88	12.00	0.64	1.39	-0.82	-0.07	-0.75
3.38	12.50	0.71	1.43	-0.80	-0.08	-0.72
3.88	13.00	0.77	1.47	-0.78	-0.08	-0.70
4.38	13.50	0.83	1.50	-0.75	-0.08	-0.67
4.88	14.00	0.87	1.52	-0.73	-0.09	-0.64
5.38	14.50	0.91	1.53	-0.72	-0.09	-0.62
5.88	15.00	0.93	1.54	-0.71	-0.10	-0.61
6.38	15.50	0.95	1.55	-0.70	-0.10	-0.60
6.88	16.00	0.96	1.56	-0.70	-0.11	-0.59
7.38	16.50	0.98	1.56	-0.70	-0.11	-0.59
7.88	17.00	0.99	1.57	-0.70	-0.12	-0.58
8.38	17.50	0.99	1.57	-0.70	-0.12	-0.58
8.88	18.00	1.00	1.57	-0.70	-0.12	-0.57
9.38	18.50	1.01	1.58	-0.70	-0.13	-0.57
9.88	19.00	1.01	1.58	-0.70	-0.13	-0.57
10.38	19.50	1.02	1.58	-0.70	-0.13	-0.56
10.88	20.00	1.02	1.58	-0.70	-0.14	-0.56

Table 6

(d) M-CHLOROBENZIL

EXCESS ENERGY (EV)	ELECTRON ENERGY (EV)	LOGARITHMIC INTENSITY RATIOS				
		FX/FM	FH/FM	FX/L-FM	FH/L-FM	FX/FH
-1.00	8.16	0.0	0.0	0.0	0.0	0.0
-0.50	8.66	0.0	0.0	0.0	0.0	0.0
0.0	9.16	0.0	0.0	0.0	0.0	0.0
0.50	9.66	0.0	0.49	0.0	0.00	0.0
1.00	10.16	-1.39	0.76	-2.15	-0.00	-2.15
1.50	10.66	-0.85	0.95	-1.81	-0.01	-1.90
2.00	11.16	-0.58	1.07	-1.66	-0.01	-1.65
2.50	11.66	-0.41	1.16	-1.58	-0.01	-1.57
3.00	12.16	-0.29	1.21	-1.51	-0.01	-1.50
3.50	12.66	-0.17	1.25	-1.44	-0.02	-1.42
4.00	13.16	-0.06	1.30	-1.38	-0.02	-1.36
4.50	13.66	0.03	1.33	-1.32	-0.02	-1.30
5.00	14.16	0.11	1.35	-1.27	-0.02	-1.24
5.50	14.66	0.16	1.36	-1.23	-0.03	-1.20
6.00	15.16	0.20	1.38	-1.21	-0.03	-1.17
6.50	15.66	0.23	1.39	-1.19	-0.04	-1.15
7.00	16.16	0.26	1.39	-1.18	-0.04	-1.14
7.50	16.66	0.27	1.40	-1.17	-0.05	-1.13
8.00	17.16	0.29	1.41	-1.17	-0.05	-1.12
8.50	17.66	0.30	1.41	-1.17	-0.06	-1.11
9.00	18.16	0.32	1.42	-1.16	-0.06	-1.10
9.50	18.66	0.33	1.42	-1.16	-0.07	-1.10
10.00	19.16	0.33	1.42	-1.16	-0.07	-1.09
-1.16	8.00	0.0	0.0	0.0	0.0	0.0
-0.66	8.50	0.0	0.0	0.0	0.0	0.0
-0.16	9.00	0.0	0.0	0.0	0.0	0.0
0.34	9.50	0.0	0.30	0.0	0.00	0.0
0.84	10.00	0.0	0.68	0.0	-0.00	0.0
1.34	10.50	-1.00	0.89	-1.90	-0.01	-1.89
1.84	11.00	-0.66	1.04	-1.71	-0.01	-1.70
2.34	11.50	-0.46	1.13	-1.61	-0.01	-1.60
2.84	12.00	-0.33	1.20	-1.54	-0.01	-1.52
3.34	12.50	-0.21	1.24	-1.46	-0.02	-1.45
3.84	13.00	-0.09	1.28	-1.39	-0.02	-1.38
4.34	13.50	-0.00	1.32	-1.34	-0.02	-1.32
4.84	14.00	0.08	1.34	-1.28	-0.02	-1.26
5.34	14.50	0.15	1.36	-1.24	-0.03	-1.21
5.84	15.00	0.19	1.37	-1.21	-0.03	-1.18
6.34	15.50	0.22	1.38	-1.19	-0.03	-1.16
6.84	16.00	0.25	1.39	-1.18	-0.04	-1.14
7.34	16.50	0.27	1.40	-1.18	-0.04	-1.13
7.84	17.00	0.29	1.41	-1.17	-0.05	-1.12
8.34	17.50	0.30	1.41	-1.17	-0.06	-1.11
8.84	18.00	0.31	1.42	-1.16	-0.06	-1.10
9.34	18.50	0.32	1.42	-1.16	-0.06	-1.10
9.84	19.00	0.33	1.42	-1.16	-0.07	-1.09
10.34	19.50	0.34	1.43	-1.16	-0.07	-1.09
10.84	20.00	0.35	1.43	-1.16	-0.07	-1.08

Table 6

(e) M-BROMOBENZIL

EXCESS ENERGY (EV)	ELECTRON ENERGY (EV)	LOGARITHMIC INTENSITY RATIOS				
		FX/FM	FH/FM	FX/I-FM	FH/I-FM	FX/FH
-1.00	8.10	0.0	0.0	0.0	0.0	0.0
-0.50	8.60	0.0	0.0	0.0	0.0	0.0
0.0	9.10	0.0	0.0	0.0	0.0	0.0
0.50	9.60	0.0	0.46	0.0	0.0	0.0
1.00	10.10	-1.74	0.76	-2.50	-0.00	-2.50
1.50	10.60	-1.12	0.99	-2.11	-0.00	-2.11
2.00	11.10	-0.72	1.14	-1.87	-0.01	-1.86
2.50	11.60	-0.47	1.22	-1.70	-0.01	-1.69
3.00	12.10	-0.29	1.28	-1.58	-0.01	-1.57
3.50	12.60	-0.15	1.33	-1.49	-0.01	-1.48
4.00	13.10	-0.04	1.37	-1.42	-0.02	-1.41
4.50	13.60	0.06	1.40	-1.35	-0.02	-1.34
5.00	14.10	0.14	1.42	-1.30	-0.02	-1.28
5.50	14.60	0.21	1.43	-1.25	-0.03	-1.22
6.00	15.10	0.26	1.45	-1.22	-0.03	-1.19
6.50	15.60	0.29	1.45	-1.19	-0.03	-1.16
7.00	16.10	0.32	1.46	-1.18	-0.04	-1.14
7.50	16.60	0.34	1.47	-1.17	-0.04	-1.13
8.00	17.10	0.36	1.47	-1.16	-0.04	-1.12
8.50	17.60	0.37	1.48	-1.15	-0.05	-1.11
9.00	18.10	0.38	1.48	-1.15	-0.05	-1.10
9.50	18.60	0.39	1.49	-1.14	-0.05	-1.09
10.00	19.10	0.40	1.49	-1.14	-0.05	-1.08
-1.10	8.00	0.0	0.0	0.0	0.0	0.0
-0.60	8.50	0.0	0.0	0.0	0.0	0.0
-0.10	9.00	0.0	0.0	0.0	0.0	0.0
0.40	9.50	0.0	0.36	0.0	-0.00	0.0
0.90	10.00	-2.03	0.71	-2.74	-0.00	-2.74
1.40	10.50	-1.22	0.95	-2.17	-0.00	-2.16
1.90	11.00	-0.79	1.12	-1.91	-0.01	-1.90
2.40	11.50	-0.51	1.21	-1.73	-0.01	-1.72
2.90	12.00	-0.32	1.27	-1.60	-0.01	-1.59
3.40	12.50	-0.18	1.32	-1.51	-0.01	-1.49
3.90	13.00	-0.06	1.36	-1.44	-0.02	-1.42
4.40	13.50	0.04	1.39	-1.37	-0.02	-1.35
4.90	14.00	0.13	1.41	-1.31	-0.02	-1.29
5.40	14.50	0.20	1.43	-1.26	-0.03	-1.23
5.90	15.00	0.25	1.44	-1.22	-0.03	-1.19
6.40	15.50	0.29	1.45	-1.20	-0.03	-1.17
6.90	16.00	0.31	1.46	-1.18	-0.03	-1.15
7.40	16.50	0.34	1.47	-1.17	-0.04	-1.13
7.90	17.00	0.35	1.47	-1.16	-0.04	-1.12
8.40	17.50	0.37	1.48	-1.15	-0.04	-1.11
8.90	18.00	0.38	1.48	-1.15	-0.05	-1.10
9.40	18.50	0.39	1.49	-1.14	-0.05	-1.09
9.90	19.00	0.40	1.49	-1.14	-0.05	-1.09
10.40	19.50	0.41	1.49	-1.13	-0.05	-1.08
10.90	20.00	0.42	1.49	-1.13	-0.05	-1.08

Table 6

(f) P-BROMOBENZIL

EXCESS ENERGY (EV)	ELECTRON ENERGY (FV)	LOGARITHMIC INTENSITY RATIOS				
		FX/FM	FH/FM	FX/I-FM	FH/I-FM	FX/FH
-1.00	8.11	0.0	0.0	0.0	0.0	0.0
-0.50	8.61	0.0	0.0	0.0	0.0	0.0
0.0	9.11	0.0	0.0	0.0	0.0	0.0
0.50	9.61	-0.17	0.74	-0.76	-0.05	-0.91
1.00	10.11	0.18	0.97	-0.86	-0.06	-0.80
1.50	10.61	0.40	1.13	-0.81	-0.07	-0.73
2.00	11.11	0.56	1.24	-0.76	-0.08	-0.67
2.50	11.61	0.67	1.31	-0.73	-0.09	-0.64
3.00	12.11	0.75	1.35	-0.70	-0.10	-0.61
3.50	12.61	0.80	1.39	-0.68	-0.10	-0.58
4.00	13.11	0.86	1.42	-0.67	-0.11	-0.56
4.50	13.61	0.91	1.44	-0.65	-0.11	-0.54
5.00	14.11	0.95	1.46	-0.63	-0.12	-0.52
5.50	14.61	0.97	1.48	-0.62	-0.12	-0.50
6.00	15.11	0.99	1.49	-0.62	-0.13	-0.49
6.50	15.61	1.01	1.50	-0.62	-0.13	-0.49
7.00	16.11	1.02	1.50	-0.62	-0.14	-0.48
7.50	16.61	1.03	1.51	-0.62	-0.14	-0.47
8.00	17.11	1.04	1.51	-0.62	-0.15	-0.47
8.50	17.61	1.05	1.52	-0.62	-0.16	-0.47
9.00	18.11	1.06	1.52	-0.63	-0.16	-0.46
9.50	18.61	1.06	1.52	-0.63	-0.17	-0.46
10.00	19.11	1.07	1.53	-0.63	-0.17	-0.46
-1.11	8.00	0.0	0.0	0.0	0.0	0.0
-0.61	8.50	0.0	0.0	0.0	0.0	0.0
-0.11	9.00	0.0	0.0	0.0	0.0	0.0
0.39	9.50	-0.27	0.65	-0.98	-0.05	-0.93
0.89	10.00	0.11	0.93	-0.88	-0.06	-0.81
1.39	10.50	0.35	1.10	-0.82	-0.07	-0.75
1.89	11.00	0.53	1.22	-0.77	-0.08	-0.68
2.39	11.50	0.65	1.29	-0.73	-0.09	-0.64
2.89	12.00	0.73	1.35	-0.71	-0.09	-0.61
3.39	12.50	0.79	1.38	-0.69	-0.10	-0.59
3.89	13.00	0.85	1.41	-0.67	-0.10	-0.57
4.39	13.50	0.90	1.44	-0.65	-0.11	-0.54
4.89	14.00	0.94	1.46	-0.64	-0.11	-0.52
5.39	14.50	0.97	1.47	-0.63	-0.12	-0.51
5.89	15.00	0.99	1.49	-0.62	-0.12	-0.50
6.39	15.50	1.01	1.49	-0.62	-0.13	-0.49
6.89	16.00	1.02	1.50	-0.62	-0.14	-0.48
7.39	16.50	1.03	1.51	-0.62	-0.14	-0.47
7.89	17.00	1.04	1.51	-0.62	-0.15	-0.47
8.39	17.50	1.05	1.52	-0.62	-0.16	-0.47
8.89	18.00	1.06	1.52	-0.63	-0.16	-0.46
9.39	18.50	1.06	1.52	-0.63	-0.17	-0.46
9.89	19.00	1.07	1.53	-0.63	-0.17	-0.46
10.39	19.50	1.07	1.53	-0.63	-0.18	-0.46
10.89	20.00	1.07	1.53	-0.63	-0.18	-0.46

Table 6

(g) M-METHYLBENZIL

EXCESS ENERGY (eV)	ELECTRON ENERGY (eV)	LOGARITHMIC INTENSITY RATIOS				
		FX/FM	FH/FM	FX/1-FM	FH/1-FM	FX/FH
-1.00	8.05	0.0	0.0	0.0	0.0	0.0
-0.50	8.55	0.0	0.0	0.0	0.0	0.0
0.0	9.05	0.0	0.0	0.0	0.0	0.0
0.50	9.55	0.19	-1.31	-0.01	-1.51	1.50
1.00	10.05	0.51	-0.70	-0.03	-1.24	1.21
1.50	10.55	0.70	-0.42	-0.03	-1.15	1.12
2.00	11.05	0.82	-0.24	-0.04	-1.10	1.07
2.50	11.55	0.90	-0.12	-0.04	-1.06	1.02
3.00	12.05	0.96	-0.02	-0.04	-1.02	0.98
3.50	12.55	1.00	0.06	-0.05	-0.99	0.94
4.00	13.05	1.04	0.13	-0.05	-0.96	0.91
4.50	13.55	1.07	0.20	-0.06	-0.92	0.87
5.00	14.05	1.08	0.25	-0.06	-0.89	0.83
5.50	14.55	1.10	0.29	-0.06	-0.87	0.81
6.00	15.05	1.11	0.31	-0.07	-0.86	0.80
6.50	15.55	1.11	0.33	-0.07	-0.86	0.78
7.00	16.05	1.12	0.35	-0.08	-0.85	0.77
7.50	16.55	1.13	0.36	-0.08	-0.85	0.77
8.00	17.05	1.13	0.37	-0.09	-0.85	0.76
8.50	17.55	1.13	0.38	-0.09	-0.85	0.76
9.00	18.05	1.14	0.39	-0.10	-0.85	0.75
9.50	18.55	1.14	0.39	-0.10	-0.85	0.75
10.00	19.05	1.14	0.40	-0.11	-0.85	0.74
-1.05	8.00	0.0	0.0	0.0	0.0	0.0
-0.55	8.50	0.0	0.0	0.0	0.0	0.0
-0.05	9.00	0.0	0.0	0.0	0.0	0.0
0.45	9.50	0.16	-1.32	-0.01	-1.49	1.48
0.95	10.00	0.49	-0.72	-0.03	-1.24	1.21
1.45	10.50	0.69	-0.44	-0.03	-1.16	1.13
1.95	11.00	0.81	-0.26	-0.04	-1.11	1.07
2.45	11.50	0.90	-0.13	-0.04	-1.06	1.02
2.95	12.00	0.95	-0.03	-0.04	-1.03	0.98
3.45	12.50	0.99	0.05	-0.05	-0.99	0.95
3.95	13.00	1.03	0.12	-0.05	-0.96	0.91
4.45	13.50	1.07	0.19	-0.05	-0.93	0.87
4.95	14.00	1.08	0.25	-0.06	-0.89	0.83
5.45	14.50	1.10	0.28	-0.06	-0.88	0.81
5.95	15.00	1.11	0.31	-0.07	-0.87	0.80
6.45	15.50	1.11	0.33	-0.07	-0.86	0.78
6.95	16.00	1.12	0.34	-0.08	-0.85	0.78
7.45	16.50	1.13	0.36	-0.08	-0.85	0.77
7.95	17.00	1.13	0.37	-0.09	-0.85	0.76
8.45	17.50	1.13	0.38	-0.09	-0.85	0.76
8.95	18.00	1.14	0.39	-0.10	-0.85	0.75
9.45	18.50	1.14	0.39	-0.10	-0.85	0.75
9.95	19.00	1.14	0.40	-0.11	-0.85	0.74
10.45	19.50	1.15	0.40	-0.11	-0.85	0.74
10.95	20.00	1.15	0.41	-0.11	-0.85	0.74

Table 6

(h) M-METHOXYBENZIL

EXCESS ENERGY (EV)	ELECTRON ENERGY (EV)	LOGARITHMIC INTENSITY RATIOS				
		FX/FM	FH/FM	FX/I-FM	FH/I-FM	FX/FH
-1.00	7.75	0.0	0.0	0.0	0.0	0.0
-0.50	8.25	0.0	0.0	0.0	0.0	0.0
0.0	8.75	0.0	0.0	0.0	0.0	0.0
0.50	9.25	-0.61	0.0	0.0	0.0	0.0
1.00	9.75	-0.18	0.0	0.00	0.0	0.0
1.50	10.25	0.05	-1.12	-0.03	-1.20	1.17
2.00	10.75	0.23	-0.80	-0.04	-1.07	1.03
2.50	11.25	0.35	-0.60	-0.05	-1.00	0.95
3.00	11.75	0.43	-0.47	-0.05	-0.95	0.87
3.50	12.25	0.49	-0.37	-0.06	-0.91	0.85
4.00	12.75	0.54	-0.27	-0.06	-0.87	0.81
4.50	13.25	0.59	-0.18	-0.07	-0.84	0.77
5.00	13.75	0.64	-0.10	-0.07	-0.81	0.74
5.50	14.25	0.67	-0.04	-0.08	-0.79	0.71
6.00	14.75	0.69	0.01	-0.08	-0.77	0.69
6.50	15.25	0.71	0.04	-0.09	-0.76	0.67
7.00	15.75	0.73	0.07	-0.09	-0.75	0.66
7.50	16.25	0.74	0.09	-0.10	-0.75	0.65
8.00	16.75	0.75	0.11	-0.10	-0.75	0.64
8.50	17.25	0.76	0.13	-0.11	-0.75	0.64
9.00	17.75	0.77	0.14	-0.11	-0.75	0.63
9.50	18.25	0.78	0.15	-0.12	-0.75	0.63
10.00	18.75	0.79	0.16	-0.13	-0.75	0.62
-0.75	8.00	0.0	0.0	0.0	0.0	0.0
-0.25	8.50	0.0	0.0	0.0	0.0	0.0
0.25	9.00	0.0	0.0	0.0	0.0	0.0
0.75	9.50	-0.34	0.0	0.0	0.0	0.0
1.25	10.00	-0.06	-1.38	-0.02	-1.34	1.32
1.75	10.50	0.15	-0.92	-0.04	-1.10	1.06
2.25	11.00	0.29	-0.69	-0.04	-1.03	0.99
2.75	11.50	0.39	-0.54	-0.05	-0.97	0.92
3.25	12.00	0.46	-0.41	-0.05	-0.93	0.87
3.75	12.50	0.52	-0.31	-0.06	-0.87	0.83
4.25	13.00	0.57	-0.22	-0.07	-0.86	0.79
4.75	13.50	0.62	-0.14	-0.07	-0.83	0.76
5.25	14.00	0.65	-0.07	-0.08	-0.80	0.72
5.75	14.50	0.68	-0.01	-0.08	-0.78	0.70
6.25	15.00	0.70	0.03	-0.09	-0.76	0.68
6.75	15.50	0.72	0.06	-0.09	-0.76	0.66
7.25	16.00	0.74	0.08	-0.10	-0.75	0.65
7.75	16.50	0.75	0.10	-0.10	-0.75	0.65
8.25	17.00	0.76	0.12	-0.11	-0.75	0.64
8.75	17.50	0.77	0.14	-0.11	-0.75	0.63
9.25	18.00	0.78	0.15	-0.12	-0.75	0.63
9.75	18.50	0.78	0.16	-0.12	-0.75	0.63
10.25	19.00	0.79	0.17	-0.13	-0.75	0.62
10.75	19.50	0.80	0.18	-0.13	-0.75	0.62
11.25	20.00	0.80	0.19	-0.14	-0.76	0.62

Table 6

(i) P-PHENYLBENZIL

EXCESS ENERGY (eV)	ELECTRON ENERGY (eV)	LOGARITHMIC INTENSITY RATIOS				
		FX/FM	FH/FM	FX/1-FM	FH/1-FM	FX/FH
-1.00	7.59	0.0	0.0	0.0	0.0	0.0
-0.50	8.09	0.0	0.0	0.0	0.0	0.0
0.0	8.59	0.0	0.0	0.0	0.0	0.0
0.50	9.09	0.12	0.0	-0.00	0.0	0.0
1.00	9.59	0.47	0.0	-0.00	0.0	0.0
1.50	10.09	0.68	-1.75	-0.00	-2.44	2.43
2.00	10.59	0.85	-1.36	-0.00	-2.22	2.22
2.50	11.09	0.97	-1.10	-0.00	-2.07	2.07
3.00	11.59	1.03	-0.92	-0.00	-1.96	1.95
3.50	12.09	1.11	-0.77	-0.01	-1.89	1.88
4.00	12.59	1.16	-0.63	-0.01	-1.80	1.79
4.50	13.09	1.21	-0.52	-0.01	-1.73	1.73
5.00	13.59	1.24	-0.40	-0.01	-1.65	1.64
5.50	14.09	1.26	-0.31	-0.01	-1.58	1.57
6.00	14.59	1.28	-0.25	-0.01	-1.54	1.53
6.50	15.09	1.29	-0.21	-0.02	-1.52	1.50
7.00	15.59	1.30	-0.18	-0.02	-1.50	1.48
7.50	16.09	1.31	-0.15	-0.02	-1.48	1.46
8.00	16.59	1.32	-0.13	-0.03	-1.47	1.45
8.50	17.09	1.32	-0.11	-0.03	-1.47	1.44
9.00	17.59	1.33	-0.10	-0.04	-1.46	1.43
9.50	18.09	1.33	-0.09	-0.04	-1.46	1.42
10.00	18.59	1.34	-0.08	-0.04	-1.46	1.41
-0.59	8.00	0.0	0.0	0.0	0.0	0.0
-0.09	8.50	0.0	0.0	0.0	0.0	0.0
0.41	9.00	-0.10	0.0	0.0	0.0	0.0
0.91	9.50	0.43	0.0	-0.00	0.0	0.0
1.41	10.00	0.65	-1.86	-0.00	-2.51	2.51
1.91	10.50	0.83	-1.42	-0.00	-2.25	2.24
2.41	11.00	0.95	-1.14	-0.00	-2.09	2.09
2.91	11.50	1.02	-0.95	-0.00	-1.97	1.97
3.41	12.00	1.10	-0.80	-0.01	-1.90	1.90
3.91	12.50	1.15	-0.66	-0.01	-1.82	1.81
4.41	13.00	1.20	-0.54	-0.01	-1.75	1.74
4.91	13.50	1.23	-0.42	-0.01	-1.66	1.65
5.41	14.00	1.26	-0.33	-0.01	-1.59	1.58
5.91	14.50	1.27	-0.26	-0.01	-1.55	1.54
6.41	15.00	1.29	-0.22	-0.02	-1.52	1.50
6.91	15.50	1.30	-0.18	-0.02	-1.50	1.48
7.41	16.00	1.31	-0.16	-0.02	-1.48	1.46
7.91	16.50	1.32	-0.13	-0.03	-1.47	1.45
8.41	17.00	1.32	-0.12	-0.03	-1.47	1.44
8.91	17.50	1.33	-0.10	-0.04	-1.46	1.43
9.41	18.00	1.33	-0.09	-0.04	-1.46	1.42
9.91	18.50	1.34	-0.08	-0.04	-1.46	1.41
10.41	19.00	1.34	-0.07	-0.05	-1.46	1.41
10.91	19.50	1.34	-0.06	-0.05	-1.46	1.40
11.41	20.00	1.35	-0.05	-0.06	-1.46	1.40

Table 6

(j) M-FORMYLBENZIL

EXCESS ENERGY (EV)	ELECTRON ENERGY (EV)	LOGARITHMIC INTENSITY RATIOS				
		FX/FM	FH/FM	FX/1-FM	FH/1-FM	FX/FH

-1.00	8.14	0.0	0.0	0.0	0.0	0.0
-0.50	8.64	0.0	0.0	0.0	0.0	0.0
0.0	9.14	0.0	0.0	0.0	0.0	0.0
0.50	9.64	0.0	0.07	0.0	0.0	0.0
1.00	10.14	-1.25	0.71	-1.96	-0.00	-1.95
1.50	10.64	-0.83	1.01	-1.84	-0.01	-1.84
2.00	11.14	-0.57	1.18	-1.76	-0.01	-1.75
2.50	11.64	-0.41	1.28	-1.69	-0.01	-1.69
3.00	12.14	-0.29	1.35	-1.64	-0.01	-1.63
3.50	12.64	-0.18	1.39	-1.59	-0.01	-1.58
4.00	13.14	-0.08	1.44	-1.53	-0.01	-1.52
4.50	13.64	0.03	1.48	-1.46	-0.02	-1.45
5.00	14.14	0.12	1.50	-1.40	-0.02	-1.38
5.50	14.64	0.19	1.52	-1.35	-0.02	-1.33
6.00	15.14	0.24	1.54	-1.32	-0.02	-1.30
6.50	15.64	0.28	1.55	-1.30	-0.03	-1.28
7.00	16.14	0.30	1.56	-1.29	-0.03	-1.26
7.50	16.64	0.33	1.57	-1.28	-0.03	-1.24
8.00	17.14	0.34	1.58	-1.27	-0.04	-1.23
8.50	17.64	0.36	1.58	-1.26	-0.04	-1.22
9.00	18.14	0.37	1.59	-1.26	-0.04	-1.22
9.50	18.64	0.38	1.59	-1.25	-0.05	-1.21
10.00	19.14	0.39	1.60	-1.25	-0.05	-1.20
-1.14	8.00	0.0	0.0	0.0	0.0	0.0
-0.64	8.50	0.0	0.0	0.0	0.0	0.0
-0.14	9.00	0.0	0.0	0.0	0.0	0.0
0.36	9.50	0.0	0.0	0.0	0.0	0.0
0.86	10.00	-1.39	0.62	-2.02	-0.00	-2.01
1.36	10.50	-0.91	0.94	-1.86	-0.01	-1.85
1.86	11.00	-0.63	1.14	-1.78	-0.01	-1.78
2.36	11.50	-0.45	1.26	-1.71	-0.01	-1.70
2.86	12.00	-0.32	1.33	-1.66	-0.01	-1.65
3.36	12.50	-0.21	1.38	-1.60	-0.01	-1.59
3.86	13.00	-0.11	1.42	-1.54	-0.01	-1.53
4.36	13.50	0.01	1.47	-1.48	-0.01	-1.46
4.86	14.00	0.10	1.50	-1.41	-0.02	-1.40
5.36	14.50	0.13	1.52	-1.36	-0.02	-1.34
5.86	15.00	0.23	1.54	-1.33	-0.02	-1.31
6.36	15.50	0.27	1.55	-1.31	-0.03	-1.28
6.86	16.00	0.30	1.56	-1.29	-0.03	-1.26
7.36	16.50	0.22	1.57	-1.28	-0.03	-1.25
7.86	17.00	0.34	1.57	-1.27	-0.04	-1.24
8.36	17.50	0.35	1.58	-1.27	-0.04	-1.23
8.86	18.00	0.37	1.59	-1.26	-0.04	-1.22
9.36	18.50	0.38	1.59	-1.26	-0.04	-1.21
9.86	19.00	0.39	1.59	-1.25	-0.05	-1.20
10.36	19.50	0.40	1.60	-1.25	-0.05	-1.20
10.86	20.00	0.41	1.60	-1.25	-0.05	-1.20

Table 6

(k) m-CYANOBENZIL

EXCESS ENERGY (EV)	ELECTRON ENERGY (EV)	LOGARITHMIC		INTENSITY RATIOS		RATIOS
		FX/FM	FH/FM	FX/1-FM	FH/1-FM	
-1.00	8.30	0.0	0.0	0.0	0.0	0.0
-0.50	8.80	0.0	0.0	0.0	0.0	0.0
0.0	9.30	0.0	0.0	0.0	0.0	0.0
0.50	9.80	0.0	0.88	0.0	0.00	0.0
1.00	10.30	0.0	1.23	0.0	0.0	0.0
1.50	10.80	-2.13	1.50	-3.63	-0.00	-3.63
2.00	11.30	-1.42	1.67	-3.09	-0.00	-3.09
2.50	11.80	-1.15	1.77	-2.92	-0.00	-2.92
3.00	12.30	-0.96	1.84	-2.80	-0.00	-2.80
3.50	12.80	-0.82	1.89	-2.71	-0.00	-2.71
4.00	13.30	-0.65	1.93	-2.59	-0.00	-2.58
4.50	13.80	-0.49	1.95	-2.44	-0.00	-2.44
5.00	14.30	-0.31	1.98	-2.29	-0.00	-2.29
5.50	14.80	-0.16	1.99	-2.16	-0.00	-2.16
6.00	15.30	-0.03	2.00	-2.05	-0.01	-2.04
6.50	15.80	0.05	2.01	-1.97	-0.01	-1.96
7.00	16.30	0.12	2.02	-1.92	-0.01	-1.91
7.50	16.80	0.16	2.03	-1.89	-0.02	-1.87
8.00	17.30	0.20	2.04	-1.86	-0.02	-1.84
8.50	17.80	0.23	2.04	-1.84	-0.03	-1.81
9.00	18.30	0.25	2.05	-1.83	-0.03	-1.79
9.50	18.80	0.27	2.05	-1.81	-0.04	-1.78
10.00	19.30	0.29	2.05	-1.80	-0.04	-1.76
-1.30	8.00	0.0	0.0	0.0	0.0	0.0
-0.30	8.50	0.0	0.0	0.0	0.0	0.0
-0.30	9.00	0.0	0.0	0.0	0.0	0.0
0.20	9.50	0.0	0.68	0.0	-0.00	0.0
0.70	10.00	0.0	1.03	0.0	0.00	0.0
1.20	10.50	0.0	1.36	0.0	0.00	0.0
1.70	11.00	-1.69	1.58	-3.27	-0.00	-3.27
2.20	11.50	-1.31	1.71	-3.02	-0.00	-3.02
2.70	12.00	-1.06	1.80	-2.86	-0.00	-2.86
3.20	12.50	-0.90	1.86	-2.76	-0.00	-2.76
3.70	13.00	-0.75	1.91	-2.66	-0.00	-2.66
4.20	13.50	-0.59	1.94	-2.53	-0.00	-2.53
4.70	14.00	-0.42	1.96	-2.38	-0.00	-2.38
5.20	14.50	-0.25	1.98	-2.24	-0.00	-2.24
5.70	15.00	-0.11	2.00	-2.11	-0.01	-2.11
6.20	15.50	0.01	2.01	-2.01	-0.01	-2.00
6.70	16.00	0.03	2.02	-1.95	-0.01	-1.94
7.20	16.50	0.14	2.03	-1.91	-0.02	-1.89
7.70	17.00	0.18	2.03	-1.87	-0.02	-1.85
8.20	17.50	0.21	2.04	-1.85	-0.03	-1.83
8.70	18.00	0.24	2.04	-1.83	-0.03	-1.80
9.20	18.50	0.26	2.05	-1.82	-0.04	-1.78
9.70	19.00	0.28	2.05	-1.81	-0.04	-1.77
10.20	19.50	0.30	2.05	-1.80	-0.04	-1.76
10.70	20.00	0.31	2.06	-1.79	-0.05	-1.74

Table 6

(1) M-TRIFLUOROMETHYLBENZIL

EXCESS ENERGY (EV)	ELECTRON ENERGY (EV)	LOGARITHMIC INTENSITY RATIOS				
		FX/FM	FH/FM	FX/1-FM	FH/1-FM	FX/FH
-1.00	8.34	0.0	0.0	0.0	0.0	0.0
-0.50	8.84	0.0	0.0	0.0	0.0	0.0
0.0	9.34	0.0	0.0	0.0	0.0	0.0
0.50	9.84	0.0	1.10	0.0	0.00	0.0
1.00	10.34	-1.42	1.37	-2.79	-0.00	-2.79
1.50	10.84	-0.92	1.56	-2.48	-0.00	-2.48
2.00	11.34	-0.70	1.67	-2.38	-0.00	-2.38
2.50	11.84	-0.52	1.77	-2.30	-0.00	-2.30
3.00	12.34	-0.33	1.84	-2.22	-0.00	-2.22
3.50	12.84	-0.24	1.89	-2.13	-0.00	-2.13
4.00	13.34	-0.12	1.92	-2.05	-0.00	-2.05
4.50	13.84	-0.00	1.97	-1.97	-0.00	-1.97
5.00	14.34	0.12	2.01	-1.90	-0.01	-1.89
5.50	14.84	0.22	2.04	-1.83	-0.01	-1.82
6.00	15.34	0.30	2.07	-1.77	-0.01	-1.76
6.50	15.84	0.36	2.09	-1.73	-0.01	-1.72
7.00	16.34	0.41	2.10	-1.71	-0.02	-1.69
7.50	16.84	0.45	2.12	-1.69	-0.02	-1.67
8.00	17.34	0.48	2.13	-1.68	-0.03	-1.65
8.50	17.84	0.50	2.14	-1.67	-0.03	-1.64
9.00	18.34	0.52	2.15	-1.66	-0.04	-1.63
9.50	18.84	0.54	2.16	-1.66	-0.04	-1.62
10.00	19.34	0.55	2.16	-1.65	-0.04	-1.61
-1.34	8.00	0.0	0.0	0.0	0.0	0.0
-0.84	8.50	0.0	0.0	0.0	0.0	0.0
-0.34	9.00	0.0	0.0	0.0	0.0	0.0
0.16	9.50	0.0	0.81	0.0	0.00	0.0
0.66	10.00	0.0	1.17	0.0	0.0	0.0
1.16	10.50	-1.16	1.43	-2.59	-0.00	-2.59
1.66	11.00	-0.83	1.60	-2.44	-0.00	-2.44
2.16	11.50	-0.64	1.71	-2.35	-0.00	-2.35
2.66	12.00	-0.48	1.80	-2.28	-0.00	-2.28
3.16	12.50	-0.34	1.85	-2.19	-0.00	-2.19
3.66	13.00	-0.20	1.90	-2.11	-0.00	-2.10
4.16	13.50	-0.09	1.93	-2.03	-0.00	-2.02
4.66	14.00	0.04	1.98	-1.95	-0.01	-1.94
5.16	14.50	0.15	2.02	-1.87	-0.01	-1.87
5.66	15.00	0.25	2.05	-1.81	-0.01	-1.80
6.16	15.50	0.33	2.07	-1.76	-0.01	-1.75
6.66	16.00	0.38	2.09	-1.73	-0.01	-1.71
7.16	16.50	0.42	2.11	-1.70	-0.02	-1.68
7.66	17.00	0.46	2.12	-1.67	-0.02	-1.66
8.16	17.50	0.48	2.13	-1.66	-0.03	-1.65
8.66	18.00	0.51	2.14	-1.67	-0.03	-1.63
9.16	18.50	0.53	2.15	-1.66	-0.04	-1.62
9.66	19.00	0.54	2.16	-1.65	-0.04	-1.61
10.16	19.50	0.56	2.16	-1.65	-0.04	-1.61
10.66	20.00	0.57	2.17	-1.64	-0.05	-1.60

Table 6

(m) M-NITROBENZIL

EXCESS ENERGY (EV)	ELECTRON ENERGY (EV)	LOGARITHMIC INTENSITY RATIOS				
		FX/FM	FH/FM	FX/1-FM	FH/1-FM	FX/FH
-1.00	8.33	0.0	0.0	0.0	0.0	0.0
-0.50	8.83	0.0	0.0	0.0	0.0	0.0
0.0	9.33	0.0	0.0	0.0	0.0	0.0
0.50	9.83	0.0	0.73	0.0	-0.00	0.0
1.00	10.33	0.0	1.02	0.0	-0.01	0.0
1.50	10.83	0.0	1.24	0.0	-0.01	0.0
2.00	11.33	-2.14	1.38	-3.54	-0.01	-3.53
2.50	11.83	-1.78	1.47	-3.27	-0.01	-3.26
3.00	12.33	-1.53	1.54	-3.08	-0.01	-3.07
3.50	12.83	-1.33	1.59	-2.93	-0.01	-2.92
4.00	13.33	-1.14	1.63	-2.79	-0.01	-2.77
4.50	13.83	-0.94	1.67	-2.63	-0.01	-2.62
5.00	14.33	-0.77	1.70	-2.49	-0.01	-2.47
5.50	14.83	-0.62	1.72	-2.36	-0.01	-2.35
6.00	15.33	-0.50	1.74	-2.26	-0.02	-2.24
6.50	15.83	-0.41	1.75	-2.18	-0.02	-2.16
7.00	16.33	-0.35	1.76	-2.13	-0.02	-2.11
7.50	16.83	-0.30	1.77	-2.10	-0.03	-2.07
8.00	17.33	-0.26	1.78	-2.07	-0.03	-2.04
8.50	17.83	-0.24	1.78	-2.05	-0.04	-2.02
9.00	18.33	-0.21	1.79	-2.04	-0.04	-2.00
9.50	18.83	-0.19	1.79	-2.03	-0.04	-1.98
10.00	19.33	-0.18	1.79	-2.02	-0.05	-1.97
-1.33	8.00	0.0	0.0	0.0	0.0	0.0
-0.83	8.50	0.0	0.0	0.0	0.0	0.0
-0.33	9.00	0.0	0.0	0.0	0.0	0.0
0.17	9.50	0.0	0.36	0.0	0.0	0.0
0.67	10.00	0.0	0.84	0.0	-0.01	0.0
1.17	10.50	0.0	1.10	0.0	-0.01	0.0
1.67	11.00	0.0	1.30	0.0	-0.01	0.0
2.17	11.50	-1.97	1.42	-3.40	-0.01	-3.39
2.67	12.00	-1.67	1.50	-3.13	-0.01	-3.17
3.17	12.50	-1.46	1.56	-3.03	-0.01	-3.02
3.67	13.00	-1.26	1.60	-2.87	-0.01	-2.86
4.17	13.50	-1.07	1.65	-2.72	-0.01	-2.71
4.67	14.00	-0.88	1.68	-2.58	-0.01	-2.57
5.17	14.50	-0.72	1.71	-2.44	-0.01	-2.43
5.67	15.00	-0.58	1.73	-2.32	-0.01	-2.31
6.17	15.50	-0.47	1.74	-2.23	-0.02	-2.21
6.67	16.00	-0.39	1.75	-2.16	-0.02	-2.14
7.17	16.50	-0.33	1.76	-2.12	-0.02	-2.09
7.67	17.00	-0.29	1.77	-2.09	-0.03	-2.06
8.17	17.50	-0.25	1.78	-2.07	-0.03	-2.03
8.67	18.00	-0.23	1.78	-2.05	-0.04	-2.01
9.17	18.50	-0.21	1.79	-2.04	-0.04	-1.99
9.67	19.00	-0.19	1.79	-2.02	-0.05	-1.98
10.17	19.50	-0.17	1.80	-2.01	-0.05	-1.97
10.67	20.00	-0.16	1.80	-2.01	-0.05	-1.96

Table 7

Logarithmic Intensity Ratios^a for Substituted Benzils (70 eV)

Substituent	F_X/F_M	F_H/F_M	$F_X/1-F_M$	$F_H/1-F_M$	F_X/F_H
(a) H	-	1.26	-	-0.20	0.0
(b) <i>m</i> -F	0.80	1.63	-1.12	-0.29	-0.83
(c) <i>p</i> -F	1.24	1.60	-0.68	-0.32	-0.36
(d) <i>m</i> -Cl	0.83	1.63	-1.05	-0.25	-0.80
(e) <i>m</i> -Br	0.83	1.75	-1.12	-0.20	-0.92
(f) <i>p</i> -Br	0.91	1.33	-0.75	-0.33	-0.42
(g) <i>m</i> -CH ₃	1.22	0.79	-0.34	-0.77	0.43
(h) <i>m</i> -CH ₃ O	0.96	0.58	-0.32	-0.70	0.38
(i) <i>p</i> -C ₆ H ₅	1.92	1.19	-0.39	-1.12	0.73
(j) <i>m</i> -CHO	0.77	1.69	-1.11	-0.19	-0.92
(k) <i>m</i> -CN	0.90	2.22	-1.56	-0.24	-1.32
(l) <i>m</i> -CF ₃	0.61	1.61	-1.21	-0.21	-1.00
(m) <i>m</i> -NO ₂	0.73	2.31	-1.76	-0.19	-1.58

^a F_M = fractional intensity of M⁺;

F_X = fractional intensity of XC₆H₄CO⁺;

F_H = fractional intensity of C₆H₅CO⁺.

5.5 APPEARANCE POTENTIALS

The individual measurements of the appearance potentials and their mean values (section 4.3) are given in Table 8 (a-m). The ionization potentials (IP), the appearance potentials of the substituted (AP_X) and unsubstituted (AP_H) benzoyl ions, and their differences (AP_X-IP , AP_H-IP , AP_X-AP_H) used in correlating the results are tabulated in Table 9 (a-m). The estimated standard deviations of all these values are given in brackets.

Table 8

Ionization and Appearance Potentials

Ion <i>m/e</i>	<u>Individual Measurements (e.s.d.)</u>				<u>Mean (e.s.d.)</u>
	$v_i (\sigma_i)$				$\bar{v} (\sigma_{\bar{v}})$
(a) Benzil					
210	9.19 (.05)	9.18 (.08)	9.27 (.07)	9.16 (.05)	9.20 (.03) (lit. ^a 8.78)
105	9.88 (.05)	9.93 (.04)	9.82 (.04)		9.87 (.03) (lit. ^a 9.70)
77	14.06 (.07)	14.00 (.10)	13.66 (.07)	13.60 (.06)	13.8 (.1) (lit. ^a 15.1)
(b) <i>m</i> -Fluorobenzil					
228	9.16 (.08)	9.28 (.05)	9.25 (.05)	9.21 (.04)	9.23 (.02)
123	10.42 (.09)	10.42 (.05)			10.42 (.05)
105	9.70 (.05)	9.89 (.06)	9.75 (.03)		9.76 (.05)
95	13.95 (.07)	13.56 (.06)			13.7 (.2)
77	14.03 (.06)	13.63 (.04)			13.8 (.2)

^a P. Natalis and J.L. Franklin, J. Chem. Phys. 69, 2943 (1965).

Table 8

Ionization and Appearance Potentials

<u>Ion</u> <u>m/e</u>	<u>Individual Measurements (e.s.d.)</u> $v_i(\sigma_i)$				<u>Mean (e.s.d.)</u> $\bar{v}(\sigma_{\bar{v}})$
(c) <i>p</i> -Fluorobenzil					
228	9.17 (.05)	9.15 (.05)	9.10 (.05)	9.09 (.04)	9.12 (.02)
123	10.14 (.05)	10.02 (.04)			10.07 (.04)
105	9.77 (.04)	9.70 (.03)			9.73 (.02)
95	14.20 (.05)	13.87 (.07)			14.1 (.1)
77	13.82 (.04)	13.60 (.05)			13.7 (.1)
(d) <i>m</i> -Chlorobenzil					
244	9.00 (.08)	9.29 (.08)	9.12 (.06)	9.22 (.05)	9.16 (.05)
139	10.36 (.08)	10.29 (.05)			10.31 (.05)
105	9.80 (.09)	9.74 (.05)			9.76 (.04)
111	14.21 (.09)	13.51 (.07)			13.8 (.3)
77	14.63 (.07)	13.77 (.04)			14.0 (.4)

Table 8

Ionization and Appearance Potentials

<u>Ion</u> <u>m/e</u>	<u>Individual Measurements (e.s.d.)</u> $v_i(\sigma_i)$				<u>Mean (e.s.d.)</u> $\bar{v}(\sigma_{\bar{v}})$
(e) m -Bromobenzil					
228	9.14 (.07)	9.13 (.09)	9.17 (.05)	9.02 (.05)	9.10 (.03)
183	10.38 (.07)	10.33 (.10)	10.55 (.05)		10.47 (.06)
105	9.69 (.07)	9.86 (.06)	9.64 (.05)		9.72 (.06)
155	14.20 (.09)	14.10 (.09)	14.19 (.07)	13.66 (.05)	13.9 (.1)
77	13.86 (.09)	13.38 (.10)	13.88 (.04)	13.61 (.05)	13.7 (.1)
(f) p -Bromobenzil					
288	9.12 (.06)	9.24 (.06)	8.96 (.03)		9.11 (.08)
183	9.84 (.05)	9.93 (.04)			9.90 (.05)
105	9.59 (.05)	9.62 (.03)			9.61 (.03)
155	13.83 (.08)	13.94 (.04)			13.90 (.06)
77	13.58 (.07)	13.57 (.09)			13.58 (.05)

Table 8

Ionization and Appearance Potentials

<u>Ion</u> <u>m/e</u>	<u>Individual Measurements (e.s.d.)</u> $v_i(\sigma_i)$			<u>Mean (e.s.d.)</u> $\bar{v}(\sigma_{\bar{v}})$
(g) m -Methylbenzil				
224	9.08 (.06)	9.06 (.05)	9.04 (.04)	9.05 (.03)
119	9.60 (.04)	9.55 (.04)		9.57 (.03)
105	9.95 (.06)	9.92 (.04)		9.93 (.03)
91	13.59 (.05)	13.61 (.05)		13.60 (.04)
77	13.97 (.06)	13.99 (.05)	14.13 (.08)	14.01 (.05)
(h) m -Methoxybenzil				
240	8.72 (.06)	8.78 (.09)	8.76 (.04)	8.75 (.03)
135	9.64 (.07)	9.51 (.04)	9.46 (.06)	9.52 (.04)
105	9.93 (.07)	9.89 (.08)		9.91 (.05)
107	13.55 (.07)	14.25 (.10)	13.47 (.06)	13.6 (.2)
77	15.21 (.04)	15.40 (.07)	14.54 (.08)	15.1 (.2)

Table 8

Ionization and Appearance Potentials

<u>Ion</u> <u>m/e</u>	<u>Individual Measurements (e.s.d.)</u> $v_i(\sigma_i)$			<u>Mean (e.s.d.)</u> $\bar{v}(\sigma_{\bar{v}})$
(i) <i>p</i> -Phenylbenzil				
286	8.59 (.03)			8.59 (.03)
181	9.25 (.08)			9.25 (.08)
105	10.12 (.06)			10.12 (.06)
153	13.78 (.04)			13.8 (.1)
152	15.8 (.1)			15.8 (.2)
77	13.3 (.1)			13.3 (.2)
(j) <i>m</i> -Formylbenzil				
238	9.03 (.06)	9.17 (.08)	9.19 (.04)	9.14 (.05)
133	10.34 (.08)	10.34 (.06)		10.34 (.05)
105	9.86 (.06)	9.89 (.05)		9.88 (.04)
77	13.67 (.07)	13.67 (.06)		13.67 (.05)

Table 8

Ionization and Appearance Potentials

<u>Ion</u> <u>m/e</u>	<u>Individual Measurements (e.s.d.)</u> $v_i(\sigma_i)$			<u>Mean (e.s.d.)</u> $\bar{v}(\sigma_{\bar{v}})$
(k) m -Cyanobenzil				
235	9.13 (.04)	9.34 (.06)	9.53 (.06)	9.3 (.1)
130	11.13 (.08)	11.44 (.05)	10.81 (.10)	11.2 (.2)
105	9.96 (.07)	10.07 (.05)	9.99 (.05)	10.01 (.03)
102	15.30 (.09)	15.61 (.10)	15.19 (.14)	15.4 (.1)
77	14.31 (.07)	14.29 (.09)	13.93 (.07)	14.2 (.1)
(l) m -Trifluoromethylbenzil				
278	9.31 (.15)	9.26 (.08)	9.40 (.07)	9.34 (.05)
173	10.55 (.08)	10.78 (.06)		10.69 (.1)
105	10.11 (.07)	9.74 (.06)	9.91 (.04)	9.9 ₁ (.1)
145	14.77 (.12)	14.31 (.06)	14.95 (.05)	14.7 (.2)
77	14.34 (.08)	13.81 (.05)	14.12 (.08)	14.0 (.1)

Table 8

Ionization and Appearance Potentials

<u>Ion</u> <u>m/e</u>	<u>Individual Measurements (e.s.d.)</u> $v_i(\sigma_i)$		<u>Mean (e.s.d.)</u> $\bar{v}(\sigma_{\bar{v}})$
(m) m -Nitrobenzil			
255	9.32 (.05)	9.34 (.04)	9.33 (.03)
150	11.54 (.09)	11.53 (.10)	11.54 (.07)
134	10.10 (.07)	10.14 (.05)	10.13 (.04)
105	9.96 (.04)	10.07 (.04)	10.01 (.04)
104	12.88 (.06)	12.71 (.05)	12.78 (.08)
77	13.92 (.05)	13.76 (.05)	13.84 (.08)

Table 9

Energy Parameters in Substituted Benzils

Substituent	IP ^a	AP _X ^b	AP _H ^c	AP _X -IP	AP _H -IP	AP _X -AP _H
(a) H	9.20 (.03)	9.87 (.03)	9.87 (.03)	0.67 (.04)	0.67 (.04)	0.00
(b) <i>m</i> -F	9.23 (.02)	10.42 (.05)	9.76 (.05)	1.19 (.05)	0.53 (.05)	0.66 (.07)
(c) <i>p</i> -F	9.12 (.02)	10.07 (.04)	9.73 (.02)	0.95 (.04)	0.61 (.04)	0.34 (.05)
(d) <i>m</i> -Cl	9.16 (.05)	10.31 (.05)	9.76 (.04)	1.15 (.06)	0.60 (.06)	0.55 (.06)
(e) <i>m</i> -Br	9.10 (.03)	10.47 (.06)	9.72 (.06)	1.37 (.08)	0.62 (.08)	0.75 (.10)
(f) <i>p</i> -Br	9.11 (.08)	9.90 (.05)	9.61 (.03)	0.79 (.09)	0.50 (.09)	0.29 (.06)
(g) <i>m</i> -CH ₃	9.05 (.03)	9.57 (.03)	9.93 (.03)	0.52 (.04)	0.88 (.04)	-0.36 (.04)
(h) <i>m</i> -CH ₃ O	8.75 (.03)	9.52 (.04)	9.91 (.05)	0.77 (.05)	1.16 (.06)	-0.39 (.06)
(i) <i>p</i> -C ₆ H ₅	8.59 (.03)	9.25 (.08)	10.12 (.06)	0.66 (.09)	1.53 (.07)	-0.87 (.10)
(j) <i>m</i> -CHO	9.14 (.05)	10.34 (.05)	9.88 (.04)	1.20 (.07)	0.74 (.06)	0.46 (.06)
(k) <i>m</i> -CN	9.3 (.1)	11.2 (.1)	10.01 (.03)	1.9 (.2)	0.7 (.1)	1.2 (.2)
(l) <i>m</i> -CF ₃	9.34 (.05)	10.7 (.1)	9.9 (.1)	1.35 (.1)	0.57 (.1)	0.78 (.14)
(m) <i>m</i> -NO ₂	9.33 (.03)	11.54 (.07)	10.01 (.04)	2.21 (.08)	0.68 (.04)	1.53 (.08)

^a IP is the ionization potential of the substituted benzil.

^b AP_X is the appearance potential of the substituted benzoyl ion (XC₆H₄CO⁺).

^c AP_H is the appearance potential of the unsubstituted benzoyl ion (C₆H₅CO⁺).

(The e.s.d. of each value is given in brackets.)

5.6 CORRELATION OF RESULTS

The linear correlations of the results were obtained from a standard least squares program (LINEAR) which calculated the intercept and slope parameters (and their standard deviations) of the regression line. The correlation coefficient (r), and the standard deviation (e) of a point of unit weight from the line were also computed to provide measures of the agreement obtained. All points were given unit weight in these correlations, and the results are tabulated in Tables 10-17. The substituent constants (σ , σ^+) were obtained from the compilations by Brown^{106,107}.

Table 10

Correlation of Energy Parameters^a with Substituent Constants.

Correlation	r ^b	e ^c	Slope (e.s.d.)	Intercept (e.s.d.)
(a) IP vs. σ	0.64	0.17	0.6 (.2)	8.95 (.08)
IP vs. σ^+	0.73	0.16	0.6 (.2)	8.97 (.06)
(b) AP _H vs. σ	0.04	0.15	0.0 (.2)	9.86 (.06)
AP _H vs. σ^+	0.00	0.15	0.0 (.2)	9.86 (.06)
(c) AP _X vs. σ	0.94	0.24	2.6 (.3)	9.6 (.1)
AP _X vs. σ^+	0.93	0.26	2.2 (.3)	9.7 (.1)
(d) (AP _H -IP) vs. σ	-0.47	0.27	-0.6 (.3)	0.9 (.1)
(AP _H -IP) vs. σ^+	-0.55	0.25	-0.6 (.3)	0.9 (.1)
(e) (AP _X -IP) vs. σ	0.95	0.16	2.0 (.2)	0.60 (.07)
(AP _X -IP) vs. σ^+	0.90	0.22	1.6 (.2)	0.74 (.08)
(f) (AP _X -AP _H) vs. σ	0.92	0.28	2.6 (.3)	-0.3 (.1)
(AP _X -AP _H) vs. σ^+	0.92	0.27	2.2 (.3)	-0.2 (.1)

^a IP = ionization potential;

AP_H = appearance potential of C₆H₅CO⁺;

AP_X = appearance potential of XC₆H₄CO⁺.

^b r = correlation coefficient.

^c e = standard deviation.

Table 11

(a) Correlation of $\text{Log}(F_H/F_M)^a$ with Substituent Constants
as a Function of the Excess Energy, E^b .

E (eV)	Const.	r^c	e^d	Slope (e.s.d.)	Intercept (e.s.d.)
2.00	σ	0.70	0.73	2.9 (.9)	0.0 (.3)
	σ^+	0.74	0.69	2.6 (.7)	0.2 (.3)
4.00	σ	0.73	0.60	2.6 (.7)	0.4 (.3)
	σ^+	0.76	0.57	2.3 (.6)	0.5 (.2)
6.00	σ	0.75	0.53	2.4 (.6)	0.6 (.2)
	σ^+	0.78	0.50	2.2 (.5)	0.7 (.2)
8.00	σ	0.76	0.50	2.3 (.6)	0.7 (.2)
	σ^+	0.79	0.47	2.1 (.5)	0.8 (.2)
10.00	σ	0.76	0.49	2.3 (.6)	0.7 (.2)
	σ^+	0.79	0.46	2.1 (.5)	0.8 (.2)

^a F_H = fractional intensity of $C_6H_5CO^+$;
 F_M = fractional intensity of M^+ .

^b $E = V - IP$ (see section 4.4).

^c r = correlation coefficient.

^d e = standard deviation.

Table 11

(b) Correlation of $\text{Log}(F_X/F_M)^a$ with Substituent Constants
as a Function of the Excess Energy, E^b .

E (eV)	Const.	r^c	e^d	Slope (e.s.d.)	Intercept (e.s.d.)
2.00	σ	-0.97	0.24	-3.7 (.3)	0.8 (.1)
	σ^+	-0.95	0.31	-3.2 (.3)	0.5 (.1)
4.00	σ	-0.96	0.20	-2.8 (.2)	1.0 (.1)
	σ^+	-0.95	0.23	-2.4 (.2)	0.8 (.1)
6.00	σ	-0.95	0.17	-2.1 (.2)	1.1 (.1)
	σ^+	-0.94	0.18	-1.8 (.2)	1.0 (.1)
8.00	σ	-0.94	0.17	-1.8 (.2)	1.1 (.1)
	σ^+	-0.93	0.17	-1.5 (.2)	1.0 (.1)
10.00	σ	-0.93	0.17	-1.7 (.2)	1.1 (.1)
	σ^+	-0.93	0.17	-1.4 (.2)	1.0 (.1)

^a F_X = fractional intensity of $\text{XC}_6\text{H}_4\text{CO}^+$;

F_M = fractional intensity of M^+ .

^b $E = V - \text{IP}$ (see section 4.4).

^c r = correlation coefficient.

^d e = standard deviation.

Table 12

(a) Correlation of $\text{Log}(F_H/1-F_M)^a$ with Substituent Constants
as a Function of the Excess Energy, E .^b

E (eV)	Const.	r^c	e^d	Slope (e.s.d.)	Intercept (e.s.d.)
2.00	σ	0.64	0.55	1.8 (.7)	-0.9 (.2)
	σ^+	0.70	0.51	1.7 (.5)	-0.8 (.2)
4.00	σ	0.66	0.43	1.6 (.5)	-0.7 (.2)
	σ^+	0.72	0.40	1.4 (.4)	-0.7 (.2)
6.00	σ	0.68	0.36	1.4 (.4)	-0.7 (.1)
	σ^+	0.73	0.34	1.3 (.4)	-0.6 (.1)
8.00	σ	0.69	0.34	1.3 (.4)	-0.7 (.1)
	σ^+	0.74	0.32	1.2 (.3)	-0.6 (.1)
10.00	σ	0.69	0.33	1.3 (.4)	-0.7 (.1)
	σ^+	0.74	0.31	1.2 (.3)	-0.6 (.1)

^a F_H = fractional intensity of $C_6H_5CO^+$;

F_M = fractional intensity of M^+ .

^b $E = V - IP$ (see section 4.4).

^c r = correlation coefficient.

^d e = standard deviation.

Table 12

(b) Correlation of $\text{Log}(F_X/1-F_M)^a$ with Substituent Constants
as a Function of the Excess Energy, E^b .

E (eV)	Const.	r^c	e^d	Slope (e.s.d.)	Intercept (e.s.d.)
2.00	σ	-0.96	0.33	-4.8 (.4)	-0.1 (.1)
	σ^+	-0.95	0.38	-4.1 (.4)	-0.4 (.1)
4.00	σ	-0.96	0.29	-3.8 (.4)	-0.1 (.1)
	σ^+	-0.95	0.32	-3.3 (.3)	-0.4 (.1)
6.00	σ	-0.96	0.24	-3.1 (.3)	-0.2 (.1)
	σ^+	-0.95	0.25	-2.6 (.3)	-0.4 (.1)
8.00	σ	-0.95	0.22	-2.8 (.3)	-0.2 (.1)
	σ^+	-0.95	0.22	-2.4 (.2)	-0.4 (.1)
10.00	σ	-0.95	0.22	-2.7 (.3)	-0.2 (.1)
	σ^+	-0.95	0.22	-2.3 (.2)	-0.4 (.1)

^a F_X = fractional intensity of $\text{XC}_6\text{H}_4\text{CO}^+$;
 F_M = fractional intensity of M^+ .

^b $E = V - \text{IP}$ (see section 4.4).

^c r = correlation coefficient.

^d e = standard deviation.

Table 13

Correlation of $\text{Log } (F_X/F_H)^a$ with Substituent Constants
as a Function of the Excess Energy, E^b .

E (eV)	Const.	r^c	e^d	Slope (e.s.d.)	Intercept (e.s.d.)
2.00	σ	-0.92	0.71	-6.6 (.9)	0.8 (.3)
	σ^+	-0.93	0.65	-5.8 (.7)	0.4 (.2)
4.00	σ	-0.91	0.59	-5.4 (.7)	0.6 (.3)
	σ^+	-0.93	0.54	-4.7 (.6)	0.3 (.2)
6.00	σ	-0.91	0.51	-4.4 (.6)	0.5 (.2)
	σ^+	-0.92	0.46	-3.9 (.5)	0.2 (.2)
8.00	σ	-0.90	0.49	-4.1 (.6)	0.5 (.2)
	σ^+	-0.92	0.44	-3.6 (.5)	0.2 (.2)
10.00	σ	-0.90	0.48	-4.0 (.6)	0.4 (.2)
	σ^+	-0.92	0.43	-3.5 (.5)	0.2 (.2)

^a F_X = fractional intensity of $\text{XC}_6\text{H}_4\text{CO}^+$;

F_H = fractional intensity of $\text{C}_6\text{H}_5\text{CO}^+$.

^b $E = V - \text{IP}$ (see section 4.4).

^c r = correlation coefficient.

^d e = standard deviation.

Table 14

(a) Correlation of $\text{Log}(F_H/F_M)^a$ with $(AP_H - IP)^b$ as a Function of the Excess Energy, E^c

E	r^d	e^e	Slope (e.s.d.)	Intercept (e.s.d.)
2.00	-0.92	0.41	-3.1 (.4)	3.1 (.3)
4.00	-0.89	0.41	-2.6 (.4)	3.0 (.3)
6.00	-0.86	0.40	-2.3 (.4)	2.9 (.3)
8.00	-0.85	0.40	-2.2 (.4)	2.9 (.3)
10.00	-0.85	0.40	-2.1 (.4)	2.9 (.3)

^a F_H = fractional intensity of $C_6H_5CO^+$;
 F_M = fractional intensity of M^+ .

^b AP_H = appearance potential $C_6H_5CO^+$;
 IP = ionization potential.

^c $E = V - IP$ (see section 4.4).

^d r = correlation coefficient.

^e e = standard deviation.

Table 14

(b) Correlation of $\text{Log}(F_X/F_M)^a$ with $(AP_X - IP)^b$ as a Function of the Excess Energy, E^c

E (eV)	r^d	e^e	Slope (e.s.d.)	Intercept (e.s.d.)
2.00	-0.98	0.20	-1.8 (.1)	1.8 (.1)
4.00	-0.97	0.19	-1.3 (.1)	1.8 (.1)
6.00	-0.94	0.19	-1.0 (.1)	1.6 (.1)
8.00	-0.92	0.19	-0.8 (.1)	1.6 (.1)
10.00	-0.91	0.19	-0.8 (.1)	1.6 (.1)

^a F_X = fractional intensity of $\text{XC}_6\text{H}_4\text{CO}^+$;
 F_M = fractional intensity of M^+ .

^b AP_X = appearance potential of $\text{XC}_6\text{H}_4\text{CO}^+$;
 IP = ionization potential.

^c $E = V - IP$ (see section 4.4).

^d r = correlation coefficient.

^e e = standard deviation.

Table 15

(a) Correlation of $\text{Log}(F_H/1-F_M)^a$ with $(AP_H-IP)^b$ as a Function of the Excess Energy, E^c

E (eV)	r^d	e^e	Slope (e.s.d.)	Intercept (e.s.d.)
2.00	-0.95	0.23	-2.2 (.2)	1.3 (.2)
4.00	-0.94	0.20	-1.8 (.2)	1.0 (.2)
6.00	-0.93	0.19	-1.5 (.2)	0.9 (.2)
8.00	-0.92	0.18	-1.4 (.2)	0.8 (.1)
10.00	-0.92	0.18	-1.4 (.2)	0.7 (.1)

^a F_H = fractional intensity of $C_6H_5CO^+$;
 F_M = fractional intensity of M^+ .

^b AP_H = appearance potential of $C_6H_5CO^+$;
 IP = ionization potential.

^c $E = V - IP$ (see section 4.4).

^d r = correlation coefficient.

^e e = standard deviation.

Table 15

(b) Correlation of $\text{Log}(F_X/1-F_M)^a$ with $(AP_X-IP)^b$ as a
Function of the Excess Energy, E^c

E (eV)	r^d	e^e	Slope (e.s.d.)	Intercept (e.s.d.)
2.00	-0.97	0.30	-2.3 (.2)	1.2 (.2)
4.00	-0.96	0.28	-1.8 (.2)	0.9 (.2)
6.00	-0.95	0.26	-1.5 (.2)	0.7 (.2)
8.00	-0.94	0.26	-1.3 (.2)	0.5 (.2)
10.00	-0.93	0.25	-1.3 (.2)	0.5 (.2)

^a F_X = fractional intensity of $\text{XC}_6\text{H}_4\text{CO}^+$;
 F_M = fractional intensity of M^+ .

^b AP_X = appearance potential of $\text{XC}_6\text{H}_4\text{CO}^+$;
IP = ionization potential.

^c $E = V - IP$ (see section 4.4).

^d r = correlation coefficient.

^e e = standard deviation.

Table 16

(a) Correlation of $\text{Log}(F_X/F_H)^a$ with $(AP_X - AP_H)^b$ as a
Function of the Excess Energy, E^c

E (eV)	r^d	e^e	Slope (e.s.d.)	Intercept (e.s.d.)
2.00	-0.990	0.26	-2.6 (.1)	-0.06 (.08)
3.00	-0.985	0.27	-2.3 (.1)	-0.06 (.09)
4.00	-0.984	0.26	-2.1 (.1)	-0.06 (.09)
5.00	-0.982	0.25	-1.9 (.1)	-0.05 (.08)
6.00	-0.979	0.25	-1.7 (.1)	-0.05 (.08)
7.00	-0.975	0.25	-1.6 (.1)	-0.05 (.08)
8.00	-0.975	0.25	-1.6 (.1)	-0.05 (.08)
9.00	-0.974	0.25	-1.6 (.1)	-0.05 (.08)
10.00	-0.974	0.25	-1.6 (.1)	-0.04 (.08)

^a F_X = fractional intensity of $\text{XC}_6\text{H}_4\text{CO}^+$;

F_H = fractional intensity of $\text{C}_6\text{H}_5\text{CO}^+$.

^b AP_X = appearance potential of $\text{XC}_6\text{H}_4\text{CO}^+$;

AP_H = appearance potential of $\text{C}_6\text{H}_5\text{CO}^+$.

^c $E = V - IP$ (see section 4.4).

^d r = correlation coefficient.

^e e = standard deviation.

Table 16

(b) Correlation of $\text{Log}(F_X/F_H)^a$ with $(AP_X - AP_H)^b$ as a Function of the Ionizing Voltage, V .^c

V (eV)	r^d	e^e	Slope (e.s.d.)	Intercept (e.s.d.)
12.00	-0.986	0.27	-2.3 (.1)	-0.09 (.09)
13.00	-0.984	0.26	-2.1 (.1)	-0.08 (.09)
14.00	-0.983	0.25	-1.9 (.1)	-0.07 (.08)
15.00	-0.980	0.25	-1.7 (.1)	-0.06 (.08)
16.00	-0.977	0.25	-1.7 (.1)	-0.05 (.08)
17.00	-0.975	0.25	-1.6 (.1)	-0.05 (.08)
18.00	-0.974	0.25	-1.6 (.1)	-0.05 (.08)
19.00	-0.974	0.25	-1.6 (.1)	-0.05 (.08)
20.00	-0.973	0.25	-1.5 (.1)	-0.05 (.08)

^a F_X = fractional intensity of $\text{XC}_6\text{H}_4\text{CO}^+$;

F_H = fractional intensity of $\text{C}_6\text{H}_5\text{CO}^+$.

^b AP_X = appearance potential of $\text{XC}_6\text{H}_4\text{CO}^+$;

AP_H = appearance potential of $\text{C}_6\text{H}_5\text{CO}^+$.

^c V = corrected ionizing voltage.

^d r = correlation coefficient.

^e e = standard deviation.

Table 17

(a) Correlation of Logarithmic Intensity Ratios^a at
70 eV with Substituent Constants.

Correlation	r ^b	e ^c	Slope (e.s.d.)	Intercept (e.s.d.)
Log (F _H /F _M) vs. σ	0.86	0.27	1.9 (.3)	1.0 (.1)
" vs. σ ⁺	0.80	0.32	1.5 (.3)	1.1 (.1)
Log (F _X /F _M) vs. σ	-0.64	0.27	-0.9 (.3)	1.3 (.1)
" vs. σ ⁺	-0.73	0.24	-0.9 (.3)	1.2 (.1)
Log (F _H /1-F _M) vs. σ	0.75	0.20	0.9 (.2)	-0.65 (.09)
" vs. σ ⁺	0.79	0.18	0.8 (.2)	-0.61 (.07)
Log (F _X /1-F _M) vs. σ	-0.97	0.12	-1.9 (.15)	-0.41 (.05)
" vs. σ ⁺	-0.95	0.16	-1.6 (.16)	-0.54 (.06)
Log (F _X /F _H) vs. σ	-0.93	0.26	-2.8 (.3)	0.2 (.1)
" vs. σ ⁺	-0.94	0.26	-2.4 (.3)	0.1 (.1)

^a F_M = fractional intensity of M⁺;
F_X = fractional intensity of XC₆H₄CO⁺;
F_H = fractional intensity of C₆H₅CO⁺.

^b r = correlation coefficient.

^c e = standard deviation.

Table 17

(b) Correlation of Logarithmic Intensity Ratios^a at
70 eV with Energy Parameters.^b

Correlation	r^c	e^d	Slope (e.s.d.)	Intercept (e.s.d.)
Log (F_H/F_M) vs. (AP_H-IP)	-0.47	0.47	-0.8 (.5)	2.1 (.4)
Log (F_X/F_M) vs. (AP_X-IP)	-0.52	0.30	-0.4 (.2)	1.4 (.2)
Log ($F_H/1-F_M$) vs. (AP_H-IP)	-0.89	0.14	-0.9 (.1)	0.3 (.1)
Log ($F_X/1-F_M$) vs. (AP_X-IP)	-0.96	0.13	-0.9 (.1)	0.1 (.1)
Log (F_X/F_H) vs. (AP_X-AP_H)	-0.98	0.14	-1.06 (.06)	-0.11 (.04)

^a F_M = fractional intensity of M^+ ;

F_X = fractional intensity of $XC_6H_4CO^+$;

F_H = fractional intensity of $C_6H_5CO^+$.

^b IP = ionization potential;

AP_X = appearance potential of $XC_6H_4CO^+$;

AP_H = appearance potential of $C_6H_5CO^+$.

^c r = correlation coefficient.

^d e = standard deviation.

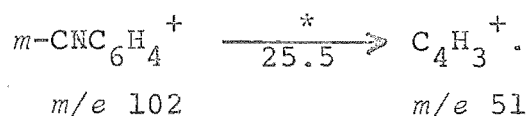
C H A P T E R 6DISCUSSION6.1 GENERAL DESCRIPTION OF MASS SPECTRA (Table 3)

The fragmentation patterns (Scheme 2) of the monosubstituted benzils studied in this work were generally straightforward. The primary fragmentations of the molecule-ion occurred by scission of the central carbon-carbon bond to give the substituted and unsubstituted benzoyl ions. Weak normal metastable ions corresponding to the more favourable of these decompositions were observed for all the compounds. The benzoyl ions decomposed by losing CO to form the substituted and unsubstituted phenyl ions, XC_6H_4^+ and C_6H_5^+ ; these decompositions were always accompanied by intense metastable ions. Further decomposition of the unsubstituted phenyl ions involved the loss of C_2H_2 to give C_4H_3^+ (m/e 51) - a process which is observed quite generally for aromatic compounds. However the substituted phenyl ions often decomposed by different pathways, usually involving the loss of part, or all, of the substituent. For example when the substituent (X) was a halogen or cyano group, HX was lost to give the ion C_6H_3^+ ($m/e = 75$). Normal metastable ions, often very weak, were observed for nearly all of these tertiary decompositions. Some of the spectra warrant further comment, and these are discussed below.

For *m*-formylbenzil (j), the structure of the ion (m/e 105) formed from the *m*-formylbenzoyl ion (m/e 133) by loss of CO is not known. It is represented by the *m*-formylphenyl structure

(by analogy with the other benzils), but may in fact have the benzoyl ion structure. The two possibilities cannot be distinguished with the information available.

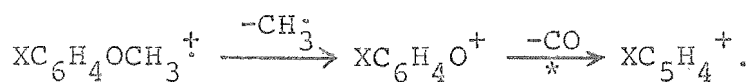
In *m*-cyanobenzil (k), a weak metastable ion is observed for the decomposition



This fragmentation corresponds to the loss of cyanoacetylene, and competes with the loss of HCN which gives a ten-fold stronger normal metastable ion ($m^* 55.1$). Normal metastable ions corresponding to the loss of a substituted acetylene fragment from the substituted phenyl ions were not observed for the other benzils, so this fragmentation may be specific for *m*-cyanobenzil. A study of the defocussed metastable ions for the formation of the C_4H_3^+ ion ($m/e 51$) would be required to confirm this.

The $m\text{-CH}_3\text{OC}_6\text{H}_4\text{CO}^+$ ion ($m/e 135$) formed in the mass spectrum of *m*-methoxybenzil (h), decomposes by two routes. The major one corresponds to the usual loss of CO by a direct cleavage reaction to give $m\text{-CH}_3\text{OC}_6\text{H}_4^+$ ($m/e 107$, $m^* 84.8$). The competing decomposition, which is much less favourable, gives the ion-radical $\text{C}_6\text{H}_4\text{O}^{\cdot+}$ ($m/e 92$, $m^* 62.7$), and possibly occurs by the consecutive loss of $\text{CH}_3\cdot$ and CO. However, the intermediate ion in this pathway ($m\text{-OC}_6\text{H}_4\text{CO}^{\cdot+}$, $m/e 120$) is not observed, and decomposition may occur by rearrangement loss of an acetyl radical. Such a rearrangement is more likely to give rise to the observed weak metastable ion in competition with the more favourable direct cleavage reaction²⁶. The ion-radical $\text{C}_6\text{H}_4\text{O}^{\cdot+}$ decomposes further by the expulsion of CO to give $\text{C}_5\text{H}_4^{\cdot+}$ (m/e

64, m^* 44.5); a similar loss of CO from phenoxy ions is observed in substituted anisoles¹⁰⁸,



The $m\text{-CH}_3\text{OC}_6\text{H}_4^+$ ion (m/e 107), formed from the m -methoxybenzoyl ion (m/e 135), loses CH_2O to give C_6H_5^+ (m/e 77, m^* 55.4); this rearrangement reaction is characteristic of methoxy-substituted aromatic compounds^{60,108}.

m -Trifluoromethylbenzil (1) loses a fluorine atom from the molecule-ion to give the ion m/e 259, as observed in other trifluoromethyl-substituted compounds¹⁰⁹. It is of minor importance compared to the usual decompositions of the benzil molecule-ions. The m -trifluoromethylphenyl ion (m/e 145) shows an unusual loss of C_4H_2 to form $\text{C}_3\text{H}_2\text{F}_3^+$ (m/e 95, m^* 62.3), which decomposes further by loss of HF to give C_3HF_2^+ (m/e 75, m^* 59.2).

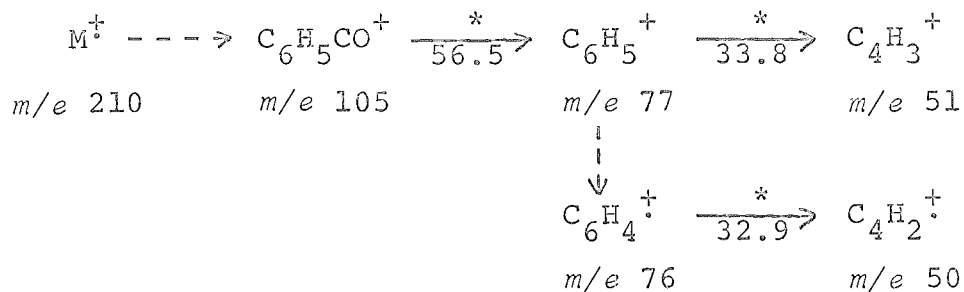
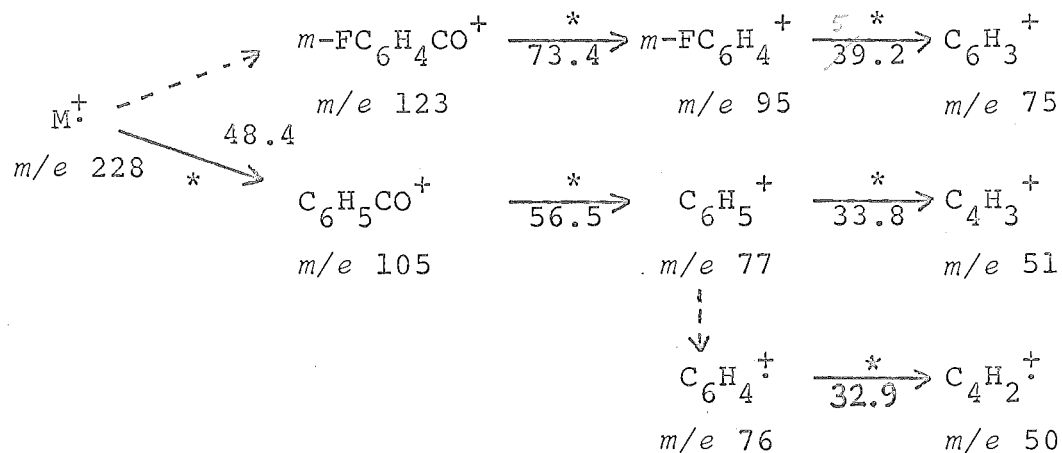
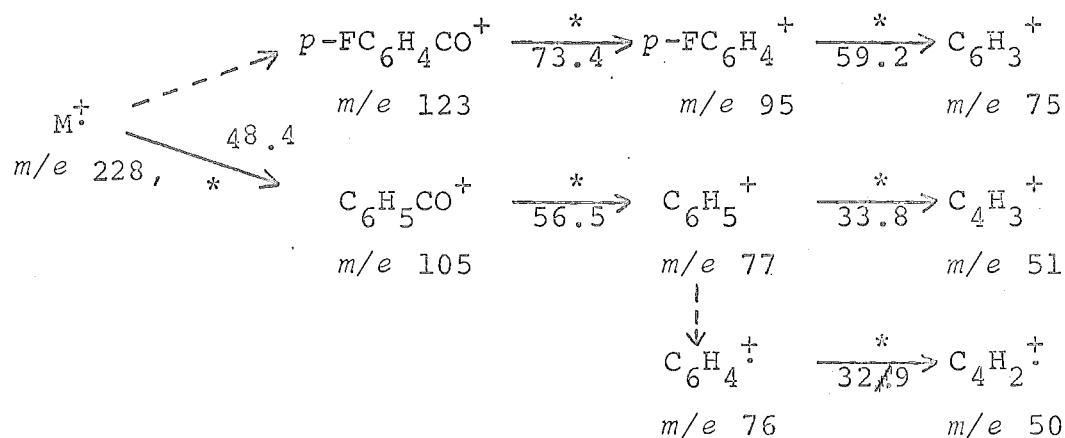
m -Nitrobenzil (m) was the only compound to give important primary or secondary fragmentations which differed from the usual fragmentations for the other benzils. These unusual decompositions can only be explained by assuming that they are controlled by the nitro group rather than the carbonyl group(s). The m -nitrobenzoyl ion (m/e 150) loses the $\text{NO}_2\cdot$ radical to give the ion-radical $\text{C}_6\text{H}_4\text{CO}^\dagger$ (m/e 104, m^* 72.1), rather than expelling CO as do the other substituted benzoyl ions. This behaviour has been observed for m -nitrobenzoyl ions generated from other compounds¹¹⁰, and is readily understandable since the activation energy for the formation of the unstable $\text{C}_6\text{H}_4\text{NO}_2^+$ ion would be expected to be much higher than that for the formation of $\text{C}_6\text{H}_4\text{CO}^\dagger$. In agreement with previous

observations¹¹⁰, decomposition of $m\text{-NO}_2\text{C}_6\text{H}_4\text{CO}^+$ by rearrangement loss of $\text{NO}\cdot$ to give $m\text{-OC}_6\text{H}_4\text{CO}^\ddagger$ (m/e 120) is negligible. The ion-radical $\text{C}_6\text{H}_4\text{CO}^\ddagger$ decomposes by losing CO to give $\text{C}_6\text{H}_4^\ddagger$ (m/e 76, m^* 55.6), which then loses C_2H_2 to form $\text{C}_4\text{H}_2^\ddagger$ (m/e 50, m^* 32.9). A more unusual decomposition of the m -nitrobenzil molecule-ion involves the formation of the m -nitrosobenzoyl ion, $m\text{-NOC}_6\text{H}_4\text{CO}^+$ (m/e 134). Since its appearance potential is lower than that for the m -nitrobenzoyl ion (Table 7(m)), it cannot be formed by the loss of an oxygen atom from m/e 150 (at least at its threshold energy). It is probably formed by a rearrangement process resulting in the loss of the benzoyloxy radical ($\text{C}_6\text{H}_5\text{CO}_2\cdot$) from the molecule-ion. The $m\text{-NOC}_6\text{H}_4\text{CO}^+$ ion loses $\text{NO}\cdot$ to give $\text{C}_6\text{H}_4\text{CO}^\ddagger$ (m/e 104, m^* 80.7).

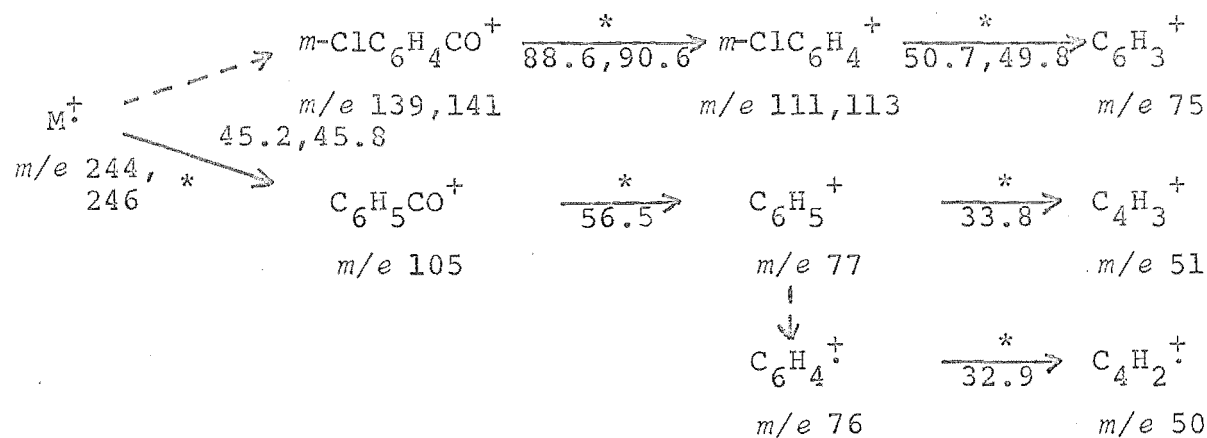
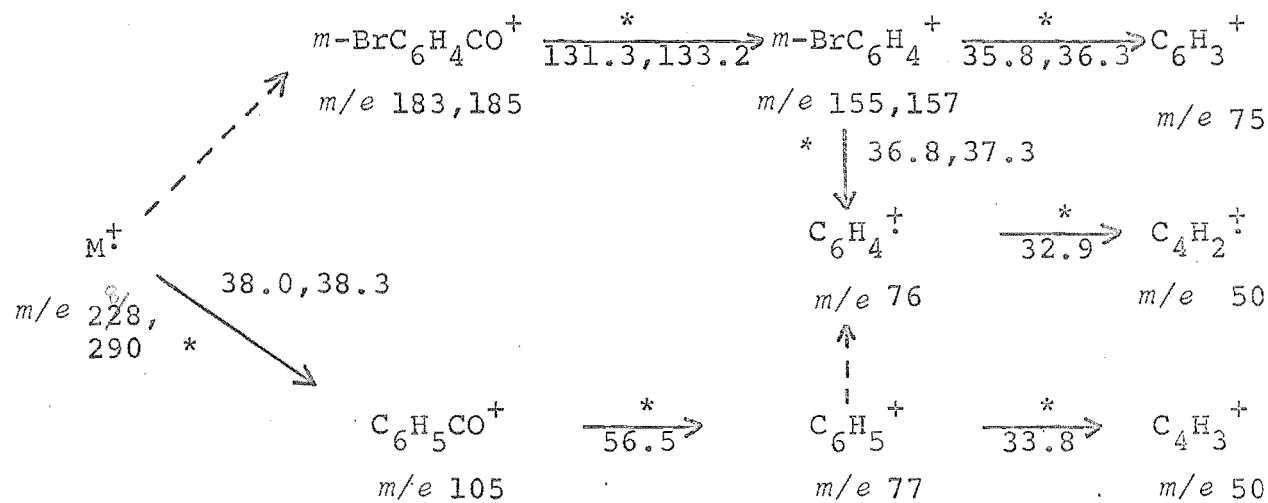
Although these proposed fragmentation schemes are consistent with all the available information, the lack of defocussed metastable ion data leaves the possibility of alternative pathways open to question. A metastable scan device was constructed in this department but the results obtained in this and other work so far were not reliable enough to be useful.

Scheme 2

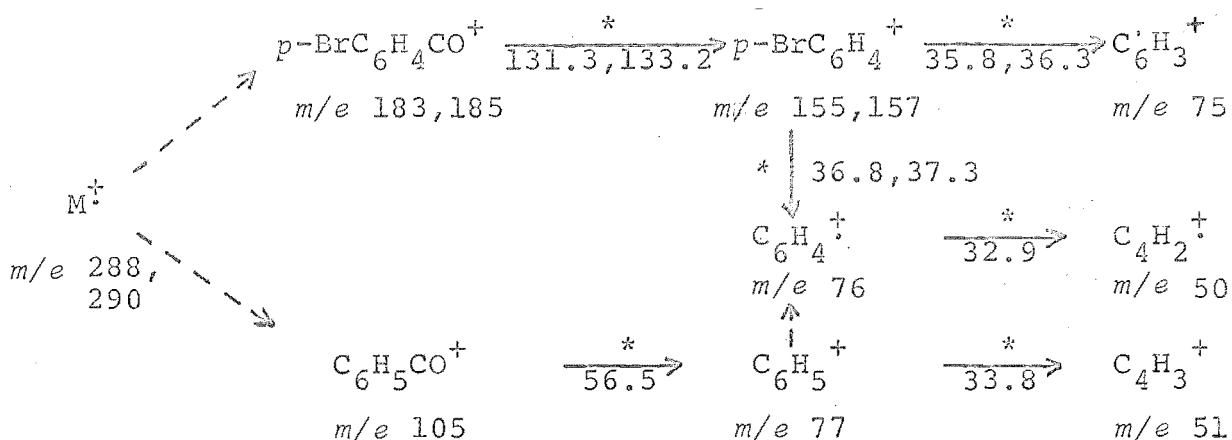
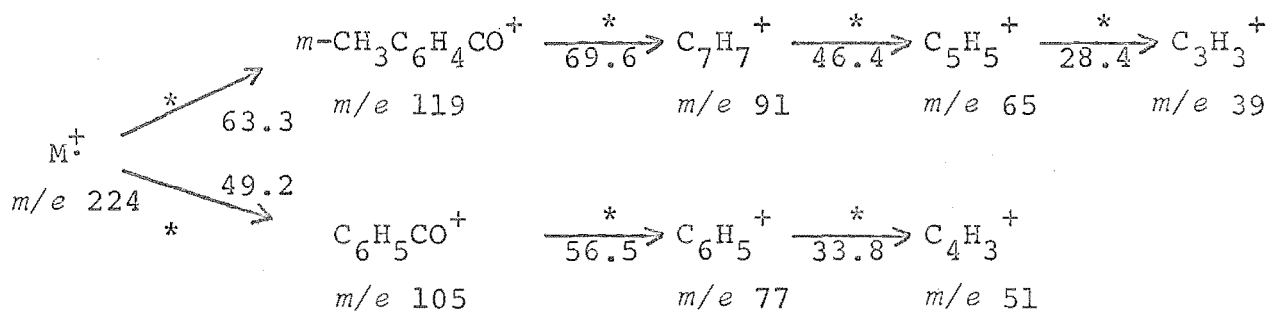
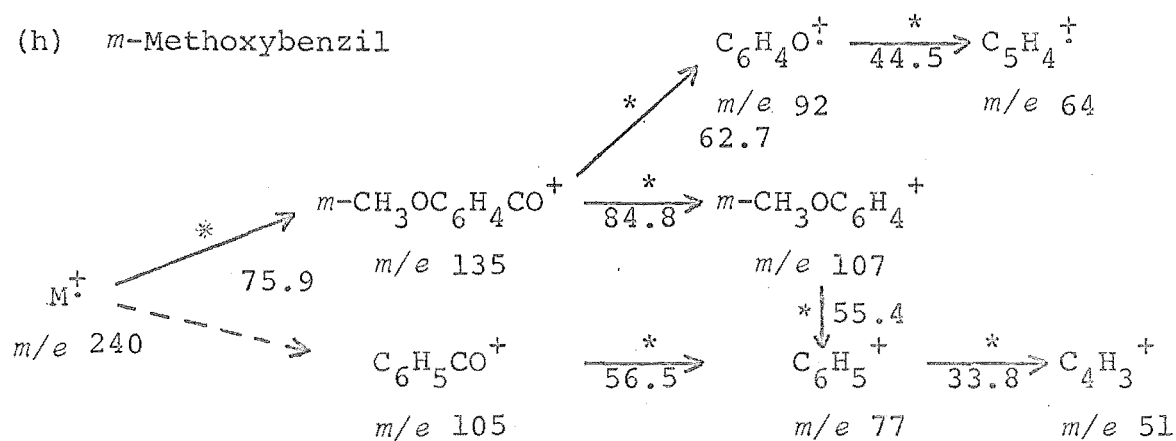
1 (a) Benzil:

2 (b) *m*-Fluorobenzil:3 (c) *p*-Fluorobenzil:

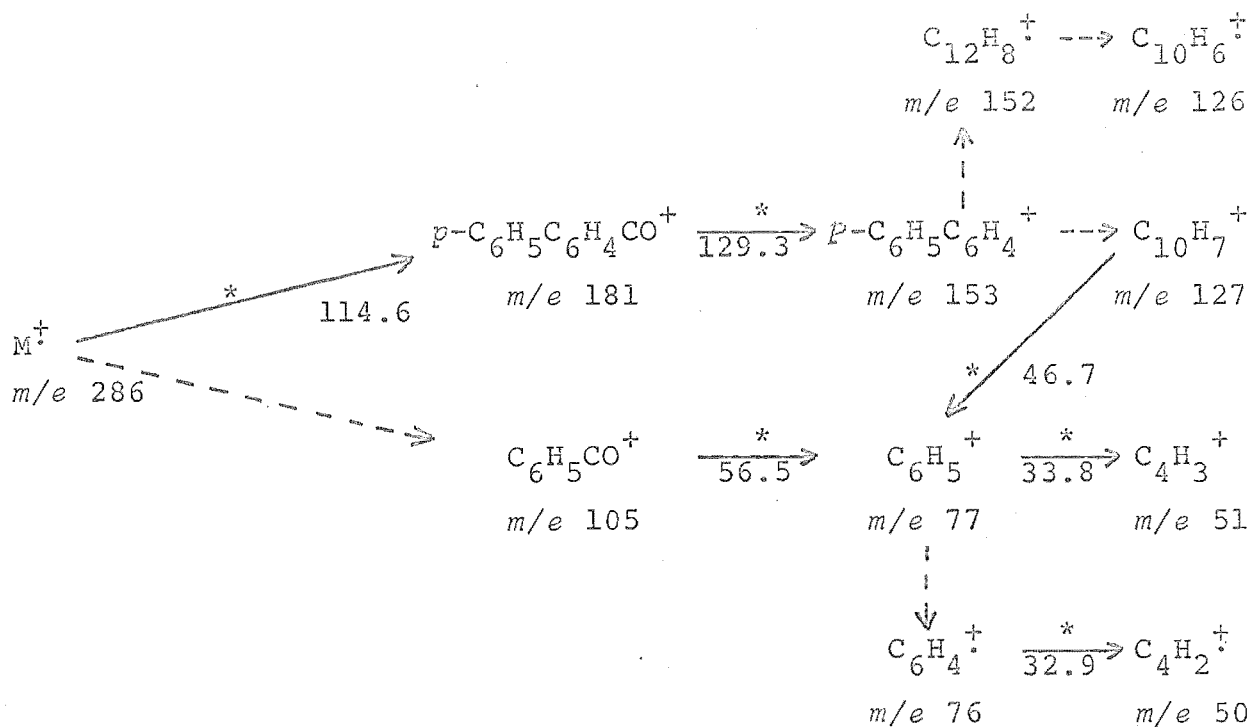
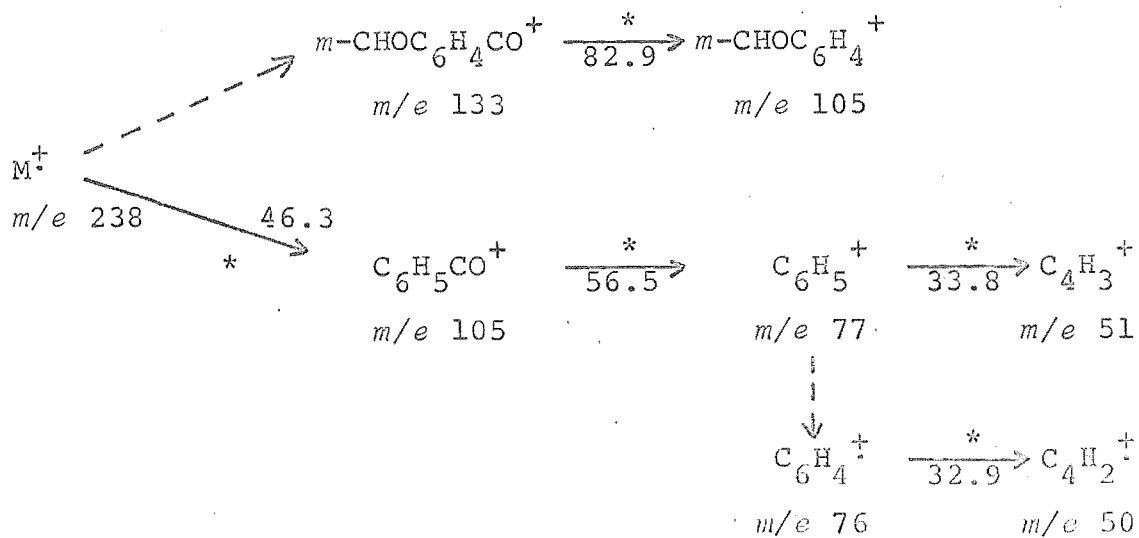
Scheme 2

A (d) *m*-Chlorobenzil:5 (e) *m*-Bromobenzil:

Scheme 2

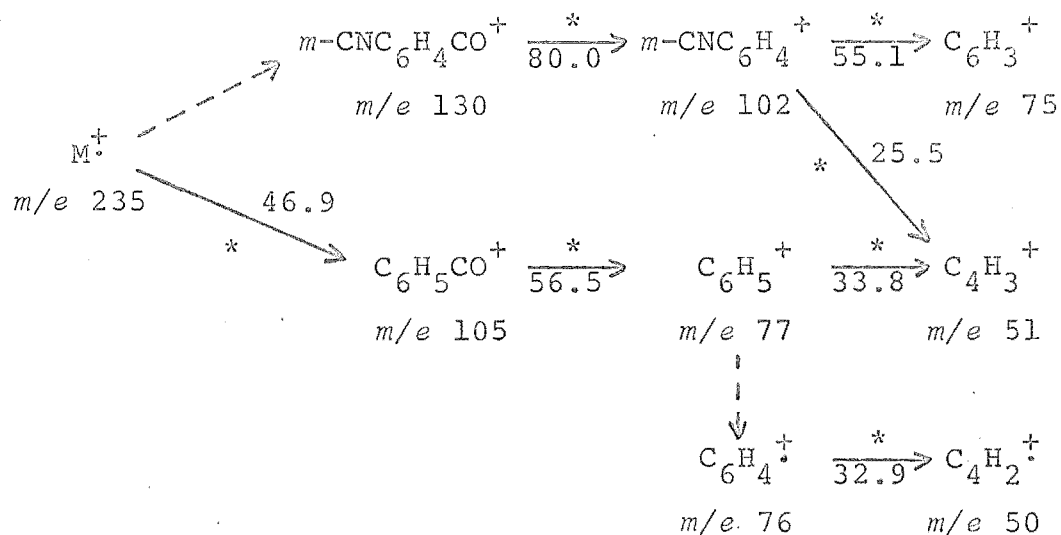
6 (f) *p*-Bromobenzil7 (g) *m*-Methylbenzil8 (h) *m*-Methoxybenzil

Scheme 2

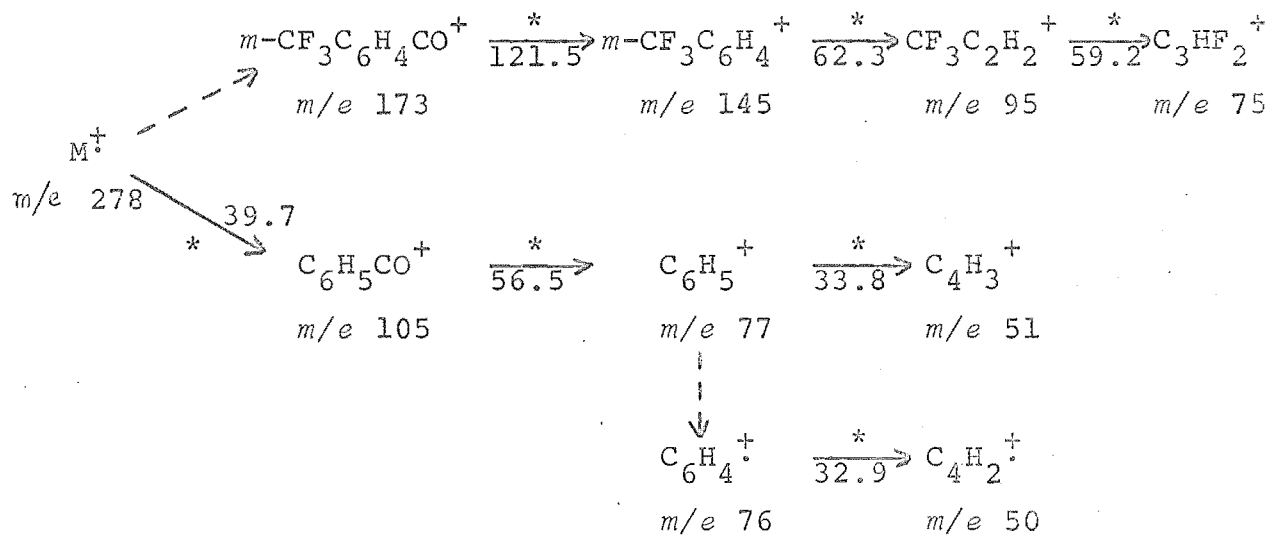
9 (i) *p*-Phenylbenzil:(j) *m*-Formylbenzil:

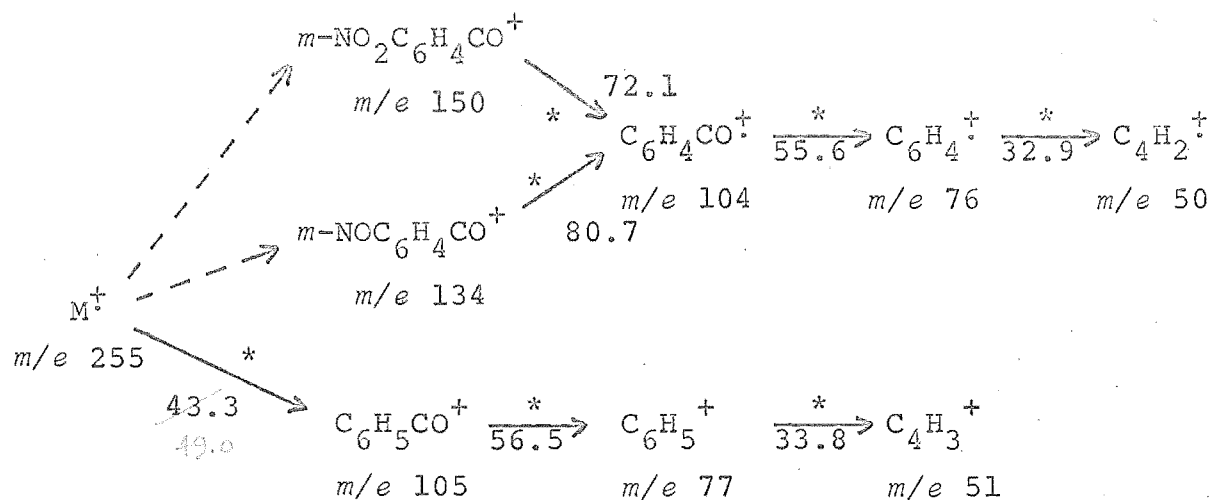
Scheme 2

(k) *m*-Cyanobenzil:



(l) *m*-Trifluoromethylbenzil:



Scheme 2B (m) *m*-Nitrobenzil:

6.2 INTERPRETATION OF ENERGY AND INTENSITY DATA

The behaviour of the monosubstituted benzils (see section 6.1) is ideally suited to a detailed investigation of substituent effects in mass spectra. The molecule-ions decompose by only two well-defined pathways to give the substituted and unsubstituted benzoyl ions (except for *m*-nitrobenzil which undergoes a competing rearrangement decomposition). This lack of alternative competing decompositions of the molecule-ions removes many of the complications which have interfered with the interpretation of other work on substituent effects^{9,26,111}. Secondary decompositions of the primary fragment ions do not become significant in the benzils until energies at least 5 eV above the ionization potential are reached; they occur by the same loss of CO for all the benzoyl ions (except for $m\text{-NO}_2\text{C}_6\text{H}_4\text{CO}^+$ and $m\text{-NOC}_6\text{H}_4\text{CO}^+$). Hence at low voltages the ion intensities reflect solely the effects of the substituents on the competitive formation of the substituted and unsubstituted primary fragment ions. This very simple situation should allow definitive conclusions to be reached about the way in which substituents influence mass spectral reactions.

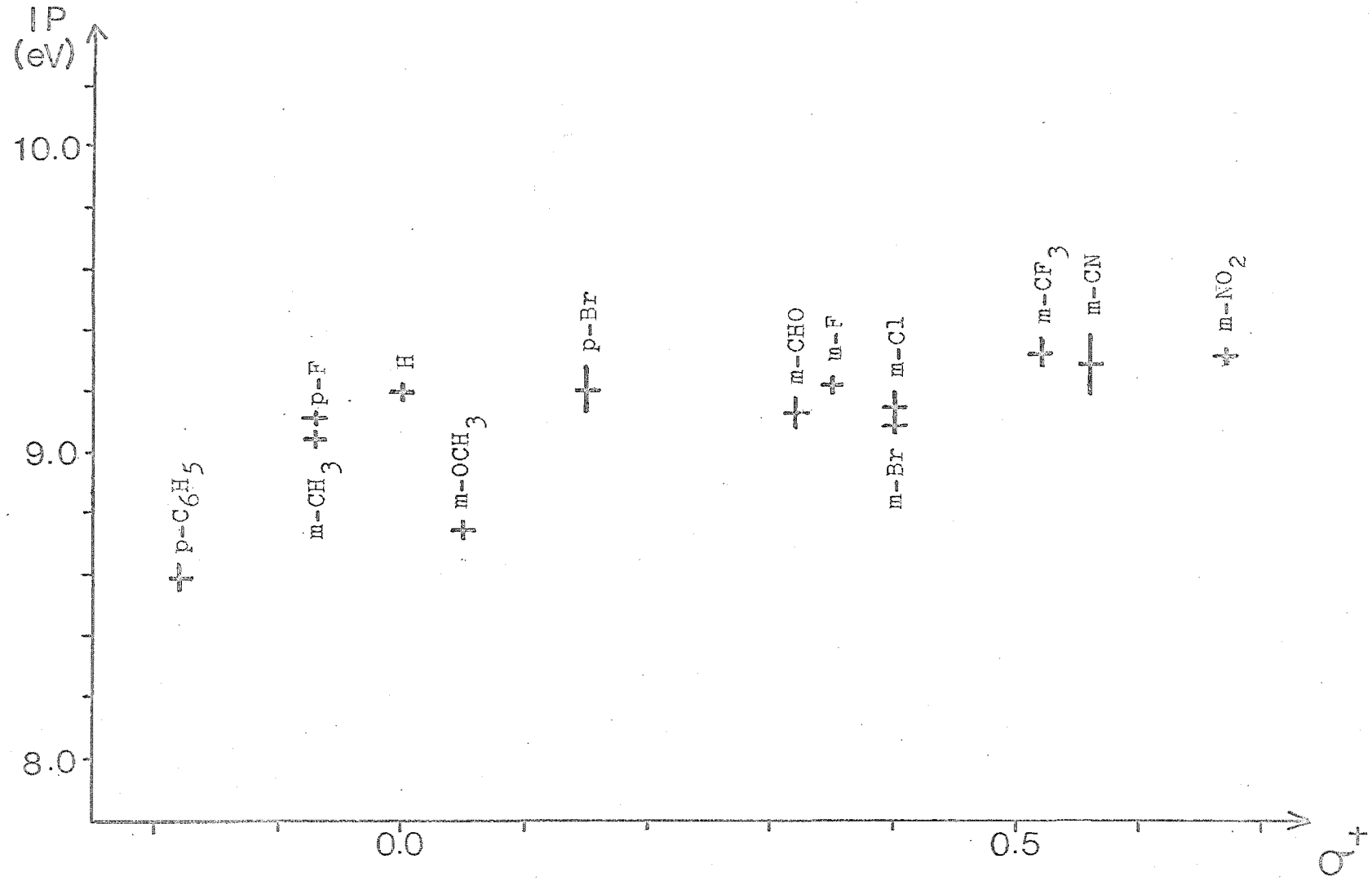
A number of approaches have been used to interpret substituent effects on ion intensities, ionization potentials, and appearance potentials^{6-8,61-63,111-127}. In this section the results of this study are used to examine these treatments, which include the correlations of substituent constants (σ, σ^+) with: ionization potentials (IP), appearance potentials of the primary fragment ions (AP_X, AP_H), energy parameters ($\text{AP}_X\text{-IP}, \text{AP}_H\text{-IP}, \text{AP}_X\text{-AP}_H$), and the logarithms of the intensity

ratios (F_X/F_M , F_H/F_M ⁶¹; $F_X/1-F_M$, $F_H/1-F_M$ ⁷; F_X/F_H ¹¹⁶). An alternative approach involving the relationship between relative ion intensities and energy parameters^{60,63,68,125,131} is then examined for the same logarithmic intensity ratios.

6.2.1 Correlation of Ionization and Appearance Potentials with Substituent Constants

The ionization potentials of the benzils are not strongly affected by the substituents used in this study; except for the *p*-phenyl and *m*-methoxy derivatives, the IP values lie within a range of 0.3 eV (*m*-CH₃ → *m*-NO₂). This range is smaller than that observed for other similarly substituted aromatic compounds (e.g. 0.6-0.7 eV for acetophenones^{7,115} and phenyl benzyl ethers⁶³, *m*-CH₃ → *m*-NO₂), suggesting that the benzil molecule-ions are stabilized primarily by the α-dicarbonyl group with the ring substituents having a smaller influence than usual. The correlation of the ionization potentials with σ or σ^+ is poor (Fig. 18; Table 10(a)). A similar lack of correlation for *meta*-substituted aromatic compounds was observed by Pignataro et al.¹¹⁵, who found that the ionization potentials of *meta*-substituted acetophenones and toluenes gave satisfactory linear correlations with σ_p^+ , whereas the correlations with σ_m^+ were widely scattered. They also noted that the IP values for the *para*- and *meta*-isomers were nearly equal and attributed this lack of a *meta-para* orientation effect to an ionization mechanism involving the loss of a π -electron from the aromatic ring (rather than a non-bonding electron from the carbonyl group, for example). A sufficient number of *para*-substituted benzils have not been studied in this work to make a similar comparison between the

Fig. 18. IP versus σ^+ .



meta- and *para*-isomers, however the correlation of IP with σ_p^+ ($r = 0.75$, $e = 0.15$) for the benzils is not significantly better than that observed with σ^+ ($r = 0.73$, $e = 0.16$). The argument that the lack of a *meta-para* orientation effect is due to ionization of an electron from a molecular orbital of the ring π -system requires that this orbital be symmetrical with respect to the *meta* and *para* ring positions. This is unlikely to be true, particularly if the delocalized π -system extends over the carbonyl group adjacent to the (substituted) ring, since the symmetry of the *meta* and *para* positions differ with respect to the carbonyl group.

No substituent effect is observed on the appearance potential (AP_H) of the unsubstituted benzoyl ion (Fig. 19; Table 10(b)); AP_H has an almost constant value of 9.86 (e.s.d. 0.06) eV. The same behaviour was observed for the appearance potential of the benzyl ion in a series of monosubstituted phenyl benzyl ethers⁶³ and bibenzyls⁸, but only for those bibenzyls in which the formation of the unsubstituted benzyl ion was favoured over the competitive formation of the substituted benzyl ion. This distinction between the results for the bibenzyls and the benzils is believed to be due only to the lack of substituents with large negative σ^+ values (e.g. *p*-NH₂, *p*-CH₃O) in the series of benzils which were studied. Further comment about the likely effect this will have on the observed correlations is made in the next section (6.2.2). When the unsubstituted benzyl ion is the less favoured primary fragment ion in the bibenzyls⁸, its appearance potential is much higher (about 2-4 eV) than in the opposite case. This is believed to be due to the competitive

Fig. 19. AP_H versus σ^+ .

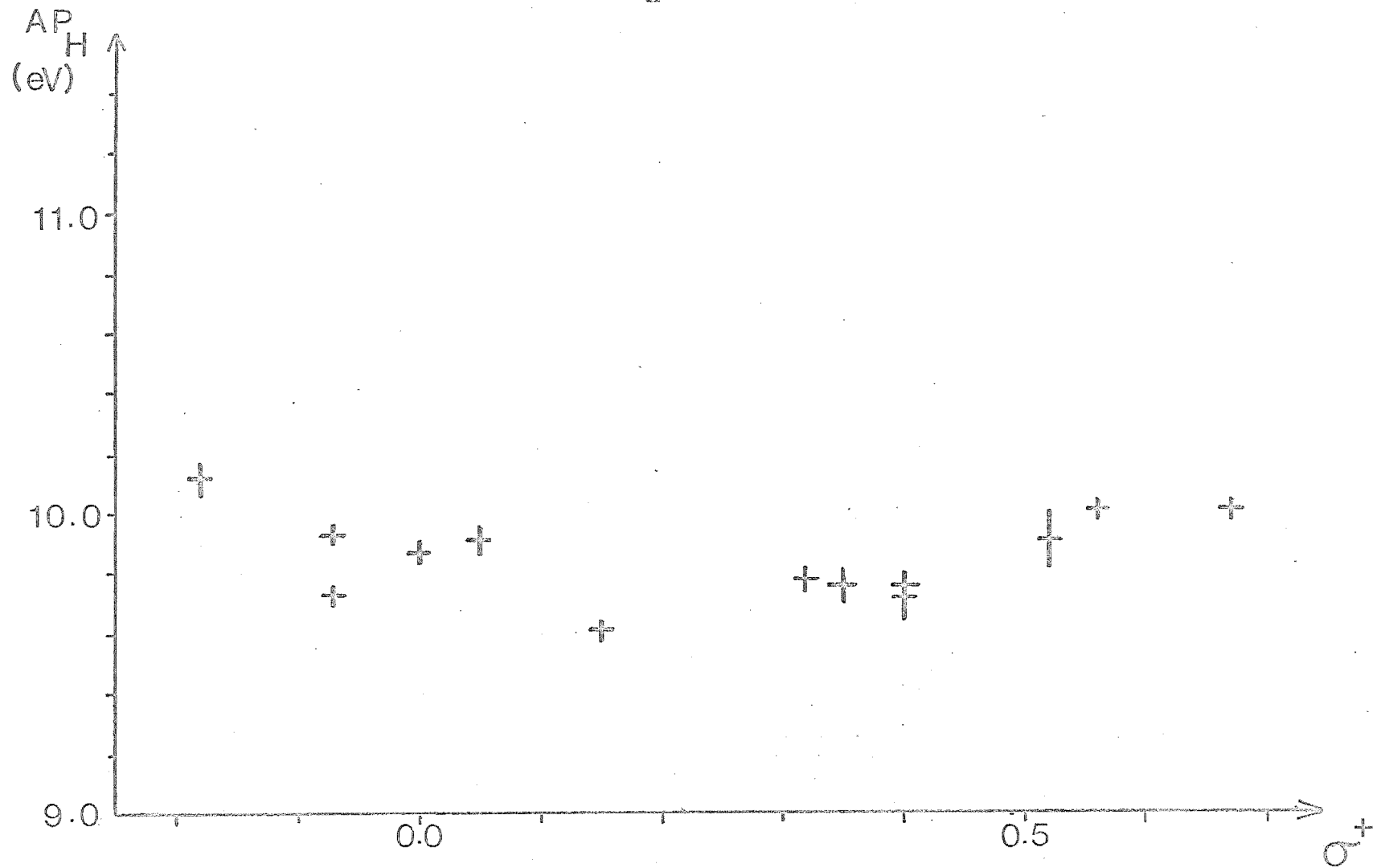
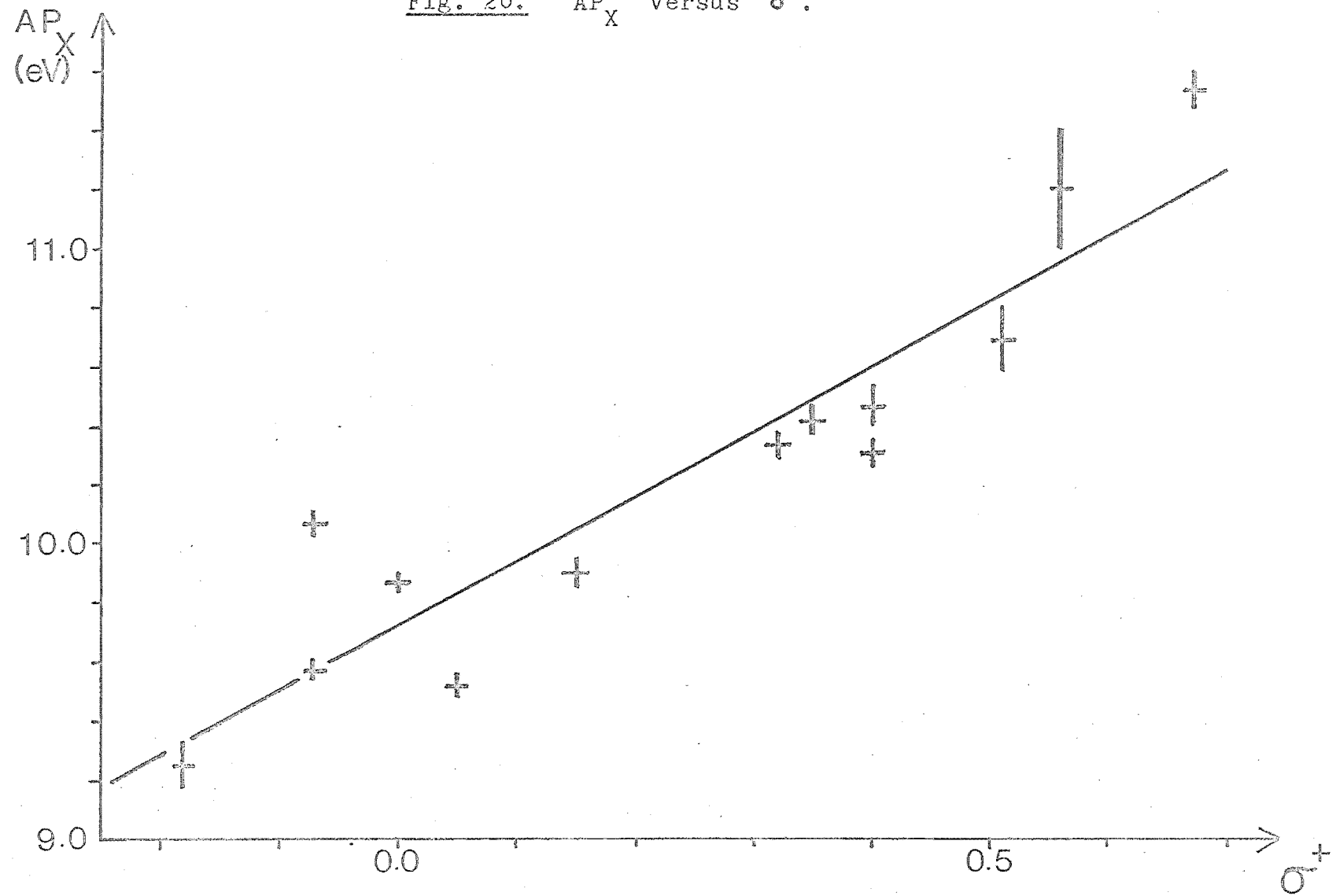


Fig. 20. AP_X versus σ^+ .



shift effect, and this also is discussed in section 6.2.2 after further consideration of the energy data for the benzils.

In contrast to the lack of variation in AP_H for the benzils, there is a marked variation in the appearance potential (AP_X) of the substituted benzoyl ion with change in substituent (Fig. 20; Table 9(c)); although the correlation between AP_X and σ^+ is fair ($r = 0.93$, $e = 0.26$), there is considerable scatter about the regression line. A similar, but even larger, variation with change in substituent was observed for the appearance potentials of the substituted benzyl ions from bibenzyls⁸ (e.g. a difference of about 4 eV from *p*-F to *m*-CN). The results for the benzils clearly demonstrate that these substituents exert their major effect on the appearance potential of the substituted benzoyl ion, rather than the unsubstituted benzoyl ion or the molecule-ion. However, the apparently ambiguous results for the bibenzyl series indicate that further consideration of this energy data is necessary. This is done in the next section, where the energy parameters obtained from the differences between the appearance and ionization potentials are discussed.

6.2.2 Correlations of Energy Parameters with Substituent Constants

The difference between the appearance potential of a primary fragment ion and the ionization potential (AP-IP) has been taken as a measure of the activation energy for the corresponding primary decomposition of the molecule-ion¹¹⁹. This approximation ignores the contributions to the appearance potential of the kinetic and competitive shift effects (see section 2.2.3(iii)), as well as any excess energy required in the decomposition process²⁶, but has been used¹¹⁹⁻¹²⁵ in the

absence of better measurements of activation energies.

The effect of substituents on these "activation energies", ΔE_H ($= AP_H - IP$) and ΔE_X ($= AP_X - IP$), for the formation of the unsubstituted and substituted benzoyl ions are shown in Figs 21 and 22 respectively. The fair correlation observed between ΔE_X and σ^+ (or σ) with a positive slope (Table 10(e)) contrasts directly with the poor correlation observed for ΔE_H which has a small negative slope (Table 10(d)). These results for the benzils are opposite to those expected by Einolf and Munson for the similar benzophenone series¹¹⁷. They argued by analogy with the appearance potential data for a series of substituted acetophenones⁷, where it was found that $AP(XC_6H_4CO^+) - IP(XC_6H_4COCH_3)$ was approximately constant for most substituents. Einolf and Munson therefore expected that AP-IP would show only a small variation with change in substituent for the formation of the substituted benzoyl ion in the benzophenone series, but a large variation for the unsubstituted benzoyl ion, with AP-IP decreasing with increasing σ^+ . However no appearance potential data were reported, and their arguments ignore the competitive shift effect.

A recent study of a series of unsubstituted bibenzyls⁸ can be usefully compared with the present results for the closely similar benzils, and Fig. 23(a,b) shows plots of ΔE_H and ΔE_X versus σ^+ for the formation of the unsubstituted and substituted benzyl ions respectively from monosubstituted bibenzyls (using IP and AP data reported by McLafferty⁸). The most striking feature of these plots is the opposite effect of the substituents on ΔE_H compared with ΔE_X ; where ΔE_H is almost constant with change in substituent ($\sigma^+ > 0$), ΔE_X varies

Fig. 21. $AP_H - IP$ versus σ^+ .

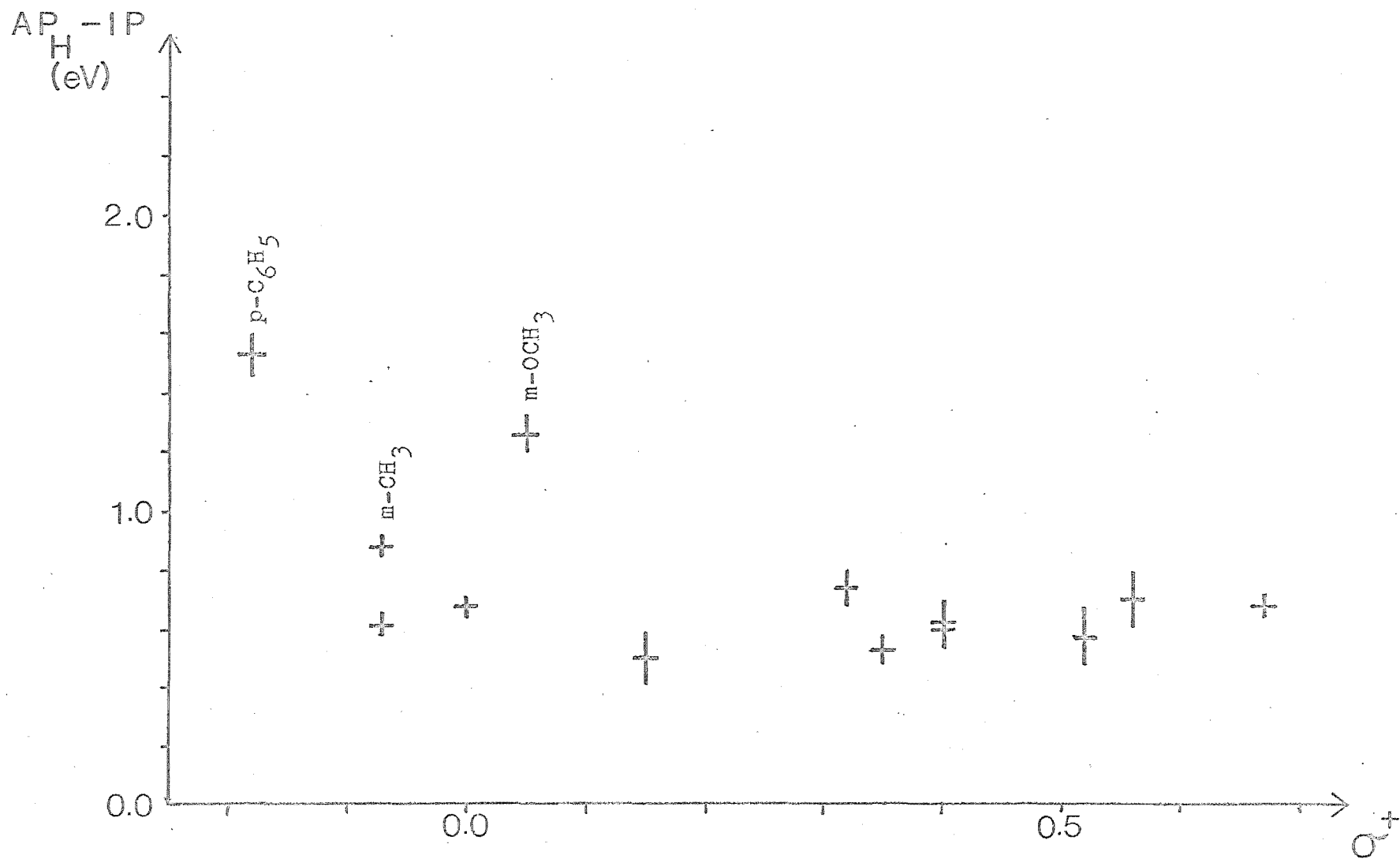


Fig. 22. $AP_X - IP$ versus σ^+ .

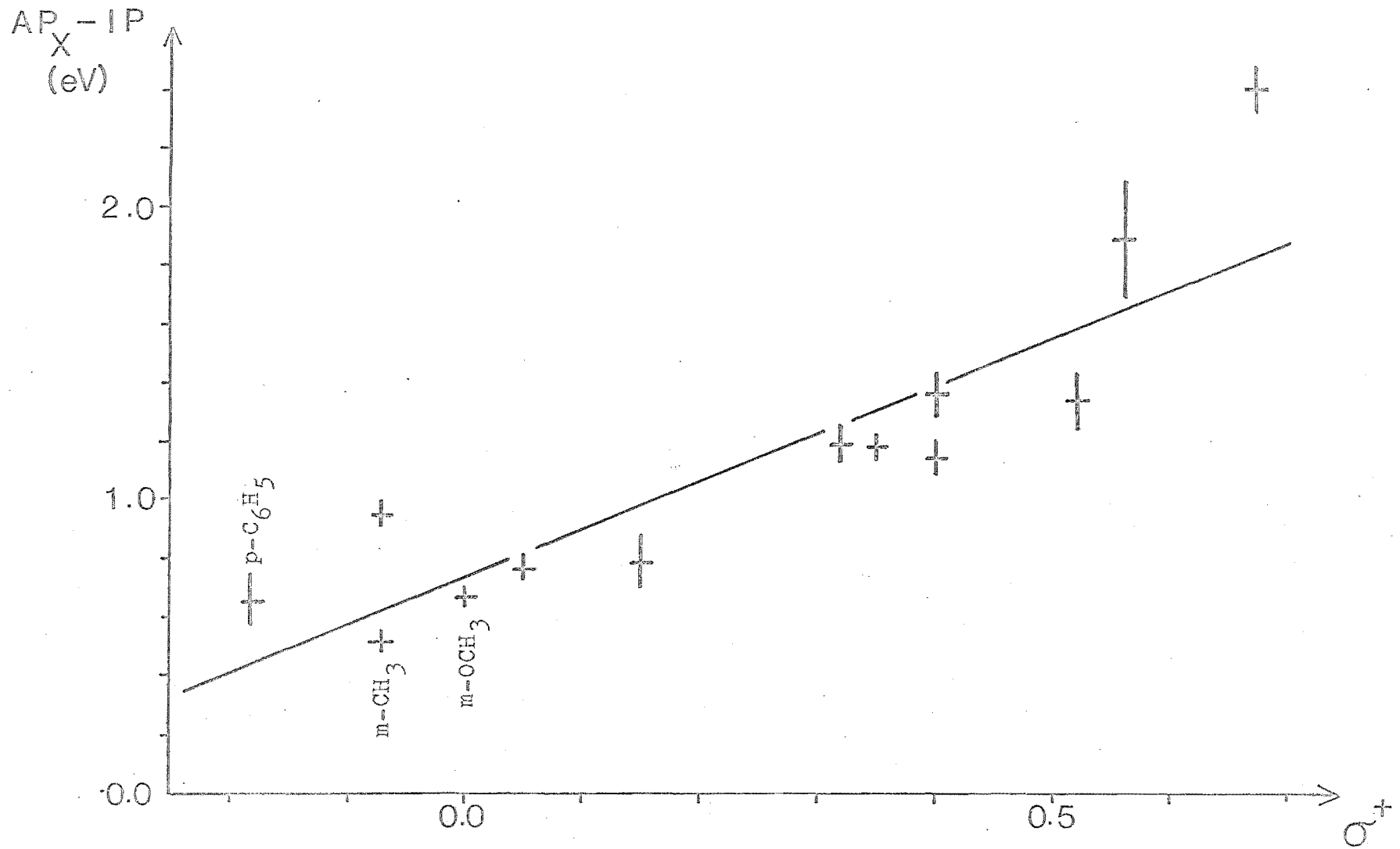


Fig. 23(a). $AP'_H - IP'$ versus σ^+ for Bibenzyls.

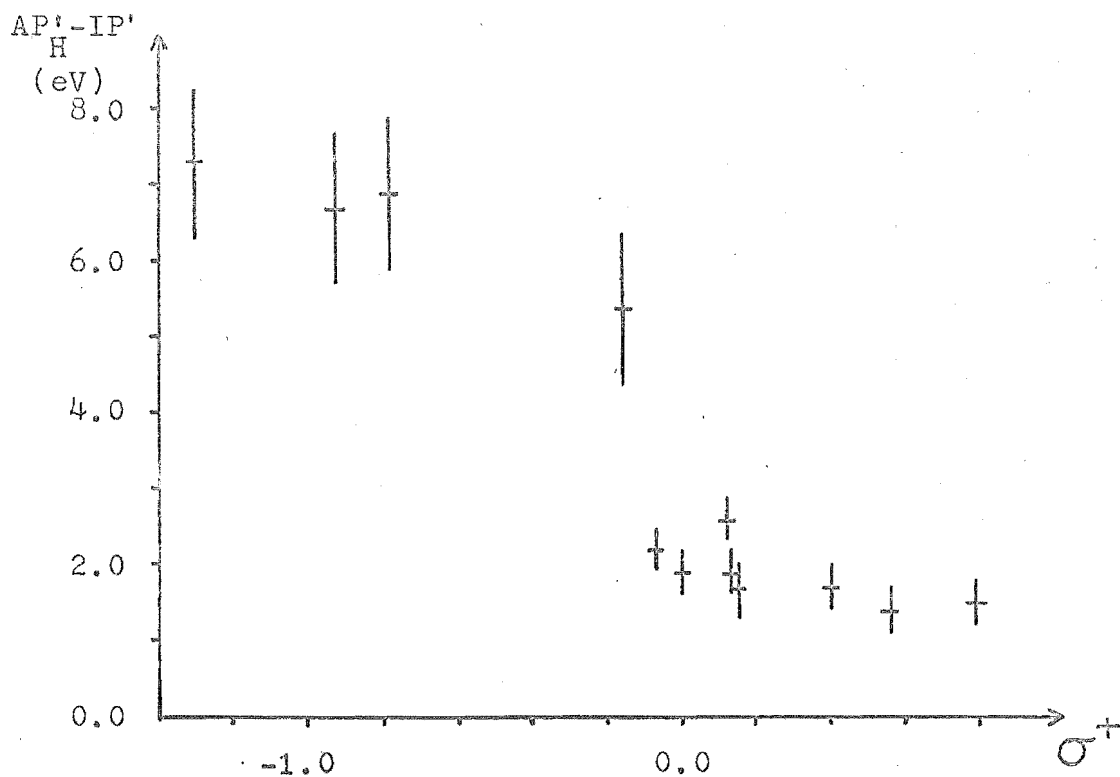
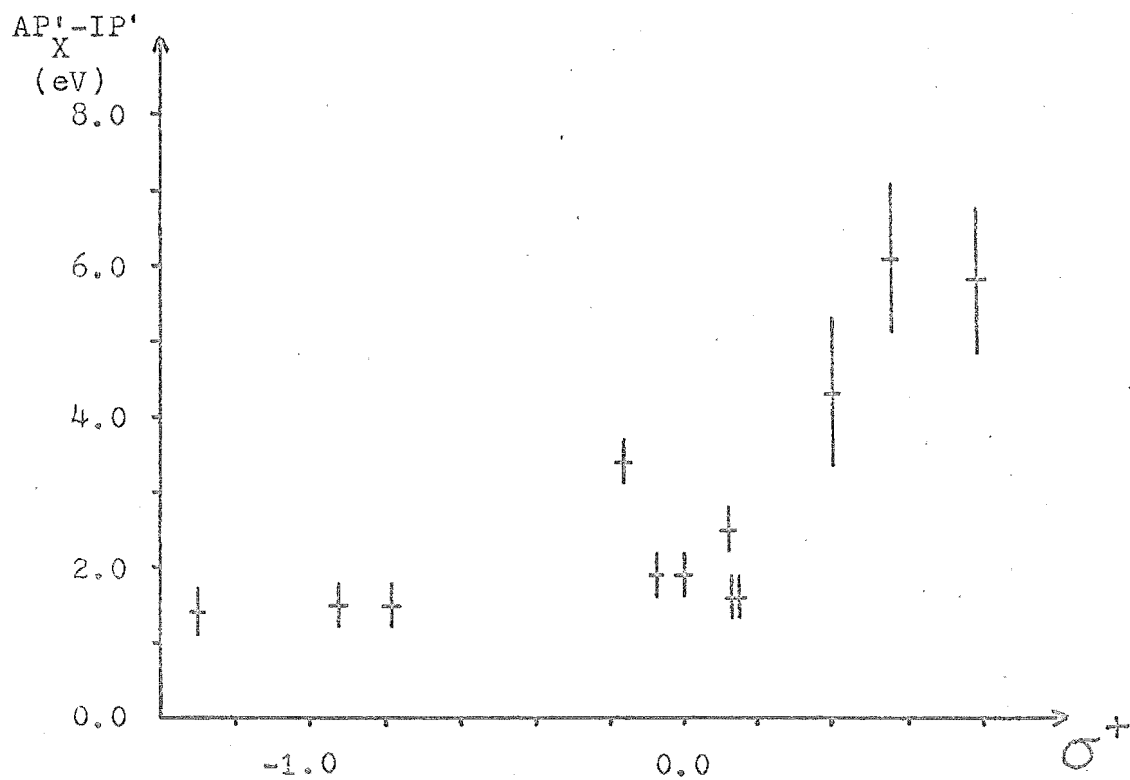


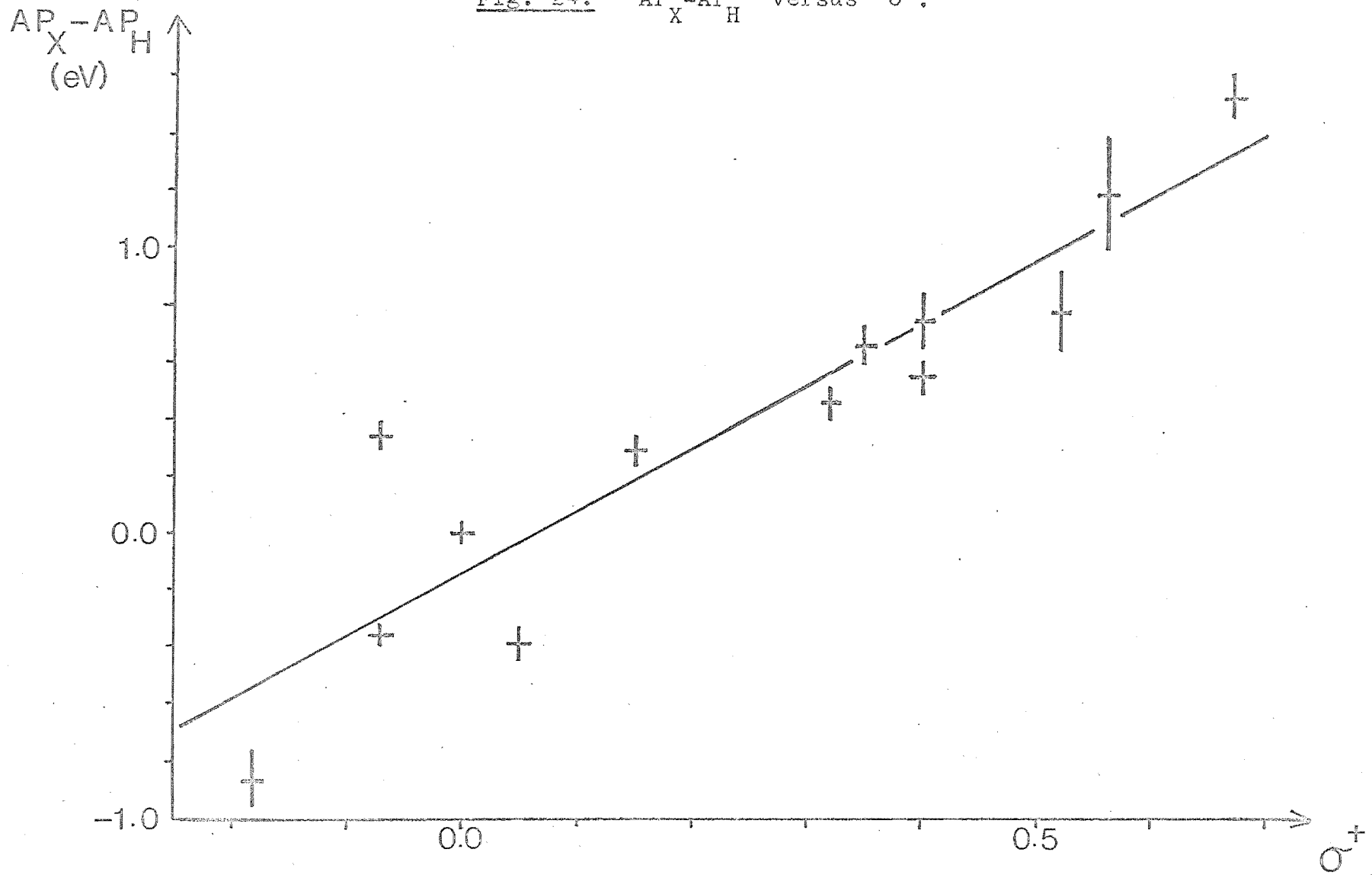
Fig. 23(b). $AP'_X - IP'$ versus σ^+ for Bibenzyls.



markedly. The reverse is true when $\sigma^+ < 0$. Furthermore, the value of ΔE for the more favourable primary decomposition of each substituted bibenzyl molecule-ion is approximately constant (about 1.5 eV). These observations are confirmed by the results for the benzils. Comparison of Fig. 21 and 22 shows that ΔE for the more favourable primary decomposition of the substituted benzils has an almost constant value of 0.65 eV. For most of the substituents used in this work, this decomposition corresponds to the formation of the unsubstituted benzoyl ion, i.e. $\Delta E_H < \Delta E_X$ (Table 9). However $\Delta E_X < \Delta E_H$ for the *p*-phenyl, *m*-methoxy and *m*-methyl substituents, and in these cases ΔE_X is also about 0.65 eV. Hence the apparent correlation between ΔE_X and $\sigma^+(\sigma)$ probably reflects only the limited range of σ^+ values covered by these substituents. If substituents with large negative σ^+ values were available, the plot of ΔE_X against σ^+ would probably show two distinct regions - a line with zero slope for $\sigma^+ < 0$ joining a curve of positive slope for $\sigma^+ > 0$ (c.f. Figs 22 and 23(b)). Conversely the plot of ΔE_H versus σ^+ would show a line of zero slope for $\sigma^+ > 0$ joining a curve of negative slope for $\sigma^+ < 0$ (c.f. Figs 21 and 23(a)).

The energy parameter $AP_X - AP_H$, which is equivalent to $\Delta E_X - \Delta E_H$, might be expected to measure the difference in the activation energies for the formation of the substituted (E_X^0) and unsubstituted (E_H^0) benzoyl ions from the molecule-ions of the substituted benzils. A fair linear correlation ($r = 0.92$, $e = 0.27$) is observed between $AP_X - AP_H$ and $\sigma^+(\sigma)$ (Fig. 24; Table 10(f)), however comparison with the correlation of AP_X with $\sigma^+(\sigma)$ (Fig. 20; Table 10(c)) indicates that the observed variation of $AP_X - AP_H$ with change in substituent is

Fig. 24. $AP_X - AP_H$ versus σ^+ .



entirely due to the variation in AP_X . If the differences in the activation energies ($E_X^0 - E_H^0$) for the competing primary decompositions of the benzil or bibenzyl molecule-ions were in fact as large as $\Delta E_X - \Delta E_H$ (see Figs 21-24), then the less favourable primary fragment ion would not contribute significantly to the total ion current because its formation could not compete effectively with the more favourable decomposition for most of the substituents.

For this reason the unusual behaviour of ΔE_H and ΔE_X with change in substituent (Figs 21-23), and the large slope of the regression line of $AP_X - AP_H$ against σ^+ (Fig. 24) are believed to be dependent on the large variation of the competitive shift effect with (small) differences in the activation energies, $E_X^0 - E_H^0$. Suppose that the activation energy for the formation of the substituted primary fragment ion (E_X^0) actually followed a linear correlation with σ^+ having a small positive slope, and that E_H^0 was independent of substituent. For substituents with positive σ^+ values, E_X^0 would then become progressively greater than E_H^0 with increasing σ^+ . The competitive shift effect on AP_X would magnify this difference, so that ΔE_X would become increasingly greater than E_X^0 with higher σ^+ values. Hence a plot of ΔE_X against σ^+ would show a linear portion of small positive slope for $\sigma^+ < 0$ (where the formation of the substituted ion would be the more favourable decomposition, so that ΔE_X would approximately parallel E_X^0), with the slope becoming increasingly greater for $\sigma^+ > 0$ (where the formation of the substituted ion would now be the less favourable decomposition, so that ΔE_X would become progressively greater than E_X^0). Similar arguments would apply to the correlation of ΔE_H with σ^+ , though here the deviations would occur for

negative values of σ^+ . Some of the factors contributing to the size of the competitive shift for these types of ion decompositions have been discussed by McLafferty⁸ (see also section 2.2.3 (iii)). The large size of the competitive shift effect compared with the differences in the activation energies for competitive decompositions, as indicated by this and other work^{8,120,126,132}, makes it almost impossible to derive activation energies from ionization and appearance potential measurements.

The competitive shift effect has generally been ignored by other workers who have used AP-IP as a measure of the activation energies for decompositions of molecule-ions^{60,63,119-125}. Fair correlations of AP-IP with σ or σ^+ were obtained by Brown for apparently competing direct cleavage and rearrangement decompositions of substituted anisoles¹²¹ and nitrobenzenes¹²². However his interpretation of these correlations, in terms of substituent effects on the activation energies for these competing decompositions is hazardous because of the unknown magnitude of the competitive shift which presumably affects the appearance potentials. The absolute values for the slopes of the regression lines of AP-IP against σ^+ were greater for the energetically less favourable competing primary decomposition in both the nitrobenzene¹²² and phenyl benzyl ether^{63,121} series. These results are consistent with the conclusions of this work as being due, at least in part, to the operation of the competitive shift effect. On the other hand, Brown observed¹²¹ that AP-IP for the rearrangement reaction, $\text{XC}_6\text{H}_4\text{OCH}_3^{\ddagger} \xrightarrow{-\text{CH}_2\text{O}} \text{XC}_6\text{H}_5^{\ddagger}$, was always less than that for the apparently competing cleavage reaction,

$\text{XC}_6\text{H}_4\text{OCH}_3^+ \xrightarrow{-\text{CH}_3^\cdot} \text{XC}_6\text{H}_4\text{O}^+$, yet the slope of the regression line of AP-IP against σ^+ was greater for the energetically more favourable rearrangement process (+ 0.62) than for the direct cleavage process (+ 0.45). Such a result would not have been expected if the competitive shift effect were operating, and suggests that these apparently competing decompositions of the anisole molecule-ions may be occurring from separate electronic states.

Neglecting excess energy terms, the activation energies for the competing primary decompositions of the benzils are given by the respective bond dissociation energies of the molecule-ions⁶⁸ (see section 2.3.2(ii)),

$$E_{\text{H}}^0 = \text{IP}(\text{C}_6\text{H}_5\text{CO}^\cdot) - \text{IP}(\text{XC}_6\text{H}_4\text{COCOC}_6\text{H}_5) + \text{D}(\text{XC}_6\text{H}_4\text{CO} - \text{COC}_6\text{H}_5) \quad (32a)$$

$$E_{\text{X}}^0 = \text{IP}(\text{XC}_6\text{H}_4\text{CO}^\cdot) - \text{IP}(\text{XC}_6\text{H}_4\text{COCOC}_6\text{H}_5) + \text{D}(\text{XC}_6\text{H}_4\text{CO} - \text{COC}_6\text{H}_5) \quad (32b)$$

Using this approximation the differences in these activation energies are given simply by the differences in the ionization potentials of the substituted benzoyl radicals,

$$E_{\text{X}}^0 - E_{\text{H}}^0 = \text{IP}(\text{XC}_6\text{H}_4\text{CO}^\cdot) - \text{IP}(\text{C}_6\text{H}_5\text{CO}^\cdot) \quad (33)$$

Unfortunately values are not available for these ionization potentials, so that this measure of the activation energy differences due to the substituents cannot be compared with that using $\text{AP}_{\text{X}} - \text{AP}_{\text{H}}$ to gain an indication of the size of the competitive shift effect on the appearance potentials.

However, such data has been obtained for some substituted benzyl radicals and provides an interesting comparison with the analogous data for the bibenzyls⁸; $\text{IP}(\text{XC}_6\text{H}_4\text{CH}_2^\cdot)$ gives a

reasonable linear correlation with σ^+ , with a slope of about 1.2 eV¹²⁷. The large errors in the appearance potentials (AP_H' , AP_X') of some of the (substituted) benzyl ions formed from the bibenzyls make it impossible to accurately determine the slope of the regression line of $AP_X' - AP_H'$ against σ^+ , but it is about five times greater than that for $IP(XC_6H_4CH_2\cdot)$. This result gives some idea of the size of the competitive shift to be expected for these ion decompositions - it is much larger than the corresponding differences in the activation energies. The same data also shows how E_X^0 and E_H^0 are expected to vary with change in the substituent for symmetrical systems like the bibenzyls and benzils. Referring to equations 32(a,b), the activation energies will be determined mainly by the differences in the ionization potential terms, since the bond strength term is not expected to vary much with change in the substituent¹²⁸. E_H^0 will therefore decrease slowly with increasing σ^+ (i.e. more electron-withdrawing substituents), due solely to the effect of the substituent on the molecular ionization potential. On the other hand the variation of E_X^0 with substituent will be determined by the differences between the ionization potentials of the substituted radical and molecule. For the substituted benzyl radicals and bibenzyls, $IP(XC_6H_4CH_2\cdot)$ increases more rapidly with σ^+ (slope ≈ 1.2 eV) than does $IP(XC_6H_4CH_2CH_2C_6H_5)$ (slope ≈ 0.5 eV), so that E_X^0 increases with increasing σ^+ and does so more rapidly (slope 0.7 eV) than E_H^0 decreases (slope ≈ -0.5 eV). These conclusions conflict with those of Einolf and Munson¹¹⁷ who expected that E_X^0 would show a smaller variation with change in substituent than E_H^0 , because E_X^0 involved the difference between two terms

which varied in the same direction. They apparently did not recognize how large this difference might be compared with the generally small variation in the molecular ionization potentials. It is expected that the activation energies in the benzil series will follow the same trends as observed for the bibenzyls, because the substituent effect on the ionization potentials of the benzils is considerably smaller than that observed for the bibenzyls, causing the variation of E_H^0 with change in substituent to be correspondingly smaller. For the same reason the variation of E_X^0 with change in substituent should be similar to, or larger than, that observed in the bibenzyl series, unless the ring substituents happen to have a very much smaller effect on $IP(XC_6H_4CO^+)$ compared with $IP(XC_6H_4CH_2^+)$.

6.2.3 Variation of Fractional Ion Intensities with Energy

The fractional ion intensities (F) of the major ions in the mass spectra of the benzils are shown (Fig. 17(a-m); Table 5(a-m)) as a function of the excess energy, E ($= V - IP$, see section 4.4). This quantity measures the amount of the ionizing energy which is available as internal energy in the molecule-ion to cause fragmentation; for each value of E there will be an internal energy distribution in the molecule-ion extending from zero to about $E + 0.6$ eV (the extra 0.6 eV is due to the energy spread of the electron beam). This energy scale was used to correct for the differences in the ionization potentials, so that the intensity data for each compound are directly comparable at equal values of E . Although this correction from the true ionizing voltage (V) is not large for these compounds, because of the small differences in their ionization potentials (Fig. 18; Table 8),

it might well be significant for other compounds and therefore affect correlations of ion intensities at low ionizing voltages.

The fractional intensity curves (Fig. 17(a-m)) clearly show the effect of the competition between the formation of the two primary fragment ions on their relative intensities. The more favourable primary fragment ion shows a very rapid increase in fractional intensity (with a corresponding decrease in the fractional intensity of the molecule-ion), which then gradually falls off as the less favourable primary fragment ion competes more effectively at higher energies. This behaviour is expected from the quasi-equilibrium theory since the rate constants for similar competing decompositions become more comparable at higher energies (see section 2.3.2(ii)). The rate of increase of the fractional intensity of the less favourable primary fragment ion with increasing energy depends markedly on the differences in the threshold energies of the two ions. For substituents where this difference is small (e.g. *p*-F (c), *p*-Br (f)), these fractional intensity curves rise rapidly to a value which then increases very slowly with energy. On the other hand, for substituents with a larger difference between threshold energies of the two curves (e.g. *m*-Br (e), *m*-CN (k), *m*-CF₃ (l)), the rate of increase of the fractional intensity of the less favourable primary fragment ion with increasing energy is much slower and smoother. The points of inflection observed in some of these curves (e.g. *m*-formylbenzil (j)) are probably not significant; they may be artificially introduced by the linear extrapolation used to extend the measured IE curves to higher energies (see section 4.4). The measured fractional ion intensities were not

obtained at close enough energy intervals to decide whether the effect was real or artificial.

The fractional intensities of the molecule-ions drop very quickly to a low value with the onset of the primary decompositions. The most notable exception to this behaviour occurs for *m*-methoxybenzil (h), where the fractional intensity of the molecule-ion (F_M) decreases quite slowly with increasing energy and has an unusually large value of about 12% at $E = 8.0$ eV. Similar, though less marked, behaviour is shown by *m*-methylbenzil (g) and *p*-phenylbenzil (i), and this may reflect an increased stability towards decomposition for these molecule-ions. Howe (ref. 59, p.67) has suggested that the overall effect in the majority of cases is for electron-donating substituents to increase the difference between the ionization potential and the lowest (fragment ion) appearance potential. This generalization was based on IP and AP data for the energetically most favourable decompositions of acetophenones^{7,113}, methyl benzoates⁶⁰, phenyl benzyl ethers⁶³ and methyl butyrates¹¹¹. The quantity $AP - IP$, for the lowest appearance potential (AP_{min}), is closely related to the fraction of molecule-ions with insufficient energy to decompose (i.e. "sub-decomposition energy" ions) given by F_M ; $AP_{min} - IP$ is expected to be largest for those molecule-ions having the greatest value of F_M in a series of similar compounds^{8,60,63}. However, in the benzil (and bibenzyl) series, $AP_{min} - IP$ is practically constant (see Figs 21-23), whereas the fractional intensities of the molecule-ions do vary significantly (as noted above). This suggests that complicating effects due to changes in the internal energy distributions of the molecule-ions with different substituents^{8,124} may be operating,

and discernable, in these cases; similar conclusions have been reached from results for other compounds containing *meta* electron-donating substituents (e.g. *m*-OCH₃, *m*-OH, and *m*-NH₂)^{60,63} (see also section 6.2.5).

The fractional intensity curves for the secondary fragment ions are also shown in order to indicate the excess energies at which decompositions of the primary fragment ions start (usually about $E = 6$ eV). For the range of energies considered in this work they make only a small contribution to the total ion intensity, and their effect on the correlations of the primary fragment ion and molecule-ion intensities can be ignored.

6.2.4 Correlations of Logarithmic Ion Intensity Ratios with Substituent Constants

The various logarithmic intensity ratios used in this section were calculated from the fractional ion intensities (Table 5(a-m)), and are given as a function of the excess energy (E) and the corrected ionizing voltage (V) in Table 6 (a-m). The asymptotic trend of these ratios towards apparently constant values with increasing energy is easily seen in these tables; their values at the higher energies (e.g. $V = 20.0$ eV) may be compared with the corresponding values calculated from the 70 eV spectra (Table 3(a-m)) and presented in Table 7. Such comparison shows that the advent of further decompositions of the primary fragment ions at higher energies causes the ratios at 70 eV to differ significantly from those at 20 eV (for example) in many cases. No consistent trend in the differences between the ratios at high and low voltages is apparent; this is expected in view of the many and varied decomposition processes which may occur at high energies, and

which will often be quite different for different substituents.

All the correlations of the logarithmic ion intensity ratios with various parameters were tested at several energies. Unless they changed significantly with energy, the regression parameters are quoted for an excess energy $E = 6.0$ eV because at this energy secondary decompositions of the primary fragment ions are still insignificant ($< 1\%$ of total ion intensity). Above this energy the change in the ratios with energy is fairly slow, so that the regression parameters do not change much at higher energies.

(i) $\text{Log } (F/F_M)$:

The original pioneering work of Bursey and McLafferty⁶¹ tried to obtain mechanistic information on mass spectral reactions by studying the effects of substituents on ion intensities. They observed fair correlations between $\log (F/F_M)$ and substituent constants (σ, σ^+) for some series of compounds⁶, where F is the fractional intensity of a primary fragment ion and F_M that of the molecule-ion (F/F_M is equivalent to their Z -values). In attempting to relate these correlations to substituent effects on the rate constants for the corresponding fragmentation reactions, they used a "steady-state" treatment of the kinetics of ion decompositions which is now well-recognized to have severe limitations^{9,11,26,59,117,131}. These limitations arise because it takes inadequate account of the competition between the decompositions of the molecule-ion, and the further decomposition of the fragment ions - factors which are correctly dealt with by the quasi-equilibrium theory (see section 2.2.3).

The correlation of $\log (F_H/F_M)$ with σ^+ or σ (Table 11(a); Fig. 25) for the benzils is poor at all energies. On the other

Fig. 25. $\text{Log}(F_H/F_M)$ versus σ^+ , $E = 6.0 \text{ eV}$.

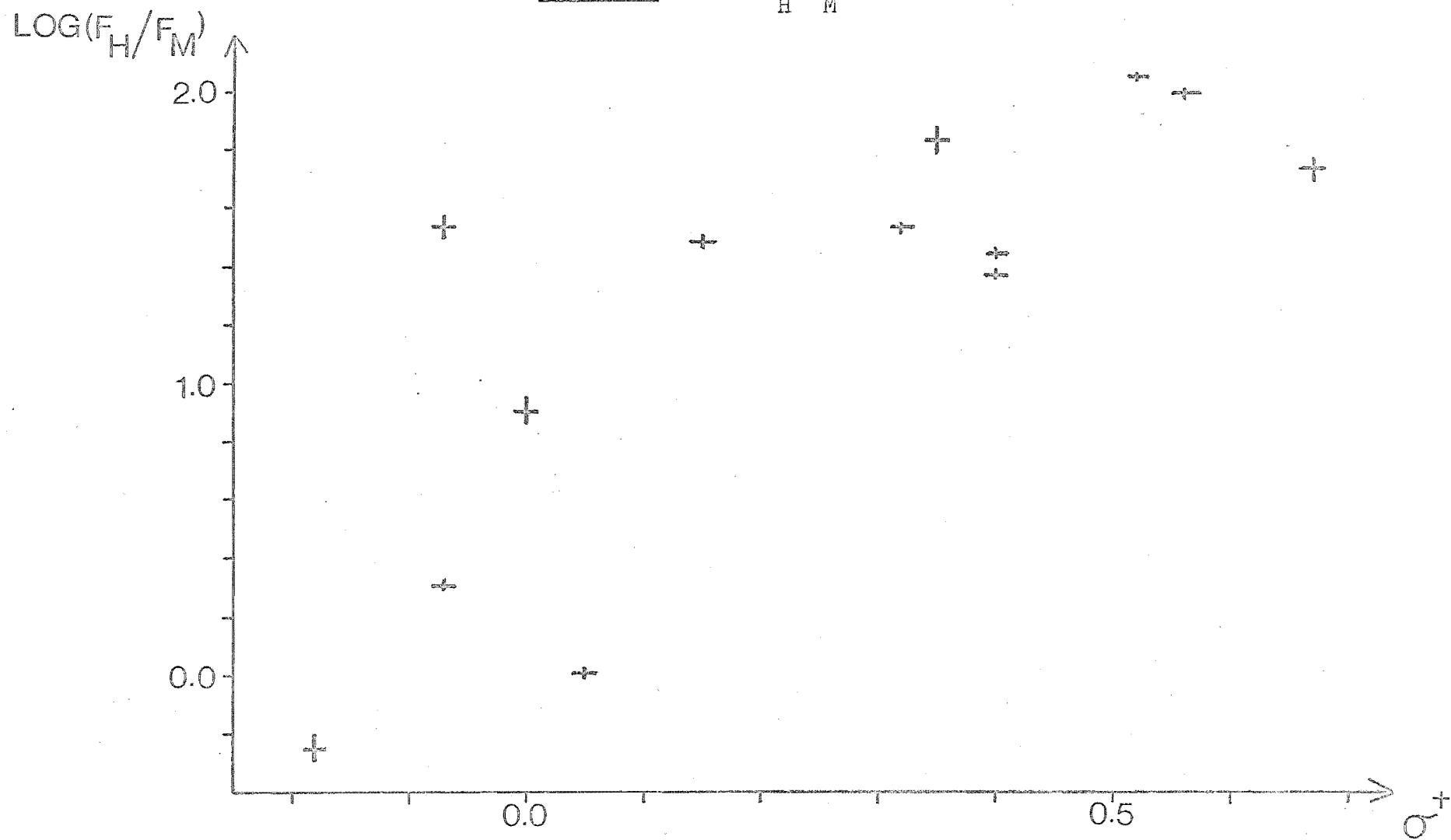
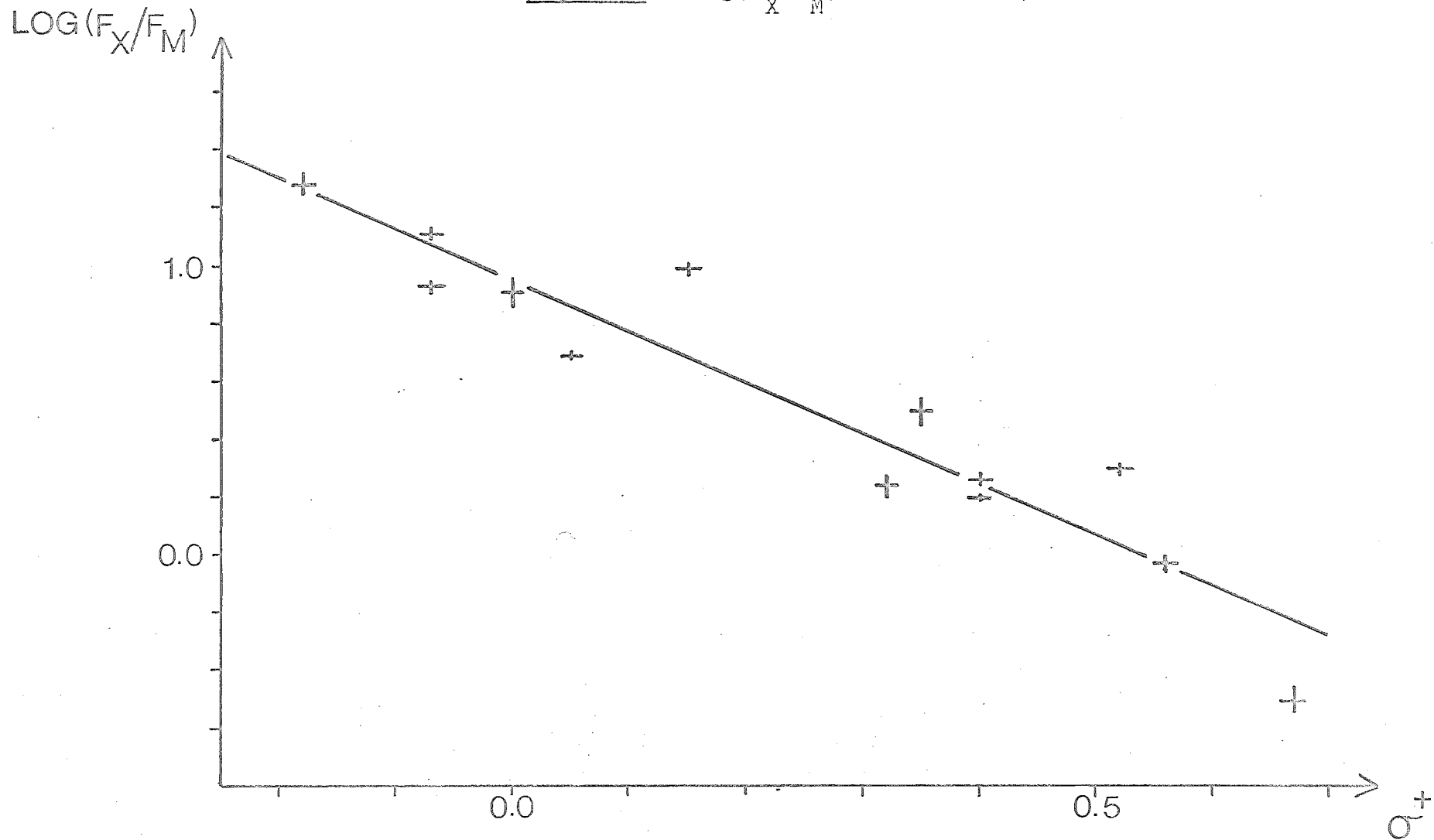


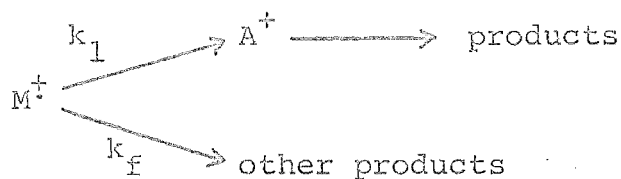
Fig. 26. $\text{Log}(F_X/F_M)$ versus σ^+ , $E = 6.0$ eV.



hand, $\log (F_X/F_M)$ gives a fair correlation with both σ^+ and σ (Table 11(b); Fig. 26) (e.g. $r = -0.94$, $e = 0.18$ at $E = 6.0$ eV) at low energies, but is much worse at 70 eV (Table 17(a)). These results serve to stress the ambiguous nature of the correlations obtained using this treatment, and since the substituent effect on these $\log (F/F_M)$ values can be influenced by a number of factors^{9,26} (see section 2.3.2) which cannot be separated, they are not discussed further. By the usual standards of solution chemistry these correlations would be considered poor. Critical workers have suggested that correlation coefficients of 0.99 (or greater) should be the requisite criterion for an acceptable correlation¹²⁹. Hardly any of the published correlations of mass spectral data (including those obtained in this work) approach this high standard, emphasizing the need for caution in the interpretation of such results.

(ii) $\log (F/1-F_M)$:

A theoretically more sound, quantitative formulation of the factors determining the effect of substituents on ion intensities^{9,26} has been given by Chin and Harrison⁷. This treatment is based on the quasi-equilibrium theory (see section 2.2.3), but includes many simplifications in order to make the kinetic analysis of the ion decompositions tractable. In particular the so-called rate constants which appear in their treatment should not be interpreted literally, since they actually represent very complicated average values. The expression obtained for the relative ion intensities in the general fragmentation scheme:



is given by

$$\frac{[\text{A}^+]}{[\text{M}_0^{\ddagger}]} = \frac{k_1}{k_t} (1-f) f' \quad (34)$$

where f is the fraction of total molecule-ions, $[\text{M}_0^{\ddagger}]$, with insufficient energy to decompose (i.e. $f = [\text{M}^{\ddagger}]/[\text{M}_0^{\ddagger}]$), f' is the fraction of total A^+ ions, $[\text{A}_0^+]$, with insufficient energy to decompose further (i.e. $f' = [\text{A}^+]/[\text{A}_0^+]$), and $k_t = k_1 + k_f$. This equation may be conveniently written in terms of fractional ion intensities as

$$\frac{F}{1-F_M} = \frac{k_1}{k_t} f' \quad (35)$$

where F is the fractional intensity of a primary fragment ion, i.e. $F = [\text{A}^+]/[\text{M}_0^{\ddagger}]$, and $F_M = [\text{M}^{\ddagger}]/[\text{M}_0^{\ddagger}] = f$. Since further decomposition of the primary fragment ions is negligible at the low ionizing voltages used in this study, $f' = 1$, so that

$$\log (F/1-F_M) = \log (k_1/k_t).$$

Also, if competing decompositions of the molecule-ion are eliminated (e.g. at energies near the threshold of the most favourable primary fragmentation), $k_t = k_1$, so that $\log (F/1-F_M) = 0$.

The lack of correlation between $\log (F_H/1-F_M)$ and $\sigma^{\ddagger}(\sigma)$ (Table 12(a); Fig. 27) appears to be due to this competition effect. For most of the substituents used in this work the

Fig. 27. $\text{Log}(F_H/1-F_M)$ versus σ^+ , $E = 6.0$ eV.

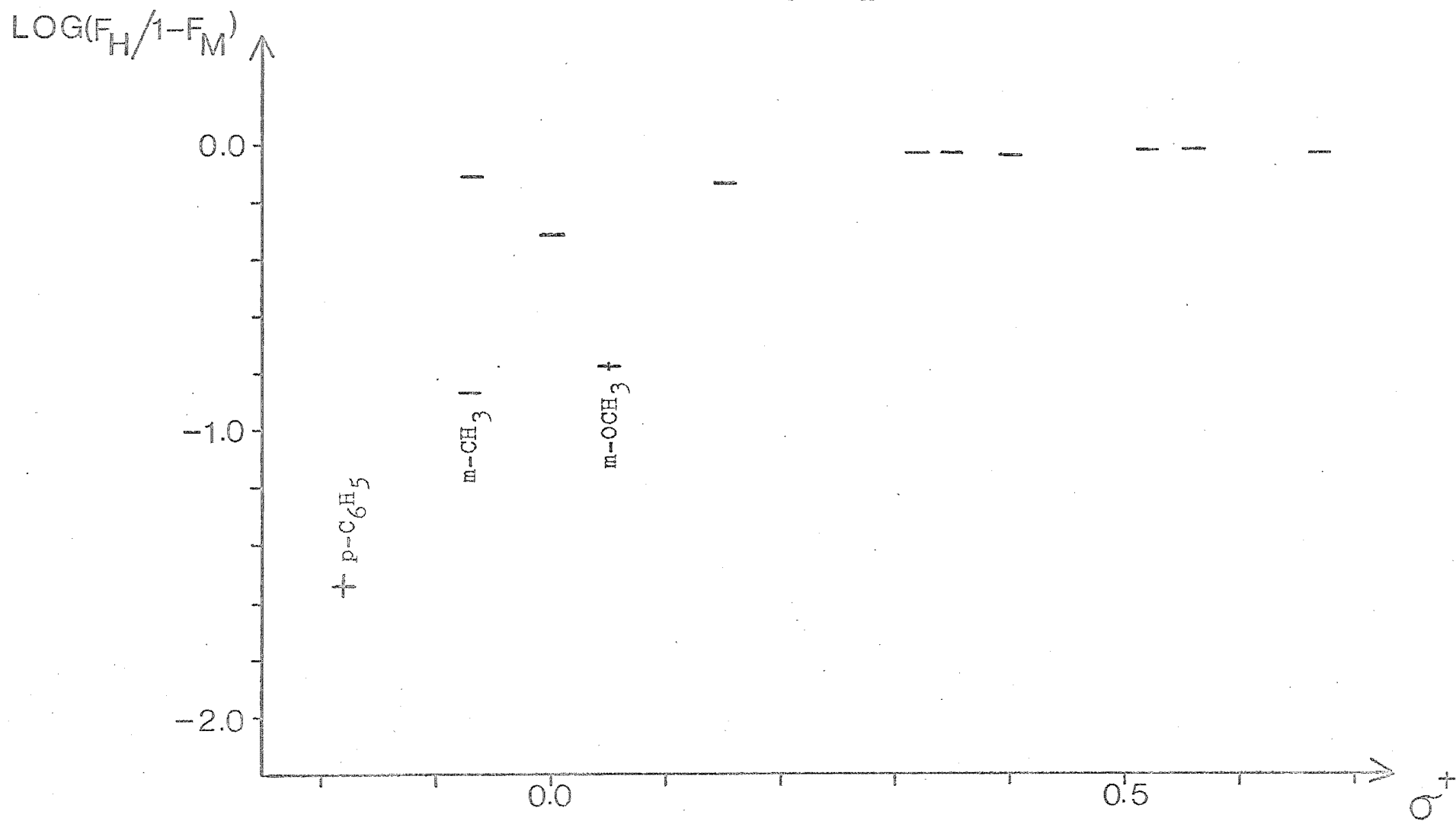


Fig. 28(a). $\text{Log}(F_X/1-F_M)$ versus σ^+ , $E = 6.0 \text{ eV}$.

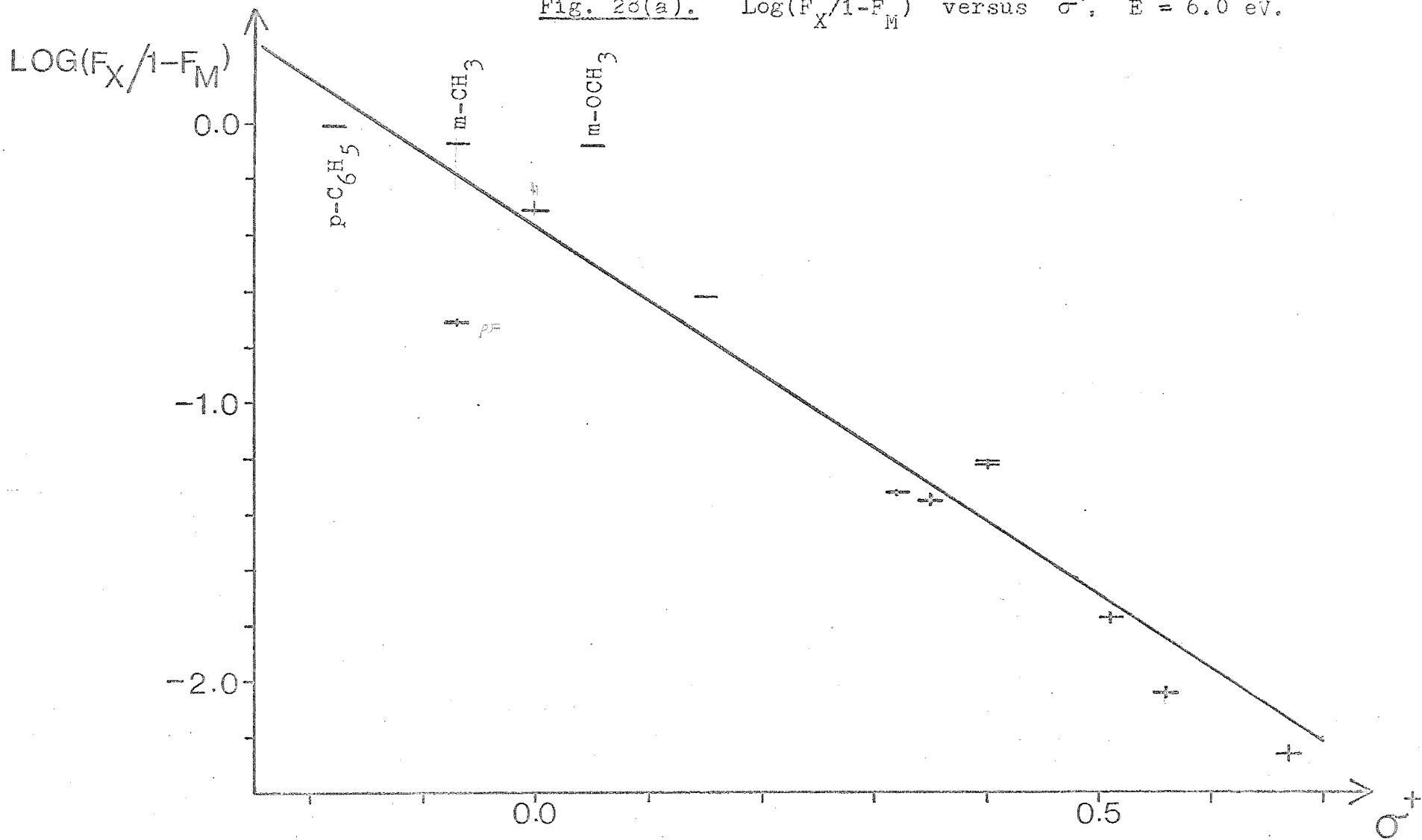
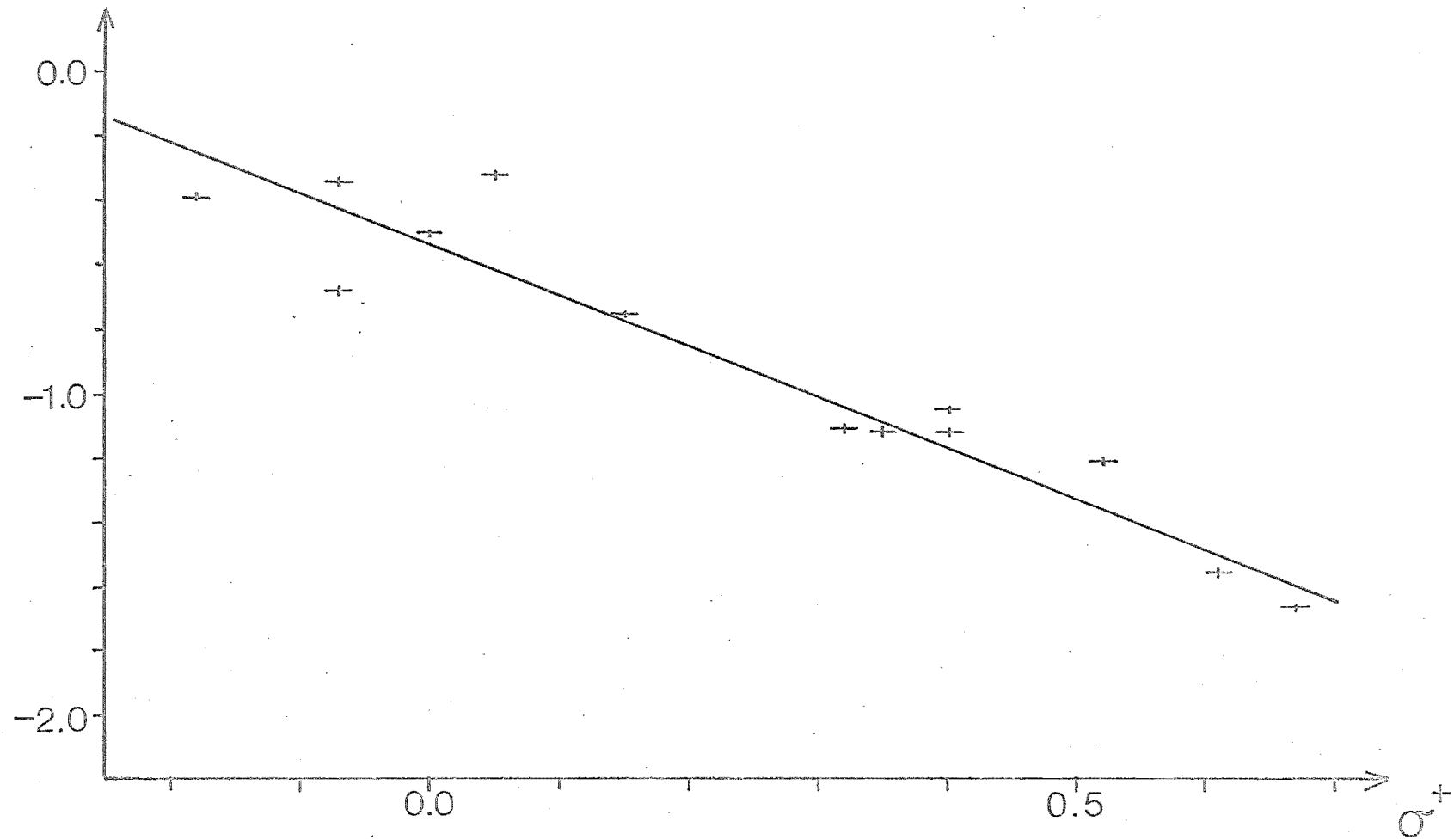


Fig. 28(b). $\text{Log}(F_X/1-F_M)$ versus σ^+ , $V = 70.0$ eV.

$\text{LOG}(F_X/1-F_M)$



more favourable primary fragmentation gives the unsubstituted benzoyl ion, and $\log (F_H/1-F_M)$ is therefore close to zero for all except the *p*-phenyl, *m*-methyl and *m*-methoxy substituents. Again, the apparently fair correlation observed between $\log (F_X/1-F_M)$ and $\sigma^+(\sigma)$ (Table 12(b); Fig. 28(a)) is almost certainly obtained only because of the limited range of $\sigma^+(\sigma)$ values covered by these substituents. If data were available for substituents with large negative σ^+ values (i.e. strongly electron-releasing *para*-substituents), these would have $\log (F_X/1-F_M)$ values close to zero - as observed for the *p*-phenyl, *m*-methyl and *m*-methoxy substituents. This would cause the correlation of $\log (F_X/1-F_M)$ with $\sigma^+(\sigma)$ to show two linear regions - one with zero slope for $\sigma^+ < 0$ and another with negative slope for $\sigma^+ > 0$ (as observed in Fig. 28). A similar effect would be expected to occur in the correlation of $\log (F_H/1-F_M)$ with $\sigma^+(\sigma)$, giving a region of zero slope for $\sigma^+ > 0$ (as observed in Fig. 27) joining a region of positive slope for $\sigma^+ < 0$. The degree of correlation observed at 70 eV is similar to that at low energies (Table 17(a); Fig. 28(b)), indicating that this treatment gives a more reliable measure of substituent effects on fragment ion intensities than does the previous "steady-state" treatment⁶¹. However, these results also show that direct information on the rate of a specific fragmentation reaction cannot be obtained from such intensity ratios, because of the unavoidable effect of competing reactions. For this reason, it is suggested that the satisfactory linear correlation observed between $\log (F(\text{CH}_3\text{CO}^+)/1-F_M)$ and σ for a series of substituted acetophenones⁷ was fortuitous, and obtained only because the CH_3CO^+ ion was always less abundant than the $\text{XC}_6\text{H}_4\text{CO}^+$ ion

formed in competition with it. $\text{Log } (F(\text{XC}_6\text{H}_4\text{CO}^+)/1-F_M)$ for the acetophenones showed practically no variation with change in substituent⁷, further confirmation that this treatment has limited usefulness in analyzing the effects of substituents on ion intensities because it scales all the fragment ion intensities relative to their total intensity. Consequently the most abundant fragment ion generally has a value for $F/1-F_M$ near unity, and variations in its relative intensity for different substituents are masked. Similar conclusions about the limited applicability of this approach for obtaining mechanistic information have been reached by Brown^{121,122}.

(iii) $\text{Log } (F_X/F_H)$:

The ratio of the fragment ion intensities for two competing decompositions of the same molecule-ion is expected to provide a measure of the relative rate constants for the two processes¹¹⁷ - although these "rate constants" again correspond to complicated average values. This intensity ratio should also show the effect of substituents on product ion stability alone - one of the major factors influencing activation energies for ion decompositions⁹ - when the competing decompositions involve the formation of substituted and unsubstituted ions of the same type. This has been demonstrated for the monosubstituted bibenzyl¹¹⁶, benzophenone¹¹⁷ and N,N'-diarylethylenediamine¹¹⁸ series.

The degree of correlation of $\text{log } (F_X/F_H)$ with $\sigma^+(\sigma)$ for the benzils (Table 13; Fig. 29(a)) is only fair (e.g. $r \approx -0.92$, $e \approx 0.5$), and remains about the same at all energies - even at 70 eV (Table 17(a); Fig. 29(b)). The major difference is the increasing magnitude of the negative slope of the regression

Fig. 29(a). $\text{Log}(F_X/F_H)$ versus σ^+ , $E = 6.0 \text{ eV}$.

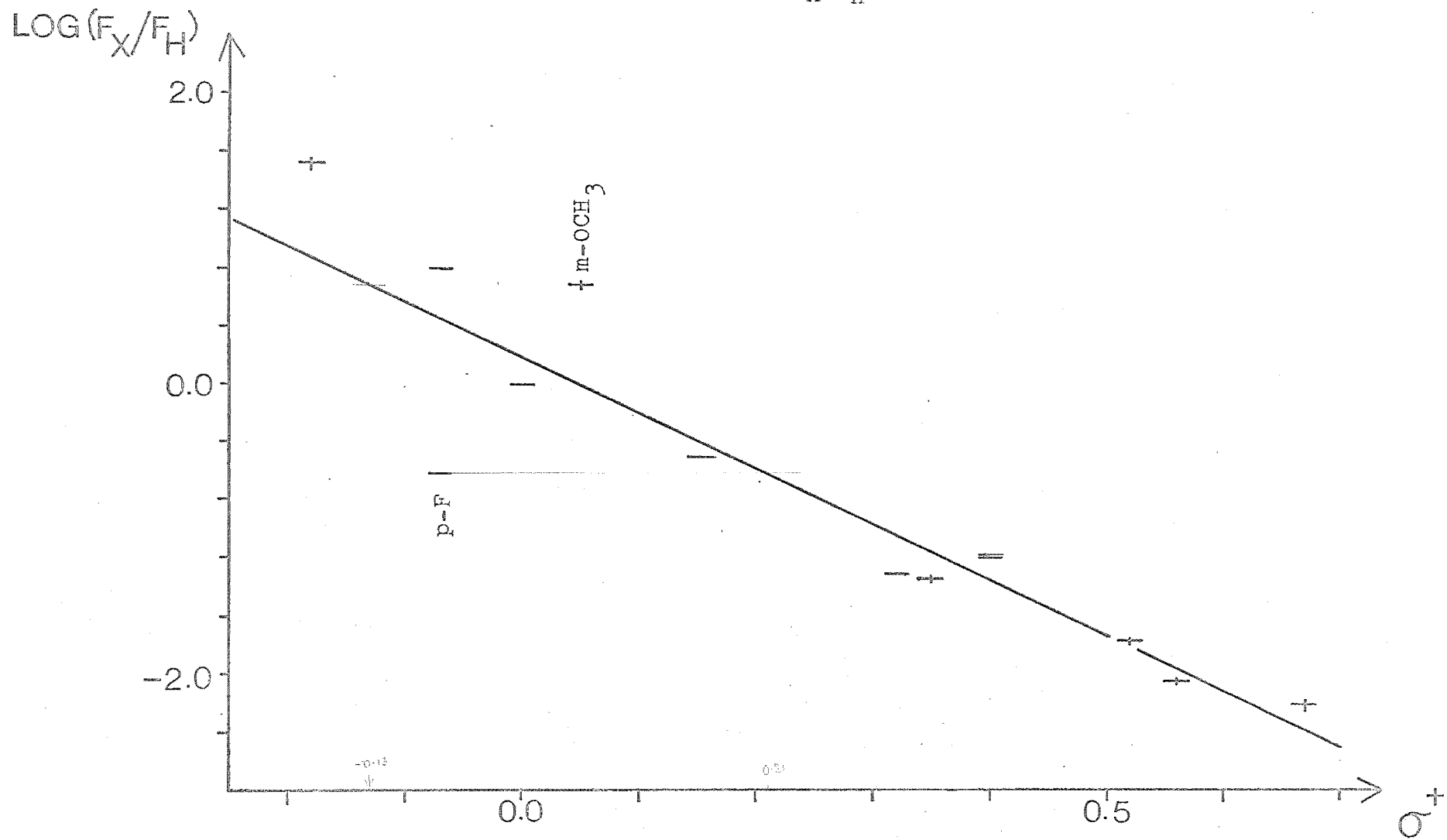
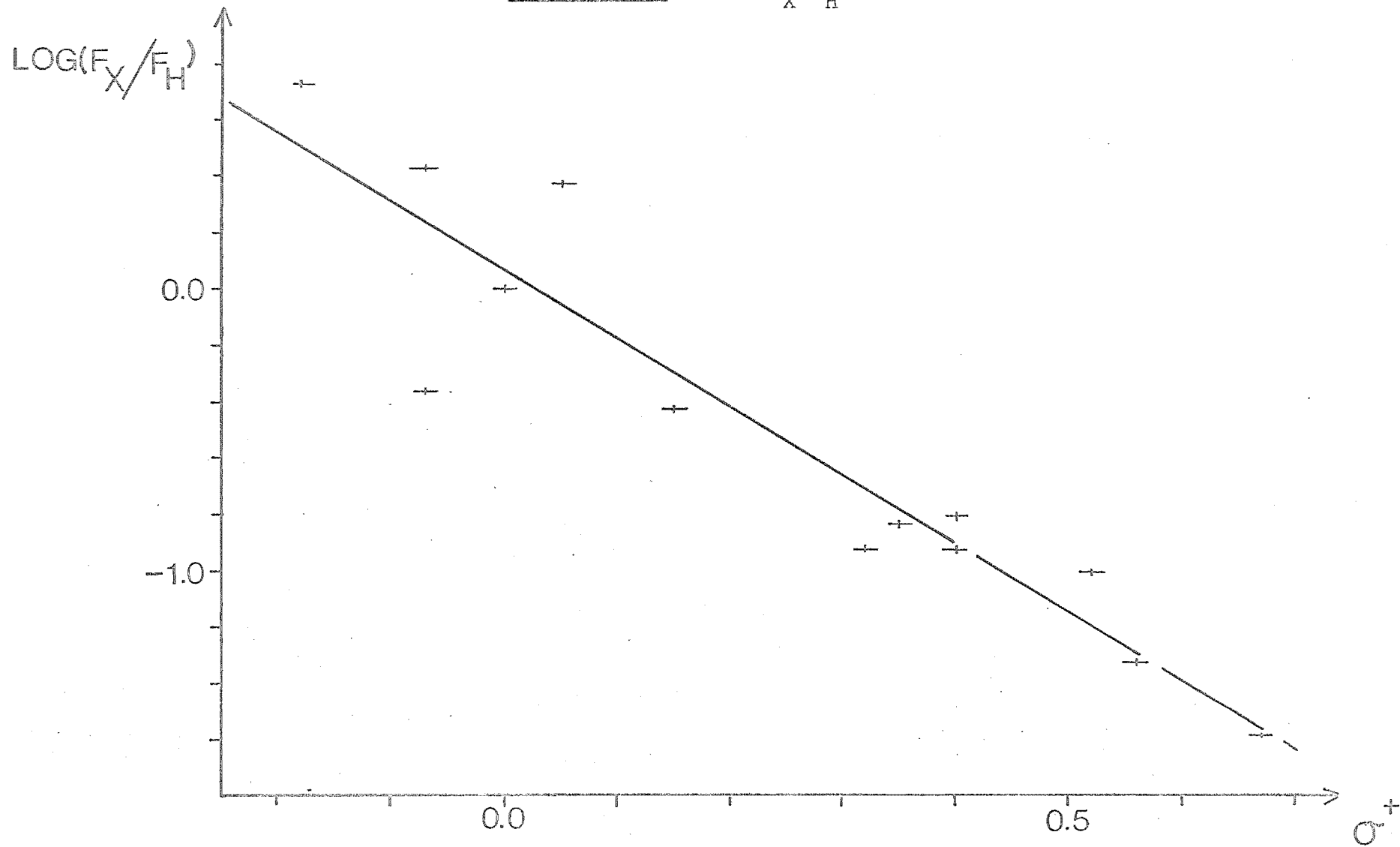


Fig. 29(b). $\text{Log}(F_X/F_H)$ versus σ^+ , $V = 70.0$ eV.



line with decreasing energy (e.g. -2.4 at 70 eV, c.f. -5.8 at $E = 2.0$ eV). These slopes may be compared with those observed for the bibenzyls¹¹⁶ (-3.3 at 15.3 eV), benzophenones¹¹⁷ (-1.5 at 15 eV), and N,N'-diarylethylenediamines¹¹⁸ (-1.0 at 20 eV). In view of the variation of these "ρ-values" with energy, and because the correlations are not of high precision, it would be unwise to draw any conclusions about the respective mechanisms of these mass spectral reactions from such comparisons. However, it may be noted that the substituent effects on the formation of the benzoyl ions from the benzils, as measured by this intensity ratio, are at least as large as those observed for any other mass spectral reactions. A significant improvement in the correlation of $\log (F_X/F_H)$ with substituent constants for the monosubstituted N,N'-diarylethylenediamines was obtained when Taft's σ^0 values¹³⁰ were used ($r = -0.98$, $e = 0.13$) instead of σ ($r = -0.92$, $e = 0.28$) or σ^+ ($r = -0.87$, $e = 0.35$)¹¹⁸. Because very few *para* substituents were available in the benzil series, a similar investigation was not attempted in this work.

Some of the deviations from the regression lines appear to be due to the σ or σ^+ values not correctly describing the effects of substituents on ion stabilities in mass spectral reactions. For example the *m*-methoxy substituent is observed to stabilize the benzoyl ion (relative to the hydrogen substituent), yet it has σ and σ^+ values greater than zero - denoting a destabilizing influence (e.g. Fig. 29). The same stabilizing effect of the *m*-methoxy substituent is observed in the N,N'-diarylethylenediamine series¹¹⁸, and in its effect

on the ionization potentials of various compounds^{7,115,121,122}. Similarly the *p*-fluoro substituent may exhibit a destabilizing effect (e.g. this work and ref. 118) or a slightly stabilizing influence^{8,117}, leading to confusion as to the correct substituent constant to use ($\sigma(p-F) > 0$, $\sigma^+(p-F) < 0$). Although σ^+ values are intuitively expected to be more suitable for mass spectral reactions (because they are derived from reactions which exhibit a similar strong electron demand^{106,107}), they do not necessarily describe the effects of substituents in ion decompositions with the precision required to allow mechanistic conclusions to be drawn from such correlations. It is therefore pertinent to consider the correlations of ion intensity functions with alternative parameters which may more adequately describe the effects of substituents in mass spectral reactions. This is done in the next section.

6.2.5 Correlations of Logarithmic Ion Intensity Ratios with Energy Parameters

The importance of "subdecomposition energy" ions (i.e. ions possessing insufficient energy to decompose^{11,26,59}) in determining the relative intensities of molecule-ions has been stressed by several workers^{7-9,60,63,111}. Howe and Williams recently suggested that $AP_{\min} - IP$ (AP_{\min} is the lowest appearance potential for the fragment ions) would provide a measure of the fraction of such molecule-ions, assuming that the shapes of the internal energy distributions were similar for different molecule-ions^{60,111}. Although this assumption is open to question^{8,124}, they observed that $\log (F/F_M)$ correlated to some extent with $AP - IP$ for the formation of the major

Fig. 30. $\text{Log}(F_H/F_M)$ versus $(AP_H - IP)$, $E = 6.0$ eV.

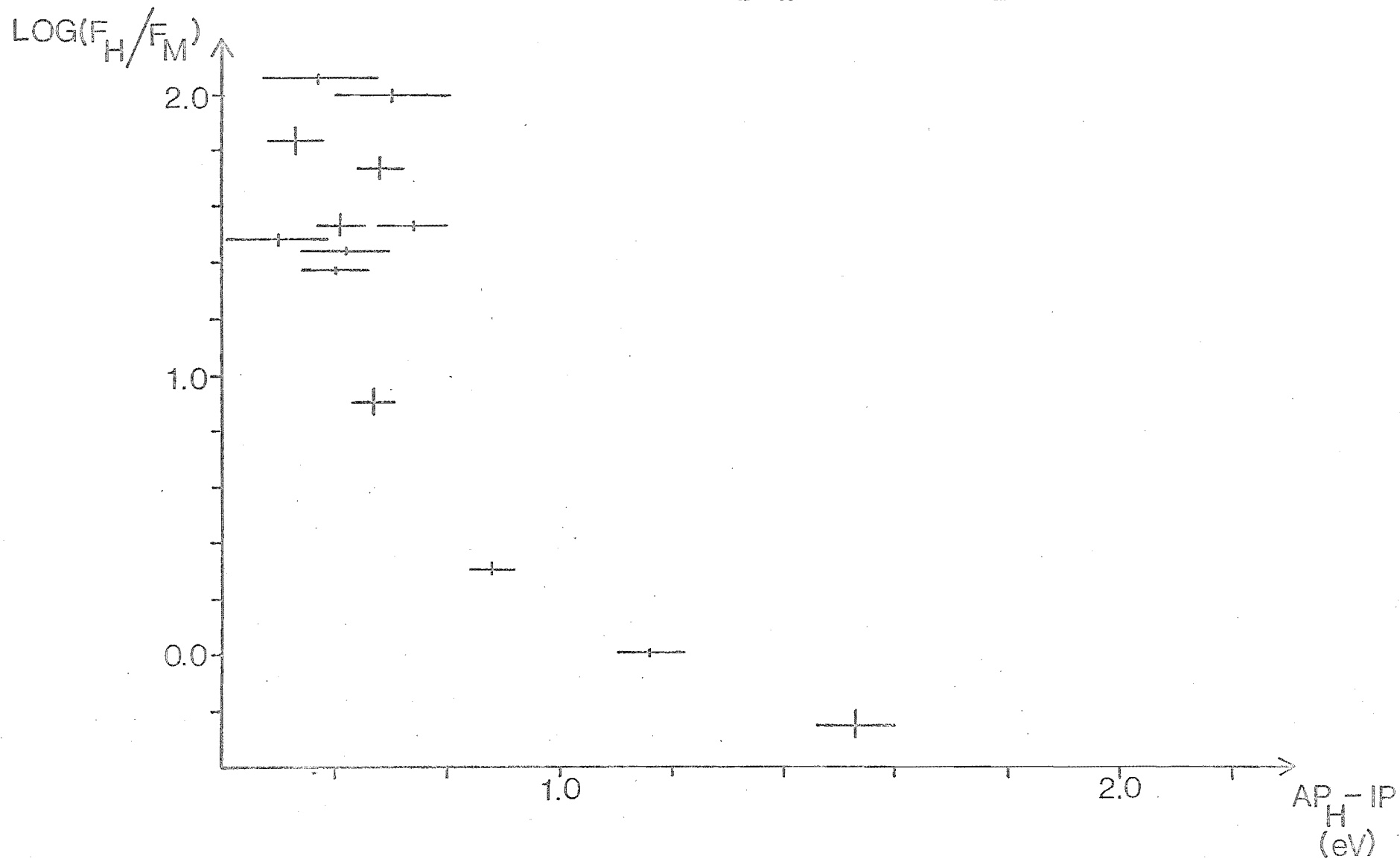
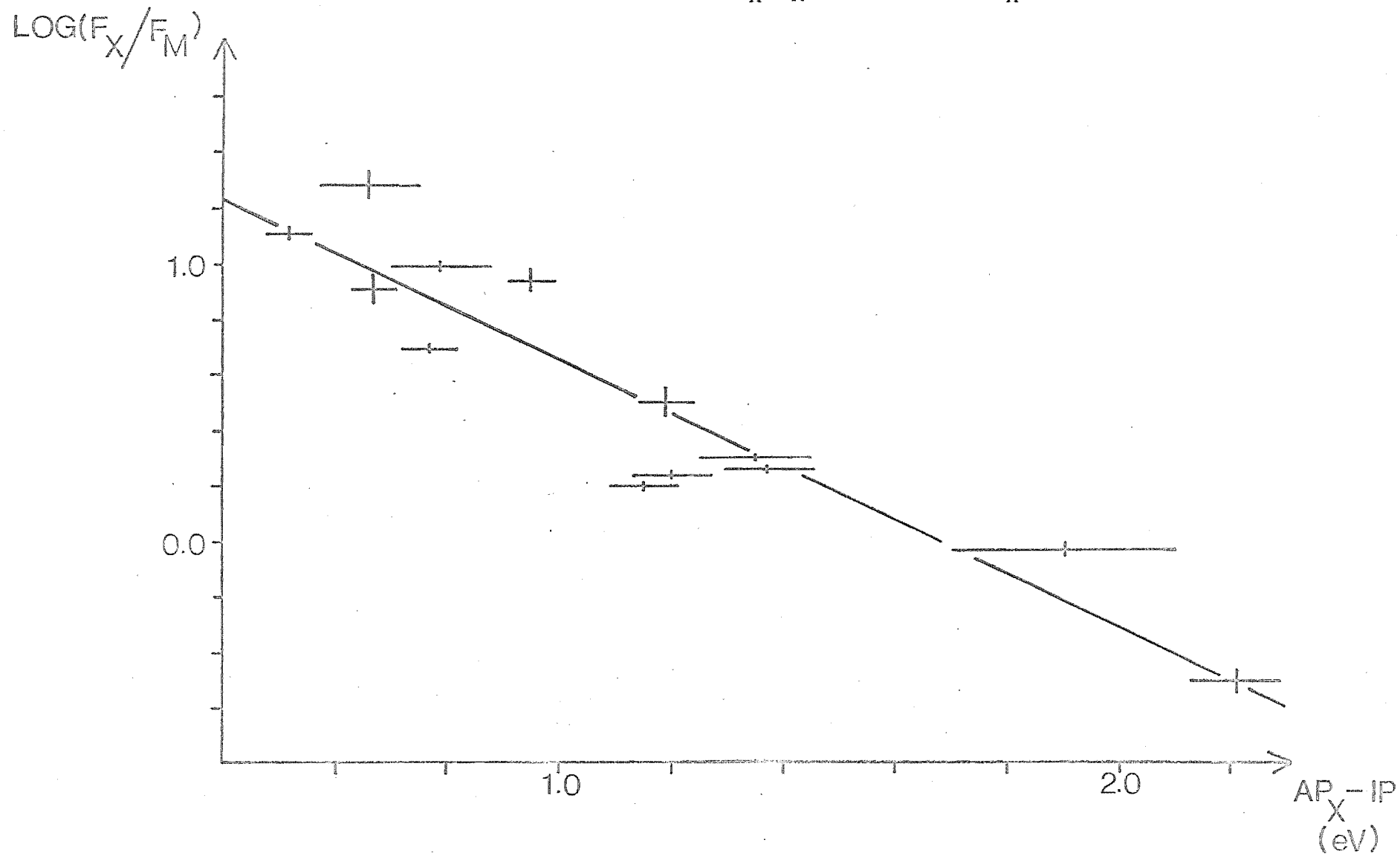


Fig. 31. $\text{Log}(F_X/F_M)$ versus $(AP_X - IP)$, $E = 6.0 \text{ eV}$.



fragment ion from monosubstituted benzenes at low energies (18 eV)⁶⁰. A similar correlation has been observed for the loss of the substituent from *ortho*-substituted thioacetanilides¹²⁵ both of these correlations show the same trend of decreasing $\log (F/F_M)$ with increasing AP-IP, but the standard deviations of the regression lines are high.

Similar results are obtained for the benzil series. The correlation of $\log (F_H/F_M)$ with AP_H -IP (Table 14(a); Fig. 30) is not good ($r = -0.86$, $e = 0.40$) - most of the points are concentrated in a small region of the plot because of the lack of variation in AP_H -IP for most of the substituted benzils (see section 6.2.2). On the other hand $\log (F_X/F_M)$ shows a reasonable correlation with AP_X -IP ($r = -0.94$, $e = 0.19$) (Table 14(b); Fig. 31). It is noticeable that although AP_{min} -IP for the more favourable fragmentation remains fairly constant (about 0.6 eV), the corresponding values of $\log (F/F_M)$ vary significantly (by up to 0.5 log units). The reasons for this are not obvious but may reflect differences in the internal energy distributions of the subdecomposition energy ions, leading to unpredictable variations in the fractional intensities of the molecule-ions. These results indicate that the interpretation of such correlations in terms of simple smoothed energy distributions^{60,111,131} should be treated with caution, particularly since the correlations are not very precise and become much worse at higher energies (see Table 17(b)) - confirming that the relation of fragment ion to molecule-ion intensities is a very complicated one depending on many factors^{59,60}.

Fig. 32. $\text{Log}(F_H/1-F_M)$ versus (AP_H-IP) , $E = 6.0$ eV.

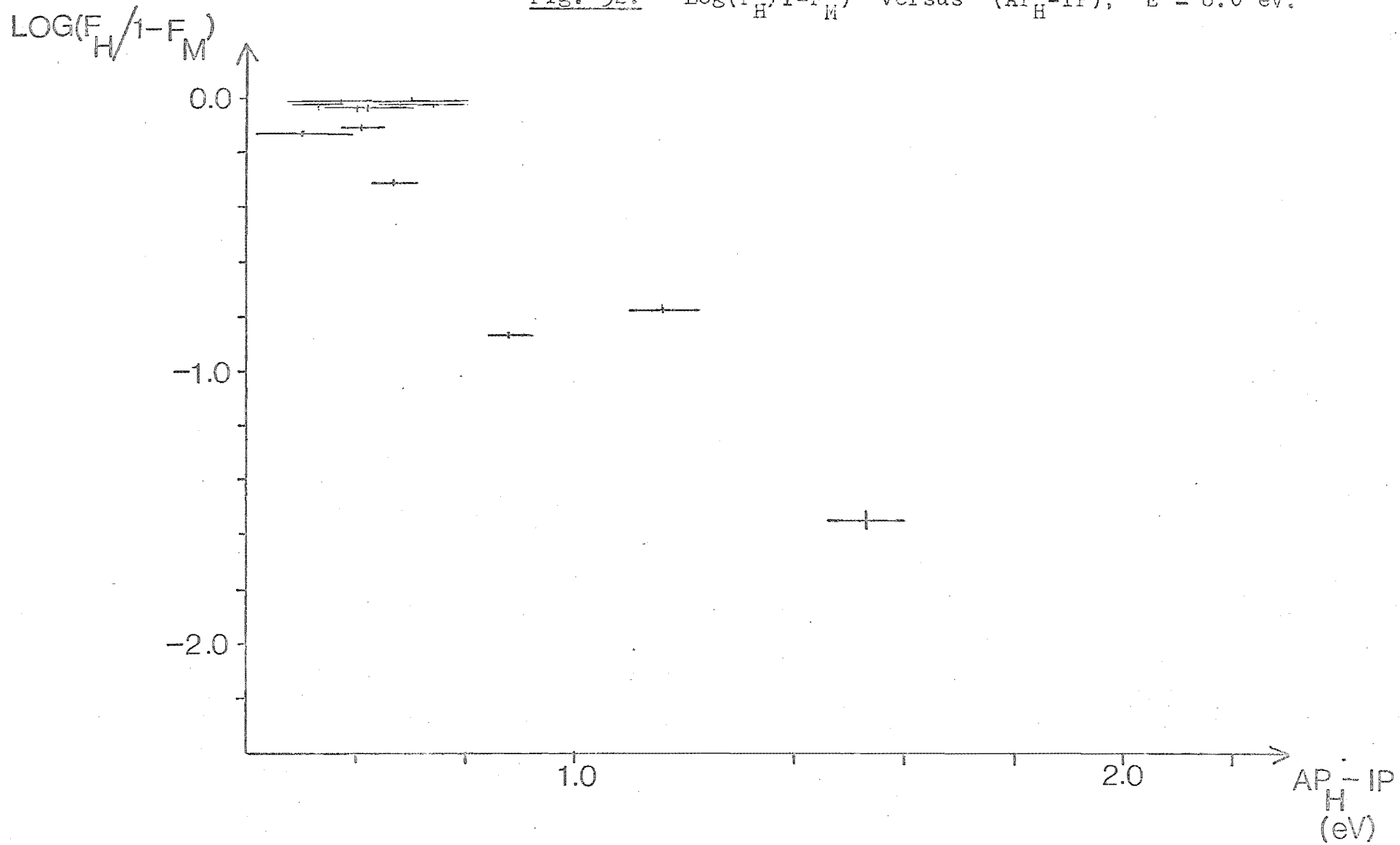
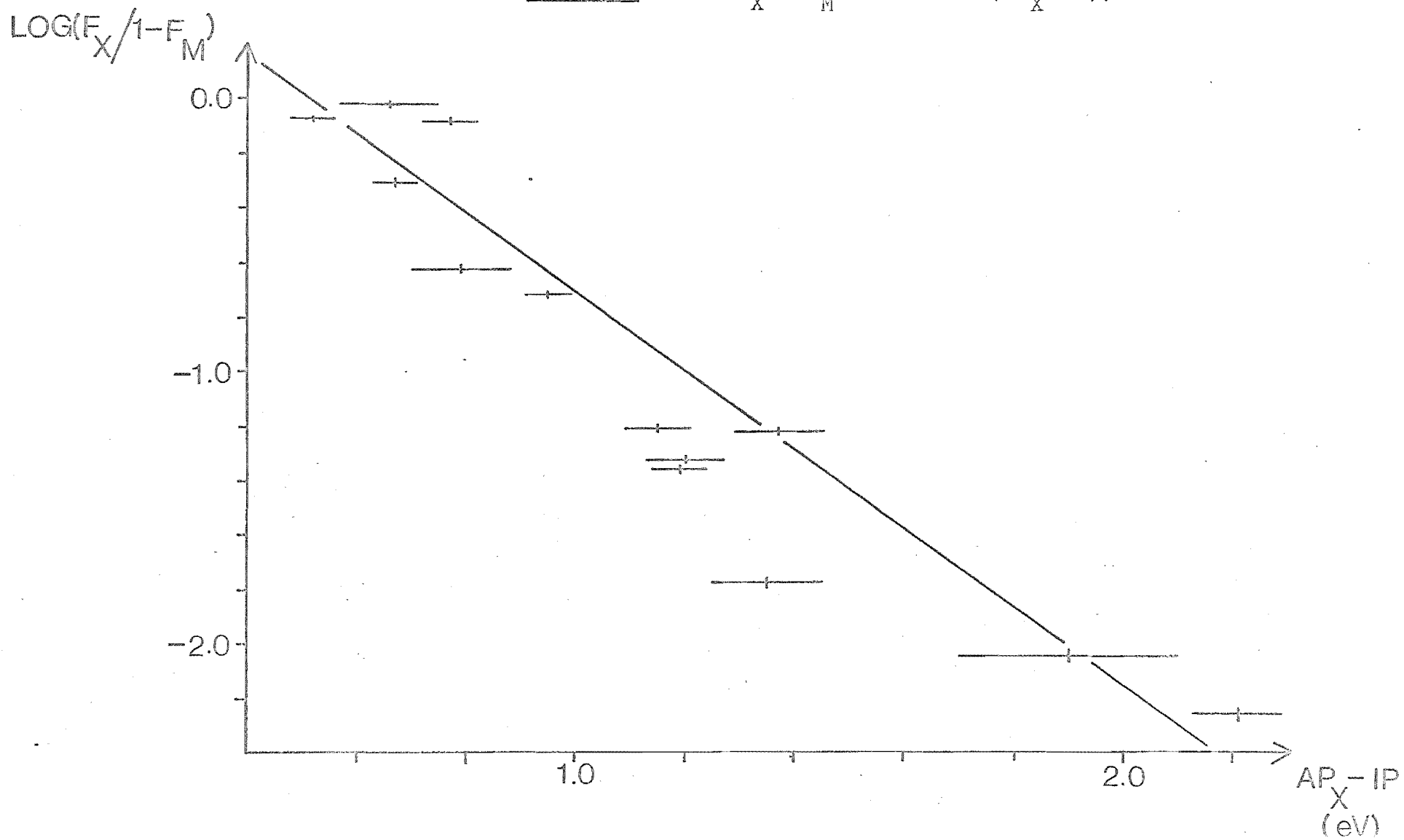


Fig. 33. $\text{Log}(F_X/1-F_M)$ versus (AP_X-IP) , $E = 6.0$ eV.



The correlations of $\log (F_H/1-F_M)$ with AP_H -IP (Table 15(a); Fig. 32) and $\log (F_X/1-F_M)$ with AP_X -IP (Table 15(b); Fig. 33) are quite good ($r \approx -0.94$, $e \approx 0.25$) and give almost identical regression lines, although the small spread of the points in Fig. 32 requires that this be treated with caution. The meaning of these results is not obvious. The intensity ratio, $F/1-F_M$, measures the fraction of the decomposing molecule-ions which form a particular fragment ion, and it might intuitively be expected to be related to the activation energy for the particular fragmentation. However, it was earlier concluded (section 6.2.2) that the quantity AP-IP does not provide a reliable measure of these activation energies; because of the competitive shift effect which can drastically affect the appearance potentials of fragment ions. Some aspects of these correlations may be explained by the special features of the decompositions of the benzils (i.e. competitive formation of only two primary fragment ions). For the more favourable primary fragmentations, AP-IP is approximately constant (see section 6.2.2) and $\log (F/1-F_M)$ is also close to zero (see section 6.2.4 (ii)), so these points are clustered around the same coordinates (0.6, 0.0) of Figs 32 and 33. Hence the similar regression lines observed in each case really reflect the differences between these quantities for the two competing fragmentations.

These considerations therefore suggest that interpretation of the correlation between $\log (F_X/F_H)$ and AP_X-AP_H (Table 16; Fig. 34(a)) might be more significant. Certainly the agreement factors observed for this correlation ($r = -0.98$, $e = 0.25$) are quite good, even at 70 eV (Table 17(b); Fig. 34(b)), and are better than any of the other correlations examined in

Fig. 34(a). $\text{Log}(F_X/F_H)$ versus $(AP_X - AP_H)$, $E = 6.0 \text{ eV}$

$\text{LOG}(F_X/F_H)$

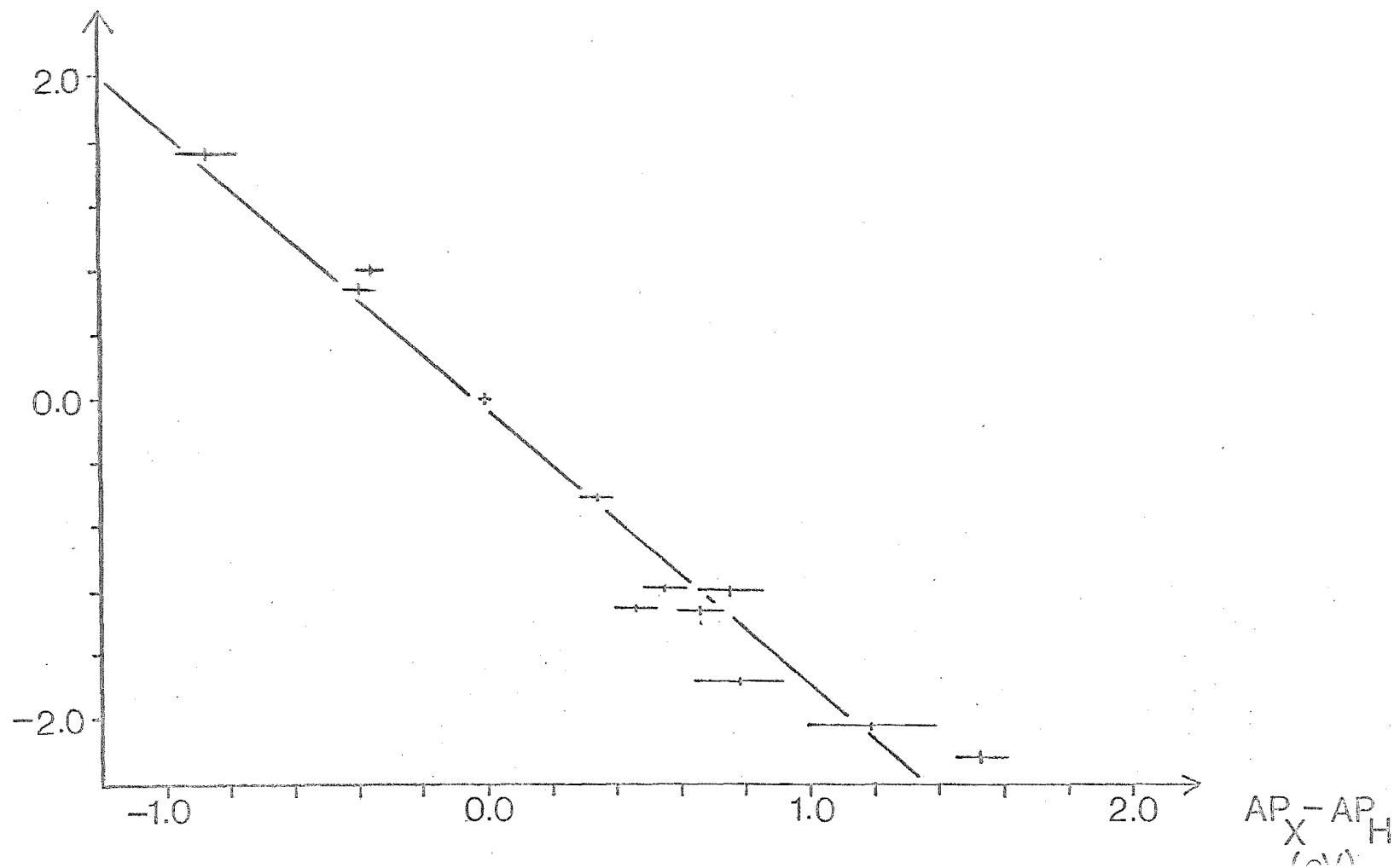
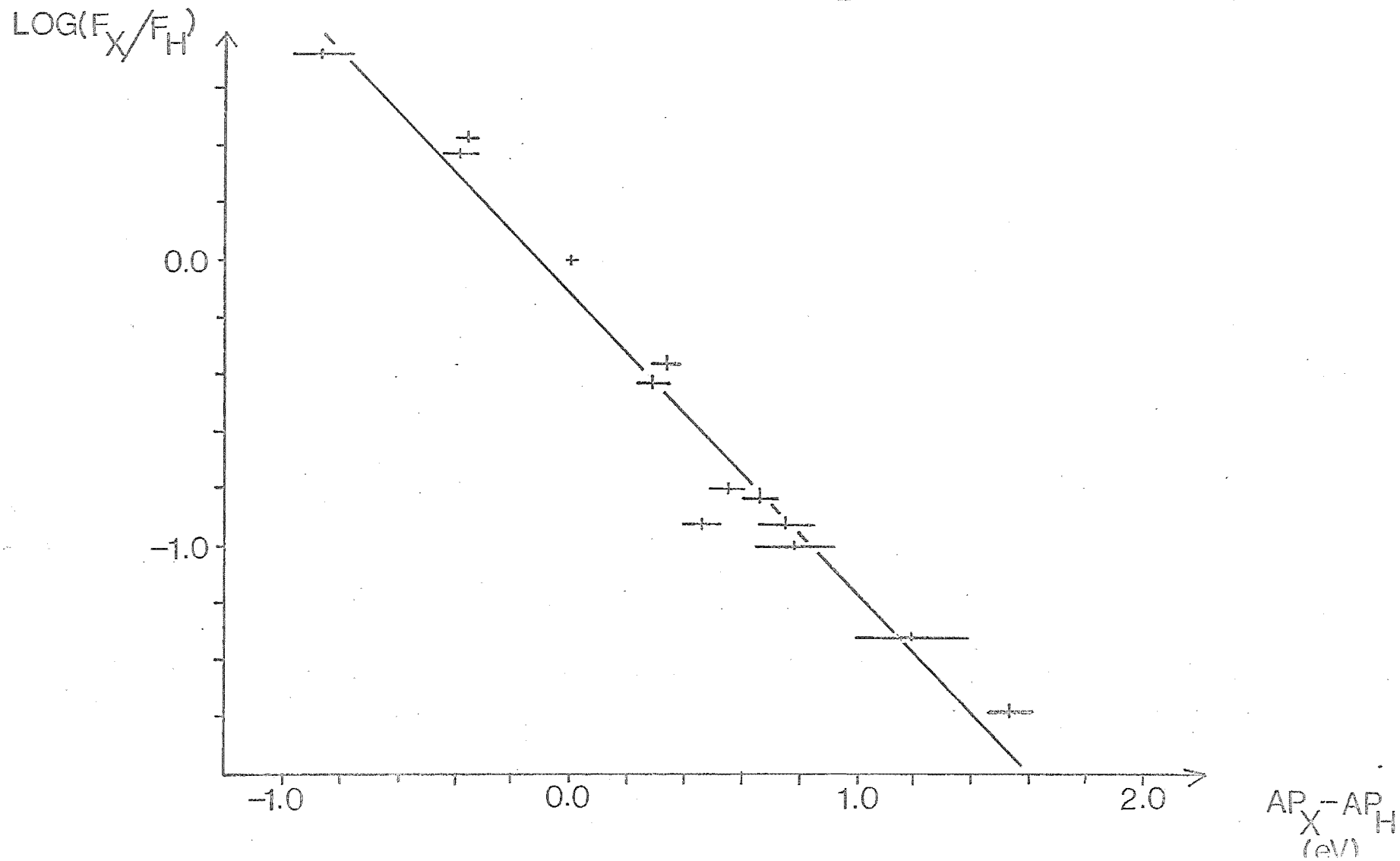


Fig. 34(b). $\text{Log}(F_X/F_H)$ versus $(AP_X - AP_H)$, $V = 70.0$ eV.



this work. The explanation of this result must lie in the fact that both these quantities depend largely on the relative stabilities of the two primary fragment ions. The effect of product ion stability on rate constants is reflected in $\log (F_X/F_H)^{116,117}$, and on the energetics of the competing decompositions of the same molecule-ion in AP_X-AP_H . In view of the earlier conclusions about the probable large competitive shift effect on AP_X-AP_H (section 6.2.2), it would be unwise to extend this argument and suggest that this correlation demonstrates especially the effect of the differences in the activation energies of the competing fragmentations on their relative intensities. Such an argument presumes that the competitive shift effect on AP_X-AP_H is proportional to the activation energy difference, $E_X^0-E_H^0$; this is possible but as yet unproven.

Similar correlations between the relative intensities of fragment ions and their appearance potentials have been observed by other workers^{60,68}, although only in a qualitative fashion, and not with the good precision obtained in this work. This is probably because the special features of the decompositions of the benzils eliminate a number of the other factors, besides ion stability, which can affect the relative intensities of fragment ions (see section 2.3.2). Harrison et al.⁶⁸ note that the differences in the activation energies for competing primary fragmentations are determined by the differences in the ionization potentials of the corresponding free radicals (see equation (33), section 6.2.2). If the ionization potentials of the substituted benzoyl radicals were available, it would be interesting to compare the correlation of $\log (F_X/F_H)$ against AP_X-AP_H with that against $IP(XC_6H_4CO^\bullet)-$

$IP(C_6H_5CO\cdot) = E_X^0 - E_H^0$ (neglecting excess energy terms). This would show whether the variations in $\log (F_X/F_H)$ with change in substituent were in fact due to differences in the activation energies of the corresponding primary decompositions.

The view that $\log (F_X/F_H)$ is determined by the differences in the activation energies is supported by the observation that the absolute magnitude of the slope of the regression line of $\log (F_X/F_H)$ against $AP_X - AP_H$ increases with decreasing energy (Table 16). It changes smoothly from a constant value of -1.6 eV^{-1} at $E = 10.0 - 7.0 \text{ eV}$ to a value of -2.6 eV^{-1} at $E = 2.0 \text{ eV}$. This behaviour is consistent with the increasing importance of the activation energy in determining the relative rate constants for ion decompositions, and hence the relative ion intensities, at low energies (see section 2.2.3).

6.3 CONCLUSION

This work clearly demonstrates that substituents have a strong influence on the mass spectra of the substituted benzils. The relative intensities of the substituted (F_X) and unsubstituted (F_H) benzoyl ions vary by more than a factor of 10^4 with change in substituent. The substituents also have large effects on the energetics of the ion decompositions studied. The appearance potentials of the substituted benzoyl ions (AP_X) differ by up to 2.5 eV, whereas those of the unsubstituted benzoyl ions (AP_H) are almost constant. The variation in the ionization potentials with change in substituent is quite small.

The effects of substituents on both ion intensity and energy parameters can be described with reasonable success

using substituent constants (σ , σ^+) derived from reactions in solution. For example, fair linear correlations of $\log (F_X/F_H)$ and $AP_X - AP_H$ with σ^+ (σ) are obtained, and the signs of the slopes of the regression lines are those expected if the decompositions are controlled by the stabilities of the product ions. Thus F_X/F_H increases, and $AP_X - AP_H$ decreases, with increasing electron-donating ability of the substituent.

However, even in the benzils, with their particularly simple mass spectral behaviour, these results do not give unambiguous information about the effects of substituents on the rate constants for the fragmentation reactions. The benzils were chosen for study because they have the special feature that the benzoyl ions are formed by competing decompositions of the same molecule-ion. This should mean that the major factors determining the benzoyl ion intensities are the rate constants for the competing decompositions, with other factors being less important. This advantage is still a limited one, since their relative intensities depend in a complicated way on the rate constants (averaged over the energy transfer function for the molecule-ion). It is therefore difficult to interpret the effects of substituents on F_X/F_H in terms of specific changes in the activation energies and frequency factors for the competing reactions. A major disadvantage with this approach is that the differences in the activation energies cannot be determined from the differences in the appearance potentials ($AP_X - AP_H$), because the appearance potentials are markedly dependent on the competitive shift. The correlation observed between $AP_X - AP_H$ and σ^+ , for example, appears to be due almost entirely to the competitive shift effect. However, the observed increase in the size of the

substituent effect on F_X/F_H with decreasing energy does suggest that the substituents are affecting the rate constants for the primary decompositions mainly by changing their activation energies.

It is now becoming clear that further progress in this field will require a more rigorous approach based on a detailed analysis of ionization efficiency curves using the quasi-equilibrium theory. To this end, time was spent during this study attempting to obtain reproducible second-derivative ionization efficiency curves which could be compared with theoretically calculated breakdown curves (section 2.2.3). A few intense ions gave satisfactory second-derivative ionization efficiency curves, but in most cases the results were not usable because the signal-to-noise ratio of the ionization efficiency curves was too low. For this reason the work has not been described; the approach should be a useful one if better raw data can be obtained from the MS902. By simulating experimental breakdown curves obtained in this way, it should be possible to derive good estimates of activation energies and frequency factors for the ion decompositions. Another approach, which appears to be capable of providing important information about the dependence of ion decompositions on the internal energy of the molecule-ion, is the determination of mass spectra using the charge-exchange technique^{133,134}.

REFERENCES

1. A. Maccoll, "Modern Aspects of Mass Spectrometry", ed. R.I. Reed, Plenum Press, New York (1968), p.143.
2. A. Maccoll, "Mass Spectrometry", ed. R.I. Reed, Academic Press, London (1965), p.429.
3. L.P. Hammett, "Physical Organic Chemistry", McGraw-Hill, New York (1940), Ch.7.
4. C.D. Ritchie and W.F. Sager, Progr. in Phys. Org. Chem. 2, 323 (1964).
5. G.G. Smith and F.W. Kelley, Prog. in Phys. Org. Chem. 8, 75 (1971).
6. M.M. Bursey, Org. Mass Spectrom. 1, 31 (1968).
7. M.S. Chin and A.G. Harrison, Org. Mass Spectrom. 2, 1073 (1969).
8. F.W. McLafferty et al., J. Am. Chem. Soc. 92, 6867 (1970).
9. F.W. McLafferty, Chem. Commun. 956 (1968).
10. J.H. Beynon, "Mass Spectrometry: Applications to Organic Chemistry", Elsevier, Amsterdam (1960).
11. T.W. Bentley and R.A.W. Johnstone, Adv. in Phys. Org. Chem. 8, 151 (1970).
12. P. Schulze and A.L. Burlingame, J. Chem. Phys. 49, 4870 (1968).
13. W.A. Chupka, J. Chem. Phys. 30, 191 (1959).
14. J.H. Beynon and A.E. Fontaine, Z. Naturforsch. 22a, 334 (1967).
15. J.A. Hipple and E.U. Condon, Phys. Rev. 68, 54 (1945).
16. J.H. Beynon, Advances in Mass Spectrometry, ed. E. Kendrick, Institute of Petroleum, London, 4, 123 (1968).

17. M. Barber and R.M. Elliott, 12th Annual ASTM-E14 Conference on Mass Spectrometry, Pittsburgh, Pa., May (1968).
18. J.E. Coutant and F.W. McLafferty, Int. J. Mass Spectrom. Ion Phys. 8, 323 (1972).
19. H.M. Rosenstock and M. Krauss, "Mass Spectrometry of Organic Ions", Ed. F.W. McLafferty, Academic Press, New York, (1963), p.1.
20. M. Krauss and V.H. Dibeler, *ibid*, p.117 (1963).
21. M.E. Wacks, "Modern Aspects of Mass Spectrometry", ed. R.I. Reed, Plenum Press, New York (1968), p.323.
22. J.E. Collin, "Modern Aspects of Mass Spectrometry", ed. R.I. Reed, Plenum Press, New York (1968), p.231.
23. A.L. Wahraftig, "Mass Spectrometry", ed. R.I. Reed, Academic Press, New York (1965), p.137.
24. F.W. McLafferty, "Topics in Mass Spectrometry", ed. A.L. Burlingame, Wiley-Interscience, New York (1970), p.223.
25. A.G. Harrison, "Topics in Mass Spectrometry", ed. A.L. Burlingame, Wiley-Interscience, New York (1970), p.121.
26. R.G. Cooks, I. Howe and D.H. Williams, Org. Mass Spectrom. 2, 137 (1969).
27. D.H. Williams, Advances in Mass Spectrometry, ed. A. Quayle, Institute of Petroleum, London, 5, 569 (1971).
28. R.S. Berry, J. Chem. Phys. 26, 714 (1957).
29. R.S. Berry, Rec. Chem. Progress 31, 9 (1970).
30. J.D. Morrison, J. Chem. Phys. 34, 578 (1961).
31. J. Jortner, S.A. Rice and R.M. Hochstrasser, Advances in Photochem. 7, 149 (1969).
32. H.M. Rosenstock, M.B. Wallenstein, A.L. Wahraftig, and H. Eyring, Proc. Natl. Acad. Sci. U.S. 38, 667 (1952);

33. H.M. Rosenstock, *Advances in Mass Spectrometry*, ed. E. Kendrick, Institute of Petroleum, London, 4, 523 (1968).
34. R.C. Tolman, "Principles of Statistical Mechanics", Oxford University Press, London (1938), pp.56, 345, 486.
35. N.B. Slater, "Theory of Unimolecular Reactions", Cornell University Press, New York (1959).
36. L.S. Kassel, "Kinetics of Homogeneous Gas Kinetics", Chemical Catalog Co., New York (1932).
37. R.A. Marcus, *J. Chem. Phys.* 43, 2658 (1965).
38. R.A. Marcus and O.K. Rice, *J. Phys. and Colloid Chem.* 55, 894 (1951).
39. S. Glasstone, K.H. Laidler and H. Eyring, "The Theory of Rate Processes", McGraw-Hill, New York (1941).
40. F.H. Mies and M. Krauss, *J. Chem. Phys.* 45, 4455 (1966).
41. F.H. Mies, *J. Chem. Phys.* 51, 787 (1969).
42. R.D. Levine, *J. Chem. Phys.* 44, 2046 (1966).
43. W. Forst, *Chem. Rev.* 71, 339 (1971).
44. M. Wolfsberg, *J. Chem. Phys.* 36, 1072 (1962).
45. P.F. Newstubb, *Int. J. Mass Spectrom. & Ion Phys.* 6, 217, 229 (1971).
46. W.A. Chupka, *J. Chem. Phys.* 30, 191 (1959).
47. C. Lifshitz and F.A. Long, *J. Chem. Phys.* 41, 2468 (1964).
48. L.P. Hills, J.H. Futrell and A.L. Wahraftig, *J. Chem. Phys.* 51, 5255 (1969).
49. B. Steiner, C.F. Giese and M.G. Inghram, *J. Chem. Phys.* 34, 189 (1961).
50. F.H. Dorman and J.D. Morrison, *J. Chem. Phys.* 34, 578, 1407 (1961).
51. S. Geltman, *Phys. Rev.* 102, 171 (1956).

52. J.D. Morrison, J. Chem. Phys. 21, 1767 (1953).
53. J.D. Morrison, J. Chem. Phys. 39, 200 (1963).
54. W.A. Chupka, J. Chem. Phys. 54, 1936 (1971).
55. M.L. Vestal, J. Chem. Phys. 43, 1356 (1965).
56. B.S. Rabinovitch and D.W. Setser, Advances in Photochem. 3, 1 (1964).
57. D.L. Bunker and M.D. Pattengill, J. Chem. Phys. 48, 772 (1968).
58. F.W. McLafferty, Anal. Chem. 31, 477 (1959).
59. I. Howe, Mass Spectrometry, The Chemical Society, 1, 31 (1971).
60. I. Howe and D.H. Williams, J. Am. Chem. Soc. 91, 7137 (1969).
61. M.M. Bursley and F.W. McLafferty, J. Am. Chem. Soc. 88, 529, 4484 (1966); 89, 1 (1967).
62. T.W. Bentley, R.A.W. Johnstone and D.W. Payling, J. Am. Chem. Soc. 91, 3978 (1969).
63. R.S. Ward, R.G. Cooks and D.H. Williams, J. Am. Chem. Soc. 91, 2727 (1968).
64. A.D. Baker, D.P. May and D.W. Turner, J. Chem. Soc. (B), 22 (1968).
65. H. Ehrhardt, F. Linder and T. Tekaat, Advances in Mass Spectrometry, ed. E. Kendrick, Institute of Petroleum, London, 4, 705 (1968).
66. M.L. Vestal, J. Chem. Phys. 43, 1356 (1965).
67. M.B. Wallenstein and M. Krauss, J. Chem. Phys. 34, 929 (1961).
68. A.G. Harrison, C.D. Finney and J.A. Sherk, Org. Mass Spectrom. 5, 1313 (1971).
69. O.K. Rice, J. Phys. Chem. 65, 1588 (1961).

70. W.A. Chupka and M. Kaminsky, J. Chem. Phys. 35, 1991 (1965).
71. Handbook of Chemistry and Physics, 48th Ed. (1967).
72. J. Cason and H. Rapoport, "Laboratory Text in Organic Chemistry", 2nd Ed. (1962), p.415.
73. L.F. Fieser, "Experiments in Organic Chemistry", 2nd Ed., p.361 (1941).
74. S.S. Jenkins, J. Am. Chem. Soc. 55, 703 (1933).
75. R.R. Otter and R.L. Shriner, J. Am. Chem. Soc. 73, 889 (1951).
76. A. Jart, Acta polytech. Scand., Ser. A 42, 1 (1965).
77. A.I. Vogel, "Practical Organic Chemistry", 3rd Ed. (1956), p.758.
78. D.E. Pearson, W.E. Stamper and B.R. Suthers, J. Org. Chem. 28, 3149 (1963).
79. L. Friedman and H. Shechter, J. Org. Chem. 26, 2522 (1961).
80. Chem. Abs. 61, 9418f (1964).
81. Organic Syntheses, Coll. Vol. 3, 627 (1955).
82. C.H. Dahl and K.G. Lewis, Austr. J. Chem. 18, 1307 (1965).
83. Beilstein's Handbuch der Organischen Chemie, E I 137 (1942).
84. C.V. Ferris and E.E. Turner, J. Chem. Soc. 1149 (1920).
85. E.H. Corey and J.P. Schaefer, J. Am. Chem. Soc. 82, 928 (1960).
86. M.T. Clark, E.C. Hendley and O.K. Neville, J. Am. Chem. Soc. 77, 3283 (1955).
87. G.G. Smith and G.O. Larson, J. Am. Chem. Soc. 82, 104 (1960).
88. H.H. Hatt, A. Pilgrim and W.J. Hurran, J. Chem. Soc. 94 (1936).
89. A. Fischer, B.A. Grigor, J. Packer and J. Vaughan, J. Am.

- Chem. Soc. 83, 4208 (1961).
90. F.D. Chattaway and E.A. Coulson, J. Chem. Soc. 1084 (1928).
 91. T. Sigmond and R.S. Sigmond, A.E.I. 7th Users Conference (1967), p.31.
 92. J.D. Morrison, Rev. Pure and Applied Chem. 5, 22 (1955).
 93. A.J.C. Nicholson, J. Chem. Phys. 29, 1312 (1958).
 94. C. La Lau, "Topics in Mass Spectrometry", ed. A.L. Burlingame, Wiley-Interscience, New York (1970), p.93.
 95. R.G. Dromey, J.C. Traeger and J.D. Morrison, Int. J. Mass Spectrom. Ion Phys. 6, 57 (1971).
 96. J.E. Collin, "Mass Spectrometry", ed. R.I. Reed, Academic Press, New York (1965), p.183, 201.
 97. H.D. Smyth, Proc. Roy. Soc. (London) A102, 283 (1922).
 98. J.W. Warren, Nature 165, 810 (1950).
 99. R.E. Honig, J. Chem. Phys. 16, 105 (1948).
 100. F.P. Lossing, A.W. Tickner and W.A. Bryce, J. Chem. Phys. 19, 1254 (1951).
 101. V.H. Dibeler and R.M. Reese, J. Res. Natl. Bur. Stand. 54, 127 (1955).
 102. W.C. Hamilton, "Statistics in Physical Science", Ronald Press, New York, (a) p.33, (b) p.42, (c) p.124, 150 (1964).
 103. W.R. Busing and H.A. Levy, "ORGLS, A General Fortran Least Squares Program", Oak Ridge National Laboratory - U.S.A.E.C., ORNL-TM-271 (1962).
 104. A. Savitzky and M.J. Golay, Anal. Chem. 36, 1627 (1964).
 105. J.S. Rollet (Ed.), "Computing Methods in Crystallography", Pergamon Press (1965), p.20.

106. H.C. Brown, *J. Org. Chem.* 23, 420 (1958).
107. H.C. Brown and Y. Okamoto, *J. Am. Chem. Soc.* 80, 4979 (1958).
108. F.W. McLafferty and M.M. Bursey, *J. Org. Chem.* 33, 124 (1968).
109. J.L. Cotter, *J. Chem. Soc. (B)*, 1162 (1967).
- 110.⁶ R.H. Shapiro and J.W. Serum, *Org. Mass Spectrom.* 2, 533 (1969).
- 111.⁷ I. Howe and D.H. Williams, *J. Am. Chem. Soc.* 90, 5461 (1968).
112. G.F. Crable and G.L. Kearns, *J. Phys. Chem.* 66, 436 (1962).
113. A. Buchs, G.P. Rossetti and B.P. Susz, *Helv. Chim. Acta* 47, 1563 (1964).
114. A. Foffani, S. Pignataro, B. Cantone and F. Grasso, *Z. Physik. Chem. (Frankfurt)* 42, 221 (1964).
- 115.¹⁰ S. Pignataro, A. Foffani, G. Inorta and G. Distefano, *Z. Physik. Chem. (Frankfurt)* 49, 291 (1966).
116. M.M. Bursey and F.W. McLafferty, *J. Am. Chem. Soc.* 90, 5299 (1968).
- 117.¹⁷ N. Einolf and B. Munson, *Org. Mass Spectrom.* 5, 397 (1971).
118. H. Giezendanner, M. Hesse and H. Schmid, *Org. Mass Spectrom.* 4, 405 (1970).
- 119.¹⁹ R.A.W. Johnstone and D.W. Payling, *Chem. Commun.* 601 (1968).
120. P. Brown, *Org. Mass Spectrom.* 3, 639 (1970).
121. } P. Brown, *Org. Mass Spectrom.* 4, 519 (1970).
122. } P. Brown, *Org. Mass Spectrom.* 4, 533 (1970).

- 123.9 R.H. Shapiro, J. Turk and J.W. Serum, *Org. Mass Spectrom.* 3, 171 (1970).
- 124.20 J. Turk and R.H. Shapiro, *Org. Mass Spectrom.* 6, 189 (1972).
- 125.91 M.A. Baldwin and A.G. Loudon, *Org. Mass Spectrom.* 2, 549 (1969).
126. P. Brown, *Org. Mass Spectrom.* 3, 1175 (1970).
- 127.92 A.G. Harrison, P. Kebarle and F.P. Lossing, *J. Am. Chem. Soc.* 83, 777 (1961).
128. T.L. Cottrell, "The Strength of Chemical Bonds", 2nd Ed., Butterworths, London (1958).
129. H.v. Bekkum, P.E. Verkade and B.M. Webster, *Rec. Trav. Chim. (Pays-Bas)* 78, 815 (1959).
130. R.W. Taft, *J. Phys. Chem.* 64, 1805 (1960).
131. R.P. Buck and M.M. Bursey, *Org. Mass Spectrom.* 3, 387 (1970).
132. R.D. Hickling and K.R. Jennings, *Org. Mass Spectrom.* 3, 1499 (1970).
133. J. Turk and R.H. Shapiro, *Org. Mass Spectrom.* 6, 189 (1972).
134. B. Andlauer and Ch. Ottinger, *J. Chem. Phys.* 55, 1471 (1971).
135. A. Causer, "PLOTAA Subroutines for the 1627 Plotter", *Memo. University of Canterbury Computer Centre* (1970).

APPENDIX ACOMPUTER PROGRAMS

Listings of the computer programs used extensively in this work are given below. They are written in the Fortran IV language, and were executed on an IBM System 360/Model 44 computer. Plots were drawn by an IBM 1620 computer with a Calcomp 1627 X-Y plotter attachment, using the PLOTAA subroutine package¹³⁵.

SMOOTH

```

SUBROUTINE SMOOTH(ORDER,MPT,MSTOP)
C
C SUBPROGRAM FOR QUADRATIC SMOOTHING OF DATA
C
COMMON /WORK/ Y(1024),X(1024)
REAL P(50)
C
C UNSMOOTHED DATA STORED IN ARRAY 'Y', AND REPLACED BY SMOOTHED DATA
C (STORED IN ARRAY 'X' DURING SMOOTHING PROCESS)
C
C INPUT PARAMETERS -
C
C ORDER = ORDER OF DERIVATIVE TO BE CALCULATED (0-2)
C MPT = NUMBER OF POINTS IN QUADRATIC SMOOTHING FUNCTION. SMOOTHED
C DATA VALUES ARE CALCULATED FROM (2*MPT+1) ORIGINAL
C POINTS
C MSTOP = NUMBER OF UNSMOOTHED DATA POINTS
C
IF(MPT.LT.2) GO TO 170
I1=MPT+1
I2=MSTOP-MPT
C CALCULATE QUADRATIC SMOOTHING FUNCTION AND STORE IN ARRAY 'P'
S0=MPT+MPT+1
S2=1.
S4=1.
DO 20 I=2,MPT
S=I*I
S2=S2+S
20 S4=S4+S*S
S2=S2*2.
S4=S4*2.
SNORM=S0*S4-S2*S2
IF(ORDER-1) 30,40,50
30 P0=S4/SNORM
DO 40 I=1,MPT
40 P(I)=(S4-S2*I*I)/SNORM
GO TO 70
50 P0=-S2/SNORM
DO 60 I=1,MPT
60 P(I)=(S0*I*I-S2)/SNORM
C CALCULATE SMOOTHED DATA VALUES
70 DO 80 I=I1,I2
X(I)=P0*Y(I)
DO 80 J=1,MPT
80 X(I)=X(I)+P(J)*(Y(I+J)+Y(I-J))
GO TO 150
90 X(I1)=0.
DO 100 J=1,MPT
100 X(I1)=X(I1)+J*(Y(I1+J)-Y(I1-J))
K1=I1+1
J1=1
J2=MPT+MPT
DO 120 I=K1,I2
J1=J1+1
J2=J2+1
X(I)=X(I-1)+MPT*(Y(J1-1)+Y(J2+1))
DO 120 J=J1,J2
120 X(I)=X(I)-Y(J)
DO 140 I=I1,I2
140 X(I)=X(I)/S2
C REPLACE UNSMOOTHED DATA BY SMOOTHED DATA
150 DO 160 I=I1,I2
160 Y(I)=X(I)
WRITE(6,99) ORDER,S0
GO TO 200
170 WRITE(6,98) MPT
200 RETURN
99 FORMAT(//IX,'LENGTH OF INTERVAL FOR QUADRATIC SMOOTHING OF',I3,'-1
ORDER DERIVATIVE =',F5.0,' POINTS')
98 FORMAT(//IX,'VALUE OF MPT=',I3,' IS INSUFFICIENT FOR QUADRATIC S
MOOTHING OF DATA')
END

```

LINEAR

SUBROUTINE LINEAR(NSTART,NLINE,IFWT,IFNPT)

SUBPROGRAM TO FIT A STRAIGHT LINE TO AN INTERVAL OF DATA BY LINEAR LEAST SQUARES.

COMMON /WORK/ Y(1024),X(1024),W(1024)
COMMON /LINPAR/ CONST,SLOPE,ESDC,ESDS,ESD,CORR
DOUBLE PRECISION WW,WX,WY,SW,SX,SY,SXX,SYY,SXY,DX,DY,XI,YI

OBSERVED DEPENDENT VARIABLE (ORDINATE) STORED IN ARRAY 'Y',
INDEPENDENT VARIABLE (ABSCISSA) IN ARRAY 'X', WEIGHTING FACTORS
(IF USED) IN ARRAY 'W'.

INPUT PARAMETERS -

NSTART = I1-1, WHERE I1 IS THE FIRST POINT OF THE INTERVAL.
NLINE = NUMBER OF POINTS IN THE INTERVAL.
IFWT = WEIGHT INDICATOR - ZERO IF UNIT WEIGHTS TO BE USED,
NON-ZERO IF WEIGHTS TO BE USED.
IFNPT = ERROR INDICATOR - 1 IF NUMBER OF DEGREES OF FREEDOM
(DOF) IS LESS THAN ONE, 0 OTHERWISE

OUTPUT PARAMETERS -

CONST = INTERCEPT OF REGRESSION LINE, ESDC = E.S.D.
SLOPE = GRADIENT OF REGRESSION LINE, ESDS = E.S.D.
ESD = STANDARD DEVIATION OF REGRESSION.
CORR = LINEAR CORRELATION COEFFICIENT OF REGRESSION.

I1=NSTART+1
I2=NSTART+NLINE

DOF=-2.

WW=1.

SW=0.

SX=0.

SY=0.

SXX=0.

SYY=0.

SXY=0.

DO 40 I=I1,I2

XI=X(I)

YI=Y(I)

CALCULATE WEIGHTED VALUES OF DATA.

IF(IFWT.NE.0) GO TO 10

WX=XI

WY=YI

GO TO 30

10 IF(W(I).EQ.0.) GO TO 40

WW=W(I)

WX=X(I)*W(I)

WY=Y(I)*W(I)

30 DOF=DOF+1.

CALCULATE SUMS FOR LINEAR LEAST SQUARES ANALYSIS.

SW=SW+WW

SX=SX+WX

SY=SY+WY

SXX=SXX+WX*XI

SYY=SYY+WY*YI

SXY=SXY+WX*YI

40 CONTINUE

IF(DOF.LT.1.) GO TO 100

CALCULATE LINEAR LEAST SQUARES ESTIMATES FOR PARAMETERS (WITH
STANDARD DEVIATIONS) AND AGREEMENT FACTORS OF THE REGRESSION.

DX=SW*SXX-SX*SX

DY=SW*SYY-SY*SY


```

WX=SXX*SY-SX*SXY
WY=SW*SXY-SX*SY
WW=WY/DX
SLOPE=WW
CONST=WX/DX
IF(DY.EQ.0.) GO TO 80
CORR=WY/DSQRT(DX*DY)
WW=DARS(DY/DX-WW*WW)
ESDS=WW
WW=WW/SW
ESD=WW*UX
ESDC=WW*SXX
ESD=SQRT(ESD/DOF)
ESDS=SQRT(ESDS/DOF)
ESDC=SQRT(ESDC/DOF)
GO TO 90
80 CORR=1.
SLOPE=0.
ESD=0.
ESDS=0.
ESDC=0.
90 RETURN
100 IFMPT=1
WRITE(6,99)
GO TO 90
99 FORMAT(//1X,'NUMBER OF D.O.F. IS INSUFFICIENT FOR LINEAR L-S ANAL
CSIS')
END

```

LINFIT

SUBROUTINE LINFIT(NC, NP, LSTART, LSTOP, SIGMA, DTEST, ISTOP)

SUBPROGRAM TO FIT A FUNCTION TO AN INTERVAL OF DATA BY THE GENERAL LEAST SQUARES TECHNIQUE (ADAPTED FROM 'ORGLS', A GENERAL FORTRAN LEAST SQUARES PROGRAM).

COMMON /INFD/ YD(1024), SIGYD(1024), X(1024), P(60), SP(60), KI(60),
CDP(60), V(60), DC(60), DV(60), DD(60), DIAG(60), PD(60), ROW(60), AM(2000)
C, SQSIG(2)
INTEGER RDR, PTR, PCH

OBSERVED DEPENDENT VARIABLE STORED IN ARRAY YD, ITS ESTIMATED STANDARD DEVIATION IN ARRAY SIGYD, AND THE INDEPENDENT VARIABLE IN ARRAY X.

NO = NUMBER OF OBSERVATIONS.
NV = NUMBER OF PARAMETERS TO BE VARIED.

INPUT PARAMETERS -

NC = NUMBER OF CYCLES OF REFINEMENT.
NP = TOTAL NUMBER OF FUNCTION PARAMETERS.
LSTART, LSTOP = INPUT PARAMETERS FOR S/R 'PRELIM' TO DEFINE THE INTERVAL OF ORIGINAL DATA TO BE FITTED.
SIGMA = SCALING FACTOR FOR ESTIMATED STANDARD DEVIATIONS.
DTEST = TEST PARAMETER TO REJECT DATA IF WEIGHTED RESIDUAL EXCEEDS DTEST.
ISTOP = ERROR INDICATOR. 1 IF MATRIX IS SINGULAR, 0 OTHERWISE

OUTPUT PARAMETERS -

P = ESTIMATED VALUES OF FUNCTION PARAMETERS.
SP = ESTIMATED STANDARD DEVIATIONS OF FUNCTION PARAMETERS.
ROW = ROW OF CORRELATION MATRIX.
DOF = NUMBER OF DEGREES OF FREEDOM, NO-NR-NV (NR = NO. OF REJECTED DATA POINTS).
SIG = SUM OF SQUARES OF WEIGHTED RESIDUALS.
SQSIG = ERROR OF FIT, SQRT(SIG/DOF).

SET CONTROL PARAMETERS.

RDR=5
PTR=6
PCH=7
ID=0
IP=0
IW=0

IF(SIGMA.LE.0.) IW=1

ENTER USERS SUBROUTINE TO SET UP DATA ARRAYS, AND OBTAIN VARIABLE NP, NV, NO, IT, IZ.

CALL PRELIM(LSTART, LSTOP, SIGMA, NP, NV, NO, IT, IZ)

IF(ID)206,204,206

204 WRITE(PTR,58)

GO TO 207

206 WRITE(PTR,59)

207 IF(IW)210,208,210

208 WRITE(PTR,61)

GO TO 211

210 WRITE(PTR,62)

211 IF(IP)212,212,214

212 WRITE(PTR,63)

GO TO 215

214 WRITE(PTR,64)IP

215 IF(IT-1)216,218,221

216 WRITE(PTR,94)

GO TO 301

218 WRITE(PTR,95)

```

      GO TO 301
221  WRITE(PTR,76)
301  WRITE(PTR,54) NC,NP,NV,NC
      IF(NC)1601,1601,1301
1301  IF(ID) 1501,1611,1501
1501  READ(RDR,66) ((KI(I),DP(I)),I=1,NP)
      GO TO 1621
1601  DO 1602 I=1,NP
1602  KI(I)=0
1611  DO 1612 I=1,NP
1612  DP(I)=0.0
C    INITIALIZE PROBLEM.
1621  NM=(NV*(NV+1))/2
      SCSIG(1)=0.0
C    PUT OUT TRIAL PARAMETERS, KEY INTEGERS, AND PARAMETER INCREMENTS
      WRITE(PTR,92)
      DO 1653 I=1,NP
1653  WRITE(PTR,93)I,P(I),KI(I),DP(I)
C    START LOOP TO PERFORM NC CYCLES AND ONE FINAL CALCULATION OF Y
      NCY=NC+1
      DO 8501 IC=1,NCY
C    CLEAR ARRAYS AM AND V EXCEPT ON LAST CYCLE
      IF(IC-NCY)1851,2001,2001
1851  DO 1852 I=1,NM
1852  AM(I)=0.0
1902  DO 1902 I=1,NV
1902  V(I)=0.0
C    INITIALIZE FOR CYCLE IC
2001  SCSIG(2)=SCSIG(1)
      SIG=0.0
      DOF=NO-NV
      WRITE(PTR,72)IC
      IF(IC.GT.1) WRITE(PTR,74)
C    START LOOP THROUGH NO OBSERVATIONS
2201  DO 5101 I=1,NO
C    ENTER USERS SUBROUTINE TO COMPUTE Y(CALC) AND DERIVATIVES
      CALL CALC(NP,I,YC,DC)
C    OBTAIN WEIGHT AND CALCULATE QUANTITIES FROM Y(OBS)-Y(CALC)
      IF(IW)2601,2501,2601
2501  SQRTW=1.0/SIGYD(I)
      GO TO 2701
2601  SIGYD(I)=1.0
      SQRTW=1.0
2701  DY=YC(I)-YC
      WDY=SQRTW*DY
C    TEST WEIGHTED RESIDUALS TO REJECT POOR DATA.
      IF(IC.EQ.1) GO TO 2801
      IF(ABS(WDY).LE.DTEST) GO TO 2801
      DOF=DOF-1.
      SQRTW=0.
      J=IZ+I
      WRITE(PTR,75) J,I,YO(I),YC,DY,WDY
      GO TO 2901
2801  SIG=SIG+WDY*WDY
C    BY-PASS DERIVATIVE AND MATRIX SET-UP ON FINAL CALC OF Y
2901  IF(IC-NCY) 3001,5101,5101
3001  IF(SQRTW) 3101,5101,3101
C    START LOOP TO STORE AN ARRAY OF NV DERIVATIVES
3101  J=1
      DO 4101 K=1,NP
      IF(KI(K))4101,4101,3201
3201  IF(ID)3401,3301,3401
C    OBTAIN DERIVATIVE FROM THOSE PROGRAMMED BY USER
3301  DV(J)=SQRTW*DC(K)
      GO TO 4001
C    OBTAIN DERIVATIVE NUMERICALLY UNLESS PARAMETER
C    INCREMENT IS ZERO
3401  DPK=DP(K)
      IF(DPK)3601,3301,3601
3601  PSAVE=P(K)

```

```

          P(K)=PSAVE+DPK
CALL CALC(NP,T,YD,DD)
          DV(J)=SQRTW*(YD-YC)/DPK
          P(K)=PSAVE
4001      J=J+1
4101      CONTINUE
          C      END LOOP TO OBTAIN DERIVATIVES
          C      START LOOP TO STORE MATRIX AND VECTOR.
          C      1604 OR GLS STORAGE SCHEME IS REVERSE OF 7090 OR GLS
          C      JK=1
          DC 5001 J=1,NV
4301      TEMP=DV(J)
          C      IF(TEMP)4501,4401,4501
          C      BY-PASS IF DERIVATIVE IS ZERO
4401      JK=JK+NV+1-J
          C      GO TO 5001
4501      DC 4801 K=J,NV
          C      AM(JK)=AM(JK)+TEMP*DV(K)
          C      JK=JK+1
4801      CONTINUE
          C      V(J)=V(J)+TEMP*WDY
5001      CONTINUE
          C      END LOOP TO STORE MATRIX AND VECTOR
5101      CONTINUE
          C      END LOOP THROUGH NO OBSERVATIONS
          C      COMPUTE AND PUT OUT AGREEMENT FACTORS
5301      SQSIG(1)=SQRT(SIG/DOF)
          C      WRITE(PTR,80) IC,DOF,SIG,SQSIG(1)
          C      BY-PASS MATRIX INVERSION AND PARAMETER OUTPUT ON FINAL CYCLE
          C      IF(IC-NCY)5401,8701,8701
          C      START LOOP TO TEST FOR ZERO DIAGONAL ELEMENT
5401      ISING=0
          C      II=1
          C      IID=NV
          C      DO 5801 I=1,NV
          C      IF(AM(II))5701,5601,5701
5601      ISING=1
          C      WRITE(PTR,83) I
5701      II=II+IID
          C      IID=IID-1
5801      CONTINUE
          C      END LOOP TO TEST FOR ZERO DIAGONAL ELEMENT
          C      TERMINATE JOB IF ZERO DIAGONAL ELEMENT WAS FOUND
          C      IF(ISING)10301,6001,10301
          C      ENTER SUBROUTINE TO REPLACE MATRIX WITH INVERSE
6001      CALL MATINV(AM,NV,ISING)
          C      IF(ISING)6201,6301,6201
          C      TERMINATE JOB IF SINGULAR MATRIX WAS FOUND
6201      WRITE(PTR,85)
          C      WRITE(PTR,87) ISING
          C      GO TO 10301
          C      START LOOP FOR MATRIX VECTOR MULTIPLICATION FOR
6301      DO 7201 I=1,NV
          C      PDI=0.0
          C      IJ=I
          C      IJD=NV-1
          C      DO 7001 J=1,NV
          C      PDI=PDI+AM(IJ)*V(J)
          C      IF(J-1)6701,6801,6901
6701      IJ=IJ+IJD
          C      IJD=IJD-1
          C      GO TO 7001
          C      SAVE DIAGONAL ELEMENTS OF INVERSE MATRIX
6801      DIAG(I)=AM(IJ)
6901      IJ=IJ+1
7001      CONTINUE
          C      PD(I)=PDI
          C      SIG=SIG-PDI*V(I)
7201      CONTINUE
          C      END LOOP FOR MATRIX VECTOR MULTIPLICATION

```

```

C          RECOMPUTE AGREEMENT FACTOR USING MODIFIED SIG
C          IF(SIG.LT.0.) SIG=0.
C          SQSIG(1)=SQRT(SIG/DOF)
C          PUT OUT CAPTION FOR LIST OF CORRECTED PARAMETERS
C          WRITE(PTR,86)IC
C          START LOOP TO CORRECT AND PUT OUT PARAMETERS
C          J=1
C          DO 8001 I=1,NP
C              IF(KI(I))7601,7601,7701
7601          WRITE(PTR,88)I,P(I),P(I)
C              GO TO 8001
7701          POLD=P(I)
C              P(I)=POLD+PD(J)
C          SIGP=SQRT(DIAG(J))*SQSIG(1)
C          SP(I)=SIGP
C              WRITE(PTR,89)I,POLD,PD(J),P(I),SIGP
C              J=J+1
C          CONTINUE
C          END LOOP TO CORRECT AND PUT OUT PARAMETERS
C          PUT OUT ESTIMATED AGREEMENT FACTORS
C          WRITE(PTR,81) IC,DOF,SIG,SQSIG(1)
C          ENTER USERS SUBROUTINE TO TEST AND MODIFY PARAMETERS
C          ISTOP=0
C          CALL TEST(NP,ISTOP)
C          IF(ISTOP) 8101,8201,8101
8101        WRITE(PTR,90) ISTOP
C          GO TO 8701
C          WRITE CORRECTED PARAMETERS ON CARDS IF DESIRED
8201        IF(IY-1) 8501,8301,8401
8301        CONTINUE
8401        WRITE(PCH,91) ((P(I),SP(I)),I=1,NP)
8501        CONTINUE
C          END LOOP THROUGH NC CYCLES AND FINAL CALC OF Y
C          TERMINATE JOB
8701        IF(NC)10501,10501,8801
C          CALCULATE AND PUT OUT CORRELATION MATRIX
8801        WRITE(PTR,97)
C          DO 9101 I=1,NV
C          DIAG(I)=1.0/SQRT(DIAG(I))
9101        CONTINUE
C          IJ=1
C          DO 10201 I=1,NV
C              DO 9601 J=1,NV
C                  RCW(J)=0.0
9601          CONTINUE
C          I1=I-1
C          DO 10001 J=I,NV
C              ROW(J-I1)=AM(IJ)*DIAG(I)*DIAG(J)
C              IJ=IJ+1
10001        CONTINUE
C          J1=NV-I1
C          WRITE(PTR,98)I,(ROW(J),J=1,J1)
10201        CONTINUE
C          GO TO 10501
10301        ISTOP=ISING
10501        RETURN
54        FORMAT(33HONUMBER OF CYCLES IN THIS JOB IS I3/30HONUMBER OF PARA
C          CTERS READ IS I3/38HONUMBER OF PARAMETERS TO BE VARIED IS I3/32HO
C          CMBER OF OBSERVATIONS READ IS I5)
58        FORMAT(31HODERIVATIVES PROGRAMMED BY USER)
59        FORMAT(57HONUMERICAL DERIVATIVES UNLESS PARAMETER INCREMENT IS Z.
10)
61        FORMAT(31HOWEIGHTS TO BE SUPPLIED BY USER)
62        FORMAT(34HOUNIT WEIGHTS TO BE SET BY PROGRAM)
63        FORMAT(41HOPARAMETERS TO BE ESTIMATED FROM RAW DATA)
64        FORMAT(34HOPARAMETERS TO BE TAKEN FROM CYCLEI2,16H OF PREVIOUS J
1)
65        FORMAT(8F10.3)
66        FORMAT(I3,F7.3)
72        FORMAT(46HOCALCULATED Y BASED ON PARAMETERS BEFORE CYCLEI2)

```

```

74 FORMAT(/IX,' REJECTED DATA POINTS  -',11X,'TORIG',7X,'I',8X,'YC(I
   C)',11X,'YC',13X,'DY',12X,'WDY'/)
75 FORMAT(31X,2110,4E15.6)
80 FORMAT(51H0AGREEMENT FACTORS BASED ON PARAMETERS BEFORE CYCLE I2/
   C21H0NUMBER OF D.O.F. IS F5.0/20H0SUM(W*(O-C)**2) IS F11.3/35H0SQRT
   CF(SUM(W*(O-C)**2)/(D.O.F.)) IS F10.4)
81 FORMAT(60H0ESTIMATED AGREEMENT FACTORS BASED ON PARAMETERS AFTER C
   CYCLE I2/21H0NUMBER OF D.O.F. IS F5.0/20H0SUM(W*(O-C)**2) IS F11.3/
   C35H0SQRTF(SUM(W*(O-C)**2)/(D.O.F.)) IS F10.4)
83 FORMAT(62H MATRIX HAS A ZERO DIAGONAL ELEMENT CORRESPONDING TO PAR
   AMETER I3,16H OF THOSE VARIED)
85 FORMAT(40H0SINGULARITY RETURN FROM MATRIX INVERTER)
86 FORMAT(37H0PARAMETERS AFTER LEAST SQUARES CYCLE I3//14X,'OLD',11X,
   C'CHANGE',10X,'NEW',11X,'ERROR'/)
87 FORMAT(1X,'DUE TO ELEMENT',I4,' OF MATRIX')
88 FORMAT(1X,I5,E15.4,15X,E15.4)
89 FORMAT(1X,I5,4E15.6)
90 FORMAT(66H0SUBROUTINE TEST INDICATES THAT JOB IS TO BE TERMINATED
   FOR PEASONI2)
91 FORMAT(8E10.4)
92 FORMAT(11H0INPUT DATA//5X,'I',7X,'P(I)',6X,'KI(I)',5X,'DP(I)'/)
93 FORMAT(1X,2(I5,E15.6))
94 FORMAT(51H0CORRECTED PARAMETERS NOT TO BE SAVED FOR LATER USE)
95 FORMAT(51H0CORRECTED PARAMETERS TO BE WRITTEN ON PRIVATE TAPE)
96 FORMAT(51H0CORRECTED PARAMETERS TO BE WRITTEN FOR CARD OUTPUT)
97 FORMAT(19H0CORRELATION MATRIX)
98 FORMAT(1H0I3,2X,20F6.3/(6X,20F6.3))
END

```

```

SUBROUTINE MATINV(AM,N,NFAIL)
C
C SUBPROGRAM TO OBTAIN INVERSE OF A SYMMETRIC MATRIX BY CHCLESKI
C PROCEDURE.
C
C DIMENSION AM(2000)
C
C ***** SEGMENT 1 OF CHCLESKI INVERSION *****
C ***** FACTOR MATRIX INTO LOWER TRIANGLE X TRANSPOSE *****
K=1
IF(N-1)10,8,9
8 AM(1)=1.0/AM(1)
GO TO 204
C ***** LOOP M OF A(L,M) *****
9 DO 7 M=1,N
IMAX=M-1
C ***** LOOP L OF A(L,M) *****
DO 6 L=M,N
SUMA=0.0
KLI=L
KMI=M
IF(IMAX)23,23,1
C *****SUM OVER I=1,M-1 A(L,I)*A(M,I) *****
1 DO 2 I=1,IMAX
SUMA=SUMA+AM(KLI)*AM(KMI)
J=M-I
KLI=KLI+J
2 KMI=KMI+J
C *****TERM=C(L,M)-SUM *****
23 TERM=AM(K)-SUMA
IF(L-M)3,3,5
3 IF(TERM)10,10,4
C ***** A(M,M)=SQRT(TERM) *****
4 DENOM= SQRT(TERM)
AM(K)=DENOM
GO TO 6
10 NFAIL= K

```

```

      GO TO 300
C     ***** A(L,K)=TERM/A(M,M) *****
      AM(K)=TERM/DENOM
      K=K+1
      7 CONTINUE
C
C     ***** SEGMENT 2 OF CHOLESKI INVERSION *****
C     ***** INVERSION OF TRIANGULAR MATRIX *****
      100 AM(1)=1.0/AM(1)
      KDM=1
C     ***** STEP L OF B(L,M) *****
      DO 104 L=2,N
      KDM=KDM+N-L+2
C     ***** RECIPROCAL OF DIAGONAL TERM *****
      TERM = 1.0/AM(KDM)
      AM(KDM)=TERM
      KMI=0
      KLI=L
      IMAX=L-1
C     ***** STEP M OF B(L,M) *****
      DO 103 M=1,IMAX
      K=KLI
C     ***** SUM TERMS *****
      SUMA=0.0
      DO 102 I=M,IMAX
      II=KMI+I
      SUMA=SUMA-AM(KLI)*AM(II)
      102 KLI=KLI+N-I
C     ***** MULT SUM * RECIP OF DIAGONAL *****
      AM(K)=SUMA*TERM
      J=I-M
      KLI=K+J
      103 KMI=KMI+J
      104 CONTINUE
C
C     ***** SEGMENT 3 OF CHOLESKI INVERSION *****
C     ***** PREMULIPLY LOWER TRIANGLE BY TRANSPOSE *****
      200 K=1
      DO 203 M=1,N
      KLI=K
      DO 202 L=M,N
      KMI=K
      IMAX=N-L+1
      SUMA=0.0
      DO 201 I=1,IMAX
      SUMA=SUMA+AM(KLI)*AM(KMI)
      KLI=KLI+1
      201 KMI=KMI+1
      AM(K)=SUMA
      202 K=K+1
      203 CONTINUE
      204 NFAIL=0
      300 RETURN
      END

```

TAPED

```

C PROGRAM TO READ ANY NUMBER OF TAPES AND PUNCH DATA ON CARDS.
C
COMMON /INFO/ ARRAY(3072),RDATA(1024),DATA(2050)
INTEGER*2 IDATA(1024)
LOGICAL TITLE(20)
C
ICH=1501
CALL PSTART(ARRAY,6000,NRESID)
120 CALL PSTART(ARRAY(ICH),6000,NRESID)
IF(NRESID) 504,503,140
140 ICH=NDP(ICH+1500,3000)
NREAD=6000-NRESID
IF(NREAD) 120,502,150
150 DO 160 I=1,1024
160 RDATA(I)=0.
C DECODE PAPER-TAPE DATA AND STORE RAW-DATA VALUES IN 'RDATA'.
CALL BNMCM(ARRAY(ICH),NREAD,RDATA)
DO 180 I=1,1024
180 IDATA(I)=RDATA(1025-I)
READ(5,94) TITLE
C PRINT AND PUNCH DECODED DATA.
WRITE(6,93) TITLE
WRITE(6,96) IDATA
WRITE(7,95) IDATA
GO TO 120
501 STOP 1
502 WRITE(6,99)
STOP 2
503 WRITE(6,98)
STOP 3
504 STOP 4
97 FORMAT(//1X,'INPUT RECORD EMPTY')
98 FORMAT(//1X,'INPUT RECORD TOO LARGE')
96 FORMAT(1X,20I6)
95 FORMAT(20I4)
94 FORMAT(20A4)
93 FORMAT(1H8/1H1,25X,20A4/26X,80('*')////)
END

```

```

C SUBROUTINE 'TRANS' TO DECODE PAPER TAPE DATA FROM MS902
C
BNMCM START 0 TRANSLATION ROUTINE FOR PAPER TAPE
USING *,15 FROM THE MS9
ST 2,28(,13)
ST 3,32(,13) USAGE - CALL BNMCM(ARRAY,N,DATA)
ST 4,36(,13) ARRAY IS THE ADDRESS OF THE P.T. RECORD
ST 5,40(,13) N IS THE NO. OF CHARACTERS IN THE RECORD
ST 6,44(,13) DATA IS THE ADDRESS OF THE DATA ARRAY
L 2,0(,1)
L 3,4(,1) EACH DATUM ON THE TAPE OCCUPIES 5 CHARS.
L 3,0(,3) THE FIRST OF THESE HAS BIT 1 BLANK
LA 3,1(,3) THE CHANNEL NO. IS IN BITS 2-6 OF THE
L 4,8(,1) FIRST TWO CHARS. (AS THE BINARY COMPLE-
BEGIN TH 0(2),X'40' MENT)
BC 8,DECODE THE DATA WORD IS IN BITS 2-7 OF THE
LA 2,1(,2) LAST THREE CHARACTERS (ALSO AS THE
SH 3,H1 BINARY COMPLEMENT)
BC 2,BEGIN THE DECODED DATA WORD IS PLACED IN THE
RETURN L 2,28(,13) DATA ARRAY ACCORDING TO THE CHANNEL NO.
L 3,32(,13)
L 4,36(,13)
L 5,40(,13)
L 6,44(,13)
MVI 12(13),X'FF'
BR 14
-DECODE OI 0(2),X'40'

```



```

SR      0,0
LA      5,2
LOOP1  TM      0(2),X'40'
        BC      8,DECODE
        IC      1,0(,2)
        SLL     1,26
        SLDL    0,5
        LA      2,1(,2)
        SH      3,H1
        BC      8,RETURN
        BCT     5,LOOP1
        LR      6,0
SR      0,0
LA      5,3
LOOP2  TM      0(2),X'40'
        BC      8,DECODE
        IC      1,0(,2)
        SLL     1,26
        SLDL    0,6
        LA      2,1(,2)
        SH      3,H1
        BC      8,RETURN
        BCT     5,LOOP2
        X       0,MASKD
        A       0,FLOAT
        ST      0,TEMP
        LE      0,TEMP
        AE      0,FLOAT
        X       6,MASKC
        PC      4,*+8
        LA      6,1024
        BCTR    6,0
        SLL     6,2
        STE     0,0(6,4)
        B       BEGIN
TEMP    DS      F
FLOAT   DC      X'46000000'
MASKD   DC      X'000003FF'
MASKC   DC      X'0001FFFF'
H1      DC      H'1'
END

```

RAWFIT

```

C PROGRAM TO FIT A SEQUENCE OF LINEAR SEGMENTS TO OBSERVED I.E.
C CURVES BY LEAST SQUARES.
C
COMMON /WORK/ RY(1024),RX(1024)
COMMON /PARAMS/ FP(60),SFP(60),VPI,VPF,VPX,VDEL
LOGICAL TITLE(20)
DIMENSION IDATA(1024)
EQUIVALENCE (IDATA(1),RY(1))
C
CONTROL PARAMETERS -
C
C NRUN = NUMBER OF I.E. CURVES IN DATASET.
C NCYC = NUMBER OF REFINEMENT CYCLES.
C
EXPERIMENTAL PARAMETERS -
C
C VMIN,VMAX = CORRECTED IONIZING VOLTAGE AT START AND FINISH OF
C I.E. CURVE.
C SIGMA = SCALE FACTOR FOR E.S.D. OF ION CURRENT.
C DTEST = TEST PARAMETER FOR REJECTION OF POOR DATA.
C VPI,VPF = INITIAL AND FINAL VOLTAGES FOR SEQUENCE OF LINEAR
C SEGMENTS.
C VPX = VOLTAGE LENGTH OF A SEGMENT.
C
READ CONTROL PARAMETERS.
100 READ(5,89,END=201) NRUN,NCYC
WRITE(6,88) NRUN
IRUN=0
110 IRUN=IRUN+1
IF(IRUN.GT.NRUN) GO TO 100
C READ OBSERVED I.E. DATA AND EXPERIMENTAL PARAMETERS.
READ(5,87) TITLE,IDATA
READ(5,85) VMIN,VMAX,SIGMA,DTEST
READ(5,85) VPI,VPF,VPX
WRITE(6,86) IRUN,TITLE,IDATA
WRITE(6,84) VMIN,VMAX,SIGMA,DTEST
WRITE(6,82) VPI,VPF,VPX
VDEL=(VMAX-VMIN)/1023.
RY(I)=IDATA(I)
RX(1)=VMIN
DO 120 I=2,1024
RY(I)=IDATA(I)
120 RX(I)=RX(I-1)+VDEL
C CALCULATE INITIAL AND FINAL INDICES FOR INTERVAL OF DATA TO BE
C FITTED.
I=0
140 I=I+1
IF(VPI.LE.RX(I)) GO TO 150
GO TO 140
150 LSTART=I
I=1025
160 I=I-1
IF(VPF.GE.RX(I)) GO TO 170
GO TO 160
170 LSTOP=I
C ENTER S/R 'LINFIT' TO CALCULATE LEAST SQUARES ESTIMATES OF
C END-POINTS OF LINEAR SEGMENTS.
CALL LINFIT(NCYC,NPAR,LSTART,LSTOP,SIGMA,DTEST,IFSTOP)
IF(IFSTOP) 202,200,202
C PUNCH FINAL PARAMETER ESTIMATES ON CARDS.
200 WRITE(7,81) VPI,VPF,VPX,NPAR,(FP(I),I=1,NPAR)
GO TO 110
201 STOP 1
202 STOP 2
89 FORMAT(5I5)
88 FORMAT(1H8,'DATASET CONTAINS ',I5,' RECORDS')
87 FORMAT(20A4/(20I4))
86 FORMAT(1H8/1H1,'RECORD NUMBER',I5,5X,20A4/24X,80(' '*))///1X,'OBSER
VED I.E. CURVE'/(5X,20I6))
85 FORMAT(5F5.2)

```

```

84 FORMAT(///1X,'EXPERIMENTAL DATA -'/25X,'INITIAL SCAN VOLTAGE =',F
  C6.2/26X,'FINAL SCAN VOLTAGE =',F6.2/27X,'EST ERROR CONSTANT =',F6
  C.2/28X,'MAX ERROR ALLOWED =',F6.2//)
82 FORMAT(1H1,'LEAST-SQUARES FIT OF LINEAR SEGMENTS TO EXPERIMENTAL D
  CATA'//1X,'SEQUENCE PARAMETERS -'/25X,'INITIAL VOLTAGE =',F6.2/25X,
  C,'FINAL VOLTAGE =',F6.2/25X,'SEGMENT LENGTH =',F6.2//)
81 FORMAT(3F5.2,I5/(10F8.2))
END

```

```

SUBROUTINE PRELIM(LSTART,LSTOP,SIG,NP,NV,NO,IT,I1)

```

```

C
C SUBPROGRAM TO SET UP DATA ARRAYS AND INITIALIZE PARAMETERS FOR
C S/R 'LINFIT'.
C
COMMON /WORK/ RY(1024),RX(1024)
COMMON /INFO/ YO(1024),SIGYO(1024),X(1024),P(60),SP(60),KI(60)
COMMON /PARAMS/ FP(60),SFP(60),VPI,VPF,VPX,VDEL
C
IT=0
I1=LSTART-1
NO=LSTOP-I1
C TRANSFER OBSERVED DATA AND CALCULATE ESTIMATED STANDARD DEVIATIONS
DO 60 I=1,NO
  II=I+1
  X(I)=RX(II)
  YO(I)=RY(II)
  SIGYO(I)=SIG*SQRT(RY(II))
  IF(SIGYO(I).EQ.0.) SIGYO(I)=1.0
60 CONTINUE
C CALCULATE NUMBER OF PARAMETERS (NP), AND OBTAIN TRIAL VALUES.
NP=(VPF-VPI)/VPX+1.5
NV=NP
IX=VPX/VDEL+0.5
XI=(VPI-RX(1))/VDEL+1.5
II=XI
IF(XI.LT.0.) II=II-1
DO 100 N=1,NP
  KI(N)=1
  SP(I)=0.
  IF(II.GT.0) GO TO 70
  P(N)=RY(1)
  GO TO 100
70 IF(II.LT.1025) GO TO 90
  P(N)=RY(1024)
  GO TO 100
90 P(N)=RY(II)
100 II=II+IX
RETURN
END

```

```

SUBROUTINE CALC(NP,IX,Y,D)

```

```

C
COMMON /INFO/ DUMMY(2048),X(1024),P(60)
COMMON /PARAMS/ FP(60),SFP(60),VPI,VPF,VPX,VDEL
C
DIMENSION D(60)
F=(X(IX)-VPI)/VPX
I1=F
F=F-II
I1=I1+1
I2=I1+2
Y=P(I1)+(P(I2)-P(I1))*F

```

```
DO 20 I=1,NP  
20 D(I)=0.  
D(I1)=1.-F  
D(I2)=F  
RETURN  
END
```

```
SUBROUTINE TEST(NP,ISTOP)
```

```
C  
COMMON /INFO/ DUMMY(3072),P(60),SP(60)  
COMMON /PARAMS/ FP(60),SFP(60)
```

```
C  
DO 20 I=1,NP  
20 FP(I)=P(I)  
SFP(I)=SP(I)  
RETURN  
END
```

SLOG

```

C PROGRAM TO NORMALIZE SEMILOG I.E. CURVES, FOR DETERMINATION OF
C APPEARANCE POTENTIALS.
C
COMMON /WORK/ Y(1024),X(1024),W(1024)
COMMON /LINPAR/ CONST,SLOPE,ESDC,ESDS,ESD,CORR
LOGICAL TITLE(20)
DIMENSION IDATA(1024)
EQUIVALENCE (IDATA(1),Y(1))
C
CONTROL PARAMETERS -
C
C NRUN = NUMBER OF I.E. CURVES IN DATASET.
C MPT = SMOOTHING PARAMETER.
C
EXPERIMENTAL PARAMETERS -
C
C VMIN,VMAX = NOMINAL IONIZING VOLTAGE AT START AND FINISH OF
C I.E. CURVE.
C LSTART,LSTOP = INITIAL AND FINAL INDICES OF REGION OVER WHICH
C LINEAR SEGMENTS ARE FITTED TO SEMILOG CURVE.
C LLINE = LENGTH OF LINEAR SEGMENTS.
C SCALE = SCALE FACTOR FOR PLOT OF SEMILOG CURVE.
C SLIM = LIMITING VALUE FOR SLOPE OF SEMILOG CURVE.
C DPT = ORDINATE VALUE AT WHICH 'VPT' IS CALCULATED.
C DZERO = ZERO CORRECTION PARAMETER FOR SEMILOG CURVE.
C
READ CONTROL PARAMETERS.
100 READ(5,89,END=201) NRUN,MPT
WRITE(6,88) NRUN
IRUN=0
110 IRUN=IRUN+1
IF(IRUN.GT.NRUN) GO TO 100
C READ OBSERVED I.E. DATA AND EXPERIMENTAL PARAMETERS.
READ(5,87) TITLE,IDATA
READ(5,83) VMIN,VMAX
READ(5,81) LSTART,LSTOP,LLINE,SCALE,SLIM,DPT,DZERO
WRITE(6,86) TITLE
WRITE(6,84) VMIN,VMAX
VDEL=(VMAX-VMIN)/1023.
DO 120 I=1,1024
120 Y(I)=IDATA(I)
CALL SMOOTH(0,MPT,1024)
X(1)=VMIN
DO 140 I=2,1024
140 X(I)=X(I-1)+VDEL
C CALCULATE NORMALIZING CONSTANT, AND OBTAIN NORMALIZED SEMILOG I.E.
C CURVE.
CALL LINEAR(0,50,0,IFNPT)
YZERO=SLOPE*VMIN+CONST-DZERO
DO 160 I=1,1024
Y(I)=Y(I)-YZERO
160 IF(Y(I).LT.1.) Y(I)=1.0
Y(I)=ALOG10(Y(I))
WRITE(6,82) DZERO,YZERO
WRITE(6,80) DPT,SLIM,SCALE
C FIT LINEAR SEGMENTS TO SEMILOG CURVE, AND OBTAIN APPROXIMATE
C VALUES FOR 'VPT' AND 'EPT'.
L1=LSTART
190 L1=L1+20
L2=L1+LLINE
IF(L2.GT.LSTOP) GO TO 200
CALL LINEAR(L1,LLINE,0,IFNPT)
IF(SLOPE.LT.SLIM) GO TO 190
EPT=-CONST/SLOPE
VPT=EPT+DPT/SLOPE
WRITE(6,78) L1,L2,CONST,ESDC,SLOPE,ESDS,CORR,EPT,VPT
GO TO 190
C PLOT NORMALIZED SEMILOG CURVE ON LINE-PRINTER.
200 CALL SPLOT(SCALE,1.5,10,1000,10)
GO TO 110

```

```

201 STOP 1
80 FORMAT(2I5)
82 FORMAT(1H8/1H1,'DATASET CONTAINS',I4,' RECORDS')
87 FORMAT(20A4/(20I4))
86 FORMAT(1H8/1H1,20X,20A4/21X,80('*'))///)
84 FORMAT(1X,'EXPERIMENTAL DATA -'/27X,'INITIAL SCAN VOLTAGE =' ,F5.2/
C29X,'FINAL SCAN VOLTAGE =' ,F5.2//)
83 FORMAT(2F5.2)
82 FORMAT(1H1,'ZERO THRESHOLD CORRECTION -'/30X,'ADJUSTED ZERO VAL
CUE =' ,F6.2//30X,'CALCULATED CORRECTION =' ,F6.2//)
81 FORMAT(3I5,4F5.2)
80 FORMAT(1H8/1H1,'SEMI-LOG PLOT PARAMETERS -'/30X,'LOG10(I.E.) AT V
CPT =' ,F6.2 //30X,'MINIMUM SLOPE VALUE =' ,F6.2 //30X,'PLOT SCALE
C FACTOR =' ,F6.2 /1H1,'CALCULATED APPEARANCE POTENTIAL VALUES -'/4
CX,'INTERVAL',12X,'CONST(ESD)',19X,'SLOPE(ESD)',13X,'CORR',8X,'EPT'
C,8X,'VPT'/)
78 FORMAT(1X,I6,'-',I4,E17.5,'(',E10.4,')',E17.5,'(',E10.4,')',F11.4,
C2F11.2)
END

```

```

SUBROUTINE SPLIT(SCALE,ZERO,ISTART,ISTOP,ISTEP)
C
C SUBPROGRAM TO PLOT NORMALIZED SEMILOG I.E. CURVE ON LINE-PRINTER.
C
COMMON /WORK/ Y(1024),X(1024)
INTEGER*2 LINE(101),BLANK/' '/,DOT/'.'/,POINT/'+'/
C
WRITE(6,99)
DO 10 I=1,101
10 LINE(I)=DOT
WRITE(6,98) LINE
DO 20 I=1,101
20 LINE(I)=BLANK
DO 40 K=ISTART,ISTOP,ISTEP
LPOINT=Y(K)*SCALE+ZERO
LINE(LPOINT)=POINT
WRITE(6,97) K,LINE,Y(K),X(K)
40 LINE(LPOINT)=BLANK
RETURN
99 FORMAT(1H8/1H1,T2,'INDEX',T53,'LOG(I.E.)',T112,'VALUE',T125,'ELECT
CRON'/1X,T126,'ENERGY'/)
98 FORMAT(6X,'0',9X,'1',9X,'2',9X,'3',9X,'4',9X,'5',9X,'6',9X,'7',9X,
C'8',9X,'9',9X,'10'/6X,101A1)
97 FORMAT(1X,I4,'-',I4,E12.5,F10.2)
END

```

SLAP.

```

C PROGRAM TO CALCULATE NOMINAL APPEARANCE POTENTIALS FROM THE
C NORMALIZED SEMILOG I.E. CURVES (OBTAINED FROM PROGRAM 'SLOG').
C
COMMON /WORK/ RY(1024),RX(1024),W(1024)
COMMON /LINPAR/ CONST,SLOPE,ESDC,ESDS,ESD,CORR
COMMON /PARAMS/ FP(60),SFP(60)
LOGICAL TITLE(20)
DIMENSION IDATA(1024)
EQUIVALENCE (IDATA(1),RY(1))

C CONTROL PARAMETERS -
C
C     NRUN = NUMBER OF I.E. CURVES IN DATASET.
C     NCYC = NUMBER OF REFINEMENT CYCLES.
C     MPT = SMOOTHING PARAMETER.
C     DPT = ORDINATE VALUE AT WHICH A.P. IS CALCULATED.
C
C EXPERIMENTAL PARAMETERS -
C
C     VMIN,VMAX = NOMINAL IONIZING VOLTAGE AT START AND FINISH OF
C     I.E. CURVE.
C     SIGMA = SCALING FACTOR FOR E.S.D. OF ION CURRENT.
C     DTEST = TEST PARAMETER FOR REJECTION OF POOR DATA.
C     LSTART,LSTOP = INITIAL AND FINAL INDICES OF LINEAR REGION OF
C     SEMILOG I.E. CURVE.
C     DZERO = ZERO CORRECTION PARAMETER FOR SEMILOG I.E. CURVE.
C
C READ CONTROL PARAMETERS.
100 READ(5,89,END=201) NRUN,NCYC,MPT,DPT
WRITE(6,88) NRUN
IRUN=0
110 IRUN=IRUN+1
IF(IRUN.GT.NRUN) GO TO 100
C READ OBSERVED I.E. DATA, AND EXPERIMENTAL PARAMETERS.
READ(5,87) TITLE,IDATA
READ(5,85) VMIN,VMAX,SIGMA,DTEST
READ(5,83) LSTART,LSTOP,DZERO
WRITE(6,86) IRUN,TITLE
WRITE(6,84) VMIN,VMAX,SIGMA,DTEST
VDEL=(VMAX-VMIN)/1023.
DO 120 I=1,1024
120 RY(I)=IDATA(I)
CALL SMOOTH(0,MPT,1024)
RX(1)=VMIN
DO 140 I=2,1024
140 RX(I)=RX(I-1)+VDEL
C CALCULATE NORMALIZING CONSTANT, AND OBTAIN NORMALIZED I.E. CURVE.
CALL LINEAR(0,50,0,IFNPT)
YZERO=SLOPE*VMIN+CONST-DZERO
DO 160 I=1,1024
RY(I)=RY(I)-YZERO
IF(RY(I).LT.1.0) RY(I)=1.0
160 CONTINUE
WRITE(6,82) DZERO,YZERO,DPT,LSTART,LSTOP
C CALCULATE LEAST SQUARES ESTIMATES OF STRAIGHT LINE PARAMETERS FOR
C LINEAR REGION OF SEMILOG I.E. CURVE.
CALL LINFIT(NCYC,NPAR,LSTART,LSTOP,SIGMA,DTEST,IFSTOP)
IF(IFSTOP) 202,170,202
C CALCULATE NOMINAL VALUES OF APPEARANCE POTENTIAL (AND E.S.D.).
170 EPT=-FP(1)/FP(2)
S1=SFP(1)/FP(1)
S2=SFP(2)/FP(2)
SEPT=EPT*SQRT(S1*S1+S2*S2)
VPT=DPT-FP(1)
S1=SFP(1)/VPT
VPT=VPT/FP(2)
SVPT=VPT*SQRT(S1*S1+S2*S2)
WRITE(6,80) EPT,SEPT,VPT,SVPT
WRITE(7,78) EPT,SEPT,VPT,SVPT
GO TO 110

```

```

201 STOP 1
202 STOP 2
86 FORMAT(3I5,F5.2)
88 FORMAT(148,'DATASET CONTAINS ',I5,' RECORDS')
87 FORMAT(20A4/(20I4))
85 FORMAT(2H8/1H1,'RECORD NUMBER',I5,5X,20A4/24X,80('*')//)
86 FORMAT(5F5.2)
84 FORMAT(///IX,'EXPERIMENTAL DATA -'/25X,'INITIAL SCAN VOLTAGE =',F
6.2/26X,'FINAL SCAN VOLTAGE =',F6.2/27X,'EST ERROR CONSTANT =',F6
6.2/28X,'MAX ERROR ALLOWED =',F6.2//)
83 FORMAT(2I5,F5.2)
82 FDRMAT(///IX,'ADJUSTED ZERO VALUE =',F6.2/24X,'CALCULATED CORREC
TION =',F6.2/24X,'LOG10(I.E.) AT VPT =',F6.2///25X,'INTERVAL F
COR L-S FIT -'/25X,'INITIAL DATA POINT =',I6/26X,'FINAL DATA
POINT =',I6/1H8/1H1,'LEAST-SQUARES FIT OF STRAIGHT LINE TO SEMI-LO
CG I.E. CURVE -'///)
80 FORMAT(///'CALCULATED APPEARANCE POTENTIAL - EPT (E.S.D.)
C VPT (E.S.D.)'//34X,2(F10.4,' (',F6.4,')'))
78 FORMAT(4F10.5)
END

```

```

SUBROUTINE PRELIM(LSTART,LSTOP,SIG,NP,NV,NO,IT,L1)
C
C SUBPROGRAM TO SET UP DATA ARRAYS AND INITIALIZE PARAMETERS FOR
C S/R 'LINFIT'.
C
COMMON /WORK/ RY(1024),RX(1024),W(1024)
COMMON /INFO/ YO(1024),SIGYO(1024),X(1024),P(60),SP(60),KI(60)
C
IT=0
L1=LSTART-1
NO=LSTOP-L1
SIGLOG=SIG/2.3026
C TRANSFER OBSERVED DATA AND CALCULATE ESTIMATED STANDARD DEVIATIONS
DO 20 I=1,NO
L=I+L1
X(I)=RX(L)
IF(RY(L).EQ.1.0) GO TO 10
YO(I)=ALOG10(RY(L))
SIGYO(I)=SIGLOG/SQRT(RY(L))
GO TO 20
10 YO(I)=0.
SIGYO(I)=1.0
20 CONTINUE
C CALCULATE NUMBER OF PARAMETERS (NP), AND OBTAIN TRIAL VALUES.
NV=2
DO 40 I=1,NV
SP(I)=0.
40 KI(I)=1
NP=2
P(1)=-10.
P(2)=1.
RETURN
END

```



```
SUBROUTINE CALC(NP,IX,Y,D)
```

```
C  
COMMON /INFO/ DUMMY(2048),X(1024),P(60)  
DIMENSION D(60)
```

```
C  
Y=P(1)+P(2)*X(IX)  
D(1)=1.  
D(2)=X(IX)  
RETURN  
END
```

```
SUBROUTINE TEST(NP,ISTOP)
```

```
C  
COMMON /INFO/ DUMMY(3072),P(60),SP(60)  
COMMON /PARAMS/ FP(60),SFP(60)
```

```
C  
DO 20 I=1,NP  
FP(I)=P(I)  
20 SFP(I)=SP(I)  
RETURN  
END
```

FIX

```

C PROGRAM TO CALCULATE FRACTIONAL ION INTENSITIES AND LOGARITHMIC
C INTENSITY RATIOS USING SMOOTHED I.E. CURVES (OBTAINED FROM PROGRAM
C 'RAWFIT').
COMMON /XDATA/ DATA(1024,8)
COMMON /WORK/ Y(1024),X(1024)
COMMON /INFO/ DUMMY(5020),TITLE,IONAME
COMMON /PARAMS/ P(60),VPI,VPF,VPX,NP
LOGICAL TITLE(10),IONAME(10,8),BLANK/' '/
DIMENSION NN(10)
REAL GAIN,ISOTOP

CONTROL PARAMETERS -

NRUN = NUMBER OF IONS CONTRIBUTING TO TOTAL ION INTENSITY
      (= NUMBER OF I.E. CURVES IN DATASET).
MPT = SMOOTHING PARAMETER.
VINCR = ENERGY INCREMENT.
VIP = IONIZATION POTENTIAL.
VEE = SHIFT PARAMETER FOR ENERGY SCALE.
ISTART,ISTOP = INITIAL AND FINAL INDICES FOR CALCULATION OF
              FRACTIONAL ION INTENSITIES.
ISTEP = NUMBER OF ENERGY INCREMENTS BETWEEN CALCULATED
        FRACTIONAL ION INTENSITIES.

EXPERIMENTAL PARAMETERS -

ISOTOP = ISOTOPIC CORRECTION.
GAIN = ELECTRON-MULTIPLIER GAIN.
CORR = INTENSITY CORRECTION.
VMIN,VMAX = INITIAL AND FINAL VALUES OF IONIZING VOLTAGE FOR
            CALCULATION OF SMOOTHED I.E. CURVE.

100 DO 120 I=1,10
    TITLE(I)=BLANK
    DO 120 J=1,8
120 IONAME(I,J)=BLANK
C READ CONTROL PARAMETERS.
READ(5,89,END=501) TITLE,NRUN,MPT,VINCR
READ(5,83) VIP,VEE,ISTART,ISTOP,ISTEP
WRITE(6,86) TITLE,NRUN
IRUN=0
150 IRUN=IRUN+1
IF (IRUN.GT.NRUN) GO TO 300
C READ EXPERIMENTAL PARAMETERS, AND PARAMETERS TO CALCULATE SMOOTHED
C I.E. CURVE (OBTAINED FROM PROGRAM 'RAWFIT').
READ(5,87) (IONAME(I,IRUN),I=1,10),ISOTOP,GAIN,CORR,VPI,VPF,VPX,NP
READ(5,85) (P(I),I=1,NP)
READ(5,83) VMIN,VMAX
WRITE(6,86) IRUN,(IONAME(I,IRUN),I=1,10)
WRITE(6,84) NP,VPI,VPF,VPX,ISOTOP,GAIN,CORR
C ENTER S/R 'DATCOM' TO CALCULATE SMOOTHED I.E. CURVE.
CALL DATCOM(IRUN,MPT,VIP,VEE,VMIN,VMAX,VINCR,IPT)
C CONVERT CALCULATED I.E. CURVE TO SAME RELATIVE INTENSITY SCALE,
C AND STORE CORRECTED I.E. CURVE.
DFACT=ISOTOP*CORR/GAIN
DO 220 I=1,IPT
220 Y(I)=Y(I)*DFACT
WRITE(6,82) (Y(I),I=1,IPT)
DO 240 I=1,IPT
240 DATA(I,IRUN)=Y(I)
GO TO 150
C ENTER S/R 'FLOG' TO CALCULATE FRACTIONAL ION INTENSITIES AND
C LOGARITHMIC INTENSITY RATIOS.
300 CALL FLOG(VIP,VEE,VINCR,NRUN,ISTART,ISTOP,ISTEP)
C ENTER S/R 'PLOT' TO OBTAIN PLOT OF FRACTIONAL ION INTENSITY CURVES
C ON 'CALCOMP 1627' PLOTTING.
READ(5,81) I1,I2,I3,NN
CALL PLOT(I1,I2,I3,NN,VINCR)
GO TO 100

```

```

501 STOP 1
6) FORMAT(10A4,2I5,F5.2)
83 FORMAT(14B/14I1,43X,10A4/44X,40('*')// 'ODATASET CONTAINS',I3,' REC
CORDS')
87 FORMAT(10A4/F10.3,F10.1,F10.2/3F5.2,I5)
85 FORMAT(////// 'ORECORD NUMBER',I5,25X,10A4/44X,40('*')////)
85 FORMAT(10F8.2)
84 FORMAT(1X,'EXPERIMENTAL DATA (FITTED BY LINEAR SEGMENTS)'//1X,'NUM
BER OF PARAMETERS =',I6//6X,'INITIAL VOLTAGE =',F6.2//7X,'FINAL VO
LTAGE =',F6.2//7X,'SEGMENT LENGTH =',F6.2//6X,'ISOTOPIIC FACTOR =',F
6.3//6X,'MULTIPLIER GAIN =',F6.2//6X,'INTENSITY CORRN =',F6.2)
87 FORMAT(2F5.2,3I5)
82 FORMAT(////1X,'CALCULATED I.E. CURVE - (CORRECTED)'//(5X,20F6.1
C))
81 FORMAT(3I5,10I2)
END

```

```

SUBROUTINE DATCOM(IRUN,MPT,VIP,VEE,VMIN,VMAX,VINCR,IPT)
C
C SUBPROGRAM TO RECONSTRUCT SMOOTHED I.E. CURVES OVER ANY DESIRED
C ENERGY RANGE, USING LINEAR SEGMENTS FITTED TO OBSERVED I.E. CURVE
C BY PROGRAM 'RAWFIT'.
C
COMMON /XDATA/ DATA(1024,8)
COMMON /WORK/ RY(1024),RX(1024)
COMMON /PARAMS/ P(60),VPI,VPE,VPX,NP
C
INITIALISE ENERGY PARAMETERS AND INDICES.
VO=VIP-VEE
VX=VO-VPI
I1=(VMIN-VO)/VINCR+0.5
I2=(VMAX-VO)/VINCR+0.5
VINIT=VO+I1*VINCR
VFINAL=VO+I2*VINCR
IPT=I2-I1+1
IMAX=I2+MPT
PEND=P(NP)-P(NP-1)
FM=NP-1
C
RECONSTRUCT I.E. CURVE USING LINEAR SEGMENTS.
DO 20 I=1,IMAX
F=(VX+I*VINCR)/VPX
IF(F.GE.FM) GO TO 10
IP=F
IF(IP.LT.0) IP=0
F=F-IP
RY(I)=P(IP+1)+(P(IP+2)-P(IP+1))*F
GO TO 20
10 RY(I)=P(NP)+PEND*(F-FM)
20 CONTINUE
C
OBTAIN SMOOTHED I.E. CURVE.
CALL SMOOTH(0,MPT,IMAX)
I3=I1-1
DO 40 I=1,IPT
RY(I)=RY(I3+I)
40
C
FIND MINIMUM OF I.E. CURVE AND SET TO ZERO.
YZERO=RY(1)
IM=1
I3=IPT/10
DO 60 I=2,I3
IF(RY(I).GT.YZERO) GO TO 60
YZERO=RY(I)
IM=I
60 CONTINUE
DO 80 I=1,IM
RY(I)=0.
IM=IM+1

```

```

DO 100 I=1M,IPT
100 RY(I)=RY(I)-YZTRD
WRITE(6,99) VMIN,VMAX,VIP,VEE,VINIT,VFINAL,VINCR,IPT
WRITE(6,98) (RY(I),I=1,IPT)
190 DATA(1021,IRUN)=VINIT
DATA(1022,IRUN)=VFINAL
DATA(1023,IRUN)=VINCR
DATA(1024,IRUN)=IPT
200 RETURN
99 FORMAT(/////1X,'ENERGY RANGE FITTED - VMIN VMAX'//26
CX,2F10.2///'0INTERNAL ENERGY VALUES - I.P. E.E. VIN
CIT VFINAL VINCR'//26X,5F10.2//'0NO. CALCULATED POINTS -'
C,I10)
98 FORMAT(/////1X,'CALCULATED I.E. CURVE - (UNCORRECTED)'//'(5X,20F6
C.0))
END

```

```

SUBROUTINE FLOG(VIP,VEE,VINCR,NRUN,ISTART,ISTOP,ISTEP)
C
C SUBPROGRAM TO CALCULATE FRACTIONAL ION INTENSITIES AND LOGARITHMIC
C INTENSITY RATIOS AS A FUNCTION OF ENERGY.
C
COMMON /XDATA/ DATA(1024,8)
COMMON /INFO/ FAX(500,8),FTOT(500),VXS(500),FAMX(10),FASX(10),
C TITLE,IONAME
LOGICAL*1 TITLE(40),IONAME(40,8)
DIMENSION ID(10),INM(10),RA(5)
REAL VX(500)
C
V0=VIP-VEE+0.1E-05
DO 20 I=1,500
VX(I)=0.
VXS(I)=0.
FTOT(I)=0.
DO 20 J=1,8
20 FAX(I,J)=0.
C CALCULATE PARAMETERS TO CONVERT INDICES FOR CORRECTED I.E. CURVES
C TO SAME ENERGY SCALE.
DO 40 N=1,NRUN
INM(N)=DATA(1024,N)
DI=(DATA(1021,N)-V0)/VINCR
IF(DI.GE.0.) GO TO 30
ID(N)=DI-0.5
GO TO 40
30 ID(N)=DI+0.5
40 CONTINUE
C STORE CORRECTED I.E. CURVES AS A FUNCTION OF SAME ENERGY SCALE.
DO 60 I=1,ISTOP
DO 50 N=1,NRUN
IN=1-ID(N)
IF(IN.LT.1.OR.IN.GT.INM(N)) GO TO 50
FAX(I,N)=DATA(IN,N)
50 CONTINUE
VX(I)=V0+VINCR*(I-1)
60 VXS(I)=VX(I)-VIP
C OBTAIN TOTAL ION INTENSITY AT EACH ENERGY, AND NORMALIZE I.E.
C CURVES.
DO 100 I=1,ISTOP
SUM=0.
DO 80 N=1,NRUN
80 SUM=SUM+FAX(I,N)
IF(SUM.EQ.0.) GO TO 100
DO 90 N=1,NRUN
90 FAX(I,N)=FAX(I,N)/SUM
100 FTOT(I)=SUM
C PRINT-OUT FRACTIONAL ION INTENSITIES AS A FUNCTION OF ENERGY.

```

```

WRITE(6,99) TITLE
WRITE(6,98) ((IONAME(I,N),I=34,36),N=1,5)
DO 190 I=ISTART,ISTOP,ISTEP
120 WRITE(6,97) VXS(I),VX(I),(FAX(I,N),N=1,5),FTDT(I)
WRITE(6,89) TITLE
WRITE(6,88)
C CALCULATE LOGARITHMIC ION INTENSITY RATIOS (FX/FM, FH/FM, FX/1-FM,
C FH/1-FM, FX/FH). FRACTIONAL ION INTENSITIES MUST BE STORED IN THE
C ORDER - (1) FM, (2) FX, (3) FH,....
DO 200 I=ISTART,ISTOP,ISTEP
DO 160 N=1,5
160 PA(N)=0.
IF(FAX(I,1).LT.0.1E-03) GO TO 200
IF(1.-FAX(I,1).LT.0.1E-03) GO TO 200
D1=ALOG10(1.-FAX(I,1))
D2=ALOG10(FAX(I,1))
IF(FAX(I,2).LT.0.1E-03) GO TO 170
F1=ALOG10(FAX(I,2))
RA(1)=F1-D2
RA(3)=F1-D1
GO TO 180
170 F1=1.0
180 IF(FAX(I,3).LT.0.1E-03) GO TO 200
F2=ALOG10(FAX(I,3))
RA(2)=F2-D2
RA(4)=F2-D1
IF(F1.GT.0.) GO TO 200
RA(5)=F1-F2
C PRINT-OUT LOGARITHMIC ION INTENSITY RATIOS AS A FUNCTION OF ENERGY
200 WRITE(6,87) VXS(I),VX(I),RA
RETURN
99 FORMAT(148/1H1//////////T45,40A1//)
98 FORMAT(43X,'FRACTIONAL ION INTENSITIES'/44X,42('*')/21X,'
C EXCESS ELECTRON',24X,'M/E',30X,'TOTAL'/22X,'ENERGY ENERGY',5
C (6X,3A1),T95,'INTENSITY'/23X,'(EV)'(EV)',8X,'(1) (2)
C (3) (4) (5)',9X,'(ARB UNITS)'//)
97 FORMAT(17X,2F10.2,4X,5F9.4,E17.4)
89 FORMAT(148/1H1//////////T30,40A1//)
88 FORMAT(21X,' EXCESS ELECTRON',5X,'LOGARITHMIC INTENSITY RATI
C OS'/22X,'ENERGY ENERGY',4X,37('*')/23X,'(EV) (EV)',5X,'FX/
C FM FH/FM FX/1-FM FH/1-FM FX/FH'//)
87 FORMAT(17X,2F10.2,2X,5F8.2)
END

```

SUBROUTINE PLOT(I1,I2,I3,NN,ESTEP)

SUBPROGRAM TO OBTAIN PLOT OF FRACTIONAL ION INTENSITY CURVES ON
'CALCOMP 1627' PLOTTER.

```

COMMON /INFO/ FA(500,8),FTDT(500),V(500),FAMX(10),FASC(10),TITLE,
C IONAME
LOGICAL*1 NAME(20),TITLE(40),IONAME(40,8)
LOGICAL*1 NAMEX(40)/' EXCESS ENERGY, V-IP (EV) '/'
LOGICAL*1 NAMEY(40)/' FRACTIONAL ION INTENSITY (#K-) '/'
LOGICAL*1 NAMEA(15)/' ION M/E SCALE'/'
DIMENSION Y(500),X(500),MAX(10),LABEL(5),NN(10)

```

```

C EDL=ESTEP/10.
ENSPAC=ESTEP*13
WRITE(6,81) I1,I2,I3,V(I1),V(I2),ENSPAC
3 DO 6 K=1,10
N=NN(K)
IF(N.EQ.0) GO TO 6
FMAX=-1.
DO 4 I=I1,I2,I3
IF(FA(I,N).GT.FMAX)FMAX=FA(I,N)

```

```

4 CONTINUE
  FMAX(N)=FMAX
  IF(FMAX.LT.0.1E-05) GO TO 5
  MAX(N)=-ALOG10(FMAX)
  FASC(N)=10.**MAX(N)
  WRITE(6,82) N,FMAX,FASC(N)
  GO TO 6
5 FASC(N)=0.0
  NN(K)=0
6 CONTINUE
  KA=I1-I3
10 KA=KA+I3
  EA=V(KA)
  NA=EA+EDEL
  IF(EA.LT.0.) NA=EA-EDEL
  FA=ABS(EA-NA)
  IF(FA.LT.0.1E-04) GO TO 20
  IF(KA.GT.I2) GO TO 101
  GO TO 10
20 ILAB=KA
  ISP=(I2-I1)/5
30 ILAB=ILAB-ISP
  IF(ILAB.GE.I1) GO TO 30
  LABEL(L)=ILAB+ISP
  DO 50 ID=2,5
50 LABEL(ID)=LABEL(ID-1)+ISP
  NOSP=(I2-I1)/I3
  ISC=500/NOSP
  CALL AINIT(1000)
  CALL ADRIG(200,250)
  CALL AGRID(0,0,1,1,600,500,1,2)
  CALL GRID(0,0,6,10,100,50,10)
  CALL GRID(0,0,60,0,10,0,5)
  CALL ASCA(-70,45,0,50,10,10,10,1,2)
  IX=-25
  DO 60 J=1,5
  REWIND 1
  WRITE(1,96) V(LABEL(J))
  REWIND 1
  READ(1,97) (NAME(II),II=1,5)
  IX=IX+100
60 CALL ALAB(IX,-30,NAME,5,1,2)
  CALL ALAB(100,-60,NAMFX,40,1,2)
  CALL ALAB(-60,50,NAMEY,40,1,4)
  CALL ALAB(100,520,TITLE,40,1,2)
  NSPI=ISP-(LABEL(1)-I1)
  ISPI=NSPI/I3*ISC
  CALL ADRIG(200+ISPI,250)
  DO 70 J1=1,10
  N=NN(J1)
  IF(N.EQ.0) GO TO 70
  K=0
  DO 80 I=I1,I2,I3
  KJ=K
  K=K+1
  X(K)=K1*ISC
80 Y(K)=FASC(N)*FA(I,N)
  CALL ALINE(X,Y,NOSP+1,0.,0.,100.,.2,1)
  CALL AAEND
  CALL AAINIT(1000)
  CALL ADRIG(200+ISPI,250)
70 CONTINUE
  CALL ADRIG(810,250)
  CALL AGRID(0,0,1,1,170,200,1,2)
  CALL ALAB(10,170,NAMEA,15,1,2)
  I2=0
  DO 12 K5=1,10
  N5=NN(K5)
  IF(N5.EQ.0) GO TO 12
  REWIND 1

```

```

WRITE(1,84) N6,(IONAME(I,N6),I=34,36),FASC(N6)
REWIND 1
READ(1,85) (NAME(I3),I3=1,15)
CALL ALAB(0,150-I2*20,NAME,15,1,2)
I2=I2+1
17 CONTINUE
CALL AFND
100 RETURN
101 WRITE(6,99)
RETURN
99 FORMAT(//1X,'INTEGRAL ENERGY VALUE CANNOT BE FOUND')
97 FORMAT(5A1)
96 FORMAT(F5.2)
81 FORMAT(148/111,50X,'PLOT PARAMETERS'//50X,17('*'))///41X,'INDICES
C -1,3I10//41X,'ENERGIES -',3F10.2//41X,'GRAPHS - ION F
C MAX FASC')
82 FORMAT(/51X,110,F10.6,E10.2)
84 FORMAT(13,3X,3A1,F7.0)
85 FORMAT(15A1)
END

```

```

SUBROUTINE GRID(IX,IY,NX,NY,IXINC,IYINC,IHIGH)
C
C DIMENSION X(2),Y(2)
C
Y(1)=IY-IHIGH
Y(2)=IY
XOR=IX
YOR=IY
IF(NX.EQ.0) GO TO 40
DO 10 I=1,NX
X(1)=IX+I*IXINC
X(2)=X(1)
10 CALL ALINE(X,Y,2,XOR,YOR,100.,100.,1)
X(1)=IX-IHIGH
X(2)=IX
40 IF(NY.EQ.0) GO TO 50
DO 20 I=1,NY
Y(1)=IY+I*IYINC
Y(2)=Y(1)
20 CALL ALINE(X,Y,2,XOR,YOR,100.,100.,1)
X(1)=NX*IXINC+IHIGH
X(2)=NX*IXINC
DO 30 I=1,NY
Y(1)=IY+I*IYINC
Y(2)=Y(1)
30 CALL ALINE(X,Y,2,XOR,YOR,100.,100.,1)
50 RETURN
END

```

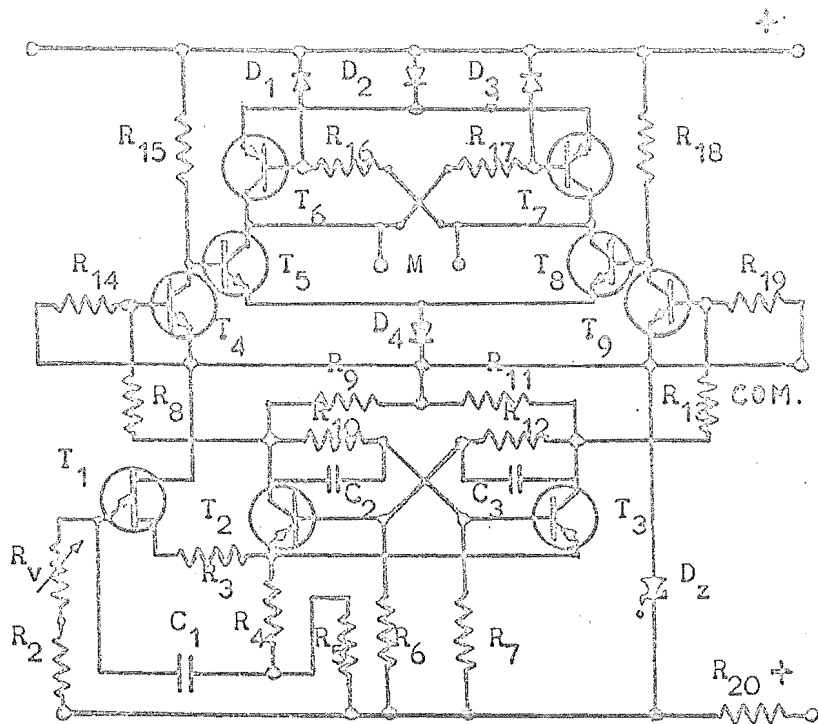
APPENDIX BELECTRONICS1. Ionizing Voltage Control Unit

This motor control unit (Fig. 35) was designed and built by A.M. Ferguson and C.R. Rowe in this department. It consists of a variable frequency, unijunction transistor pulse generator which drives a flip-flop. The flip-flop modifies the pulses to square-wave pulses of equal mark space ratio, and these drive the motor switching transistors.

2. CAT-Tape Punch Interface

This interface (Fig. 36) was designed and built by C.R. Rowe in this department.

FIG. 35 MOTOR DRIVE UNIT



Components Listing:

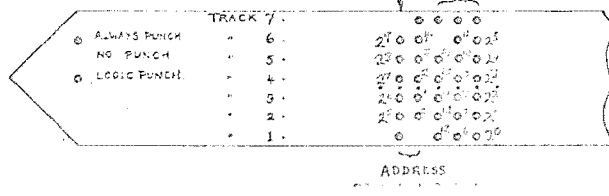
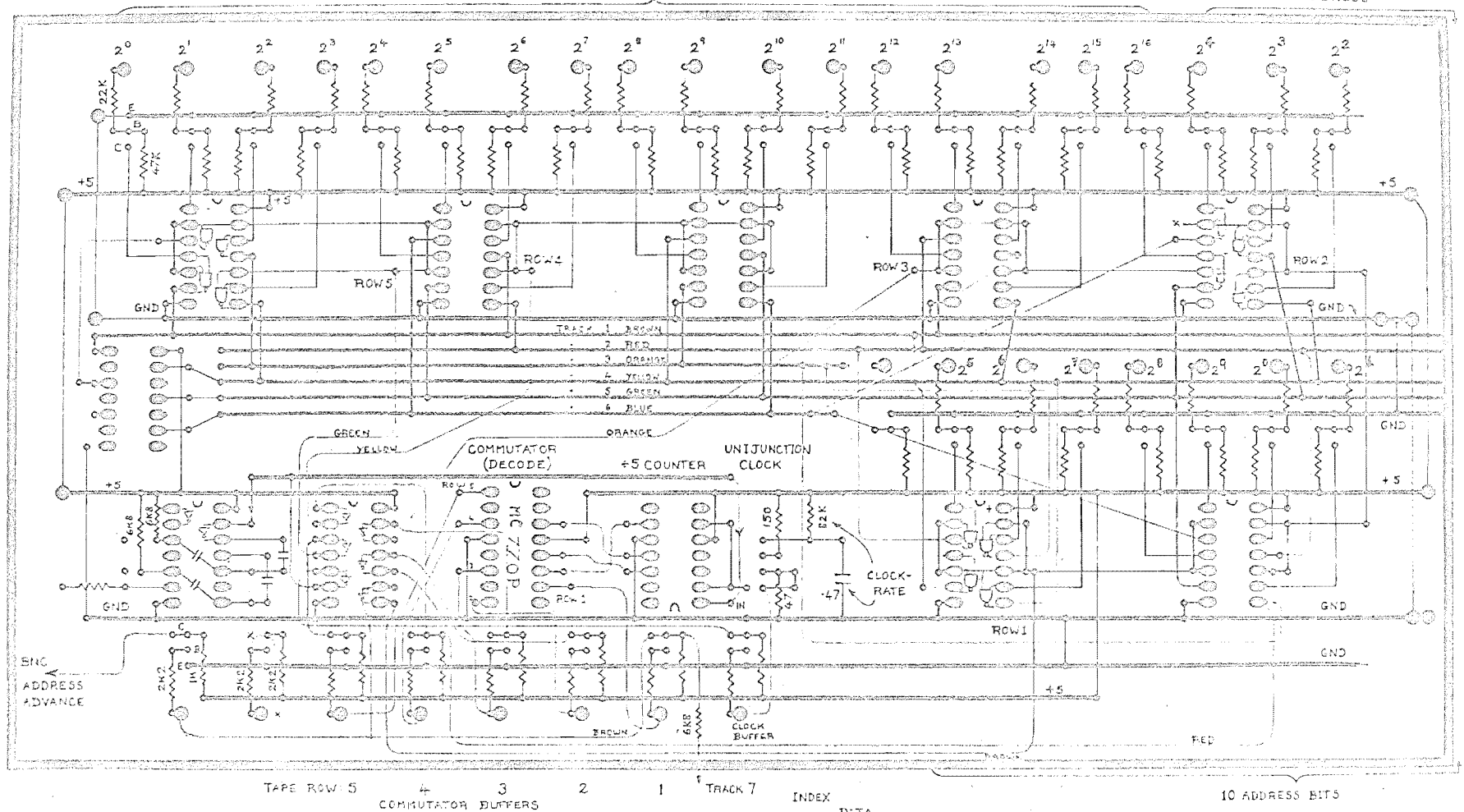
Note; First statement in line is for low voltage/power version (10-20) volt. Other versions require lower drive resistances where indicated*.

T ₁	Unijunction(TIS43A,etc)	T ₆	MT 9658*
T ₂	MT 9658	T ₇	MT 9658*
T ₃	MT 9658	T ₈	MT 9608*
T ₄	MT 9608*2N3053	T ₉	MT 9608*2N3053
T ₅	MT 9608*2N3053		
D ₁	1N914	D ₄	1N4004
D ₂	1N4004	D _Z	10 volt zener or uA723 reg.*
D ₃	1N914		
C ₁	0.39 uF polycarb.	C ₃	0.1 uF, 25 volt
C ₂	0.1 uF, 25 volt		
R _V	100 K pot. *	R ₈	4K7
R ₂	27 K *	R ₉	3K3(1K2)*
R ₃	330	R ₁₀ , R ₁₁	33K *
R ₄	220	R ₁₂	33K *
R ₅	15	R ₁₃	4K7 *
		R ₁₅	10K(3K3) *
		R ₁₆ , R ₁₇	10K (3K3) *
		R ₁₈	10K (3K3) *
		R ₁₉	2K2
		R ₂₀	2K7 *

FIG. 36

17 DATA BITS

ADDRESS



CAT TAPE-PUNCH INTERFACE

ACKNOWLEDGEMENTS

I am particularly indebted to my supervisor, Dr G.J. Wright, for providing every help and encouragement in this study. I also appreciate the skilled efforts of Mr C.R. Rowe and Mr A.M. Ferguson of the technical staff of this department, who developed the data collection system which made much of this work possible.

The work described in this thesis was carried out during the tenure of a U.G.C. (N.Z.) Post-Graduate Scholarship.